Cape Peninsula
University of Technology

PERFORMANCE EVALUATION AND IMPROVEMENT OF GRID-CONNECTED TECHNOLOGY

by

ATANDA KAMORU RAJI

Dissertation submitted in full fulfillment of the requirements for the degree

Doctor of Technology: Electrical Engineering

in the Faculty of Engineering

at the Cape Peninsula University of Technology

Supervisor: Professor MTE Kahn

Bellville

May 2012

Declaration by candidate

I Atanda Kamoru Raji hereby declare that the content of this dissertation represent my own work, and that the opinions contained are my own and not necessarily those of the Cape Peninsula University of Technology.

I ascertain that this dissertation has not previously been submitted for academic examination towards any qualification.

_____ _____

NAME DATE

Abstract

The confluence of the limited resources of fossil fuels (e.g. coal, oil and natural gas), environmental degradations leading to climate change, security of supplies and fossil fuels high costs have demanded a tremendous efforts on humanity to seek for a sustainable and unlimited natural energy sources. Amongst these renewable energy sources stands out solar energy because of its ubiquitousness. Solar energy is converted to DC electricity by the photovoltaic effect.

Photovoltaic (PV) power systems installed in commercial and industrial buildings are a good example of distributed power generation. Here the energy consumption and production match and thus electricity taken from the grid during daytime peak hours can be reduced. This is beneficial as the transmission losses in the grid are avoided and also transmission need is reduced.

The cost effectiveness of a solar energy system has hindered its wide adoption and deployment in terms of the initial capital cost even though it has a zero energy cost and very minimal operating and maintenance costs.

Different governments have instituted many financial incentives for fast adoption of PV systems for both residential and commercial applications. However, all these incentives are not sustainable in the longer term forecast.

For PV system to attain grid parity requires more than unsustainable approach of many governments providing time limited subsidies. The technical solution to the problem is to reduce the overall system cost through technical innovations. One such method is the adoption of transformerless inverter technology as the grid interface system.

Transformerless inverter topology provides galvanic isolation through innovative inverter topology and switching strategies that eliminates problems created by not employing the service of transformer.

An extensive technical literature review is carried out on interconnection standards and codes before presenting some selected distributed energy resources including energy storage systems. Many aspect of grid connected system such as the output filters and power inverter controllers for grid compatibility are highlighted in this work.

The modelling of the PV renewable energy system and experimental validation of the Centre for Distributed Power Electronics Centre is carried out. A simplified common mode voltage model that is used to determine the ground leakage current is developed and analysed in chapter five.

Full bridge transformerless PV inverter topology with bipolar and unipolar switching strategies are modelled and simulated with PSIM software for the investigation of the common mode

voltage and ground leakage current. The results of the simulation are used for the classification of its PV transformerless grid-connected suitability. Neutral point clamped derived transformerless PV inverter topologies such as H5, HERIC, REFU and Ingeteam are modelled and investigated with PSIM software. Efficiency models of convectional full bridge transformerless PV inverter topology are provided in this work.

A novel transformerless PV inverter topology called FB ZVR AC decoupling dual-parallel is developed and analysed in this dissertation. The topology proves to be efficient and safe when a bipolar switching strategy is adopted. The German VDE-026-1-1 safety code is used as the requirement that must be satisfied by PV inverter topology for grid connection.

Advantages of the proposed transformerless PV inverter topology are: better use of the DC bus voltage - the REFU inverter uses half the DC bus voltage, the proposed topology uses the full DC bus voltage providing higher root mean square quantities, DC-DC converters are not needed in the proposed topology thereby increasing the overall efficiency of the inverter topology, the problem of balancing the mid-point of the two DC capacitors is avoided in the proposed topology that may cause non symmetric output voltage and the possibility of non-symmetric AC voltage output that may result into injecting DC current into the utility grid is avoided in this topology.

Efficiency wise, the proposed inverter topology uses six semiconductor switches with two of them operated at the grid frequency while the REFU topology uses three power converter stages in the structure thereby reducing the overall system efficiency.

It is concluded that adoption of transformerless PV inverter topology increases the efficiency-cost ratio and reduces the installation cost by the avoidance of the high or low frequency isolation transformer used in some early PV inverter topology systems. The safety of such transformerless PV inverter topology is also guaranteed as seen in all new commercialized transformerless PV inverter topology in the market today.

Dedication

The work in this dissertation is wholly dedicated to my mother Kudiratu Abeni Afolabi-Raji who kept a vigilant eye on me as a 7-8 year-old boy whenever the NEPA (Nigeria Electricity Power Authority now called Power Holding Company of Nigeria) distribution servicemen worked on the lines and I satisfied by curiosity by watching to wonder what those men were doing up there. She was always around to ensure that I do not stand directly under the repaired lines keeping me away from any falling object. Thanks mother.

My appreciation to my family is undoubtedly unsolicited for their kind understanding that kept me going during my study. I thank my children Adeola, Taiye, Kehinde, Idowu (ID), Adeolu and my wife Folashade Latifat for their unrelenting supports and compassionate love.

Acknowledge

The utmost gratefulness goes to almighty Allah for granting me and my family good health to start and complete this work.

Professor MTE Kahn, my supervisor has given me a tremendous guide and support using his expert knowledge in academic research process. I would like to express my sincere appreciation to Professor MTE Kahn, for his support, guidance and encouragement. Professor MTE Kahn's broad knowledge, great intuition and accurate judgment have been the source of inspiration for my research in the Centre for Distributed Power Electronics Systems during the past years. The most precious things I have learned from him are the ability of independent research and also a long-term vision in the research.

I would also like to acknowledge my colleague Dr. Marco Adonis, an active member of the Centre for Distributed Power Electronics Systems who has been an inspirational motivator for me during my research work. I say thank you for what you have contributed to the success of this work.

I acknowledge my co-postgraduate students now doctors: Dr. Afua Mohammed, Dr Kilimo Abraham for their good work relationship and the academic advice we shared together and received from one another during their stay at the Centre for Distributed Power Electronics Systems.

The financial assistance of the Cape Peninsula University of Technology towards this research is acknowledged. Specifically funds granted to me to attend a PHD Microgrid course at the University of Aalborg Denmark and the University Research Fund (URF) for the purchase of equipment used in some of the work carried out in this dissertation.

Opinions expressed in this dissertation and the conclusions arrived at, are those of the author and are not necessarily to be attributed to the Cape Peninsula University of Technology

Table of Contents

Declaration by candidate ii

Abstract iii

Dedication v

Acknowledge vi

Table of Contents vii

List of Figures xi

List of Tables xvi

Nomenclatures xvii

Chapter 1 : INTRODUCTION 19

1.1 Problem Statement 21

1.2 Research Questions 23

1.3 Objectives 23

1.4 Delineations 24

1.5 Outline of the Thesis 24

Chapter 2 : LITERATURE REVIEW 26

2.1 Introduction 26

2.2 Interconnection Technologies 33

2.2.1 Synchronous interconnection 34

2.2.2 Induction interconnection 35

2.2.2.1 Variable-Speed wind turbines 36

2.2.2.2 Variable-speed operation of synchronous generators 36

2.2.3 Inverter interconnection 40

2.3 Grid requirements and standards for grid connected technology 42

2.3.1 IEEE 1547 Interconnection Standard for distributed Resources 42

2.3.2 IEC 61727 Characteristics of Utility Interface 43

2.3.3 VDE 0126-1-1 Safety 44

2.3.4 EN 50160 Public Distribution Voltage Quality 45

2.3.5 SA Interconnection Standard for the Interconnection of Embedded Generation 46
2.3.5.1 Excitation control and governor requirements 47
2.3.5.2 Synchronization 48
2.3.5.3 Islanded operation 49
2.3.5.4 Fault ride through capabilities 49
2.3.5.5 Under and over voltage protection 50
2.3.5.6 Under and over frequency protection 50
2.4 PV grid requirements 51
2.4.1 Response to abnormal grid conditions 51
2.4.2 Voltage deviations 51
2.4.3 Frequency deviations 52
2.4.4 Reconnection after trip 52
2.5 Power Quality 53
2.5.1 DC current injection 53
2.5.2 Current harmonics 54
2.5.3 Average power factor 55
2.6 Anti-islanding requirements 55
2.6.1 IEEE 1547/UL1741 Anti-islanding requirements 56
2.6.2 IEC 62116 Anti-islanding Requirements 58
2.6.3 VDE 0126-1-1 Anti-islanding Requirements 58
2.7 Grid filter topologies 59
2.7.1 L-filter 60
2.7.2 LC and LCL-filter 60
2.7.3 Damping 61
2.8 Grid Power Converter Control 62
2.9 DC-AC Converter control 62
2.9.1 Transformations 63
2.9.3 PI Controllers 70
2.9.4 Proportional resonant controllers 71
2.9.5 State feedback controller 72
2.9.6 Harmonic compensation 73
2.9.7 Grid synchronisation 74
2.9.7.1 Filtered Zero Cross Detection (ZCD) 74
2.9.7.2 Filtering of grid voltages 74

2.9.7.3 Phase Locked Loop (PLL) 75
2.9.7.4 Adaptive PLL 77

Chapter 3 : DISTRIBUTED ENERGY RESOURCES TECHNOLOGY 78

3.1 Wind power system 79
3.2 Fuel cell system 82
3.4 Micro turbine system 82
3.4 Combined heat and power system 84
3.5 Energy storage systems 85
3.7.1 Electrochemical battery 87
3.7.2 Flywheel 89
3.7.3 Ultracapacitor 89
3.7.4 Superconducting magnetic energy storage system 90
3.7.5 Compressed air energy storage system 91
3.8.6 Tidal power 91
3.8.7 Wave power 93
3.8.8 Biomass 95
3.8.9 Small-scale hydroelectric power generation 95

Chapter 4 : PHOTOVOLTAIC SYSTEM MODELLING AND VALIDATION 97

4.1 Photovoltaic Cells Modelling and Analysis 97
4.2 Simulations and Validation Results 101
4.3 Common mode voltage and ground leakage current analysis 107
4.3.1 Simplified common mode leakage current model 110

Chapter 5 : TRANSFORMERLESS GRID CONNECTED PHOTOVOLTAIC INVERTERS 114

5.1 Photovoltaic power conversion technology 114
5.2 Solar Power Conversion Structures 115
5.2 H-Bridge Inverter Topology 120
5.3 Neutral Point Clamped Topology 124
5.3 NPC Derived Commercialized Transformerless Topologies 130

5.3.1 H5 Inverter 130
5.3.2 HERIC Inverter 133
5.3.3 REFU Inverter 138
5.3.4 Ingeteam Inverter 142
5.3.5 FB-ZVR Inverter 147

Chapter 6 : COMMON MODE VOLTAGE AND GROUND LEAKAGE CURRENT 150

6.1 Introduction 150
6.2 Thermal module 150
6.2.1 Diode power losses calculation 151
6.2.2 IGBT power losses calculation 152
6.3 Full bridge with bipolar switching inverter: Common mode voltage and ground leakage current 153
6.5 Full bridge with unipolar switching inverter: Common mode voltage and ground leakage current 158
6.6 Energy efficiency determination of FB transformerless inverter topology 162

Chapter 7 : NOVEL TRANSFORMERLESS GRID-CONNECTED PV TOPOLOGY 168

7.1 Introduction 168
7.2 A novel transformerless grid-connected PV topology 168
7.2.1 FB VZS AC decoupling dual-parallel switch with unipolar modulator. 169
7.2.1 FB VZS AC decoupling dual-parallel switch with bipolar modulator. 173
7.3 Advantages of the proposed PV transformerless inverter topology 178
Chapter 8: CONCLUSION AND RECOMMENDED FUTURE WORKS 180

Conclusions 180
Recommended Future Works 181

REFERENCES 182

APPENDIXE A 201

A1 Model of the Power Converter 201
A2 IXYS HiPerFASTTM IGBT datasheet 205

List of Figures

Figure 2-1 Installed PV power....27
Figure 2-2 Off grid and grid connected growth share....27
Figure 2-3 Variable-speed wind turbine with synchronous generator....37
Figure 2-4Variable-speed wind turbine with squirrel cage induction generator....38
Figure 2-5 Wind turbine with WRIG and external rotor resistance....39
Figure 2-6 Test setup for the anti-islanding requirement in IEEE 1547.1....56
Figure 2-7 Test setup for anti-islanding requirement in VDE 0126-1-1....59
Figure 2-8 LC filter....60
Figure 2-9 L filter....61
Figure 2-10 LCL filter....61
Figure 2-11 Different PMW control schemes....63
Figure 2-12 abc to αβ transformation....65
Figure 2-13 αβ to dq transformation....66
Figure 2-14 Generation of carrier based PWM signals....68
Figure 2-15 Space vector representation of output voltage....69
Figure 2-16 A basic PLL circuit....75
Figure 2-17 schematic of a phase lock loop with transformation....76
Figure 3-1: Distributed Generation Technology Types....78
Figure 3-2: Wind Energy Conversion System....79
Figure 3-3: Concentrated Solar Power....81
Figure 3-4: Photovoltaic Effect and Operation....82
Figure 3-5 Single shaft microturbine....83
Figure 3-6 Double-layer Ultracapacitor Construction Details....90
Figure 3-7: Artist's impression of axial tidal current turbines....93
Figure 4-1Single diode electrical equivalent model....97
Figure 4-2 Maximum power point....100
Figure 4-3 Schematic of the PV system modelled....101
Figure 4-4 PSIM PV panel physical model....102
Figure 4-5 CDPES PV system setup....103
Figure 4-6: Solar panels mounted on the roof of Electrical Engineering Department CPUT....104
Figure 4-7 Output voltage and current waveforms of the simulated model....105
Figure 4-8 60W Linear load....106

Figure 4-9 120 W Linear load 106
Figure 4-10 180 W Linear load 107
Figure 4-11 Common mode current in a transformerless system.....108
Figure 4-12 Parasitic capacitance in PV.....109
Figure 4-13 Common mode leakage current model of single phase full bridge inverter.....110
Figure 4-14 Simplified common mode leakage current mode of a single-phase full bridge inverter.....110
Figure 4-15 Equivalent circuit model of the leakage current generated by the grid 111
Figure 4-16 Equivalent circuit of the leakage current generated by the two PWM voltage sources. 111
Figure 4-17 Equivalent circuit of the common mode leakage current model 113
Figure 5-1 PV Inverter Technologies 114
Figure 5-2 General Structure of a Transformerless Renewable Energy DPGS and its main Control Features 115
Figure 5-3 (a) Centralized technology (b) String technology.....117
Figure 5-4 Multi-string technology 118
Figure 5-5 Basic Full Bridge Inverter with PV Module.....120
Figure 5-6 Bipolar SPWM switching control logic circuit.....121
Figure 5-7 Bipolar switching waveforms 121
Figure 5-8 Unipolar SPWM switching control logic circuit 122
Figure 5-9 Unipolar switching waveforms.....122
Figure 5-10 Hybrid switching control logic circuits 123
Figure 5-11Hybrid SPWM Waveforms.....123
Figure 5-12 Neutral clamped half-bridge topology.....124
Figure 5-13 NPC Vg>0, Ig>0, S1 and S2 On, S3 and S4 Off.....125
Figure 5-14 NPC Vg>0, Ig>0, D+ and S2 On, S3, S1 and S4 Off.....125
Figure 5-15 NPC Vg<0, Ig<0, S3 and S4 On, S1 and S2 Off.....125
Figure 5-16 NPC Vg>0, Ig>0, S3 and D- On, S1, S4 and S2 Off.....126
Figure 5-17 Conergy NPC inverter topology 127
Figure 5-18 Conergy Vg>0, Ig>0, S1 = ON, S+, S- and S2 =OFF 128
Figure 5-19 Conergy Vg<0, Ig>0, S2 = ON, S+, S- and S1 =OFF 128
Figure 5-20 Conergy Vg>0, Ig>0, S+ = ON, S-, S1 and S2 =OFF 128
Figure 5-21 Conergy Vg<0, Ig<0, S- = ON, S+, S- and S2 +OFF.....129
Figure 5-22 H5 inverter topology.....130

Figure 5-23 H5 switching logic control circuit 131
Figure 5-24 H5 control signal waveforms 131
Figure 5-25 H5 Vg>0, S5, S1 and S4 On 132
Figure 5-26 H5 Vg>0, S5 and S4 Off and D3 On 132
Figure 5-27 H5 Vg>0, S5 and S4 Off, S1 and D3 On 133
Figure 5-28 H5 Vg<0, S5 and S2 Off, D1 and S3 Off 133
Figure 5-29 HERIC inverter topology 134
Figure 5-30 HERIC switching logic control circuit 135
Figure 5-31 HERIC switching waveforms 135
Figure 5-32 HERIC Vg>0, S1 and S4 On, S_ On 136
Figure 5-33 HERIC Vg>0, S1 and S4 Off, S+ and D- On 136
Figure 5-34 HERIC Vg>0, S2 and S3 On, S- On 136
Figure 5-35 HERIC Vg<0, S2 and S3 Off, S- and D+ On 137
Figure 5-36 REFU transformerless PV inverter topology 138
Figure 5-37 REFU Vg>0, Vpv<|Vg|, Ig>0. S1 and S+ = ON 140
Figure 5-38 REFU Vg>0, Vpv<|Vg|, Ig>0. S3 and S+ = ON 140
Figure 5-39 REFU Vg>0, Ig>0. S+= ON 140
Figure 5-40 REFU Vg>0, Vpv<|Vg|, Ig<0. S2 and S- = ON 141
Figure 5-41 REFU Vg<0, Vpv<|Vg|, Ig<0. S4 and S- = ON 141
Figure 5-42 REFU Vg<0, Ig<0. S-= ON 141
Figure 5-43 H6 inverter topology 142
Figure 5-44 H6 switching control logic circuit 143
Figure 5-45 H6 switching waveforms 143
Figure 5-46 Ingeteam Vg>0. S5, S6, S1 and S4 = ON 145
Figure 5-47 Ingeteam Vg<0. S5, S6, S1, S2 and S3 = ON 145
Figure 5-48 Ingeteam Vg>0. S1 and S4 = ON 145
Figure 5-49 Ingeteam Vg<0. S2 and S3 = ON 146
Figure 5-50 FB-ZVR inverter topology 147
Figure 5-51 FB-ZVR switching modulation circuit 148
Figure 5-52 FB-ZVR modulation signal waveforms 148
Figure 6-1 FB transformerless grid-connected topology with bipolar modulator 154
Figure 6-2 FB bipolar inverter output voltage 155
Figure 6-3 FB bipolar common mode voltage 155
Figure 6-4 FB bipolar grid terminal voltage 156

Figure 6-5 FB bipolar PV array terminal voltage 156
Figure 6-6 FB bipolar ground leakage current 157
Figure 6-7 Ground leakage current FFT 157
Figure 6-8 FB transformerless grid-connected topology with unipolar modulator 158
Figure 6-9 FB unipolar inverter output voltage 159
Figure 6-10 PV array terminal voltage 160
Figure 6-11 Grid terminal voltage 160
Figure 6-12 FB unipolar Common mode voltage 161
Figure 6-13 FB unipolar ground leakage current 161
Figure 6-14 FB unipolar ground leakage current FFT 162
Figure 6-15 Efficiency model of transformerless PV FB inverter topology 164
Figure 6-16 Average semiconductor power switch losses with bipolar switching 164
Figure 6-17 Average input power of FB topology with unipolar switching 165
Figure 6-18 Average semiconductor power switch losses with bipolar switching 166
Figure 6-19 Average input power of FB topology with bipolar switching 167
Figure 7-1 FB VZS AC decoupled dual-parallel switch 169
Figure 7-2 FB VZS AC decoupling dual-parallel switch unipolar modulator circuit 169
Figure 7-3 FB VZS AC decoupling dual-parallel switch inverter output voltage (Unipolar) 170
Figure 7-4 FB VZS AC decoupling dual-parallel switch common mode voltage (Unipolar) 170
Figure 7-5 FB VZS AC decoupling dual-parallel switch PV array terminal voltage (unipolar) 171
Figure 7-6 PV array terminal voltage FFT 171
Figure 7-7 FB VZS AC decoupling dual-parallel switch PV ground leakage current (Unipolar) 172
Figure 7-8 FB VZS AC decoupling dual-parallel switch PV ground leakage current FFT (Unipolar) 172
Figure 7-9 FB VZS AC decoupling dual-parallel switch with bipolar modulator 173
Figure 7-10 FB VZS AC decoupling dual-parallel switch bipolar modulator circuit 174
Figure 7-11 FB VZS AC decoupling dual-parallel switch inverter output voltage (bipolar) 175
Figure 7-12 FB VZS AC decoupling dual-parallel switching signals (bipolar) 175
Figure 7-13 FB VZS AC decoupling dual-parallel switch PV array terminal voltage (bipolar) 176
Figure 7-14 FB VZS AC decoupling dual-parallel switch PV array terminal voltage FFT (bipolar) 176
Figure 7-15 FB VZS AC decoupling dual-parallel switch Common mode voltage (bipolar) 177

Figure 7-16 FB VZS AC decoupling dual-parallel switch PV ground leakage current (Bipolar) 177
Figure 7-17 FB VZS AC decoupling dual-parallel switch PV ground leakage current FFT (Bipolar).....178
Figure A-0-1 Stationary and rotating reference frame 204

List of Tables

Table 2-1 Topology options for variable-speed wind turbine using wound rotor induction generators....40
Table 2-2 Public distribution grid voltage harmonics EN 50160....46
Table 2-3 Typical synchronizing parameter limits (IEEE 1547 p12)....48
Table 2-4 Typical settings for loss-of-grid....49
Table 2-5 Maximum operating times for voltage protection....50
Table 2-6 Disconnection time for voltage variations....51
Table 2-7 Disconnection time for frequency variations....52
Table 2-8 Conditions for reconnection after trip....52
Table 2-9 DC current injection limitations....53
Table 2-10 Maximum current harmonics....54
Table 3-1 Functionality of Storage Systems....86
Table 3-2 Characteristics of Lead-Acid Battery....88
Table 4-1 PV system theoretical calculations....105
Table 4-2 PV system simulated results....105
Table 4-3: PV system experimental works results....106
Table 6-1 Parameters used in case of the simulation....154
Table 6-2 Parameters used in case of the simulation....158
Table 6-3 Parameters used in case of the simulation (unipolar switching)....163

Nomenclatures

A:	Ampere
AC:	Alternating current
C_{PV}:	DC link PV capacitance
C_{PV_g}:	PV array parasitic capacitance to ground
DC:	Direct current
DG:	Distributed generation
dq0:	d-q-o axis
ESKOM:	South Africa electricity utility
f:	Frequency
FB:	Full bridge topology
FB-ZVR:	Full bridge zero voltage rectifier
FFT:	Fast Fourier Transform
HB:	half bridge topology
HERIC:	Highly efficient and reliable inverter concept
IEC:	International Electrotechnical commission
IEEE:	Institute of Electrical and Electronics Engineers
IGBT:	Insulated gate bipolar transistor
L:	Inductance
LC:	Inductance-capacitance
LCL:	Inductance-capacitance-inductance
MOSFET:	Metal oxide semiconductor field effect transistor
NPC:	Neutral point clamped
PI:	Proportional-Integral
PID:	Proportional-Integral-Differential
Pin:	Input power
PLL:	Phase-locked loop
Pout:	Output power
PR:	Proportional-Resonant
PWM:	Pulse width modulation
s:	Seconds
SA:	South Africa
SPWM:	Sinusoidal pulse width modulation

V:	Voltage
Vdc:	DC link voltage
VDE:	German grid compliance code
Vin:	Input voltage
Vout:	Output voltage
VSI:	Voltage source inverter
W:	Watt
ZSI:	Z-source inverter
αβ0:	Alpha-beta-o axis
ω:	Angular frequency

The need for electricity is never ending. Along with the growth in demand for electric power, sustainable development, environmental issues, power quality and reliability have become concerns. Electric utilities are becoming more and more stressed since existing transmission systems are approaching their operating limits with growing loads. Concerns on the change in the earth's climate, formalized in the Kyoto Protocol in 1997 also stimulate research promotion, development and increased use of renewable energy (Tsikalakis & Hatziargyriou, 2007; Battaglini, Lilliestam, Hass & Patt, 2009).

In South Africa, the South African Revenue Services has introduced an accelerated depreciation allowable for renewable energy projects for companies who want to roll out commercial and industrial scale under 1 MW within their organization. Companies can write off their system in three years at the rate of 50%, 30% and 20%. Companies who also invest in PV feel that PV is a great way to show that they are environmentally-conscious and sensitive about their carbon footprint.

The challenge at a residential level is the initial investment that needs to be made. For example, a competitively priced 1,1 kW_p grid connected PV system costs about R33 000. The system should produce about 6 kWh per day with a payback period of seven year, which includes the forecasted energy-price escalation from Eskom (25^o in Africa, 2012).

Over the last few years, a number of factors have led to an increased in distributed generation schemes for producing electricity: reduction in gaseous emissions (mainly CO_2), energy efficiency or rational use of energy, deregulation or liberalization, diversification of energy resources, availability of modular generating plants, easiness of finding sites for smaller generators, short construction lead time and lower capital costs for smaller plants, and generation site location closer to load which reduce transmission costs as well as power loss are some of the reasons for increasing deployment of distributed generation units.

In power systems, the application of electricity generation based on renewable sources is not new (Chicco & Mancarella, 2009), but a future large-scale implementation of these renewable energy sources will cause structural changes in the existing distribution and transmission networks (Bull & Billman, 1999; Tong, Kleinberg & Miu, 2005; Bayod-Rjula, 2009). This is due to the following:

Most renewable energy generators are connected to the distribution network (for example the solar panel on the roofs of houses, small wind farms and individual wind mills). This is in contrast with the current layout of the system, where most of the generator is connected to the transmission system (Jiayi, Chuanwen & Rong, 2008).

Most renewable energy generators depend on natural and uncontrollable sources, such as the wind and the sun, and the electrical power output cannot be controlled (Lamont, 2008). If there is no wind, the windmill does not deliver energy. However, most renewable energy generators are connected to the grid by power electronic interfaces, which offer the possibility and flexibility to control the power output given a certain power input in some way (Valtchev, Van dev Bossche, Ghijselen & Melkebeek, 2000; Gao & Iravin, 2008). In case of photovoltaic systems for example, the converter of a solar panel is programmed to maximize the energy yield by means of a maximum power point tracker (Billy & Shu-Hung 2005).

Many renewable energy generators, for example wind turbines and photovoltaic systems, have an intermittent and variability character (Abderrazzaq & Aloquili, 2008; Kudo, Takeuchi, Nozaki, Endo & Sumita, 2009; Fernandez, Garca, Saenz & Jurado, 2009). A large-scale implementation of this type of generators can lead to strong power fluctuation in the grid (Marwali, Jung & Keyhani, 2004). This will evidently make power system operation and control very difficult (if not impossible) if consideration of distributed generation system integration is not taken into account.

The term distributed generation or embedded generation refers to small generators that are usually connected to the distribution network (Ackermann, Anderson & Sder, 2001; Peppermans, Driesen, Haeseldonckx, Belmans & Dhaseleer, 2005). Distributed generation includes:

- Generators powered from renewable energy sources except large scale hydro and the largest wind farm (Mondol, Yohanis & Norton, 2007).
- Combined heat and power (CHP) system, also known as co-generation (co-gen).
- Standby generators operating in grid-connected mode, particularly when centralized generation is inadequate or expensive or unavailable.

Smaller generators are not connected to the transmission system because of the high cost of transformers and switchgears. Also, the transmission system is likely to be too far away since the geographical location of the generators is usually predetermined by the availability of the renewable energy resource.

Technical advances and institutional changes in the electric power industry have resulted in a constantly increasing penetration of distributed generation (DG) resources in the grids (Lasseter, 2007; Peas Lopes, Hatziargyriou, Mutale, Djapic & Jenkins, 2007; Ramakrishna & Bhatti, 2008). For the connection of new DG installations to the network a variety of factors are taken into account, including technical requirements imposed by utilities to ensure that the DG station does not adversely affect the operation and safety of the network (Basson, 2008).

Distributed generation offer potential benefits such as reduction in transmission and distribution losses, deferment of grid investment and improved grid asset utilisation, improved grid reliability, providing ancillary services such as voltage support or stability, contingency reserves and black start capability. Other benefits include clean energy, lower-cost energy, reduced price volatility, greater reliability and better power quality, energy and load management, and combined heat and power synergies (Siddiqui & Maribu, 2009). To reap all these benefits will require research and development on key interface, interconnection and communications and control technologies.

Distributed generation will invariably contain some kind of renewable energy source such as wind power, photovoltaic system, hydro system (ranging from micro hydro to small hydro), tidal power, wave power, biomass, alternative energy source (such as fuel cell), fossil fuel energy source generators (such as micro turbines), diesel generators etc.

1.1 Problem Statement

The standard electric power system models has been designed and developed to generate power at large-scale power plants distantly located to the load centres and distribute power to customers via power transmission lines. Power distribution infrastructure has also been designed as a unidirectional power flow conduit. In recent years, however, we have been witnessing the appearance of many small-scale power plants on power networks, as distributed power sources — such as photovoltaic power, wind power, and other alternative and renewable energy sources get connected to the transmission and distribution systems. A concern with PV and other renewable energy forms is that they are intermittent and stochastic. As more of these power sources are interconnected with power grids, various risks come into view, such as lower electric power quality, public and equipment safety as well as system stability.

Photovoltaic (PV) systems are one of the few power generation technologies that can be installed right at the point of consumption, regardless of the amount of energy demanded. This saves enormous costs in infrastructure such as cabling, transformers and switchgear.

The electric power industry liberalization, technological advancement and the concern for the environment have steered centrally generated electrical energy technology towards decentralized generation technology such as wind and solar power system (Bouffard & Kirschen, 2008). This shift is possible because of fast restructuring of the electric power industry which manifests itself under liberalization, deregulation, free market participation, and re-regulation concepts (Ackermann, 2007).

From an environmental perspective, the increase use of renewable technologies is highly desirable, as they do not emit greenhouse gasses and thus do not contribute to climate change (Bose, 2000). Nevertheless, their increase poses increasingly technical challenges on reliable operation of the interconnected grid, due to their intermittent and stochastic nature (Salam, Mohamed & Hannan, 2008).

In order to add to the supply adequacy and increase the reliability of the interconnected grid, the power electronic interface used to connect the distributed generators with the grid must comply with standards set by grid operators or owners (IEEE 1547 Standard, 2003). Harnessing the full potential of distributed energy resources will surely rely on less negative impact contributed by distribution generation integration technology (Dicorato & Trovato, 2008).

To ensure grid parity (PV electricity generation cost relative to grid electricity) for PV systems require increased efficiency-to-cost ratio. One technical method to achieve this is to increase the efficiency and decrease the system cost through the elimination of the galvanic isolation typically provided by high-frequency transformers in the DC-DC boost converter or by a line-frequency transformers on the output. Thus a typical efficiency increase of 1-2% can be obtained.

This research project evaluates the performance of PV power converter topologies that can be used without either high or line-frequency transformers and enhances the performance indices of PV grid-connected technologies notably transformerless PV inverter topologies. A novel PV transformerless inverter topology developed was evaluated for compliance to safety requirements as stipulated in the grid code.

The main performance indices evaluated are the common mode voltage and ground leakage current introduced as a result of the galvanic isolation absence.

Sub-Problems

Insight into the development of unintentional islanding detection algorithms (Brndlinger & Bletterie 2005; Chowdury, Chowdury, Ten & Crossley, 2008; Zeineldin, El-Saadany & Salama, 2006).

The issues of micro grid integration with existing power system infrastructures (Hossein, Shayanfar & Fotuhi-Firuzabad, 2009; Pedrasa & Spooner 2006).

Ancillary services provided from distributed energy resources (Yan, Tolbert, Rizy & Kueck, 2007; Li, Ding, Wang & Zhang, 2008).

1.2 Research Questions

Can a cost effective and high efficiency grid connected power inverter for solar energy distributed power generation conceptualized?

Can a cost effective and high efficiency grid connected power inverter for solar energy distributed power generation modeled and verified?

Can the technical requirements recommended in the grid codes for the conceptualised grid connected topology be met and surpassed?

Can new key performance indexes be identified in the transformerless grid connected technology arena?

What minimum set of functions should be included in a basic power inverter-based interconnection system? What are the optional additional capability functions?

1.3 Objectives

To extensively research on grid-tied technologies used to interconnect PV distributed generators to the LV distribution system in order to identify current developments in the paradigm.

To evaluate the performance indices of power electronic interface technologies that is used to make grid interconnection to conform to interconnection codes and standards.

To improve on system performance of the existing grid interconnection technologies that can possibly lead to new grid interconnection technology development.

1.4 Delineations

The scope of the research will concentrate on performance evaluation and improvement of power electronics interface grid-connected technology in conformity with international standards (e.g. IEEE 1547 – 2003, IEC61737, VDE 0126-1-1, and G8 code). Transformerless inverter topologies are thoroughly investigated for selected performance indices determination. The research will not delve into performance evaluation of induction generator grid-connected technology, synchronous generator grid-connected technology and permanent magnet synchronous generator grid-tied technology, unintentional and intentional islanding algorithms, distribution system protection schemes, protection coordination schemes, load frequency control and dispatch ability of distributed generators. However, literature reviews on some of these is provided to give a holistic view of distributed generation systems design, analysis, control, planning and operation.

1.5 Outline of the Thesis

Chapter 2 provides an extensive technical literature review of information about interconnection technologies. Synchronous, asynchronous and power electronics inverters are reviewed extensively. Interconnection technical requirements from IEEE 1547 series, German DIV VDE 0126-1-1, IEC 61727, EN 50160 and South Africa codes are reviewed. SA Interconnection Standard for the Interconnection of Embedded Generation is reviewed in details in subsection 2.3.5 providing all the important technical requirements from embedded generators particularly synchronous generators. PV technical requirements in the entire reviewed standards are presented dealing with issues like response to abnormal conditions, voltage deviation, frequency deviation and reconnection after trip. Power quality issues are discussed under various standards and codes. Two grid filters types and grid converter control systems are also reviewed in chapter one.

Main types of distributed generation systems are reviewed in chapter three. Wind power, fuel cells, micro turbine and CHP systems are reviewed from the operation point of view. Electrochemical, flywheel, ultra capacitor, superconducting, compressed air energy systems are thoroughly reviewed as these storage systems will be deployed extensively in the future smart grid technology. Other forms of distributed generation systems such as tidal, wave and biomass are also reviewed.

Chapter four presents the mathematical model of photovoltaic system. An experimental work used to validate the renewable energy system at the Centre of Distributed Power Electronics

Systems (CDPES) is presented. Common mode voltage and ground leakage current models are provided. Simplified models for both common mode voltage and ground leakage current are developed and used in the subsequent chapters.

Transformerless topologies used in photovoltaic system are presented in chapter five. Power conversion systems and photovoltaic system structures are reviewed here as well. H-bridge, neutral point clamped and NPC derived topologies. H5, HERIC, REFU, Ingeteam and FB-ZVR are analyzed and simulated. Common mode voltage and ground leakage current are the two performance indices examined to make a conclusion about the suitability of the various topologies for use as a c transformerless photovoltaic grid connected system.

Common mode voltage, ground leakage current and efficiency of conventional full bridge transformerless topologies are presented in chapter 6. Bipolar and unipolar switching strategies are applied to the conventional full bridge. The common mode voltages as well as the ground leakage currents are the indices used to decide the suitability of the topology as a transformerless photovoltaic grid connected system.

A new topology developed called FB VZS AC decoupling dual-parallel is presented in chapter seven. The new topology was examined under both bipolar and unipolar switching strategies. The common mode voltages and leakage currents are again used for the determination of the suitability of the inverter for transformerless photovoltaic grid connected system.

Chapter eight gives the conclusions of this research work based on the analysis and simulation results of the novel transformerless PV inverter topology developed and list some future works that can be considered.

2.1 Introduction

Almost all distributed generators will require power electronic interface technology to enable grid connection to either the transmission system or distribution system depending on the generation voltage level (Blaabjerg, Chen & Kjaer, 2004). Many such power electronic interface technologies have been researched on extensively based on recent journal publications and white paper reports on the subject matter (Hassaine, Olias, Quintero & Haddadi, 2009; Finney & Williams, 2009; Renders, Gussem, Ryckaert & Vandevelde, 2009; Renders, Gussem, Ryckaert & Vandevelde, 2009; Salamah, Chen & Smedley, 2008; Schimpf & Norum, 2008; Lee, Song, Park, Moon & Lee, 2008; Khajehoddin, Jain & Bakhshai, 2007; Peng F Z, Shen M & Huang Y, 2007; Blaabjerg, Teodoresu, Liserre & Timbus, 2006; Carrasco, Franquelo, Bialasiewicz, Galvn, Guisado, Prats, Len & Moreno-Alfonso, 2006; Kojabadi, Bin, Gadoura, Liuchen & Ghribi 2006; Azbe & Mihalic, 2006; Zeng & chang, 2005; Xue, Chang, Kjr, Bordonau & Shimizu, 2004; Arlampalam, Barnes, Engler Goodwin & Jenkins, 2004; Myrzik & Calais, 2003; Rodriguez, Lai & Peng, 2002, Hinz & Mutschler 1998).

The installed PV power in MW from 1992 to 2007 is shown in figure 2-1. The PV grid installation has quickly overshadowed the off grid installation systems in the early 90's to late 90's. The installed PV capacity as grid connected system continues to increase.

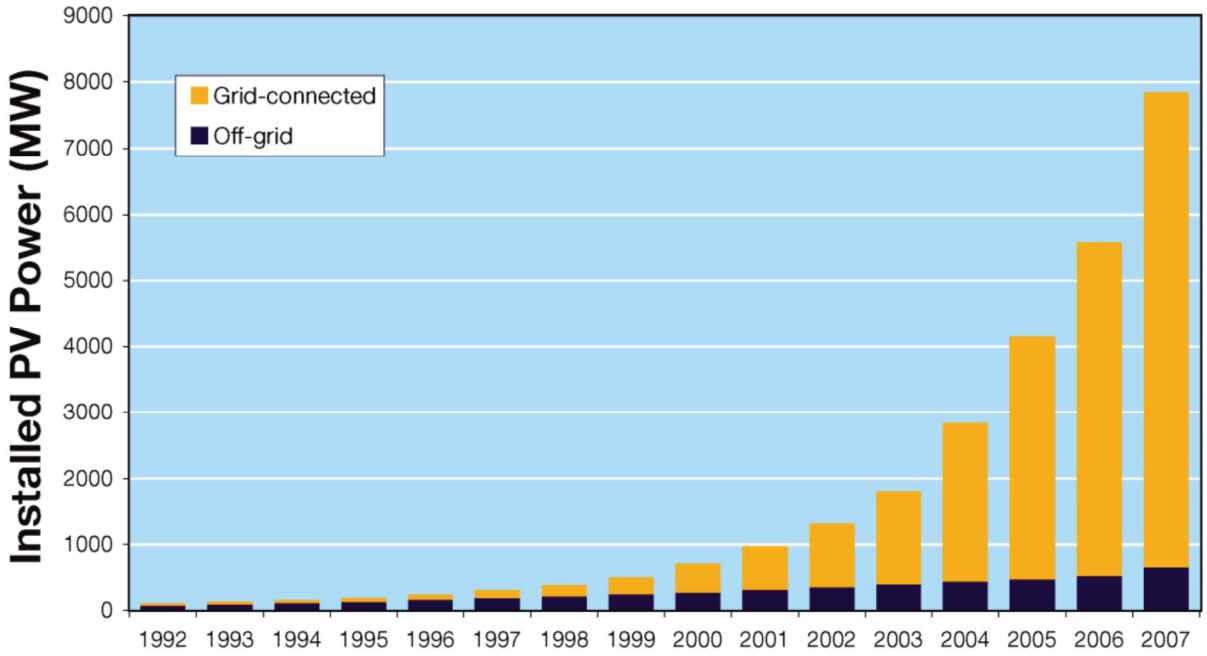

Figure 2-1 Installed PV power

The percentage contribution of PV grid connected penetration from 1990 to 2010 shows that off grid installation is relegated to remote applications where the access to the utility grid is not economically feasible because of the high cost of the electric power system extension as depicted in figure 2-2 (Mints, 2011).

Most renewable energy generators are connected to the grid by means of power electronics interfaces. This gives quite a different behaviour compared with synchronous generators used in traditional large-scale power generation units (Lasseter & Piagi, 2004).

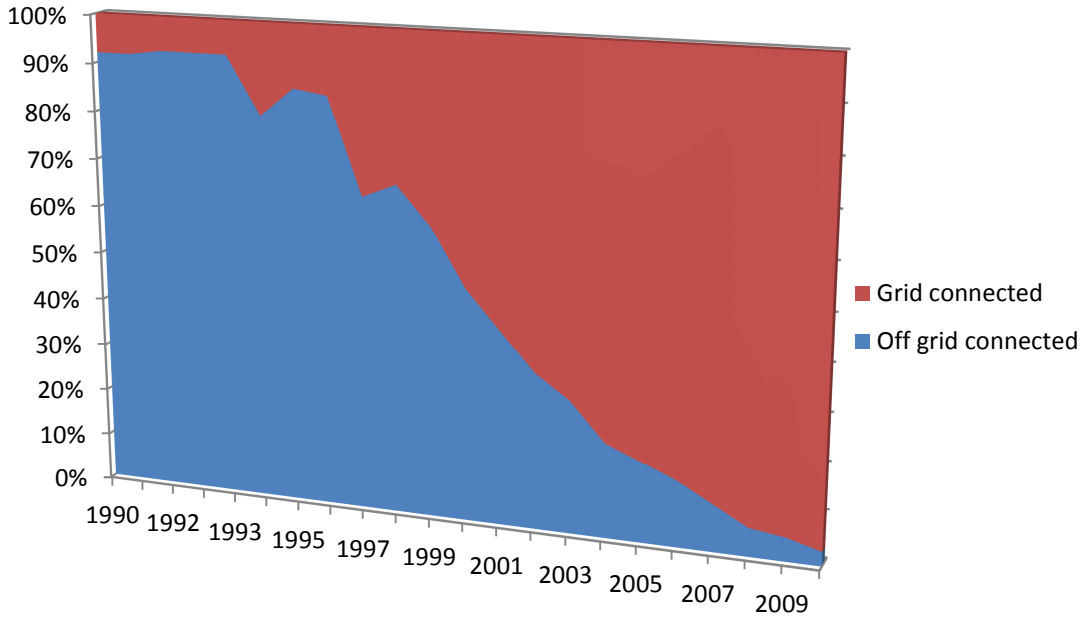

Figure 2-2 Off grid and grid connected growth share

There exist various types of distributed generation (DG) technologies, such as; microturbines, fuel cells, photovoltaic cells, wind turbines, reciprocating engines, and small hydro installations. In addition, there are storage technologies such as; batteries, flywheels, ultracapacitors and super-conducting magnetic energy storage systems. However, recent innovations and developments in power electronics technologies means that the power converter interfaced DG are gaining importance. The ability of power electronic devices to convert electric power from one frequency to another and one voltage level to another has been extensively exploited to convert the electric power from various sources to a common accepted form. For most of the micro sources, such as variable frequency alternating current microturbines, direct current fuel cells, direct current photovoltaic cells and low power variable frequency alternating current wind turbines, electrical power is generated as direct current voltage and converted to alternating current using inverter. In other words, unlike in large-scale power generating plants, a power electronics inverter system isolates the small mechanical, chemical, or solid-state generator from the power grid.

IEEE 1547 standard for interconnecting distributed resources with electric power system focuses on the technical specifications for, and the testing of the interconnection system itself. It provides requirements relevant to the performance, operation, testing, safety and maintenance of the interconnection. It covers general requirements, response to abnormal conditions, power quality, islanding and test specifications and requirements for design, production, installation evaluation, commissioning and periodic tests. These requirements are universally needed for the interconnection of distributed resources – including synchronous generators, induction generators and power inverters/converts - and will be sufficient for most installations. The IEEE 1547 standard specifies the requirements for the DG to disconnect from the grid under deviations in voltage magnitude and frequency or under grid outages (IEEE, 2003; UL 1741, 2005, IEEE 1547.1, 2005). Much work is still needed to realize a universal interconnection technology (UIT) and to understand the effect of large penetration of DG on fault currents, protection and dynamic interactions with the power system (Conti, 2009).

A distributed generation system incorporating only micro-turbines and fuel cell was modeled and simulated in MATLAB$^{(R)}$ software environment for transient analysis study by Jurado & Carpio (2005). The micro-source is capable of providing effective load-following in the distribution system. However, the results also show that the micro-source is not an uninterruptible power supply and does not protect the load from voltage instability while in grid-connect mode.

An overview of multilevel voltage source inverters for single-phase grid connected photovoltaic system is provided by Calais, Agelidis and Meinhardt, 1999. Multilevel inverter topology offers several advantages compared to their conventional counterparts by synthesizing the AC output terminal voltage from several levels of DC voltages, which approach ideal sinusoidal waveform with low harmonic distortion and filter size reduction. The need of several DC sources makes multilevel topologies attractive for photovoltaic applications.

A small-signal dynamic model (Katiraei, Iravani & Lehn, 2007) of a micro-grid including conventional and electronically interfaced distributed resources was developed for the controller design and optimization, evaluation of angle and voltage stability, investigation of torsional dynamics, controller interaction of electronically interfaced distributed generator units and low-frequency power quality issues. The study concluded that the fast control action of the electronically interfaced DG unit can be exploited to meet changes in power demand, maintain angle and voltage stability and enhance voltage quality during grid-connected and autonomous micro-grid modes of operation.

Alfred Engler (2005) implemented the conventional frequency and voltage droops in grid-connected inverter, thus down scaling the conventional grid control concept to the low voltage grid. A voltage source combined with an inductance represents a high voltage line with a stiff grid or a synchronous machine (generator). The only boundary condition is the same sign for the frequency as well as for the voltage droop factors. However, in order to improve the voltage control the partial compensation of lines was implemented.

A control method that uses only low-bandwidth data communication signals between each generating system in addition to locally measurable feedback signals for parallel operation of distributed generation systems in a standalone ac power system is proposed by Marwali el ta 2004. This is achieved by combining two control methods: droop control method and average power control method. In addition, a harmonic droop scheme for sharing harmonic content of the load current is proposed based on the voltages and currents algorithms presented.

To make parallelization possible for UPS inverter, adjustable virtual impedance is proposed by Skjellnes el ta (2002) with a feedback controller for each unit which emulates a voltage source. This impedance is implemented by using feedback from the individual currents delivered to the safe bus, creating apparent ohmic impedance without energy loss. The proposed system provides

load sharing without communication thereby enabling system frequency and voltage control as well. However, this feedback must have a certain bandwidth to be effective.

Kavidha and Rajambal (2006) developed a multilevel inverter for photovoltaic which eliminates the use of transformer. The system performance is investigated by using simulation studies for different solar intensities. The performance of multilevel inverter using fundamental switching scheme eliminate lower order dominant harmonics thereby reducing the total harmonics distortion (THD). It is concluded that the five-level multilevel inverter improved the harmonic spectrum.

A new power electronic interface suitable for transformerless grid interconnection is developed (Rahman & Zhong, 1997) that employs boost converter on the DC side followed by a PWM current-forced single-phase inverter for injecting power into the grid. The circuit has the advantage of requiring fewer switching devices. The controller for the boost rectifier in the DC side includes a discrete maximum power tracker and the current-forced inverter in the AC side autonomously feeds the maximum power available PV energy into the mains.

Gonzalez et al (2004) present a new transformerless single-phase multilevel-based photovoltaic inverter that is capable of eliminating common-mode currents and topologically guarantees that no DC is injected into the grid. Thus it improves the behavior of the inverter in term of electromagnetic interference and exhibits high efficiency. The maximum efficiency is reported to be 98,16%

A mathematical model a d performance evaluation for a single-stage grid-connected photovoltaic system is developed (Dash &Yazdani, 2008) that is useful for the design of the system controller. The proposed controller in the paper adopts an inner current-control loop and an outer DC-link voltage control loop. The current-control mechanism protected the PV system against external faults, enables control of the DC-link voltage and controls and maximizes the PV system output power. The effectiveness of the proposed strategy and the most important transient of the PV systems are evaluated through simulation studies conducted on a detailed model of the PV system.

The ground leakage current in a 1,5 kW PV installation is measured under different conditions and the results used to build a model by Lopez et al (2010). The installation includes a string of 16 PV panel, a full bridge inverter and an LCL filter at the inverter output. The model allows the study of the influence of the harmonics injected by the inverter on the ground current. It is

concluded that modulation strategy has the main influence on the ground current. Bipolar modulation causes much lower ground leakage current unipolar modulation. It is also concluded that neutral point clamper inverter has low current ripple, low filter requirements, low switching losses and low switches stress without ground the ground current problems. Elimination of ground current makes this topology very interesting for single-phase grid-connected applications, where DC sources present high ground capacitance.

Three transformerless converters for three-phase solar applications are compared concerning efficiency, leakage current and mechanical volume by Frank et al (2010). The investigated topologies are voltage source inverter, three-level neutral point clamped and Z-source inverter. The power losses, the resulting leakage current at the PV array and volume of the inverter are investigated mathematically. It is concluded that from the efficiency point of view the neutral point clamped has the best performance followed by the voltage source inverter and the Z-source inverter. The ground leakage current is acceptable for all the investigated topologies.

A thorough assessment of some topologies to minimize ground leakage currents in transformerless PV inverter is examined by Bouzguenda et al (2010). Simulation results show that the HERIC inverter can be an attractive solution for the transformerless systems. However, the major drawbacks of this inverter are that it is only ideal in case the PV system supplies the grid with active power.

A comparison among different modulation techniques to eliminate leakage currents in transformerless three-phase PV systems is studied by Cavalanti et al (2010). Based on the common mode voltage model used in the study, modulation techniques are proposed to eliminate the leakage currents in transformerless PV systems without requiring any modification on the converter and any additional hardware. It is proven that the proposed modulation for two-level and three-level inverters present the best results. Using the proposed modulation for three-level inverters guarantees low leakage currents with a gain of 50% of the maximum amplitude voltages in relation to the two-level inverters. Therefore, the technique is especially suitable if three-level inverters are used.

A modified Z-source inverter (ZSI) with specific modulation techniques is prosed to reduce leakage current in a three-phase transformerless photovoltaic systems by Bradaschia et al (2011).only an additional fast-recovery diode is added when compared with the original structure of ZSI. The PWM technique is entirely modified in order to reduce the leakage currents through

the conduction path. The results of their work confirm the effectiveness of the proposed inverter and the prosed modulation techniques in reducing the leakage currents in three-phase transformerless PV systems.

Many transformerless inverter topologies developed so far only operate with unity power factor. That is, they can only be operated to deliver active power to the grid. Higher penetration of such PV technology will eventually lead to overvoltage problems in the system. Baifeng et al (2012) proposes a high efficiency dual-buck full-bridge PV inverter for a wide range power factor operation. Additionally, a novel hybrid bipolar PWM method is proposed to achieve low ground leakage current and low output current distortion in the PV system. Simulation and experimental work are presented that effectiveness of their proposed topology and modulation scheme.

A novel transformerless grid-connected converter with negative grounding for a photovoltaic generation system is proposed and developed by Shen et al (2012). The negative terminals of the solar cell array can be directly connected to the ground in the proposed grid-connected power converter to avoid the transparent conducting oxide corrosion that occurs in some types of thin-film solar cell array. The salient features of the proposed power converter are that some power electronic switches are simultaneously used in both the DC-DC power converter and the DC-AC inverter and only two power electronics switches operate at high switching frequency at the same time. The leakage current of the PV generation system is reduced.

The design and analysis of the output filter design for a transformerless single-phase inverter presented by Azri & Rahim (2011) minimizes switching frequency current harmonics, improving the output response characteristics.

Variath & Andersen (2010) reviewed and evaluated eight different PV module inverter topologies and provides an overview of the merits and demerits of each on the basis of circuit level Pspice simulation. The complete system is modeled in Pspice and the model is made as realistic as possible by including the parasitic elements.

The problems of DC current injection into the grid that will saturate the distribution transformer along the grid and leakage current ground that increases conducted and radiated electromagnetic interference, total harmonic distortion and losses is modeled, analyzed by Suan et al (2011). Control aspects of transformerless topologies are presented as well.

Alahmad et al (2011) presented an adaptive photovoltaic inverter topology that provides flexible connection between the PV modules and the inverter to meet current condition of the PV array. Efficiency comparison between traditional PV system configurations is discussed.

A design optimization technique that focused on transformerless PV inverters is proposed by Koutroulis & Blaabjerg (2011). The influences of the electric grid regulations and standards and the PV array operational characteristic on the design of grid-connected PV inverters have been considered in their work. The simulation results verify the proposed optimization method enable the maximization of the PV energy injected into the electric grid by the optimized PV installation.

2.2 Interconnection Technologies

Prime mover or engine most often differentiates one alternative energy source form another. It is typically the most expensive subsystem of an alternative energy source technology. Prime movers may be powered by traditional fuel or renewable energy and they change energy from one form to another. For example, prime movers may use direct physical energy to rotate a shaft (e.g. in a hydro-turbine or wind energy device), or they may use chemical energy conversion to change thermodynamic energy to physical energy (e.g. by burning diesel fuel, natural gas, or propane to a piston or turbine to rotate a shaft).

The electric generator converts prime mover energy into electrical energy. Historically, most electrical generation has been accomplished via rotating machines. The prime mover drives an electric generator that is synchronous or induction (asynchronous). The generator has a stator that consists of a set of AC windings and a rotor with windings that are either AC or DC. The stator is stationary and the rotor is rotated by the prime mover. The means of power conversion is through interaction of the magnetic fields of the stator and rotor circuits.

Synchronous generators are used when power production from the prime mover is relatively constant (e.g. for internal combustion engine). Most large utility generator are synchronous. Induction generators, on the other hand, are well suited for rotating systems in which the prime mover is not constant (e.g. for wind turbines and small hydro-turbines). However, they can also be used with engines and combustion engines. Synchronous and induction generator electrical output then undergoes another power conversion to achieve the sinusoidal power quality level compatible with utility grid interconnection.

Inverters are electronic systems that convert power statically. Inverters are based on power semiconductor devices, microprocessor or digital processor technologies, and control and communications algorithms. Generally, inverters are used with prime movers that provide Dc electricity (such as fuel cells or PV) or microturbines, which are small, high speed, rotating combustion turbines coupled directly to a synchronous–type electric generator. In the case of the microturbine, the generator output voltage waveform is very high frequency, well beyond the utility grid's 50 or 60 Hz. The high-frequency waveform is rectified to DC electricity, and the DC electricity is then synthesized to a sinusoidal waveform suitable for connection with the grid.

2.2.1 Synchronous interconnection

Most generators in service today are synchronous. A synchronous generator is an AC machine in which the rotational speed of normal operation is constant and in synchronism with the frequency of the area electric power system with which it is connected. In synchronous generators, field excitation is supplied by a separate motor-generator set, a directly coupled self-excited DC generator, or a brushless exciter that does not require an outside electrical source. Therefore, this type of generator can run in stand-alone mode or interconnected with the area electric power system. When interconnected, the generator output is exactly in step with area electric power system voltage and frequency. Separately excited synchronous generators can supply sustained fault current nearly all operating conditions.

Synchronous generators require core complex control than grid-connected induction generators to synchronize with the area electric power system and control field excitation. They also require special protective equipment to isolate them from the area electric power system under fault conditions. An advantage is that this type of machine can provide during area electric power system outages. In addition, it permits area electric power system to control the power factor at their facilities by adjusting the DC field current.

2.2.2 Induction interconnection

Induction generators are asynchronous machines that require an external source to provide the magnetizing (reactive) current necessary to establish the magnetic field across the airgap between the generator stator and rotor. Without such a source, induction generators cannot supply electric power and must always operate in parallel with the utility system, a synchronous machine, or a capacitor that can supply the reactive requirements.

In certain instances, an induction generator may continue to generate electric power after the utility system source is removed. This phenomenon, known as self-excitation, can occur when there is sufficient capacitance in parallel with the induction generator to provide excitation and the load connected has certain resistive characteristics. This external capacitance may be part of the alternative energy source or may consist of power factor correction capacitors located on the utility system with which the alternative energy source is connected.

Induction generators operate at a rotational speed determine by the prime mover and slightly higher than required for exact synchronism. Below synchronous speed, these machines operate as induction motor and thus become a load on the utility system. Some advantages of induction generators are:

- Grid-connected induction generators need only basic control systems because their operation is relatively simple compared to synchronous generators.
- They do not require special procedure to synchronize with the utility system because this occurs essentially automatically.
- They will normally cease to operate when a utility system outage occurs if self-excitation system option is not implemented.

A disadvantage of induction generators is their response when connected with the utility at speeds significantly below synchronous speed. Depending on the machine class, potentially damaging inrush currents and associated torques can result. Regardless of load, induction generators draw reactive power form the utility system and adversely affect the voltage regulation on the circuit with which it is connected. Induction generators then consume Vars from the utility system. It is important to consider the addition of capacitors to improve the power factor and reduce the reactive power demand.

2.2.2.1 Variable-speed wind turbines

Variable-speed operation of wind turbines is often desirable for two reasons:

- Below rated wind-speed, the wind turbine rotor can extract the most energy if the tip speed ratio can be kept constant, requiring that the rotor speed vary with the wind speed
- Variable-speed operation of the turbine's rotor can result in reduced fluctuating stresses, and hence reduced fatigue, of the components of the drive train.

While variable-speed operation of the turbine rotor may be desirable, however, such operation complicates the generation of AC electricity at a constant frequency.
There are at least in principle, a variety of ways to allow variable-speed operation of the turbine rotor, while keeping the generating frequency constant. Nearly all the approaches to variable-speed operation of wind turbines in use today, however, are electrical. Variable-speed operation is possible with the following types of generators:

- Synchronous generators
- Squirrel cage type induction generators
- Wound rotor type induction generators
- Switched reluctance generators

Switched reluctance generators are not yet common in wind energy conversion system. The first three generators types listed above will be discussed in the following sub sections.

2.2.2.2 Variable-speed operation of synchronous generators

There are basically two types of synchronous generator:

- Those whose field windings are separately excited
- Those whose fields windings are provided by permanent magnets

In either case the output frequency is a direct function of the speed of the generator and the number of magnetic poles. For a synchronous generator to be used in variable-speed wind turbine, the output of the generator must first be rectified to DC voltage and then converted back

to AC voltage using power electronic technology. An arrangement that would allow this to take place is shown in figure2-1.

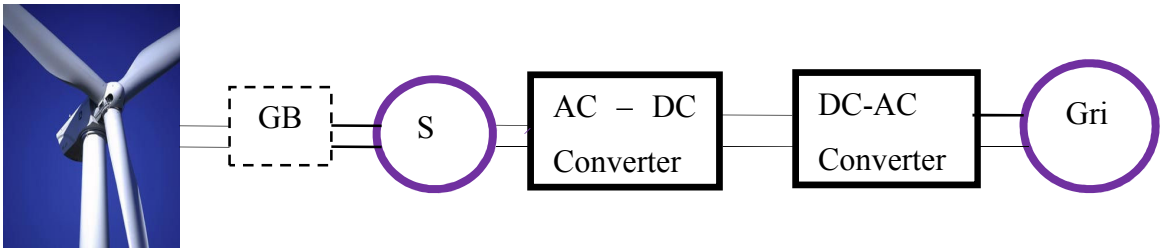

Figure 2-3 Variable-speed wind turbine with synchronous generator

In this figure the wind turbine's rotor is shown on the left-hand side. Moving progressively towards the right are the main shaft, gearbox (GB), generator (SG), rectifier (AC/DC), Dc link, inverter (DC/AC) and the electric power utility grid. The rectifier may either be a diode or a controlled type AC to DC power rectifier. The inverter may either be an SCR or a PWM inverter. In case of a separately excited synchronous generator, there may be voltage control on the generator itself. If a permanent magnet synchronous generator is used, voltage control must take place somewhere in the converter circuit. Some wind turbines use a multiple pole synchronous generator with sufficient number of poles that the generator is directly connected to the main shaft with no need for a gearbox. Accordingly the gearbox shown in figure 2-1 will not be used. It should be noted that direct drive, multipole generators are physically much larger than generators with gearboxes.

2.3.1 Variable–speed Operation of Squirrel Cage Induction Generators

Squirrel cage induction generator (SQIG) may be used in variable-speed wind turbines, although the method of doing so is not as conceptually straightforward as synchronous generators. In particular, induction generator requires source of reactive power which must be supplied by a capacitor or a power electronic reactive power generators. These power electronic power converters are expensive and introduce additional losses into the system. These losses are often of the same order of magnitude as the gains in aerodynamic efficiency, so net gain in energy production may be relatively small (Manwell el ta, 2009). In this case, the main benefit of variable-speed operation could be in the reduction of fatigue damage to the rest of the turbine.

A typical variable-speed squirrel cage induction generator configuration is illustrated in figure 2-2.

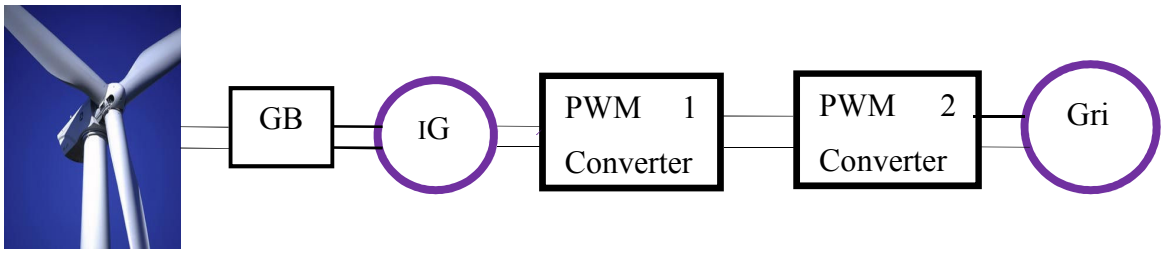

Figure 2-4 Variable-speed wind turbine with squirrel cage induction generator

This figure shows the wind turbine rotor, gearbox, induction generator, two PWM power converters, a Dc link between them and the electric power grid. In this configuration the generator side converter (PWM1) provides reactive power to the generator rotor as well as accepting real power from it. It controls the frequency to the generator rotor and hence, its speed. PWM 1 also converters the rotor power to DC. The grid side power converter (PWM 2) converters the Dc power to AC power at appropriate frequency and voltage magnitude.

2.2.3 Variable-speed Operation with wound Rotor Induction Generator

Another approach to variable-speed turbine operation is through the use of a wound rotor induction generator (WRIG). Wound rotor induction generators are similar in many ways to squirrel cage induction generators except in the design of their rotors. The rotor in WRIG has windings of copper wire rather than shorted metal bars. The stator has winding just as in the SQIG. The ends of the rotor windings are accessible and normally via brushes and slip rings. Power can either be extracted or injected into the rotor. WRIGs have many features of SQIG in that they are compact and fairly rugged (except for the brushes and slip rings). Figure 2-3 shows WRIG with an external resistor.

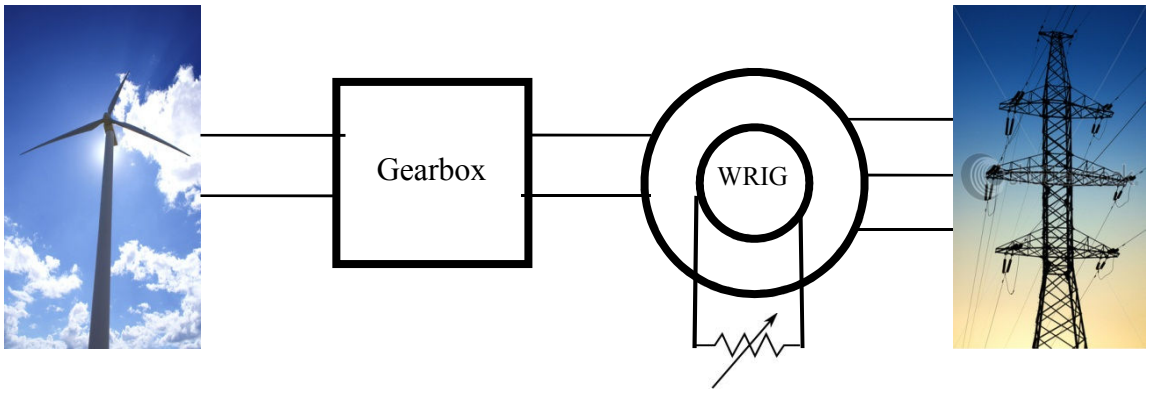

Figure 2-5 Wind turbine with WRIG and external rotor resistance

They are also less expensive than synchronous generators, although they are more expensive than SQIGs. The main advantage of the WRIG is that it is possible to have variable-speed operation of the wind turbine while using power converters of approximately one third of the capacity that would be required if all the power were to go through the converters. The converters will not only be smaller but they will be less expensive than those that would be used in either SGs or SQIGs of the same rating.

Wound rotor induction generators can be used in a variety of ways to facilitate variable-speed operation. These include:

- High slip operation
- Slip power recovery
- True variable-speed operation

Table 2-1 summarizes the key features of these topologies.

Table 2-1 Topology options for variable-speed wind turbine using wound rotor induction generators

Topology	Rotor side converter	Line side converter	Speed range
High slip	Adjustable resistor	N/A	Limited super-synchronous
Slip power recovery	Rectifier	Inverter	Super-synchronous only
	Phase controlled rectifier		Super-synchronous; limited sub-synchronous
True variable speed	PWM converter	PWM converter	Super or sub-synchronous

The slip for a given power output of a convectional generator can be increased by increasing the resistance of the rotor. This will increase the range of possible operating speeds. Accordingly, one could in principle create a variable-speed induction generator by simply increasing the rotor resistance. On the other hand, the losses in the rotor also increase with the resistance and so does the decrease of the overall system efficiency.

2.2.3 Inverter interconnection

Some alternative energy sources produce electric power with voltages not in synchronism with those of the utility system with which they are to be connected. An electric power converter provides an interface between a nonsynchronous alternative energy source and a utility system so that the two may be properly interconnected.

The two categories of nonsynchronous alternative energy source output voltage are:

- Direct-current (DC) voltages generated by DC generators, such as fuel cells, PV systems, DC energy storage system (e.g. electrochemical batteries), or AC generators through rectifiers.
- Alternating-current (AC) voltages generated by synchronous generators running at nonsynchronous speed or by asynchronous generators.

The two categories of electric power converter that can connect alternative energy sources with utility system are:

1. DC-to-AC power converters (inverters). In this case, the input voltage to the device is generally a non-regulated DC voltage. The output of the device is at the frequency and voltage magnitude specified by the local utility or grid operator. This is the dominant means of small and renewable energy interconnection.
2. AC-to-DC electric power converters. In this case, the input frequency, voltage magnitude to the device, or both does not meet the utility requirements. The output of the converter device is at the appropriate frequency and voltage magnitude as specified by the grid operator in cases in which DC power can be used. This approach is not widely used.

The profusion of data centers and other customers using DC power supplies (such as the power supplied by electronic ballast) has opened the door to either a direct DC or DC-to-AC converter designed to deliver the DC output of small alternative energy source units directly to the application.

Static power conversions are built with diodes, transistors, or thyristors and have ratings compatible with alternative energy source applications. These solid-state devices are configured into rectifiers (to convert AC power into DC power), inverters (to convert AC power into DC power) and cycloconverter (to convert AC power at one frequency into AC power at another frequency). Some types require the utility system to operate; others may continue to function normally after utility system failure. The major advantages of solid-state converters are their higher efficiency and potentially higher reliability than rotating machine power converters. In addition, this technology offers increased flexibility with the incorporation of protective relaying, coordination and communications options.

2.3 Grid requirements and standards for grid connected technology

Grid connected PV systems are being developed very fast and systems from kW to tenths of MW are now in operation. As an important source of distributed generation the PV systems need to comply to series of standard requirement in order to ensure the safety and the seamless transfer of the electrical energy to the grid.

Typically, local regulation imposed by the grid operator apply in most countries but large efforts are being made to imposed some standard grid requirements that can be adopted by many countries.

The most relevant international bodies that are developing worldwide standards are: IEEE in US, IEC in Switzerland and DKE (German commission for Electrical, Electronics and Information Technology of DIN and VDE) in Germany, the dominant PV market.

The grid requirement is a very important specification that is having a big impact on the design and performance of distributed power generation (especially PV and Wind energy system). For example in the USA market the transformerless PV inverters were only allowed in 2005. Another example is the recent three-phase mini-central PV inverter in the range 8-15 kW tailored to the new grid requirement in some European countries, which are limiting the feed-in tariff to about this level. Like any other distributed power generation system the PV industry is very sensitive to the grid regulation and is tailoring the product in accordance.

Because of many similarities between the South Africa electricity system and European countries in terms of system voltage and system frequency, we discussed at length most of the European standards and grid codes in this dissertation.

The most relevant standard requirements and the technical challenges that should be addressed by the PV inverter technology are provided in the following sub sections.

2.3.1 IEEE 1547 Interconnection Standard for distributed Resources

IEEE develops voluntary standards for electrical and electronic equipment. These standards are developed with the involvement of equipment manufacturers, users, utilities and general interest groups. Most US states public utility commission guidelines and utility interconnection requirements reference IEEE standards. In addition, most UL (underwriter laboratories) that relates to interconnection ensure that the equipment is manufactured to comply with IEEE standards.

IEEE 1547-2003, Standard for interconnecting for Distributed Resources with Electric Power Systems is the result of a recent effort by SCC21 (IEEE Standards Coordinating Committee 21)

to develop a single interconnection standard that applies to all distributed power generation technologies.

The IEEE 1547 standard focuses on the technical specifications for, and the testing of, the interconnection itself. It includes general requirements, response to abnormal conditions, power quality, islanding and test specifications as well as requirement for design, production, installation evaluation, commissioning and periodic tests. The requirements are applicable for interconnection with EPS at typical distribution levels (medium) and also low-voltage distribution network are considered.

It has evolved greatly since 2003 resulting in a number of series addressing in detail important aspects of the standard such as conformance test procedures (IEEE 1547.2), application guide (IEEE 1547.1), anti-islanding (IEEE 1547.). The standard has benefited greatly from earlier utility industry work documented in IEEE and IEC standard (e.g IEEE 929, 519, 1453; IEC EMC series 61000 etc) and ANSI C37 series of protective relaying standards. IEEE addresses all types of interconnected generation up to 10 MW and *establishes mandatory requirements*. This set it apart from several previous IEEE guides or recommended practices on DG, which convey only suggestion and recommendations.

2.3.2 IEC 61727 Characteristics of utility interface

A huge effort in harmonizing the grid requirement has been done by IEC (International Electrotechnical Commission) that promotes international corporation within standardization for electrical and electronics issues. The TC-82 Committee on Solar Photovoltaic Energy System is developing a large range of standards for the PV industry. In the grid interconnection requirement, the TC-82 has developed the standard IEC 61727 published in December 2007. The standard applies to utility-interconnected PV power system operating in parallel with the utility and utilizing static non-islanding inverters for the conversion of DC power to AC power and lays down requirement for interconnection of PV system to the utility distribution system.

Another related standard of 2005, IEC 62116, Testing Procedures of Islanding Prevention Measures for Utility Interactive Photovoltaic Inverters, describing the testing procedure for the requirement stated in IEC 61727. Although there are slight differences, the requirements from IEC 61727 are harmonising very well with the ones from IEEE 1547.

2.3.3 VDE 0126-1-1 safety

Germany is the dominant PV market and therefore the Germany regulations issued by the VDE Testing and Certification Institute is very important. ENS safety device, Automatic Disconnection Device between a Generator and the Public Low-Voltage Grid, was introduced first as an external hardware device, but later in software. According to the former VDE 0126-1999, the ENS device should be detect a jump of 0,5 Ω in the grid impedance in a power-balanced situation. This was only possible by using active methods based on distorting the grid and measuring the response. After some years of experience in the field it was agreed that the requirements are too tight and frequently led to nuisance trips affecting the yield and also power quality degradation.

Eventually, the newly revised standard VDE 0126- 2006 has relaxed the tight thresholds for disconnection in the case of abrupt grid impedance changes (from 0,5 Ω to 1,0 Ω) and even allow as an alternative method an anti-islanding requirement very similar to IEEE 1754.1 based on a resonant RLC load. These changes are expected to contribute to increased grid stability, without compromising the electrical safety.

Apart from ENS, the VDE 0126-1-1 also includes over/under voltage and frequency detection and describes the test procedures for a fail-safe protective interface that has to disconnect automatically the PV inverter from the grid in case of DC injection, fault current and low isolation to earth. In order to accommodate transformerless PV inverters, a leakage current limit (300 mA) is imposed and active monitoring of the fault current with sensitivity down to 30 mA and active monitoring of isolation (> 1 kΩ) is required. Also, for the fail-safe disconnection circuit, a redundant circuit is required. This means that additional hardware is needed in order to achieve these safety functions, thus increasing the complexity and cost.

2.2.4 IEC 61000 Electromagnetic Compatibility (EMC – low frequency)

IEC 61000-3-2 deals with the limitation of harmonic currents injected into the public supply system. It specifies limits of harmonic components of the input current, which may be produced by equipment tested under specified conditions. This part of IEC 61000 is applicable to electrical and electronic equipment having an input current up to and including 16 A per phase, and is intended to be connected to public low voltage. For equipment with current higher than 16 A but lower than 75 A the corresponding standard IEC 61000-3-12 applies.

IEC 61000-3-3 is concerned with the limitation of voltage fluctuations and flicker impressed on the public low-voltage system. It specifies with the limitation of voltage changes that may be produced by equipment tested under specified conditions and gives guidance on methods of

assessment. This part of IEC 61000 is applicable to electrical and electronic equipment having an input current equal to or less than 16 A per phase, intended to be connected to public low-voltage distribution systems of between 220 V and 250 V line to neutral at 50 H, and not subject to conditional condition. For equipment with current higher than 16 A but lower than 75 A the corresponding standard IEC 61000-3-11 applies.

2.3.4 EN 50160 public distribution voltage quality

The voltage quality in the public distribution system is regulated in Europe by EN 50160, which gives the main voltage parameters and their permissible deviation ranges at the customer's point of common coupling in public low-voltage (LV) and medium voltage (MV) electricity distribution system, under normal operating conditions. The parameters of the supply voltage shall be within the specified range during 95% of the test period, while the permitted deviations in the remaining 5% of the period are much greater. EN 50160 is principally informative and accepts no responsibility when the limits are exceeded.

The following parameters are of interest for designing the control of PV inverters.

- Voltage harmonic levels as shown in table 4.1. Maximum voltage THD is 8%
- Voltage unbalance for three-phase inverters. Maximum unbalance is 3%
- Voltage amplitude variations: maximum ±10%
- Frequency variations: maximum ±1%
- Voltage dips: duration < 1 s deep < ±60%

Table 2-2 Public distribution grid voltage harmonics EN 50160

Odd harmonics				Even harmonics	
Not multiple of 3		Multiple of 3			
Order *h*	Relative voltage (%)	**Order *h***	Relative voltage (%)	**Order *h***	Relative voltage (%)
5	6	**3**	5	**2**	2
7	5	**9**	1,5	**4**	1
11	3,5	**15**	0,5	**6 to 24**	0,5
13	3	**21**	0,5		
17	2				
19	1,5				
23	1,5				
25	1,5				

For the PV inverter, point-of-view compatibility with this voltage power quality standard is important as it can demonstrate that the inverter is able to operate with the whole range of disturbances. The voltage and frequency variations are surpassed by other PV specific standards as shown in the nest section. For the permitted disturbance in term of dips, there is not yet any ride through capability requirement for grid connected PV systems, but in the future as grid connected PV systems penetration increase such a requirement (similar to wind power grid codes) is expected.

2.3.5 SA interconnection standard for the interconnection of embedded generation

This standard sets out the minimum technical and statutory requirements for the connection of embedded generators (EG) to the Eskom distribution medium and high voltage electrical networks. Embedded generator is defined as a legal entity that operates or desire to operate a generating plant that is connected to the distribution network. This definition includes all types of connected generation, including co-generators and renewables. Alternatively, the item of generating plant that is or will be connected to the distribution network. A co-generator is defined as a source of electrical power that complies with types I, II or III below:

- Type I: projects utilizing process energy which would otherwise be underutilized or wasted (e.g. waste heat recovery)
- Type II: Primary fuel based generation projects which produces, as part of their core design, other usable energy in addition to electricity (e.g. combined heat and power or CHP projects)
- Type III: Renewable fuel based projects where the renewable fuel source is both the primary source of energy and is a co-product of an industrial process (e.g. use of bagasse and/or forestry waste from the sugar and paper industries).

The intention is that this interconnection standard, or one of broadly similar requirements, shall also apply to EGs connecting to municipal electricity networks which, in turn, are supplied by ESKOM. This way, technical requirements at the point of connection between the supply authority and the EG need not to be replicated between ESKOM and the supply authority.
The standard provides for generic interconnection requirement and shall be applicable to all different types of generators, prime movers etc. in certain cases (e.g. wind generation technology) it may be necessary to supplement the requirements of this standard with additional technology-specific requirements.
The standard encompasses issues the general requirements, legal requirements, operational safety, generator capabilities and operation, requirements for the utility network interface etc.
A closer look into the generator capabilities and operation is highlighted in this work as these functionalities plus power quality issues can be handled by power electronics grid connected system. Excitation control and governor requirements, synchronization, islanded operation (loss-of-mains protection), fault ride through capabilities, under and over voltage protection, under and over frequency protection and DC failure monitoring requirements are briefly discussed in the following sub sections.

2.3.5.1 Excitation control and governor requirements

The Distribution Code: Network code requires all embedded generators of nominal capacity greater than 10MVA to comply with section 3.1 of the South African Grid Code: Network Code. The requirements of the Grid Code apply specifically to synchronous generators and not asynchronous generators.
Synchronous generators shall be equipped with excitation controllers capable of connecting and operating on a network that may be subjected to voltage in a range between 0,95 per unit and 1,05 per unit.

Induction generators are not capable of voltage or reactive power control because they are consumer of reactive power. The EG must thus supply reactive power compensation to connect the power factor to within ±0,90, unless otherwise negotiated with ESKOM.

All EG units of nominal capacity larger than 50 MVA shall conform to the continuous and short-duration frequency operating limits in the South African Grid Code: Network Code. The code states that the continues operational range for the generation unit is between 48,5 Hz – 51,5 Hz. The same section of the code also stipulates the frequency versus guaranteed operating time capability as well as the requirement for governor control using a 4% droop characteristic required by turbo-generators.

Presently, EG units of nominal capacity less than 10 MVA are not required to comply with the governing and continuous frequency operational requirements as stated above.

2.3.5.2 Synchronization

All embedded generating plants other than mains excited asynchronous machines must be synchronized with the ESKOM supply prior to making the parallel connection.

The voltage between the unit and the system prior to synchronizing shall not differ by more than the value specified in table 2-3. Where the mode of operation of generating equipment is such that synchronizing of a machine or machines will occur at intervals of less than two hours, the voltage fluctuation at the point of generator connection resulting from the generation capacity being connected shall not be exceed 1%.

Table 2-3 Typical synchronizing parameter limits (IEEE 1547 p12)

Aggregate rating of EG (kVA)	Maximum frequency difference Δf (Hz)	Maximum voltage difference ΔV (%)	Maximum phase angle difference $\Delta\Phi$ (degrees)
S < 500	0,3	10	20
500 ≤ *S* < 1500	0,2	5	15
S ≥ 1500	0,1	3	10

2.3.5.3 Islanded operation

Intentional islanding of a generator with part of the ESKOM network is not permitted in the current standard unless specifically agreed with ESKOM. This will change as the penetration depth of embedded generating systems increases.

For unintentional islanding, where a generator is synchronized with the ESKOM network at the time that an upstream ESKOM circuit breaker opens, severing the connection between the generation supply and the grid supply, the generator shall cease to energize the local ESKOM network within 2 seconds.

A related requirement in the standard is the loss-of-mains protection. Loss-of-grid protection may take the form of rate-of-change of frequency (ROCOF) or voltage vector shift protection. Typical settings for loss-of-grid protection are depicted in table.

Table 2-4 Typical settings for loss-of-grid

ROCOF	Δf	0,2 – 1,0 Hz/s (0,4 Hz/s typical)
	Δt	40ms – 2s
	Time delay	200ms – 500ms
Voltage vector shift	ΔV	6° – 12° (6° typical, 12° on weak grid)

Where ROCOF or voltage vector shift protection is not deemed suitable, a communication-base direct transfer trip scheme may be applied such as to disconnect the embedded generator in the event of an island developing. The trend in USA and Europe now is to allow distributed energy resources to ride through faults in order to maintain the electric power system stability.

2.3.5.4 Fault ride through capabilities

This section is under consideration for future revision of the standard.

2.3.5.5 Under and over voltage protection

Under- and over-voltage protection shall be provided. The voltage protections shall detect the effective (i.e. root mean square) or the fundamental component of each phase to phase voltage. Maximum operating times for the voltage protection are indicated in table 2-4 which is adopted from IEEE 1547 standard for interconnecting distributed resources with the electric power system.

Table 2-5 Maximum operating times for voltage protection

Voltage range (% of nominal)	Maximum operation time (seconds)
V<50%	0,2
$50\% \leq V < 90\%$	2
$110\% < V < 120\%$	1
$V \geq 120\%$	0,2

In cases where the embedded generation facility may import or export power from the ESKOM network, the voltage protection may be supervised so as only to operate in the event of real and/or reactive power export by the facility to the network.

2.3.5.6 Under and over frequency protection

Under- and over frequency protection shall be provided. The under- and over-frequency protection relay shall be accurate to within 10 millihertz of setting. Where an averaging window is used for the frequency measurement, this shall be limited to a maximum length of six cycles.
The frequency protection shall be set to allow generator operation within the frequency ranges stipulate in sub-section 2.3.5.1. Operation outside this range shall cause the EG to sever the connection with the ESKOM network within 300ms.
In cases where the EG facility may import or export power from the ESKOM network, the frequency protection may be supervised so as only to operate in the event of real power export by the facility to the grid.

2.4 PV grid requirements

This section deal with specific interconnection requirements for photovoltaic grid connected systems. Issues such as response to abnormal grid condition, voltage deviations, frequency and reconnection after trip stipulated in some international interconnection standards are compared and differentiated.

2.4.1 Response to abnormal grid conditions

The PV inverters need to disconnect from the grid in case of abnormal grid conditions in terms of voltage and frequency variations outside the permitted range. This response is to ensure that the safety of utility maintenance personnel and the general public as well as avoid damage to connected system equipment including the PV system.

2.4.2 Voltage deviations

The nominal voltage refers to the system voltage at the point of common coupling point of the interconnection system. The disconnection time refers to the time between the abnormal condition occurring and the inverter ceasing to energize the utility line. Table 2-6 compares the specifications for IEEE 1547, IEC 61727 and VDE 0126-1-1.

Table 2-6 Disconnection time for voltage variations

IEEE 1547		IEC 61727		VDE 0126-1-1	
Voltage rating (%)	**Disconnection time (sec.)**	**Voltage rating (%)**	**Disconnection time (sec.)**	**Voltage rating (%)**	**Disconnection time (sec.)**
V< 50	0,16	V< 50	0,10	110≤V<85	0,20
50≤V<88	2,00	50≤V<85	2,00		
110<V<120	1,00	110<V<135	2,00		
V≥120	0,16	V≥135	0,05		

The inverter control system shall actually remain connected to the utility to allow sensing of the utility electrical conditions for use by the resynchronization system of the grid connected inverter. The purpose of the allowed time delay is to ride through short-term disturbances to avoid excessive nuisance tripping.

It is observed that required disconnection time for VDE 0126-1-1 is much shorter and thus fast voltage monitoring is required compared to IEEE 1574 and IEC 61727 standards.

2.4.3 Frequency deviations

The purpose of the allowed range and time delay is to ride through short-term disturbances to avoid excessive nuisance tripping in a weak grid system especially rural or far from the grid distribution systems. Table 2.3 shows the disconnection time for frequency variations allowed by IEEE 1547, IEC 61727 and VDE 0126-1-1 standards.

Table 2-7 Disconnection time for frequency variations

IEEE 1547		IEC 61727		VDE 0126-1-1	
Frequency range (Hz)	**Disconnection time (sec.)**	**Frequency range (Hz)**	**Disconnection time (sec.)**	**Frequency range (Hz)**	**Disconnection time (sec.)**
$59,3<f<60,5$[a]	0,16	f_n-1<f< f_n+1	0,2	$47,5<f<50,2$	0,2

[a]For systems with power > 30 kW the lower limit can be adjusted in order to allow participation in the frequency control.

It can be observed that the VDE 0126-1-1 allows a much lower frequency limit and thus frequency adaptive synchronisation is required.

2.4.4 Reconnection after trip

After disconnection caused by abnormal voltage or frequency conditions the inverter can be reconnected only in the conditions stipulated in table 2-4.

Table 2-8 Conditions for reconnection after trip

IEEE 1547	IEC 61727	VDE 0126-1-1
$88 < V < 110$ (%)	$85 <V<110$ (%)	N/A
AND	AND	
$59,3 < f < 60,5$ (Hz)	f_n-1<f< f_n+1	
	AND	
	Minimum delay of 3 minutes	

It can be observed that the time delay in IEC 61727 is an extra caution to ensure that resynchronization before reconnection in order to avoid possible damage to the interconnection system.

2.5 Power quality

The quality of the power delivered by the grid connected distributed power generation system for the utility as well as for the local load in a configuration called microgrid system is governed by practices and standards on voltage deviations, flicker, frequency fluctuations, harmonics content and power factor value. The power factor value is an indication of the amount of active power and reactive power delivered to the grid. Deviations from these standards represent out-of-bounds conditions and may require disconnection of the grid connected distributed power generation system. We discuss the DC current injection limits, current harmonics limits and power factor requirements in IEEE 1547, IEC 61727 and VDE 0126-1-1 in the following subsections.

2.5.1 DC current injection

DC current injection in the utility can saturate the distribution transformers, leading to overheating and transformer trips. For the convectional PV system with galvanic isolation, this problem is minimized, but with the new generation of transformerless PV inverters increased is required in this matter. Table 2-5 tabulates the limits of injected DC current has acceptable limits.

Table 2-9 DC current injection limitations

IEEE 1547	IEC 61727	VDE 0126-1-1
$I_{DC} < 0,5$ (%)	$I_{DC} < 1,0$ (%)	$I_{DC} < 1$ A
Of the rated RMS current	of the rated RMS current	Maximum trip time 0,2 sec.

For IEEE and IEC 61727 the DC component of the current should be measured by using harmonic analysis (fast Fourier transform or FFT) and there is no maximum trip time condition. During the test the measures DC component should be below the limits for different loading conditions (1/3, 2/3 and 3/3 of the nominal load). For VDE 0126-1-1 this condition requires a

special designed current sensor that can detect this threshold and disconnect within the required trip time

.

2.5.2 Current harmonics

The distributed power generation system should produce low current distortion levels to ensure that no adverse effects are caused to other equipment to the utility system. Table 2-6 lists the acceptable levels for IEEE 1547 and IEC 61727standards.

Table 2-10 Maximum current harmonics

IEEE 1547 and IEC 61727						
Individual harmonic order (odd)[a]	$h < 11$	$11 \leq h < 17$	$17 \leq h < 23$	$23 \leq h < 35$	$35 \geq 17$	Total harmonic distortion THD (%)
(%)	**4,0**	**2,0**	**1,5**	**0,6**	**0,3**	**5,0**

[a]Even harmonics are limited to 25% of the odd harmonics limits stated above

The test voltage for IEEE 1547 and IEC 61727 should be produced by an electronics power source with a voltage THD (thermohydrodynamic) less than 2,5% and individual voltage harmonics lower than 50% of the current harmonic limits. The practice is to use an ideal sinusoidal power source so as not to influence the results by the background distortion.

2.5.3 Average power factor

Only in IEC 61727 is stated that the grid connected distributed generators shall have an average lagging power factor greater than 0,9 when the power output is greater than 50%. Most PV inverters designed for grid connected service operate close to the unity power factor.
In IEEE 1547 there is no requirement for power factor as this is a general standard that should also allow distributed generation system to supply reactive power for voltage regulation functionality.
Usually the power factor requirement for PV inverters should now be interpreted as a requirement to operate at a quasi-unity power factor without the possibility of regulating the voltage by exchange reactive power with the utility grid. For high-power PV installations connected directly to the distribution level local grid requirement apply as they may participate in the grid control. For low-power installations it is also envisaged that in the near future the utilities will allow them to exchange reactive power when the penetration level is high (approximately greater than 30%). New regulation will be needed before this can be implemented,

2.6 Anti-islanding requirements

The most technical challenging requirement is the so called anti-islanding. Islanding for grid-connected distributed systems takes place when the distributed resource power conversion system does not disconnect for a very short time after the grid is de-energized, that is, it is continuing to operate with local load. In the typical case of a residential electrical system co-supplied by a roof-top PV system, grid disconnection can occur as a result of a local failure detected by ground fault protection or of an intentional disconnection of the line for servicing. In both situations, if the PV inverter does not disconnect the following consequence can occur:

- Retripping the line or connected equipment can cause damage due to out-of-phase closure
- Safety hazard for utility line workers who assumes de-energized lines during islanding.

In order to avoid these serious consequences safety measures are in place called anti-islanding requirements and are embodied in all grid codes for grid connected distributed generation systems.

2.6.1 IEEE 1547/UL1741 anti-islanding requirements

In IEEE 1547 the requirement is that after an unintentional islanding where the distributed resources continue to energize a portion of the electric power system through the point of common coupling (PCC), the distributed resources (DR) shall detect the islanding and cease to energize the area electric power system within 2 seconds. In IEEE 1547.1 the test setup is described as shown in figure, where the equipment under test (EUT) represents the DR under test.

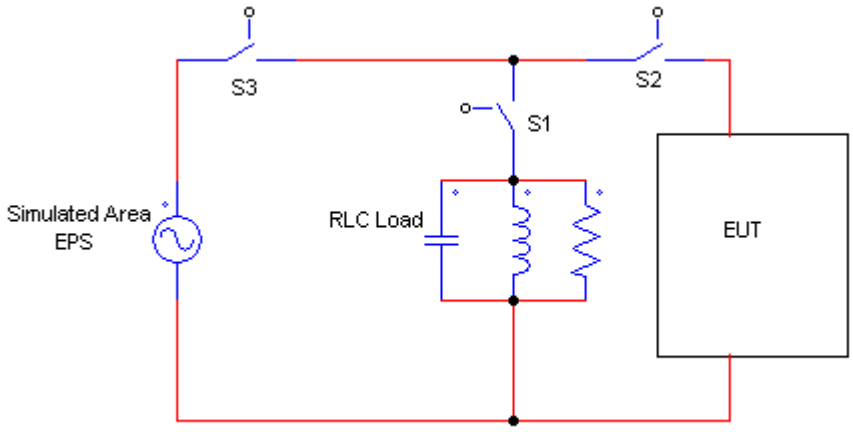

Figure 2-6 Test setup for the anti-islanding requirement in IEEE 1547.1

Notes

1- Switch S1 may be replaced with individual switches on each of the RLC load components
2- Unless the EUT has a unity output power factor, the receiver power component of the EUT is considered to be part of the islanding load circuit in the figure.

The test conditions require that an adjustable RLC load should be connected in parallel between the DR and the grid system. The resonant LC circuit should be adjusted to resonant at the at the nominal grid frequency f and to have a quality factor of Q_f = 1, that is the reactive power generated by C should equal the reactive power absorbed by L and should equal the power dissipated in resistor R at the nominal power P and nominal grid voltage V. thus the values for the RLC load can be calculated as in equation 2-1.

$$R = \frac{V^2}{P}$$
$$L = \frac{V^2}{2\pi f P Q_f} \qquad \text{2-1}$$
$$C = \frac{P Q_f}{2\pi f V^2}$$

The parameters of the RLC load should first be fine-tuned until the grid current through S3 is lower than 2% of the rated value at steady-state. In this balance condition, S3 should be opened and the time before disconnection is measured and should be lower than 2 seconds.

For three phase DR power conversion system each phase should be tested with respect to the neutral individually. For three three-wire three phase DR power conversion system the local load should be connected between the phases.

The UL 1741 standard in the US has been harmonized with the anti-islanding requirements in IEEE 1547. The main difference with respect to the previous IEEE 929-2000 standard is that the requirement for the quality factor of the local RLC load has been reduced from 2,5 to 1,0, thus making compliance easier to achieve.

2.6.2 IEC 62116 anti-islanding requirements

In the draft version of IEC 62116 – 2006 similar requirement as those for IEEE 1547 are proposed. The test can be utilized by other interconnected DR. in the normative reference IEC 61727 – 2004 the ratings of the system valid in this standard have a rating of 10 kVA or less. The test circuit is the same as in IEEE 1547.1 and a power balance is required before the island detection test. The requirement for passing the test contains more test cases but the conditions for confirming island detection do not have a significant deviation compared to IEEE 1547.1 test.
The power conversion system is tested at three levels of the output power (A: 100-105%, B;50-66% and C: 25-33% of the inverter rated output power). Case A is tested under maximum allowable input power and case C at minimum allowable inverter output power if greater than 33%. The voltage at the input of the inverter also has specific conditions. All conditions are to be tested at no deviation in real and reactive load power consumption than for condition A in a step of 5% both real and reactive power iterated deviation from -10 to 10% from the operating output power of the inverter. Condition B and C are evaluated by deviating the reactive load in an interval of ±5% in a step of 1% of the inverter output.
The maximum trip time is the same as in IEEE 1547.1 standard which is 2 seconds. In IEC 61727, there is no specific description of the anti-islanding requirement as compiling this dissertation. Instead reference is made to IEC 62116.

2.6.3 VDE 0126-1-1 anti-islanding requirements

The VDE 0126-1-1 allows the compliance with one of the following anti-islanding methods

1. Impedance measurement. The test circuit is shown in figure 2-2. The procedure is based on local balancing of the active and reactive power using the variable RLC circuit and the switch *S* is opened in order to increase the grid impedance by 1,0 Ω. The inverter should disconnect within the required time, which is 2 seconds. The test should be repeated for different values of the simulated grid impedance (R_2 and L_2) in the range of 1,0 Ω (maximum of 0,5 Ω inductive reactance).
2. Disconnection detection with RLC resonant load. The test circuit is the same as the one from IEEE 1547.1 showed in figure 2-1 and the test conditions are that the RLC resonant circuit parameters should be calculated for a quality factor greater than 2 using equation 2-1. With balanced power the inverter should disconnect after the disconnection of S2 in a maximum of 5 seconds for the following power levels: 25%, 50% and 100%.

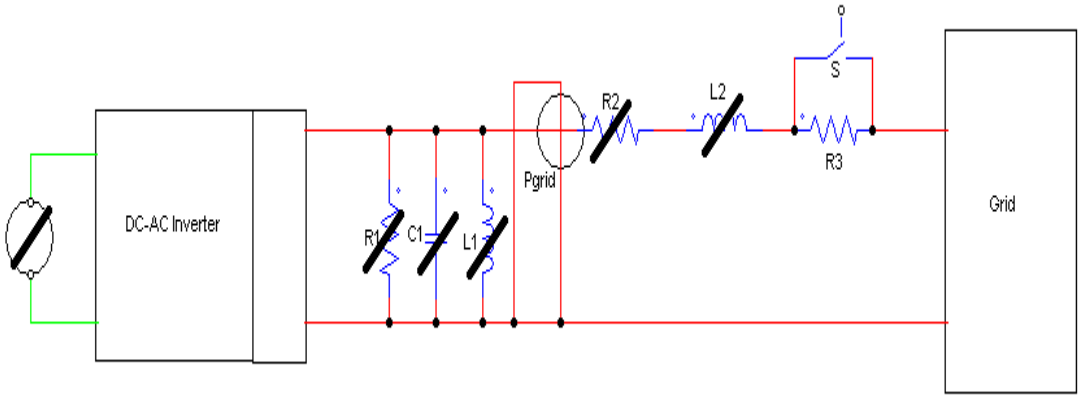

Figure 2-7 Test setup for anti-islanding requirement in VDE 0126-1-1

For three-phase PV inverters passive anti-islanding method is accepted by monitoring all three phases of voltage with respect to the neutral. This method is condition by having individual current control in each of the phases.

Finding a software-based anti-islanding has been a very challenging task, resulting in a large number of research works.

2.7 Grid filter topologies

Injection of power from the PV system to the grid is typically done through a voltage source inverter system. Harmonics in the output voltage of the inverter is usually attenuated by connecting a filter between the voltage source inverter system and the grid in order to cope with the power quality requirements of the utility. An improvement in the reactive power export to the grid is also constrained by the filter parameter. The most common filters used for this purpose are reviewed in this section.

2.7.1 L-filter

The degree of which the harmonic content is attenuated depends on the filter used. A first order filter consisting of one inductor in series with the mains and is the most commonly used filter. This is because the filter is easy to make, and it has no resonance problems as higher order filters may have. The major drawback of this filter is the size of the inductor needed to achieve a reasonable attenuation of the current harmonics. So with an attenuation of 20 dB per decade over the whole frequency range, this filter is most efficient when used with high frequency pulse width modulation switching strategy of the voltage source inverter system.

2.7.2 LC and LCL-filter

Higher order filters consisting of combinations of inductors and capacitors, can give a better attenuation of the harmonics, but they also make the design more complex. The most common higher order filters are the second order LC filter and the third order LCL filter. In grid connected systems the LC filter is seldom used, since the resonance frequency of the filter will vary with the inductance value of the grid (Blaabjerg, 2006). Instead by using a correctly designed LCL filter this problem is reduced, because the resonance frequency is mostly depending on the filter components (Blaabjerg, 2006). The LCL filter will also give a better attenuation than a LC filter given the same size. The dynamic control of the inverter is more difficult when using a LCL filter compared to using a simple L filter. With the LCL filter two more poles and two more zeroes are introduced compared to the simple L filter. So care must therefore be taken when designing the controller, and the additional poles and zeroes can make the system unstable if not proper damping is introduced. The filter topologies for both LC and LCL filters are shown in figures 2-6 and 2-7 respectively.

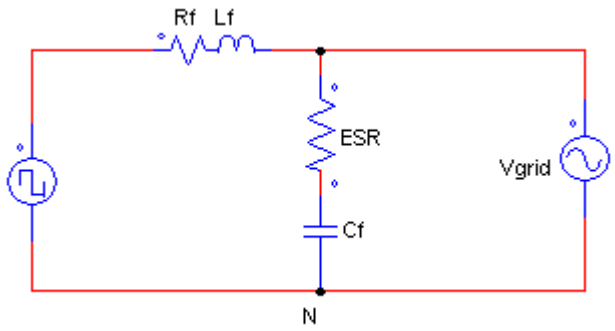

Figure 2-8 LC filter

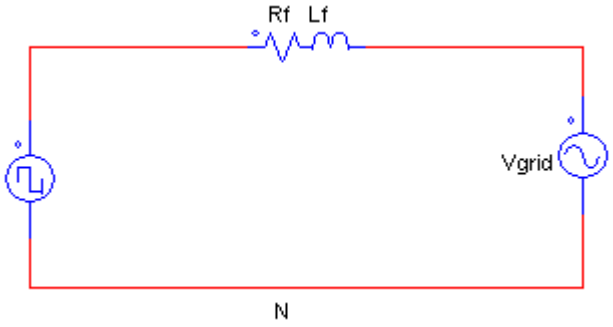

Figure 2-9 L filter

2.7.3 Damping

Damping of the LCL filter resonance can be either active using the converter, or passive using elements like resistors, capacitors and inductors. Several different methods for passive damping has been proposed, from a simple resistor in series with the capacitor, to more complex circuits including resistors, capacitors and inductors in series or parallel configurations. When a resistor is introduced in the circuit, there will be some increase in the losses, how much depends on the configuration. One should also be aware that some of the configurations might introduce resonance frequency shifts, and lower attenuation at higher frequencies compared to the undamped LCL filter. Several different approaches to active damping have been proposed in the literature. These methods often require the measurement of the capacitor voltage and/or currents, but other methods using estimated values have also been used. The use of active damping removes the losses associated with passive damping, but it increases the complexity of the control and might introduce other problems if not correctly designed. In the figure 2-8 below a LCL filter with a simple passive damping resistor in series with the filter capacitor is shown.

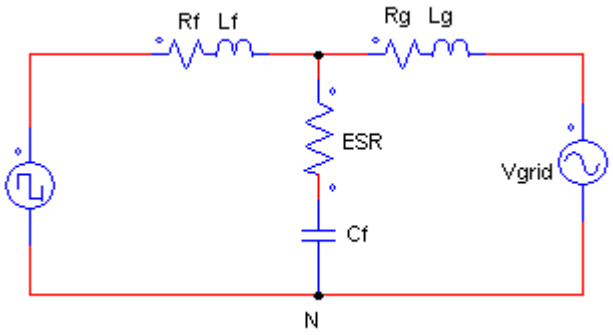

Figure 2-10 LCL filter

2.8 Grid power converter control

Two main issues in the control of grid connected technologies are the control of the DC link voltage (if there is no DC/DC converter in charge of it) and the control of AC power that is injected into the grid. The AC power can be controlled with the purpose either of feeding the utility grid or feeding the stand-alone loads or a microgrid. In the first case the distributed power system may also offer support to the grid. Once the operation mode of the grid converter is determined and the strategy to select the reference power is also selected, the power control using the instantaneous power theory in current and or voltage is adopted. In fact, the converter can be operated as a controlled current source (typically adopted if the converter is grid tied and does not offer any support to the grid) or as a controlled voltage source (typically used if the converter is in stand-alone, microgrid or grid supporting). In the second case, if an LC filter is used the current is controlled. The control of currents and voltages can be done in state variables or in a cascade structure. In case of operation in a microgrid and grid-supporting modes the droop control (or an equivalent one) is needed.

2.9 DC-AC converter control

In order to control the DC-AC converter there are two major control strategies, current control mode and voltage control mode strategies. Where current control is the most common way to control grid connected voltage source inverters. A current controller has the advantage of being less susceptible to voltage phase shifts and to distortion in the grid voltage, thus it reduces the harmonic currents to a minimum. Whereas voltage control can result in overloading of the inverter due to small phase errors, and large harmonic currents may occur if the grid voltage is distorted. If operated in standalone mode, voltage control mode would be a natural choice, but when operated in grid connected mode, current control mode is the most robust control. Figure 2-10 shows PMW control schemes used in power converter systems.

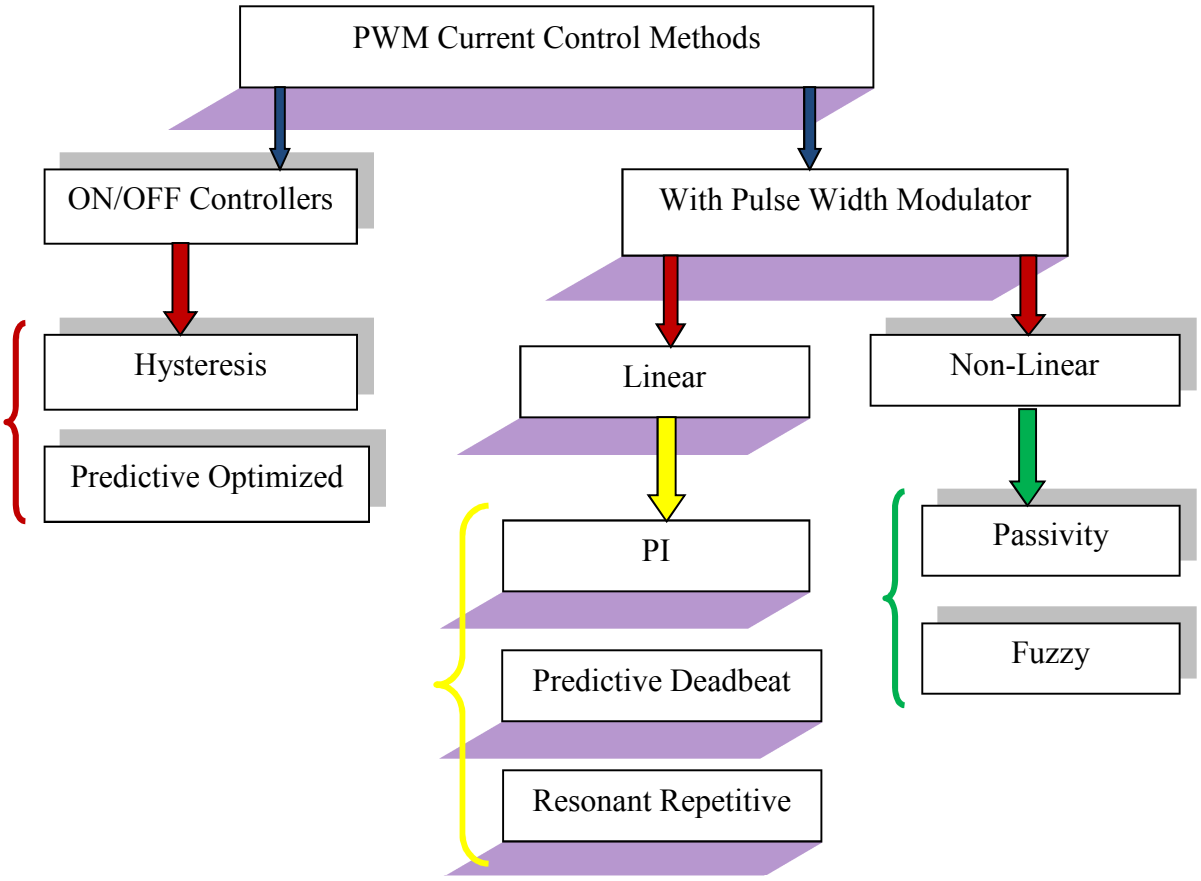

Figure 2-11 Different PMW control schemes

Some of the control schemes presented in this section will involve the use of transformations between the three-phase system and different two-phase systems; therefore the concept of transformation is defined first.

2.9.1 Transformations

In order to avoid controlling three currents and voltages separately, transformations from a three-phase system to different two-phase systems have been made. These are based on the fact that in a balanced three-phase system there are only two independent currents and voltages, thus the third current and voltage can be expressed by the other two quantities. These systems are often referred to as reference frames, where the frame is the axis system of the transformed system.

Stationary reference frame (Clarke transform)

When a three-phase system is transformed into a two-phase system, this is often called an *abc* to *αβ* (or *αβ0* when the zero vector is used) transform, or a transform into the stationary reference frame. Both the three-phase and the two-phase system is said to be stationary, because the axes is locked in one position, but the term stationary reference frame usually refers to a two-phase stationary reference frame.

The transformation is made by applying the Clarke transformation in equation 2-10, where the three-phase quantities must be phase values. By inverting the coefficient matrix, the three-phase quantities can be found as a function of the two-phase quantities.

$$\begin{bmatrix} X_\alpha \\ X_\beta \\ X_0 \end{bmatrix} = \frac{2}{3} \begin{bmatrix} 1 & -\frac{1}{2} & -\frac{1}{2} \\ 0 & \frac{\sqrt{3}}{2} & -\frac{\sqrt{3}}{2} \\ \frac{1}{2} & \frac{1}{2} & \frac{1}{2} \end{bmatrix} \begin{bmatrix} X_a \\ X_b \\ X_c \end{bmatrix} \qquad 2\text{-}2$$

The transformation can be thought of as a change of coordinate system, from a three axis (phase) system to a two axis (phase) system as shown in figure 2-11. It can be seen from the *abc* coordinate system that only two phases is needed to express the vector X_{abc}, and thus it can be expressed in the *αβ* system as the vector X_{ab} without any loss of information. In the figure ω is the angular speed of the vector, and θ is the instantaneous angle of the vector. If X is the grid voltage, then ω represents the grid frequency, and θ represents the instantaneous phase angle.

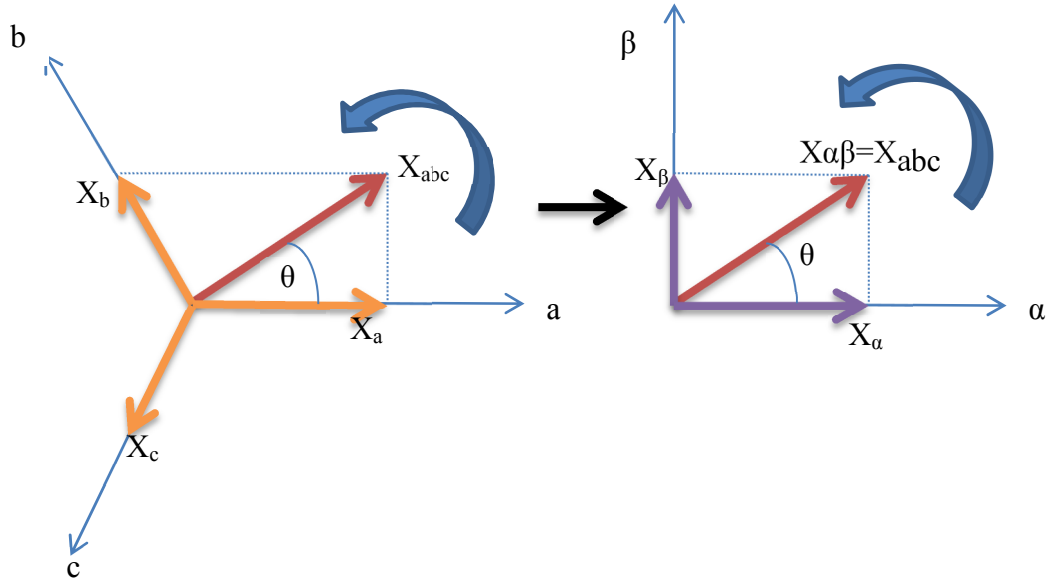

Figure 2-12 abc to αβ transformation

Usually the three-phase quantities are assumed symmetrical, and thus the zero-sequence component can be ignored. When there is no zero-sequence component the instantaneous active and reactive power is given by equations 2-11 and 2-12 respectively. The factor 3/2 is introduced in order to have the power from all three phases equal in both reference frames (power invariance identity).

$$p_{\alpha\beta} = \frac{3}{2}\left(v_\alpha i_\alpha + v_\beta i_\beta\right) \qquad 2\text{-}3$$

$$q_{\alpha\beta} = \frac{3}{2}\left(v_\beta i_\alpha - v_\alpha i_\beta\right) \qquad 2\text{-}4$$

Synchronous reference frame (Park transform)

In this system the axis system is no longer locked and rotates following an arbitrary vector, hence the term synchronous reference frame. It is sometimes also termed the *dq* system (or *dq0* if zero-vector is used).

This transformation is widely used in motor drives, where the axis system follows for instance the rotor position or rotor flux. In grid connected inverters it is most common to lock the axis system to a voltage (usually the grid voltage). In figure 2-12 the *d*-axis is locked to the vector

X_{ab}, and therefore $X_d = X_{\alpha\beta}$ and $Xq = 0$. The axis system will then rotate with an angular speed of ω, and have an instantaneous angle of θ (referred to the stationary system).

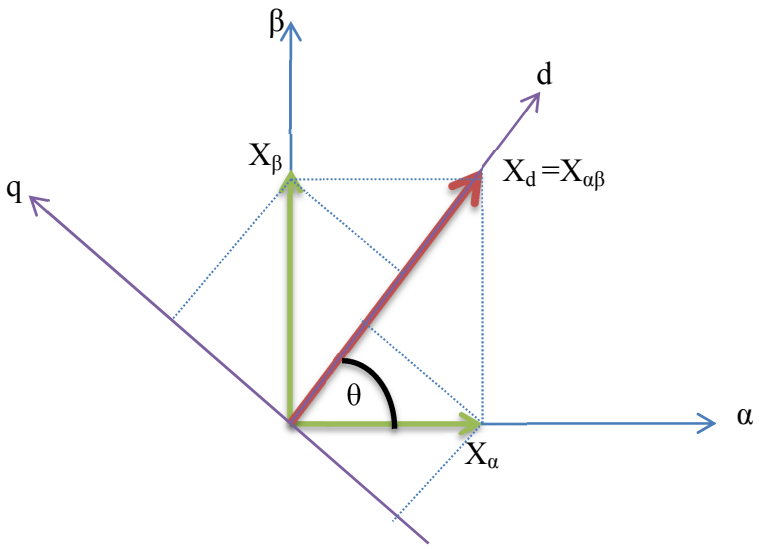

Figure 2-13 αβ to dq transformation

The transformation is made using the Park transformation shown in equation 2-13, where the stationary quantities can be found as a function of the synchronous quantities by inverting the coefficient matrix.

$$\begin{bmatrix} X_d \\ X_q \\ X_o \end{bmatrix} = \begin{bmatrix} \cos(\theta) & \sin(\theta) & 0 \\ -\sin(\theta) & \cos(\theta) & 0 \\ 0 & 0 & 1 \end{bmatrix} \begin{bmatrix} X_\alpha \\ X_\beta \\ X_o \end{bmatrix} \qquad 2\text{-}5$$

Θ – Instantaneous phase angle

If the *dq*-axis system is locked to the grid voltage, the axes will rotate with the angular frequency of 2πft, and the *dq* values will become DC-values (constants). If it is still assumed that the three-phase quantities are symmetrical, then the zero-sequence component is still zero, and the active and reactive power is given by equations 2-14 and 2-15 respectively.

$$p_{dq} = \frac{3}{2}(v_d i_d + v_q i_q) \quad 2\text{-}6$$

$$q_{dq} = \frac{3}{2}(v_q i_d - v_d i_q) \quad 2\text{-}7$$

These equations assume that both the voltage and the current are transformed into the *dq* system using the same reference frame. When the reference frame is oriented at the voltage vector, then the *d*-axis current will represent current in phase with the voltage, and thus it represents the active power in the circuit. The *q*-axis current will then represent current which is out of phase with the voltage, and thus it represents the reactive power in the circuit.
It should be noted that other versions of the Park transform exists, and in those the orientation of the *dq*-axis on the $X_{\alpha\beta}$ vector might differ. This can for instance lead to having the active power controlled by the q-axis component value.

2.9.2 Pulse Width Modulation (PWM)

The most common methods for PWM modulation is carrier based PWM (CB-PWM), space vector modulation (SVM) and random PWM. A summary of the operation in the linear modulation range is presented here.

Carrier Based (CB-PWM)

CB-PWM is the basic and most common way to modulate the switching signals. This method can be divided into methods, sinusoidal PWM and CB-PWM with zero sequence signal (ZSS). With sinusoidal PWM, three reference sinusoidal signals are compared to a triangular wave generating logical signals controlling the switches. The ZSS method is based on the sinusoidal PWM, with the addition of a zero sequence signal of third harmonic frequency. The injection of the third harmonic is not producing phase voltage distortion or affecting load average currents. It does however extend the linear region of operation; reduce the average switching frequency and the current harmonics.
The ZSS method can be further divided into continuous and discontinuous modulation (DPWM), where the most well-known method of continuous modulation is the method with sinusoidal ZSS, but also triangular ZSS is used. ZSS amplitude of 1/4 of the fundamental corresponds to the minimum of output current harmonics, and with 1/6 it corresponds to the maximum linear range. Discontinuous modulation is formed by unmodulated segments (converter power switches do not

switch) phase shifted from 0 to π/3, and can reduce the average switching frequency and switching losses, but has higher harmonic content at lower modulation ratios. The maximum output voltage in the linear region for the sine PWM and the PWM with ZSS is shown in equation 2-16

$$V_{LL\_sine} = \frac{\sqrt{3}}{2\sqrt{2}} V_{DC} = 0,612 * V_{DC}$$
$$V_{LL\_ZSS} = \frac{\sqrt{3}}{\sqrt{2}} V_{DC} = 0,707 * V_{DC} \qquad 2\text{-}8$$

The principle of the generation of switch signals is shown in figure 12-13, where a triangular carrier signal is compared to sinusoidal signals representing the phase voltages. If the sinusoidal is larger than the carrier wave, then switch turns on, and if less it turns off.

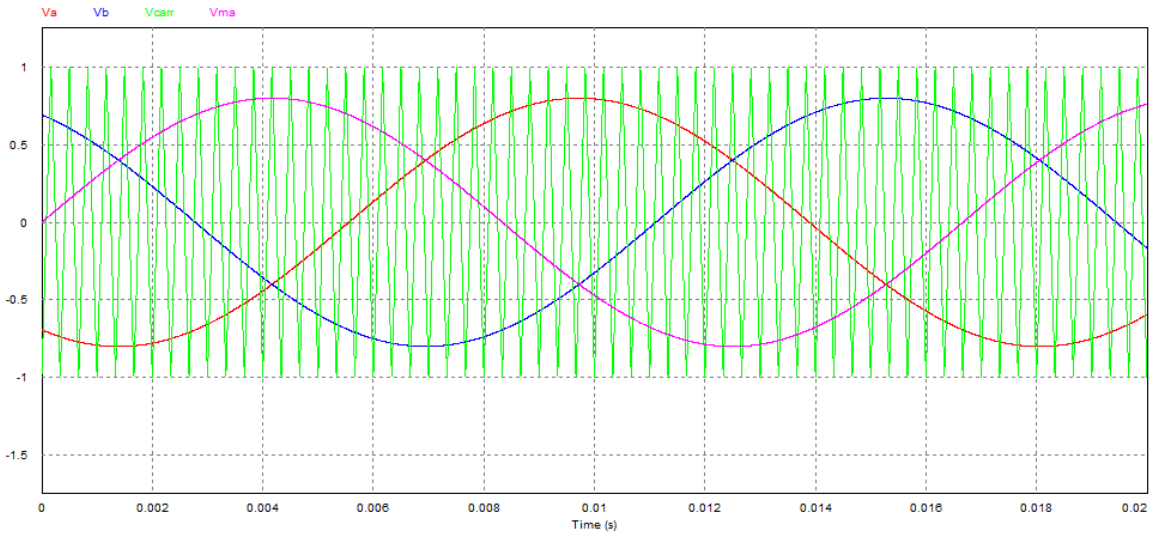

Figure 2-14 Generation of carrier based PWM signals

Space Vector Modulation (SVM)

SVM is a method based on space vector representation of the converter AC-side voltages or currents, and it is shown that the difference between SVM and CB-PWM is only the treatment of the three-phase quantities. CB-PWM operates in terms of three-phase natural components, whereas SVM uses an artificial vector transformation. With a three-phase two level inverter there are eight possible switching states, made up of six active and two zero switching states. There are several different methods for creating the switching patterns, the only difference

between them is the placement of the zero vectors. The different switching states are shown in the figure 2-14.

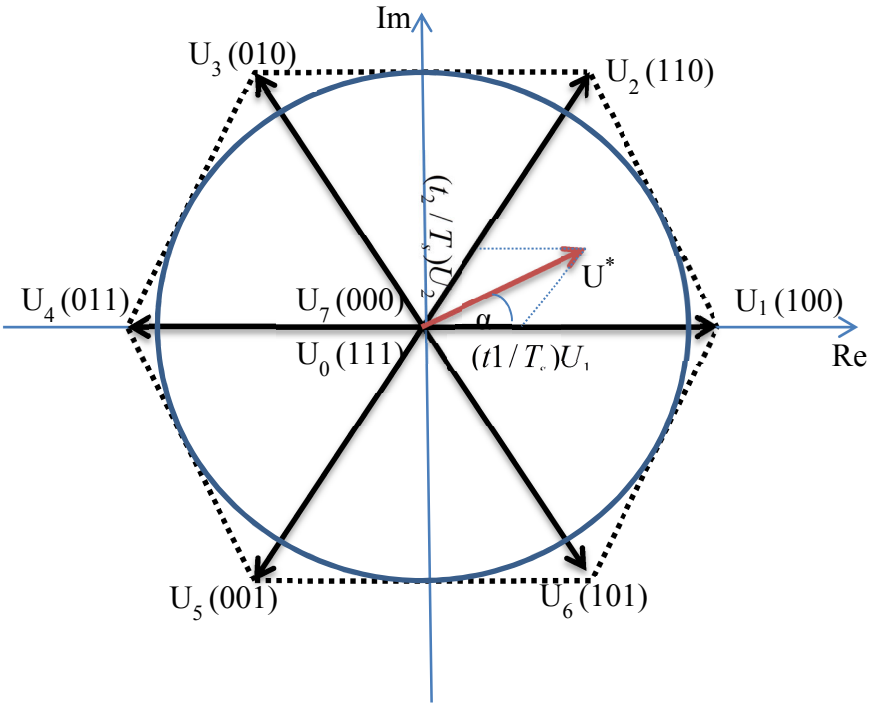

Figure 2-15 Space vector representation of output voltage

The most popular method is the three-phase SVM with symmetrical placement of zero vectors (SVPWM). This method corresponds to CB-PWM with triangular ZSS of quarter amplitude, and has almost equal harmonic content as CB-PWM with sinusoidal ZSS. It is easy to implement in a microprocessor, and is therefore the natural choice of SVM. Two other techniques for SVM is vector modulation with V_{N0}=0 (voltage between converter neutral and grid neutral = 0, equal to sine PWM), and vector modulation with third harmonic (equal to CB-PWM with sinusoidal ZCC), but these are easier to achieve with CB-PWM. Two-phase SVM is another method which is equivalent with the discontinuous CB-PWM with ZSS (DPWM). This method will have only one zero state per sampling time, and therefore a simple calculation, but is best used at high modulation ratios. The maximum line voltage with the SVPWM and also the two-phase PWM is given in equation 2-17.

$$V_{LL\_SVPWM} = \frac{1}{\sqrt{2}} V_{DC} = 0,707 * V_{DC} \qquad 2\text{-}9$$

There is also a variant of SVM called adaptive SVM (ASVM), which combines different SVM techniques into one universal solution. This method gives full control range including over modulation and six-step operation (square wave operation) and higher efficiency of the inverter, but the inverter will only mostly operate in the upper linear area of modulation, therefore this method is not of interest.
The generation of the switch signals is for the SVM based on a mathematical approach, which can easily be implemented into a microprocessor.

Random PWM
Random PWM is based on randomly varying the switching period, and thus creating harmonics more evenly distributed throughout the frequency spectrum. This has advantages as reducing the acoustic noise, and compliance with standards defining limits for emission of conducted and radiated EMI may be obtainable with less filtering and shielding efforts. The implementation of random modulation is strongly dependent on the hardware used for the PWM, and the distribution of harmonics is not well defined as it is for fixed carrier period PWM.

2.9.3 PI controllers

PI controllers can be applied both in the stationary ($\alpha\beta$) and synchronous (dq) reference frame, but by applying them to the dq system there will be DC currents stationary, and the PI compensators are able to reduce the stationary steady-state error of the fundamental to zero. This is not the case with PI controllers working in the $\alpha\beta$ system, where there is an inherent tracking error of phase and amplitude. Therefore current control in a synchronous (rotating) reference frame, using PI controllers is the typical solution in 3-phase grid connected inverters.
An advantage of current control in the dq system is the individual control of active and reactive power by orienting the dq frame on the grid voltage as discussed in the previous section. Where the active power is controlled by the d-axis current and the reactive power is controlled by the q-axis current. Some well-known drawbacks of this method is the need for many transformations, decoupling in three-phase converters, and limitations in compensating the low harmonics in order to comply with power quality standards. In its general form the PI controller is defined as

shown in equation 2-18 where T_i is the integration constant, K the controller gain and s is the Laplace operation.

$$G_{c(PI)}(s) = K\ (\frac{1+T_i s}{T_i s}) \qquad 2\text{-}10$$

If harmonic compensation is desired, it is possible to add harmonic compensators with the same method as described above, but now using reference frames rotating at the desired harmonic frequency (Teodorescu, 2006). This requires lots of computer resources for the complex computation of the algorithm.

2.9.4 Proportional resonant controllers

The proportional resonant (PR) controller is a new type of controller described in (Teodorescu et al, 2004; Blaabjerg, 2004). In this approach the PI DC-compensator is transformed into an equivalent AC compensator (using the transforms described in 2.9.1), thus giving the same frequency response characteristics in the bandwidth of concern. By using this method the complexity of the calculations will be reduced, and the cross couplings are removed. The PR controller is defined as shown in equation 2-19.

$$G_c(s) = K_P + K_1 \frac{s}{s^2 + \omega^2} \qquad 2\text{-}11$$

In combination with the PR controller it is often added a harmonic compensator (HC). The harmonic compensator consists of a sum of generalized integrators, which are tuned to have almost infinite gain at different frequencies, called resonant frequencies. Outside these frequencies the generalized integrators have almost no attenuation. This is an interesting feature of the generalized integrator, because it does not affect the dynamics of the PR controller outside the tuned frequency. Thus one can add as many generalized integrator as needed without affecting the overall system dynamics. The harmonic compensator is defined as shown in equation 2-20 where h denote the harmonic order to be compensated.

$$G_H(s) = \sum_{h=3,5,7...} K_{1h} \frac{s}{s^2 + (\omega h)^2} \qquad 2\text{-}12$$

This combination of PR controllers and harmonic compensators, can be tuned to react to the fundamental frequency for a good regulation, and tuned to harmonic frequencies in order to compensate them (Teodorescu et al, 2004).

2.9.5 State feedback controller

In the methods described above where the control processes have a mathematical description in the form of transfer functions, it is not possible to observe and control all of the internal phenomena involved in the control process. Therefore the state space method is gaining more and more attention, because this method provides a uniform and powerful representation in the time domain of multivariable systems of arbitrary order with linear, nonlinear, or time varying coefficients. There exist different ways to write the state space equations, but one way described is shown in equation 2-21.

$$\begin{aligned} \dot{\mathbf{X}}(t) &= \mathbf{A}\mathbf{x}(t) + \mathbf{B}\mathbf{u}(t) \\ \mathbf{y}(t) &= \mathbf{C}\mathbf{x}(t) + \mathbf{D}\mathbf{u}(t) \end{aligned} \qquad 2\text{-}13$$

where
x(t): State variable
u(t): Input vector
y(t): Output vector
A: State coupling matrix
B: Input coupling matrix
C: Output coupling matrix
D: Input to output coupling matrix

With this system description also the initial conditions are easy to implement, and the state feedback controller can work in both stationary and synchronous reference frame. When using this method the poles of the closed loop system can be placed in predetermined locations in the s-plane (or z-plane when discretized), and thus controlling the characteristics of the response of

the system. Also with this method harmonic compensation can be achieved, by including a model of the system at the desired harmonic frequency.

2.9.6 Harmonic compensation

Nonlinear loads have become a large part of the load profile of the grid nowadays. These loads draw currents with a harmonic spectrum where the harmonic above the fundamental becomes distinctive. When these currents go through the impedances of the grid, they create voltage harmonic drops which deteriorate the grid voltage. This deterioration of the grid voltage will affect all the grid connected equipment, and if the harmonics are sufficiently large, it can lead to damage or deterioration of this equipment. It can therefore be understood that this situation is undesirable, and some sort of compensation is needed in order to keep the harmonics at a low level.

The classical solution to this problem is installing passive filters, but these filters have some drawbacks. The source impedance will strongly affect the compensation characteristics, and they are susceptible to undesirable series and parallel resonance with source and load.

In order to alleviate these problems active filters have become more and more interesting, because they are flexible and have the ability to adapt to varying situations. An active filter can be a VSI programmed to deliver currents at the desired harmonic frequencies (harmonic compensation), and thus reduce the harmonic voltage drops. Which means that any grid connected VSI can be used as an active filter.

In order to compensate for any harmonic drawn by the load, the harmonic currents needs to be isolated and their phase and amplitude must be known. This can for instance be achieved using filtering or some FFT algorithm. Once the harmonic current is known, it can be compensated using for example one of the methods described about current control in

2.9.7 Grid synchronisation

The inverter delivers current to the grid, and the synchronization of the current with the grid voltage is important to:

- Deliver power at a power factor within the limits in the standards, or within limits given
- By the utility if there is need for reactive power compensation.
- Reduce the harmonic current content, by applying a "clean" reference current.
- Minimize the grid connection transients.

In (Teodorescue et al, 2006) several methods for grid synchronization are presented. These are summarized here, discussing their major advantages and disadvantages.

2.9.7.1 Filtered zero cross detection (ZCD)

With this method the zero-crossing of the voltage is registered, and the phase angle is calculated. The method is easy to implement and uses little computational resources, but the technique has several drawbacks. Since the technique is based on zero-crossing detection, the phase angle is only updated two times per period of the grid voltage frequency, and therefore the dynamic performance of this technique is low. Also filtering has to be applied in order to detect the zero-crossing of the fundamental frequency, and therefore a delay is introduced. This can be avoided using special high order predictive filter without delay, but then the complexity becomes very high.

2.9.7.2 Filtering of grid voltages

By filtering the grid voltage in different reference frames, such as the two-phase stationary or the synchronous frame, the phase angle can be extracted directly using the arctangent function. The filtering is done in either the stationary frame, or in the synchronous where there are DC-components. The arctangent function is always applied to the stationary frame, thus giving the instantaneous phase angle. Therefore when the filtering is done in the synchronous frame, the signal must be transformed back into the stationary frame before applying the arctangent function.

In (Timbus et al, 2005) it is reported improved performance over the zero-crossing method, but the technique encounters some difficulties in extracting the phase angle when grid variations and

or faults occur in the network. Another drawback of this method is the use of filtering, since most filter types introduces a delay, the calculated phase angle will lag the real phase angle.

2.9.7.3 Phase locked loop (PLL)

A phase locked loop (PLL) produces an output signal which synchronizes in phase and frequency with the input signal, using a negative feedback loop. The PLL controls the internal signal such that, the error in phase between input and output is kept to a minimum, and the frequency is equal at input and output. A basic PLL circuit often consists of three components, a phase detector, a loop filter and a voltage controlled oscillator. This basic circuit is shown in figure 2.9.

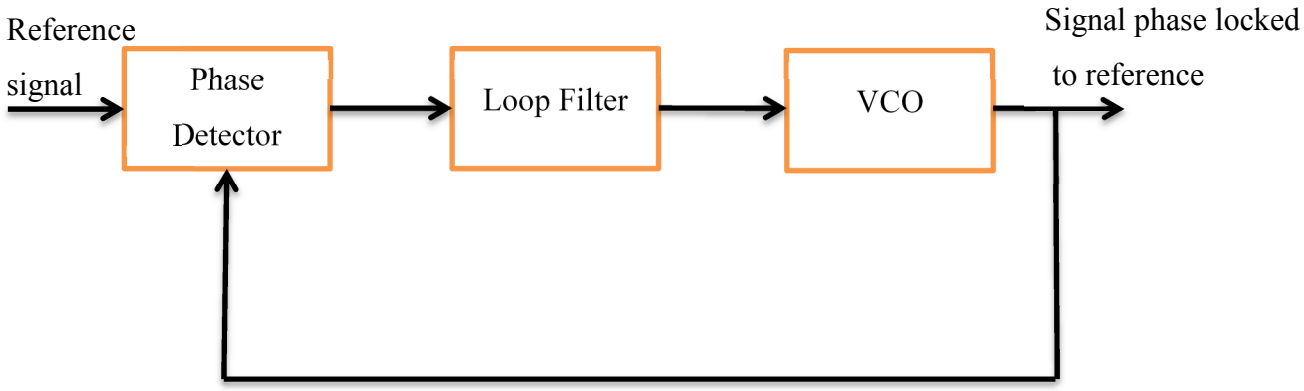

Figure 2-16 A basic PLL circuit

The phase detector is implemented by transforming the voltages into the *dq* system. By using the phase locked angle in the *dq* transformation, the phase difference between the reference signal and the phase locked signal can be extracted by applying the arctangent function. This gives the exact phase difference, but the phase difference can also indirectly be found by recognizing that the phase difference is zero when V_q equals zero. In three-phase systems the transformation is easy to implement, but in single phase systems there is only one voltage, so the orthogonal component of the voltage has to be found artificially.

The loop filter can be some sort of regulator, which brings the phase error to zero. This is usually a proportional integral regulator, but also higher order regulators can be used. A higher order system increases the dynamics of the system and enhances the filtering capabilities, but it also increases the complexity. When choosing the controller order, one must weigh what is most

important of the latter. When using a PI controller, this gives a second order system, and then the PLL bandwidth and damping factor can be set using linear system theory.

After the loop filter, which output is the frequency, a voltage controlled oscillator is applied. This is usually a simple integrator, which gives the phase locked angle as output. With the PLL no delays are introduced, so the phase locked angle will be in phase with the grid angle.

A schematic model is shown in figure 2-16. It shows the basic principle of a phase lock loop with its transformations of the three-phase voltages. In this loop the arctan2 function is applied as the phase detector, giving the exact phase difference.

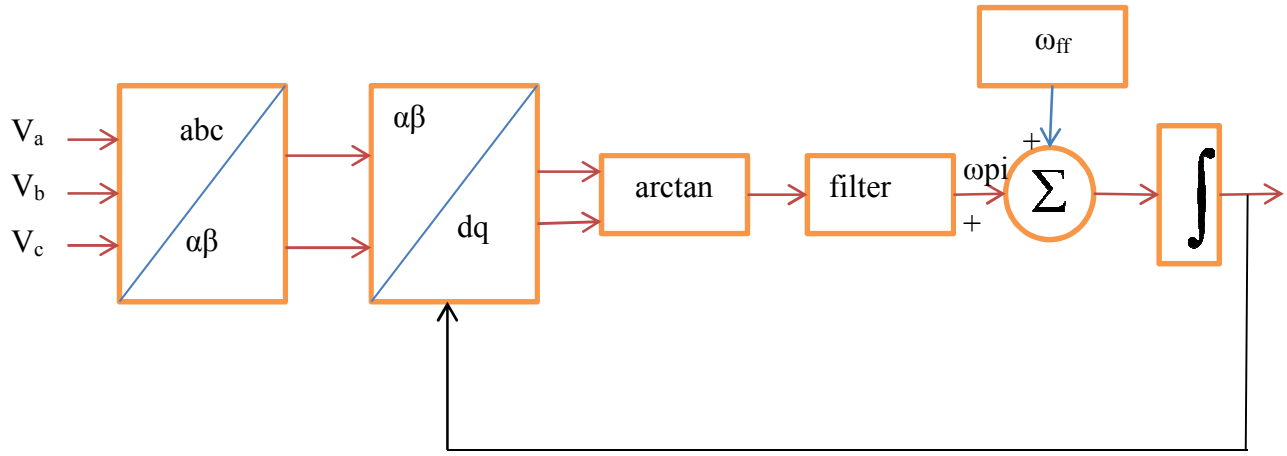

Figure 2-17 schematic of a phase lock loop with transformation

This algorithm has better rejection of grid harmonics, notches and any other kind of disturbances then the previous methods, but during grid unbalancing further improvements has to be done. In the case of a unsymmetrical voltage fault, the second harmonics produced by the negative sequence will propagate through the PLL and become reflected at the output. This means that in order to alleviate this problem, the zero sequence signal has to be filtered out, thus the PLL is only estimating the phase angle of the positive sequence signal.

2.9.7.4 Adaptive PLL

Timbus et al proposed a more advanced PLL structure that is described based on an adaptive algorithm. In these method three PLL systems is used, one for each phase. Where there are three control units that individually control the frequency, phase angle and voltage magnitude of the grid voltage. This gives precise information about each phase, and therefore this method is suitable for grid monitoring, and thus islanding detection and safety improvements. The disadvantage of this structure can be the large algorithm needed to implement the controllers (3x3 controllers in this case, but it can be less in other structures), and a moving average filter that is involved in the controllers which is computationally heavy but very precise.

Chapter 3 : DISTRIBUTED ENERGY RESOURCES TECHNOLOGY

Renewable energy for electricity generation in South Africa has largely been confined to the off-grid applications. Currently, most use of renewable energy is off-grid photovoltaic, as well as solar cooking and water heating. Photovoltaic (PV) systems are used as stand-alone sources of electricity in areas remote from grid, but are expensive compared to grid-connected electricity in South Africa. Policy options such as feed-in tariffs, renewable portfolio standards and renewable obligations for promoting renewable electricity were thoroughly reviewed (Harald, 2005).

This chapter presents a brief and brevity background on different types of DG. Wind energy conversion system, solar energy, micro-turbines, energy storage systems, combined heat and power or cogeneration, fuel cell systems.

Figure 3-1 shows the common types of energy sources that can be utilized in DG systems. Important features of these types are discussed in the following subsections.

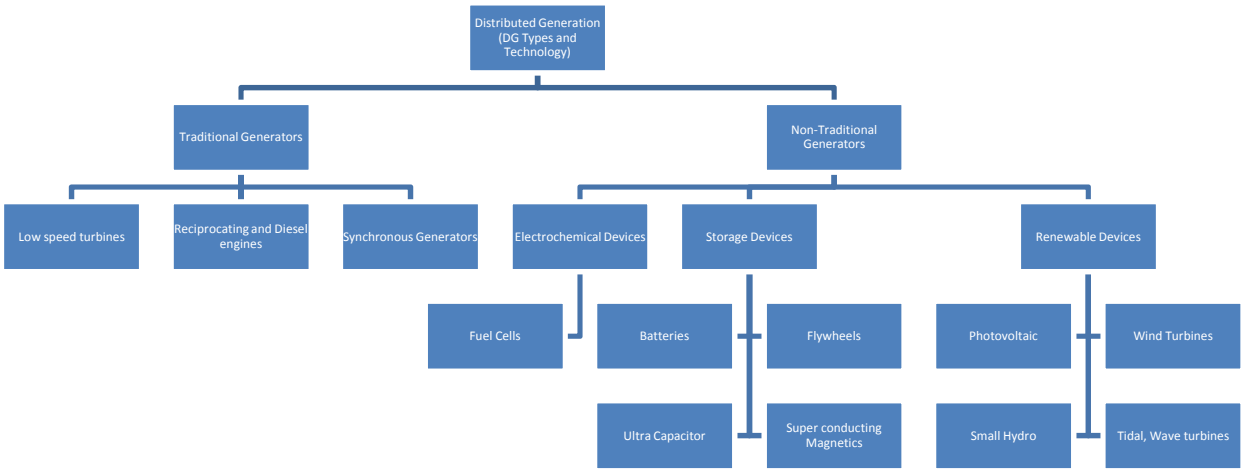

Figure 3-1: Distributed generation technology types

3.1 Wind power system

Wind power has been in use for serving mankind since centuries through what has been popularly known as “Wind-mills”. There is no “electrical” stage in old-styled uses where wind velocity is directly used for performing the jobs such as wheat-grinding, pumping water for irrigation, sailing vessels, etc. It enjoys the advantages of being plentiful, inexhaustible, renewable and non-polluting, over and above being cheap for running costs. It suffers from disadvantages of being unreliable, and being economically un-viable for large power generation until recent time. With advanced power electronics technology system, it is now possible to have suitable power control circuits on the output side of wind generators so that these can pump energy into low or medium voltage lines of the grid over a wide range of variation of wind speeds (Sørensen, 2011; Vieira da Rosa, 2009).

A wind energy conversion system consists of a rotor, turbine blades, generator, drive or coupling device, shaft and the nacelle that contains the gearbox and the generator drive. Modern wind energy conversion system can provide clean electricity as individual or as wind farms.

The energy in the wind is converted to rotational mechanical energy by the turbine which is coupled to the rotor of an electricity generator using a shaft. The electrical energy generator converts the rotational mechanical energy to the electrical energy either for grid-forming or grid-following applications Farrent & Simões, 2006. Figure 3-2 shows the wind energy conversion system.

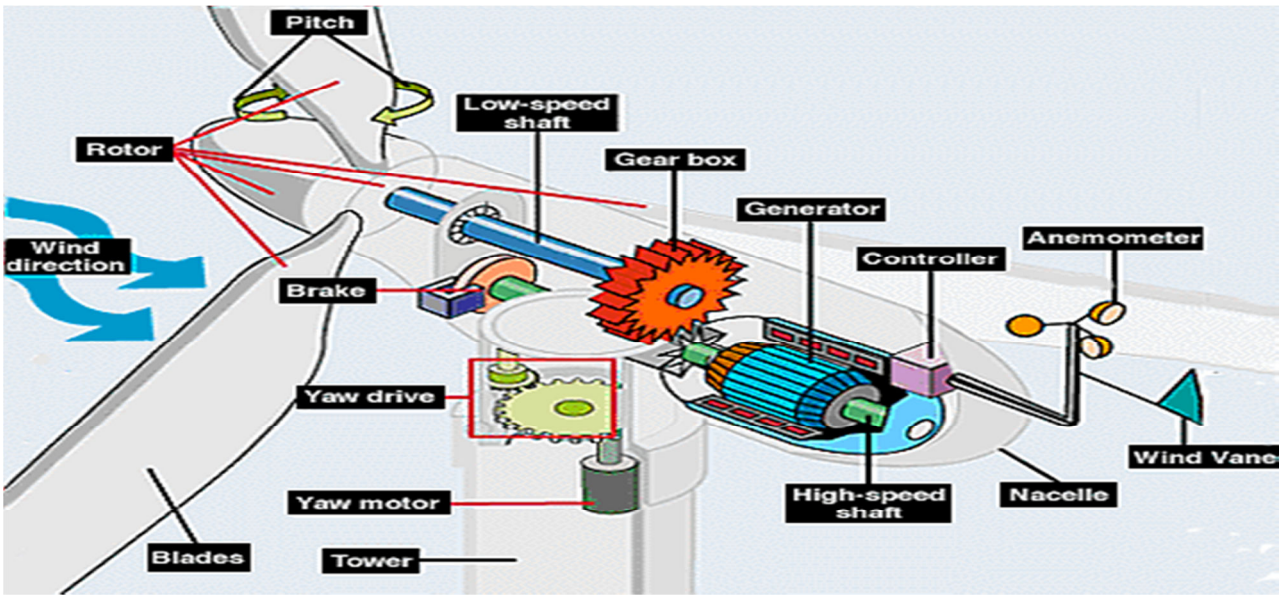

Figure 3-2: Wind energy conversion system

3.2 Solar power system

The sun is our source for light, heat and food. Fossil fuels, wood and crops are in fact an accumulation of solar energy. Also hydropower and wing power are in their origin forms of solar energy. But in the daily conversation, when we speak about solar energy, we mean the direct conversion from solar radiation into heat or electricity. In the case of heat production we speak of thermal solar energy and when the output is electricity we call it photovoltaic energy. One of the most widespread uses of thermal energy is solar water heating. Water is pumped through a collector, being black painted body with tubes inside. The collector absorbs the solar radiation and transfer the heat to the circulating water. The water rises in temperature and the hot water is stored in a boiler. The boiler acts as a heat exchanger to heat up tap water. This works well for domestic and small industrial application and the utility bills are reduced (Sørensen, 2011; Vieira da Rosa, 2009).

So-called concentrating solar power systems use the sun's heat to generate electricity. These systems consist of rows of highly reflective parabolic troughs and each parabolic trough focuses and concentrates sunlight on a central tube with heat-absorbing fluid, which is used in a heat exchanger to produce steam. The steam expands in a steam turbine, which is the prime mover for a synchronous generator. Of similar design is the solar power tower which can generate large amounts of electricity using a tall, fluid-filled tower located at the focal point of a large field of mirrors (Farrent & Simões, 2006).

Solar power towers consist of a large field of sun-tracking mirrors, called heliostats, which focus solar energy on a receiver atop a centrally located tower. The enormous amount of energy, coming out of the sun rays, concentrated at one point (the tower in the middle), produces temperatures of approx. 550°C to 1500°C. The gained thermal energy can be used for heating water or molten salt, which saves the energy for later use. Heated water gets to steam, which is used to move the turbine-generator as depicted in Figure 3-3. This way thermal energy is converted into electricity.

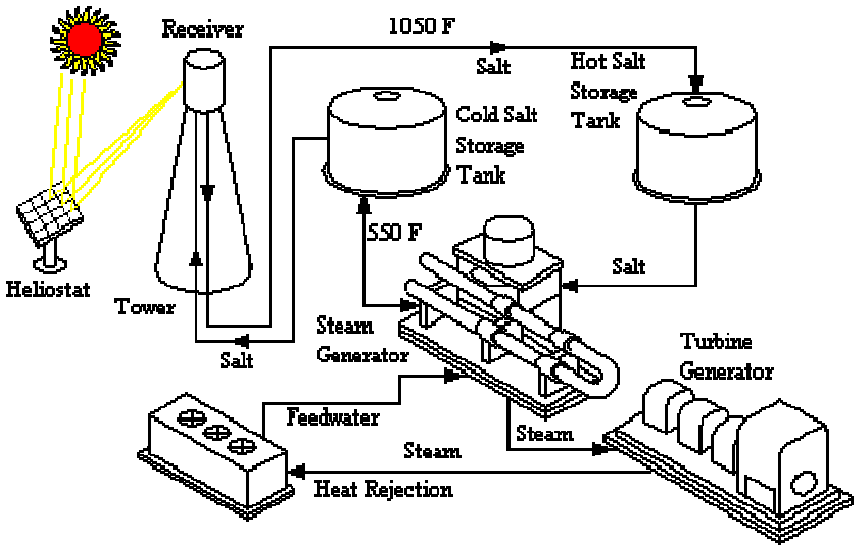

Figure 3-3: Concentrated solar power

Photovoltaic (PV) technology transforms the energy of solar photons into direct current using semiconductor materials. The smallest unit is called a solar cell or a PV cell. When photons enter the solar cell, electrons in the semiconductor material are freed, generating a DC current. The most common semiconductor materials used in PV cell manufacturing are single-crystal silicon, amorphous silicon, polycrystalline silicon, cadmium telluride, copper indium diselenide, and gallium arsenide. The most important PV cell technologies are crystalline silicon and thin films, including amorphous silicon (Sørensen, 2011; Vieira da Rosa, 2009).

PV cells connected together and sealed with an encapsulate form a PV module or panel. Their size ranges from a few watts to around 100W. Power-electronic converters convert the DC current output of a PV panel to AC current. Only a portion of the sunlight received by a PV cell is converted into electricity (Farrent & Simões, 2006).

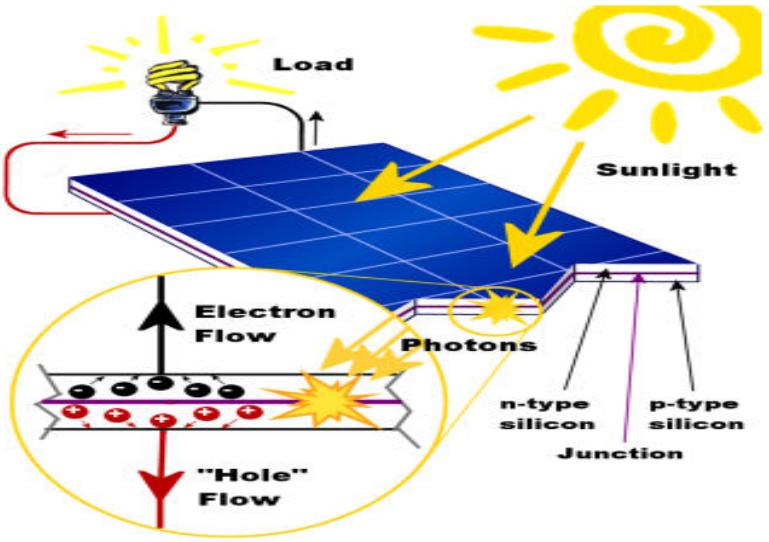

Figure 3-4: Photovoltaic effect and operation

3.2 Fuel cell system

Fuel cell is a device used to generate electric power and provide thermal energy from chemical energy through electrochemical processes. It can be considered as a battery supplying electric energy as long as its fuels are continued to supply. Unlike batteries, fuel cells do not need to be charged for the consumed materials during the electrochemical process since these materials are continuously supplied (keyhani, 2011).

Fuel cell generator is interfaced to the grid or load via power electronic converter: usually a voltage source inverter. However, in most applications a Dc-Dc converter is used to match the dc input voltage of the inverter since fuel cells is high current low voltage source. Being a dispatchable power source, fuel cells do not cause intermittent generation problems (Farrent & Simões, 2006; Sørensen, 2011; Vieira da Rosa, 2009).

3.4 Micro turbine system

Micro-turbines are small capacity combustion turbines, which can operate using natural gas, propane, diesel, kerosene and other hydrocarbon fuels to generate electrical power within 20-500 kW range. In a simple form, they consist of a compressor, combustor, heat recuperator, small turbine and generator. Single-shaft and split-shaft are two types of microturbines. Sometimes, they have only one moving shaft (Figure 3-5) and use air or oil for lubrication. Micro-turbine are small scale of 0,4-1,0 m^3 in volume and 20-500 kW in size. Unlike the traditional combustion turbines, micro-turbines run at less temperature and pressure and faster speed (up to 150 000 rpm), which sometimes require no gearbox. Output frequency of microrurbines is from about

400 Hz up to several kilo Hertz. It must be converted to 50/60 Hz using power electronics converter. The small size is a big advantage of these systems due to the use of high-speed turbines with airfoil bearings. Due to the relative low price of natural gas, low installation cost and low maintenance cost, micro-turbines are one of the most promising DG energy sources today (Sørensen, 2011; Vieira da Rosa, 2009).

A micro-turbine generator is interfaced to the grid or load via a power electronic converter; usually a voltage source inverter. However, the high frequency output of micro-turbines is decoupled from power the inverter by first converting it to Dc using a power rectifier circuit. Being a dispatchable source, micro-turbines do not cause intermittent problems (Farrent & Simões, 2006).

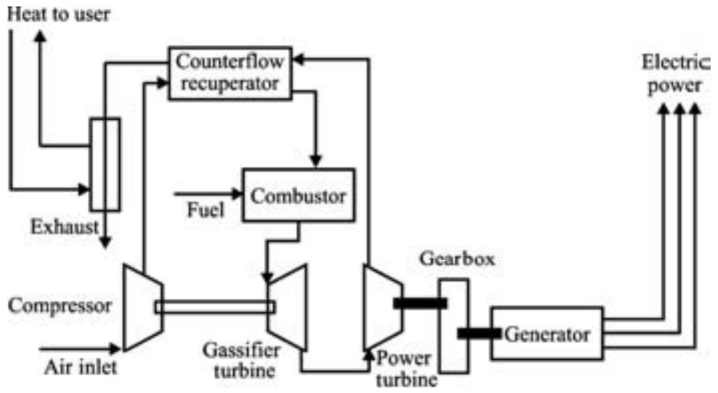

Figure 3-5 Single shaft microturbine

Microturbines have the following features:

- Size – They are relatively smaller in size as compared to other DERs.
- Fuel-to-electricity conversion – They can reach the range of 25–30%. However, if the waste heat recovery is used for CHP applications, energy efficiency levels are greater than 80%.
- NOx emissions – These are lower than 7 ppm for natural gas machines.
- Operational life – They are designed for 11,000 hours of operation between major overhauls with a service life of at least 45,000 hours.
- Economy of operation – System costs are lower than $500 per kW. Cost of electricity is competitive with alternatives including grid power for market applications.
- Fuel flexibility – It is capable of using alternative fuels, like natural gas, diesel, ethanol and landfill gas, and other biomass-derived liquids and gases.

- Noise level – It has reduced level of noise and vibrations.
- Installation – It has simpler installation procedure.

3.4 Combined heat and power system

In the early 1900s, most industries generated their own power and used the waste heat for supplemental thermal energy. This was the beginning of cogeneration. Combined heat and power or cogeneration systems are most promising as distributed energy resources for distributed generation applications. Their main advantage is the overall energy-efficient power generation by better utilisation of waste heat. Unlike fossil-fuelled power plants, combined heat and power systems capture and use the by-product heat locally for domestic and industrial/process heating purposes or district heat distribution system. Heat produced at moderate temperatures (100 – 180°C) can also be used in absorption chillers for cooling. Concurrent production of electricity, heat and cooling is known as trigeneration. By capturing the excess heat, combined heat and power system allows better usage of energy than conventional generation, potentially reaching an overall energy efficiency of more than 80%, compared with that of about 35% for conventional power plants. It is most efficient when the heat is utilised locally. Overall efficiency is reduced if heat is to be transported over long distances using heavily insulated pipes, which are both expensive and inefficient. On the other hand, electricity can be transmitted over much longer distances for lesser energy loss at the expense of transmission system infrastructure. Thus, combines heat and power plants can be located somewhat remotely from their electrical loads, but they must always be located close to the heat loads for better performance (Sørensen, 2011; Vieira da Rosa, 2009). Combined heat and power plants are commonly employed in district heating systems of big towns, hospitals, prisons, oil refineries, paper mills and industrial plants with large heat loads. Use of combined heat and power plants has been found to lead to 35% reduction in primary energy use as compared to conventional power generation and heat-only boilers, 30% reduction in emission with respect to coal-fired power plants and 10% reduction in emission with respect to combined cycle gas-turbine plants (Farrent & Simões, 2006).

3.5 Energy storage systems

Electrical energy storage has long been considered a very important technology in electric power system design, planning and operation for system reliability and stability purpose. At the onset of the twentieth century, electrochemical batteries and other forms of energy storage devices were used to power telephones and rotating generators to smooth out load variations.

Today, energy storage systems play the important role of unifying, distributing and augmenting the capabilities of alternative and renewable energy-distributed generating systems.

Energy storage technologies are classified according to the energy, time and transient response required for their operation. It is convenient to define storage capacity in terms of the time the normal energy capacity can cover the load at rated power.

Energy storage enhances DG in the following ways:

- It stabilizes and permits DG to run at a constant and stable output, despite load variations and required maintenance services.
- It provides energy to ride through instantaneous lacks of primary energy (such as those of sun, wind and small hydropower sources)
- It permits DG to operate seamlessly as a dispatchable unit.

Lead-Acid battery is used as an energy storage system in this project to function as described above.

Table 3-1 shows how storage objectives determine storage features in terms of time response requirement.

Energy storage for DG can be compared by parameters that define the performance criteria. These parameters are capacity, specific energy, energy density, specific power, efficiency, recharge rate, self-discharge, lifetime, capital cost and operating cost (Farrent & Simões, 2006).

Table 3-1 Functionality of Storage Systems

Storage Capacity	**Energy Storage Features**
Transient (microsecond)	• Compensate for voltage sags • Ride through disturbances (backup systems) • Improves harmonics distortion and power quality
Very short term (cycles of the grid frequency)	• Protect load during startup and synchronization of backup generator • Compensates transient response of renewable-based electronics converters • Increases system reliability during fault management • Keeps computer and telecommunication systems alive for safe electronic data backup
Short term (minutes)	• Protects load during short-term load peaks • Smooth renewable energy deficits for online capture of wind or solar power • Decreases needs for startup generator • Improves maintenance needs of fossil fuel-based generator • Allows ride through of critical medical, safety and financial procedures
Medium term(a few hours)	• Stores renewable energy surplus to be

	used at a later time • Compensates for load-leveling policies • Allows stored energy to be negotiated on net-metering basis • Integrates surplus energy with thermal systems
Long term (several hours to a couple of days)	• Stores renewable energy for compensation of weather-based changes • Possible elimination of fossil fuel-based generator backup • Provides reduction in fuel consumption and decreases waste of renewable energy • Produces hydrogen from renewable sources
Planning (week to months)	• Includes large power storage systems, such as pumped and compressed air systems • Uses fossil fuel storage to offset economic fluctuations • Stores hydrogen from biomass or renewable-based system

3.7.1 Electrochemical battery

The lead-acid battery is an electrochemical device invented by Planté in1859. It is made up of two electrodes that react with a sulfuric acid electrolyte. During discharge, both electrodes are converted to lead sulfate, as described by the following charge-discharge reaction:

$$\overset{\text{cathode}}{Pb} + 2H_2SO_4 + \overset{\text{anode}}{PbO_2} \underset{\text{charge}}{\overset{\text{discharge}}{\rightleftharpoons}} \overset{\text{cathode}}{PbSO_4} + 2H_2O + \overset{\text{anode}}{PbSO_4} \qquad 3\text{-}1$$

When the battery is charged, the anode is restored to lead dioxide and the cathode to metallic lead. However, irreversible changes in the electrodes limit the number of cycles, and failure may occur after a couple of thousand cycles, depending on battery design and depth of discharge.

Many rechargeable batteries are suitable for DG applications, but comprehensive descriptions are outside the scope of this thesis. The lead-acid is still the most common because of its relative economic power density. However, other technologies may surpass the lead-acid battery on the basis of energy density and lifetime. For example, nickel-cadmium batteries are common in applications that require sealed batteries capable of operating in any orientation with higher energy density. Other advanced batteries, such as nickel-metal hydride and several lithium technologies, may become cost-effective in the future for residential and commercial applications. The advantage and limitations of lead-acid batteries are listed in Table 3-2.

Table 3-2 Characteristics of Lead-Acid Battery

Advantages	**Limitations**
Inexpensive and simple to manufacture	Low energy density: poor weight-to-energy ratio limits use to stationary and wheeled applications
Mature, reliable and well-understood technology	Cannot be stored in discharged condition: cell voltage should never drop below 2,10V
When used correctly, durable and provides dependable service	Allows only a limited number of full discharge cycles: well suited for standby applications that requires only occasional deep discharge
Self-discharge is among the lowest of rechargeable battery systems	Lead content and acid electrolyte make them environmental unfriendly
Low maintenance requirements, no memory: no electrolyte to fill on sealed version	Transportation restriction on flooded lead-acid; environmental concerns regarding spillage
Capable of high discharge rate	Thermal runaway can occur with improper charging

3.7.2 Flywheel

There are two broad classes of flywheel energy storage technologies. One is a technology based on low-speed flywheel (up to 6000 rpm) with steel rotors and convectional bearings. The other one involves modern high-speed flywheel systems (up to 60 000 rpm) that are just becoming commercial and make use of advanced composite wheel that have much higher energy and power density than steel wheels. This technology requires ultralow friction bearing assemblies, such as magnetic bearings.

Most applications of flywheel in the area of renewable energy delivery are based on a typical configuration where an electrical machine (i.e. high-speed synchronous machine or induction machine) drives a flywheel, and its electrical part is connected back-to-back converter. Such configuration requires an adequate control strategy to improve power smoothing.

The basic operation could be summarized as follows. When there is excess in the generated power with respect to the demanded power, the difference is stored in the flywheel that is driven by the electrical machine operating as a motor. On the other hand, when a perturbation or a fluctuation in delivered power is detected in the load, the electrical machine is driven by the flywheel and operates as a generator supplying needed extra energy (Farrent & Simões, 2006).

3.7.3 Ultracapacitor

Ordinary capacitor store energy in the dielectric material at a value of $\frac{1}{2}CV^2$, where C is the capacitance (farad) and V (volt) is the voltage across its terminals. The maximum voltage of a regular capacitor is dependent on the breakdown characteristics of the dielectric material. The charge Q (coulombs) stored in the capacitor is given by $Q = CV$. The capacitance of the dielectric capacitor depends on the dielectric constant (ε) and the thickness (*d*) of the dielectric plus its geometric area.

$$C = \varepsilon \frac{A}{d} \qquad 3\text{-}2$$

Electric double-layer capacitor with very large capacitance values has been developed. Those capacitors are frequently called supercapacitor, ultracapacitor or electrochemical capacitors. The term ultracapacitor is used in this thesis because the power industry seems to use it more frequently. An ultracapacitor is an electrical energy storage device that is constructed much like

a battery because it has two electrodes immersed in an electrolyte with a separator between them. The electrodes are fabricated from porous high-surface-area material that has pores of diameter in the nanometer range. Charge is stored in the micropores at or near the interface between the solid electrode material and the electrolyte. The charge and energy stored are given by the same expressions as those for ordinary capacitor, but the capacitance depends on complex a phenomenon that occurs in the micropores of the electrodes. Construction details of a double-layer ultracapacitor contrasted with ordinary capacitor. The capacitor contains two particulate-carbon formed on conductive-polymer films. An ion-conductive membrane separates the two electrodes and a potassium hydroxide electrolyte permeates the capacitor. The micropores in the carbon particulates result in an enormous surface areas and yield extremely high capacitance values, which convectional capacitor cannot sustain (Farrent & Simões, 2006).

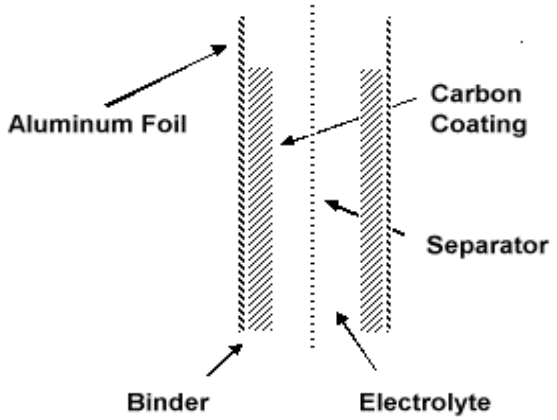

Figure 3-6 Double-layer ultracapacitor construction details

3.7.4 Superconducting magnetic energy storage system

Superconducting magnetic energy storage (SMES) system is well suited to storing and discharging energy at high rates (high power.) It stores energy in the magnetic field created by direct current in a coil of cryogenically cooled, superconducting material. If the coil were wound using a conventional wire such as copper, the magnetic energy would be dissipated as heat due to the wire's resistance to the flow of current. The advantage of a cryogenically cooled, superconducting material is that it reduces electrical resistance to almost zero. The SMES recharges quickly and can repeat the charge/discharge sequence thousands of times without any degradation of the magnet. A SMES system can achieve full power within 100 ms. Theoretically, a coil of around 150–500 m radius would be able to support a load of 18,000 GJ at 1000 MW,

depending on the peak field and ratio of the coil's height and diameter.3 Recharge time can be accelerated to meet specific requirements, depending on system capacity.

Because no conversion of energy to other forms is involved (e.g., mechanical or chemical), the energy is stored directly and round-trip efficiency can be very high. SMES systems can store energy with a loss of only 0.1%; this loss is due principally to energy required by the cooling system. Mature, commercialized SMES is likely to operate at 97%–98% round-trip efficiency and is an excellent technology for providing reactive power on demand.

3.7.5 Compressed air energy storage system

Energy storage in compressed air is made using a compressor that stores it in an air reservoir (i.e. an aquifer like the ones used for natural-gas storage, natural caverns, or mechanically formed caverns, etc.). When a grid is operating off peak, the compressor stores air in the air reservoir. During discharge at peak loads, the compressed air is released to a combustor where it is mixed with oil or gas driving a turbine. Such system are available for 100-300 MW and burn about one-third of the premium fuel of a conventional simply cycle combustion turbine (Keyhani, 2011).

An alternative to compressed air energy storage (CAES) is the use of compressed air in vessels, which operate exactly in the same way as CAES except that the air is stored in pressure vessels rather than underground reservoir. Such difference makes possible variations consisting of the use pneumatic motor acting as compressors or driving a dc motor/generator according to the operation required by the system, i.e., storing energy when there is no extra demand of energy or delivering extra power at peak loads (Farrent & Simões, 2006).

3.8.6 Tidal power

The moon and sun's gravitational fields cause the natural rise and fall of coastal tidal waters. Since the moon is closer to the earth. Albeit much less massive, it has a dominant effect upon tides. As the moon is 2,2 times more influential than the sun, it could be considered that tidal energy is mostly a form of lunar energy (Sørensen, 2011; Vieira da Rosa, 2009).

The earth rotates on its axis once every 24 hours. In the earth's frame of reference the sun orbits the earth once every 24 hours. The moon orbits the earth once every 29 days approximately. In the earth frame of reference, the moon appears to orbit the earth once every 24 hours and 50 minutes. This difference in periods between the apparent orbits of the sun and moon leads to

phase change with larger spring tides during in-phase behavior and smaller neap tides when the sun and moon are out of phase (Keyhani, 2011).

Constructing a barrage across an estuary and allowing tidal waters alternately to fill the estuary through sluice gates and then empty it through turbines can generate energy. A barrage constructed across an estuary is equipped with a series of gated sluices and a bank of low head axial turbines. Where it is necessary to maintain navigation to the upper part of the estuary, a ship-lock may be required.

Tidal barrage are a currently available technology, but very few exist worldwide. The best known example is the 240 MW scheme at La Rance in France, and smaller installations have been made in Nova Scotia, Russia and China.

One of the main disadvantages of tidal schemes is pulsed nature of their electrical output. The technology to extract energy from tidal current is conceptually simple: a turbine is placed in a suitable tidal flow, which turns the generator through a gearbox as shown in Figure 3-7. It is similar to a submerged wind turbine, except that the greater specific gravity of seawater results in much higher energy densities in tidal streams than is found in winds of the same velocity. However, the water velocities available in tidal streams (typically rated velocities of 2-3m/s on good sites) are much lower than the air velocities used by wind turbines. Although power output is proportional to be cube of the velocity, tidal stream rotors generally produce significantly greater power than wind turbine of the same size because of the massively increased water density. Compared to wind, tidal flow velocity are expected to have little turbulence and thus vary in a smooth manner, reducing fatigue loads on the rotor and generating electricity with little short time variation (Farrent & Simões, 2006).

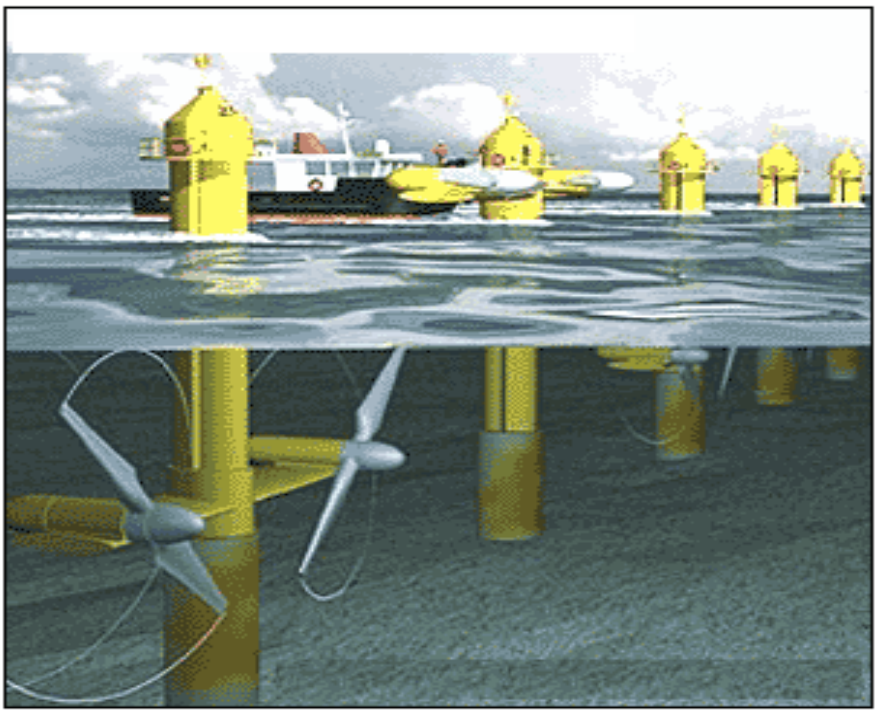

Figure 3-7: Artist's impression of axial tidal current turbines

3.8.7 Wave power

Very large energy fluxes can occur in deep water sea waves. The power in the wave is proportional to the square of the amplitude and to the period of the motion. Therefore the long period approximately 10 seconds, large amplitude approximately 2m waves have considerable interest for power generation, with energy fluxes commonly averaging between 50 kWm^{-1} and 70kWm^{-1} width of oncoming wave (Sørensen, 2011; Vieira da Rosa, 2009).

The possibility of generating electrical power from these deep water waves has been recognised for many years, and there are countless ideas for machines to extract the power. Very small scale autonomous systems are used for marine warning lights on buoys and much larger devices for grid power generation. The provision of power for marine desalination is an obvious attraction. As with all renewable energy supplies, the scale of operation has to be determined, and present trends support moderate power generation at about 100 kW–1MW from modular devices each capturing energy from about 5m to 25m of wave front. Initial designs are for operation at shore-line or near to shore to give access and to lessen, hopefully, storm damage. It is important to

appreciate the many difficulties facing wave power developments. These may be summarised here:

- Wave patterns are irregular in amplitude, phase and direction. It is difficult to design devices to extract power efficiently over the wide range of variables.
- There is always some probability of extreme gales or hurricanes producing waves of anomaly intensity. The structure of the power devices must be able to withstand this. Commonly the 50 year peak wave is 10 times the height of the average wave. Thus the structures have to withstand ~100 times the power intensity to which they are normally matched. Allowing for this is expensive and will probably reduce normal efficiency of power extraction.
- Peak power is generally available in deep water waves from open-sea swells produced from long fetches of prevailing wind, e.g. beyond the Western Islands of Scotland (in one of the most tempestuous areas of the North Atlantic) and in regions of the Pacific Ocean. The difficulties of constructing power devices for these types of wave regimes, of maintaining and fixing or mooring them in position, and of transmitting power to land, are fearsome. Therefore more protected and accessible areas near to shore are most commonly used.
- Wave periods are commonly ~5–10 s (frequency ~0_1Hz). It is extremely difficult to couple this irregular slow motion to electrical generators requiring ~500 times greater frequency.
- So many types of device may be suggested for wave power extraction that the task of selecting a particular method is made complicated and somewhat arbitrary.
- The large power requirement of industrial areas makes it tempting to seek for equivalent wave energy supplies. Consequently plans may be scaled up so only large schemes are contemplated in the most demanding wave regimes. Smaller sites of far less power potential, but more reasonable economics and security, may be ignored.
- The development and application of wave power has occurred with spasmodic and changing government interest, largely without the benefit of market incentives. Wave power needs the same learning curve of steadily enlarging application from small beginnings that has occurred with wind power.

The distinctive advantages of wave power are the large energy fluxes available and the predictability of wave conditions over periods of days. Waves are created by wind, and effectively store the energy for transmission over great distances (Farrent & Simões, 2006).

3.8.8 Biomass

Any biomass-based energy process begins with the capture of sunlight and production of a chemical compound. This complicated step, called photosynthesis, leads basically to glucose. Subsequent biochemical transformations result in the creation of a very large number of compounds, some of very great commercial value. At best, photosynthesis proceeds with efficiencies of less than 8%. By the time the final product is available for consumption, large chunks of energy have been spent in cultivation, fertilizing, harvesting, transporting the raw biomass, removing the excess water, and extracting the desired fuel. The overall efficiency is usually a fraction of 1%. This is a prime example of practical energy processes that, though extremely inefficient, are of commercial interests mainly because the economic and ecological aspects are favourable (Sørensen, 2011; Vieira da Rosa, 2009).

Different types of biomass can be used for making energy in biomass power plants. When used in this manner for commercial or home energy. Biomass originates from the following sources: agricultural crop waste (called bagasse), horticulture waste, wood and charcoal, pulp processing sludge, municipal solid waste (MSW), wastewater treatment solids, animal waste, and landfill waste. Sometimes used vegetable oils and animal fats also fit into the category of energy-producing biomass. Biomass energy offers an advantage because it can be almost any solid material that when burned releases a usable form of energy. The main types of biomass used throughout the world differ in source so they contain various constituents, which make them more or less efficient as energy sources (Farrent & Simões, 2006).

3.8.9 Small-scale hydroelectric power generation

The small-scale hydroelectric generators are effectively used for generating power onsite in distributed generation application. Extent of generation depends on the topography of an area and its annual precipitation (i.e. rainfall). These generators suffer from occasional large variations in generation due to variable water flow caused by uneven rainfall (Sørensen, 2011). This is particularly true for hydro power stations, which do not have their own storage reservoirs and for which the catchment area is spread over rocky soil without vegetation cover. Variable

water resources also lead to varying generation with a low capacity factor. The power output from a hydro turbine is given by

$$P = QH\eta\rho g \qquad 3\text{-}3$$

where P is power output (W), Q is water flow rate (m^3/s), H the effective head (m), η is the overall efficiency, ρ the water density (1000 kg/m^3) and g is the acceleration due to gravity. Equation $P = QH\eta\rho g$ 3-3 indicates that the power output can be increased by increasing both effective head and water flow rate. Penstock is the pipeline through which water is brought to the turbine (Vieira da Rosa, 2009). The cross section of the penstock is suitably designed for optimum water flow rate. Various types of water turbines are used depending on available water heads and flow rates. Usually, reaction turbines operate at lower heads (for example, Francis and Kaplan turbines) and the impulse turbines (for example, Pelton wheels) operate at higher heads. Reaction turbines extract energy from pressure drop whereas impulse turbines extract power from the kinetic energy of water jets at atmospheric pressure. Cross-flow impulse turbines are used for small hydro units where kinetic energy is extracted from water striking the turbine blades as a water sheet rather than a jet. Both synchronous and induction generators may be used for small-scale hydro generation with suitable multiple-ratio gearboxes (Farrent & Simões, 2006).

4.1 Photovoltaic cells modelling and analysis

Many different models have been proposed in the literature capturing specific details of PV cell for different parametric investigations. The single diode electrical model is detailed and used in this dissertation for the investigation of different transformerless PV topologies in chapter 6. The equivalent electrical circuit of a single PV cell is represented in figure 4.1 where the following equation can be easily derived:

$$I_o = I_\lambda - I_d - I_p \qquad 4\text{-}1$$

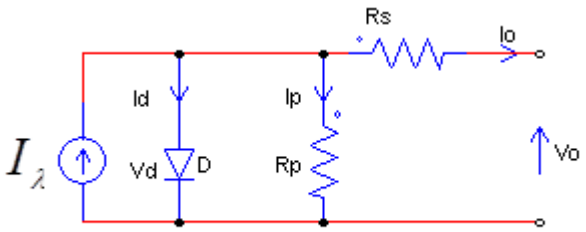

Figure 4-1Single diode electrical equivalent model

Where

I_λ = photon current, which depends on the ligth intensity and its wavelength
I_d = Shockley temperature-dependent diode current
I_p = PV cell leakage current
I_o = outpout current of the PV cell

The photon current is proportional to the illumination intensity and depends on the light wavelength, λ. The parameters of this current are related to the cell short-current, I_{sc}, and the open-circuit voltage, V_{oc}. The short-circuit current may be obtained from the I-V characteristic for a given solar cell when the PV cell output voltage is zero. In turns, the open-circuit voltage is obtained for zero output current that is under no load.

In addition, if the photon current is known for certain standard illumination intensity (say $L_s = 1$ sun) and a prescribed photon current of $I_{\lambda o}$, it is possible to obtain the photon current

approximately for every other level of illumination value if a linear relationship is assumed through the expression

$$I_\lambda = \frac{L}{L_s} I_{\lambda o} \qquad 4\text{-}2$$

The Shockley diode equation is given by the classical expression

$$I_d = I_s \left(e^{qV_d/\eta KT} - 1 \right) \qquad 4\text{-}3$$

Where

$I_s =$ reverse saturated current of the diode, typically 100 pA for the silicon diode

$K =$ $1{,}38047 \times 10^{-23}$ J/K is the Boltzmann constant

$q =$ $1{,}60210 \times 10^{-19} C$ is the electron charge

$V_d =$ diode volatge (V)

$\eta =$ empirical constant

$T =$ is the absolute temperature (K)

A parallel resistance R_p can represent the internal lossess, or leakage current, through the Schockley diode. These values usually range between 200 and 300 Ω. Also, there is a series resistance between the phone current source and the load, R_s. The usual value of this resistance is very small (0,05 to 0,10 Ω), reflecting directly on the manufacturing quality of the PV cells. Under these circumstances, equation 4.1 becomes

$$I_0 = I_\lambda - I_s \left(e^{qV_d/KT} - 1 \right) - \frac{V_d}{R_p} \qquad 4\text{-}4$$

The diode voltage is $V_d = I_o(R_s + R_L) = V_o(1 + R_s / R_L)$, being a function of the load resistance, R_L, and for this reason of the cell output power. Therefore, substituting V_d in equation 4-4, more precise output current can be obtained from

$$I_o = \frac{R_p}{R_p + R_s + R_L} \left[I_\lambda - I_s (e^{qV_d/KT} - 1) \right] \qquad 4\text{-}5$$

For large values of the load resistance with respect to the parallel resistance of the PV cell, difference in the output current values become remarkable.

It is very important to use the empirical factor, η, in the exponential term of either equations 4-4 or 4-5, so that they can be adjusted to the practical data from the manufacturer. The adjusted forms of these equations are, respectively,

$$I_0 = I_\lambda - I_s\left(e^{qV_d/\eta KT} - 1\right) - \frac{V_d}{R_p} \qquad 4\text{-}6$$

$$I_o = \frac{R_p}{R_p + R_s + R_L}\left[I_\lambda - I_s(e^{qV_d/\eta KT} - 1)\right] \qquad 4\text{-}7$$

The diode voltage and the open-circuit voltage change with the load current. For the very particular case when the output current is zero in an illumination panel, the single-cell open-circuit voltage may be obtained from equation 6-6 as

$$I_o = V_d\big|_{I_o=0} = (I_\lambda - I_d)R_p = \left[I_\lambda - I_s(e^{qV_d/\eta KT} - 1)\right]R_p$$

where the logarithmic simplified form is 4-8

$$\mathrm{V}_o = \frac{KT}{\eta q} In\left(1 + \frac{I_\lambda}{I_s} - \frac{V_{oc}}{I_s R_p}\right)$$

This is a transcendental equation that can be solved numerically. However, as V_{oc} is on the order of 0,6 V, R_p is on the order of 300 Ω and has opposite sign. Then

$$V_{oc} \approx \frac{KT}{\eta q} In \frac{I_\lambda}{I_s} \qquad 4\text{-}9$$

As the series resistance of a PV cell is very small (on the order of 0,1 Ω), when the cell is short-circuited, practically the only opposition to the current through is R_s. So the short-circuit current can be given by

$$I_{sc} \approx I_\lambda \qquad 4\text{-}10$$

The output power of the PV cell is the product of V_o by the output current given by equation 4-7, which gives

$$P_o = I_o = \frac{V_o R_p}{R_p + R_s + R_L}\left[I_\lambda - I_s (e^{qV_o(1+R_s/R_L)/\eta KT} - 1) \right] \qquad 4\text{-}11$$

The maximum power may be obtained by differentiating equation 4-11 with respect to V_o and setting the derivative equal to zero to find the external load voltage V_{om} for the maximum output power of the PV cell, which must satisfy

$$I_s e^{qV_{om}(1+R_s/R_L)/\eta KT} = \frac{I_\lambda + I_s}{1 + V_{om}^{qV_{om}(1+R_s/R_L)/\eta KT}} \qquad 4\text{-}12$$

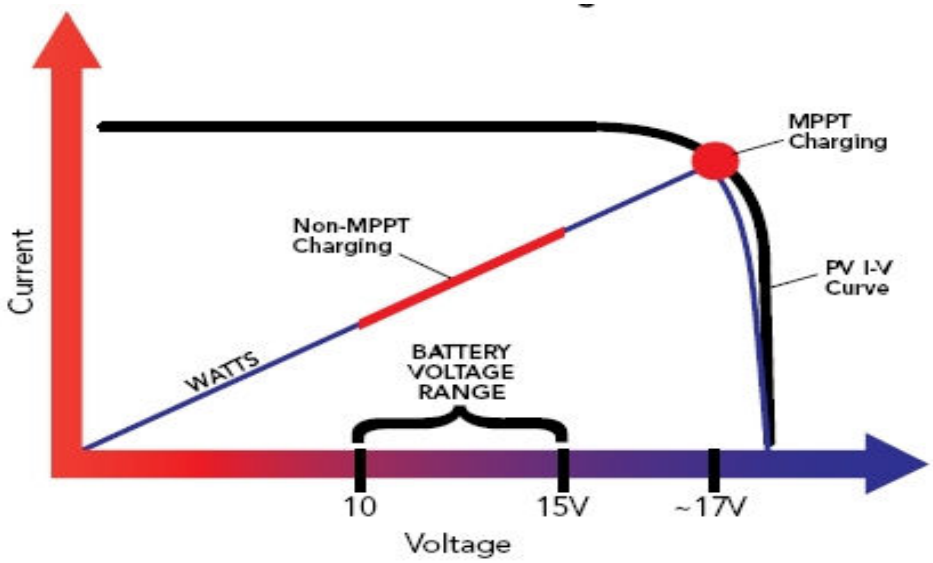

Figure 4-2 Maximum power point

Another way of doing this is by plotting equation 4-11 as shown in figure 4-2 and obtains its maximum graphically. The maximum power may be given by

$$P_m = \frac{V_{om}(I_s + I_\lambda)}{1 + \eta KT / qV_{om}(1 + R_s / R_L)} \qquad 4\text{-}13$$

If the incident flux power, P_i, on the cell is known, the conversion efficiency for the maximum power becomes

$$P_m = \frac{P_m}{P_i} = \frac{V_{om}(I_s + I_\lambda)}{P_i\left[1 + \eta KT / qV_{om}(1 + R_s / R_L)\right]} \qquad 4\text{-}14$$

4.2 Simulations and validation Results

The goal of this sub section is to verify and validate the PV system installed in the Centre for Distributed Power Electronics System at Cape Peninsula University of Technology. A typical PV system has different blocks: the PV module, DC-DC stage, charge controller, energy storage, power decoupling and the DC-AC converter as shown in figure 4-3.Computer simulation methods offer a powerful tool for the analysis of renewable energy systems, due to the possibility of reproducing the performance of a system on the computer. The philosophy behind digital simulation is that experiments which normally should be done on real systems, under high assembling costs and time consuming conditions, can be done numerically in a short time on a computer, thus saving time and investments.

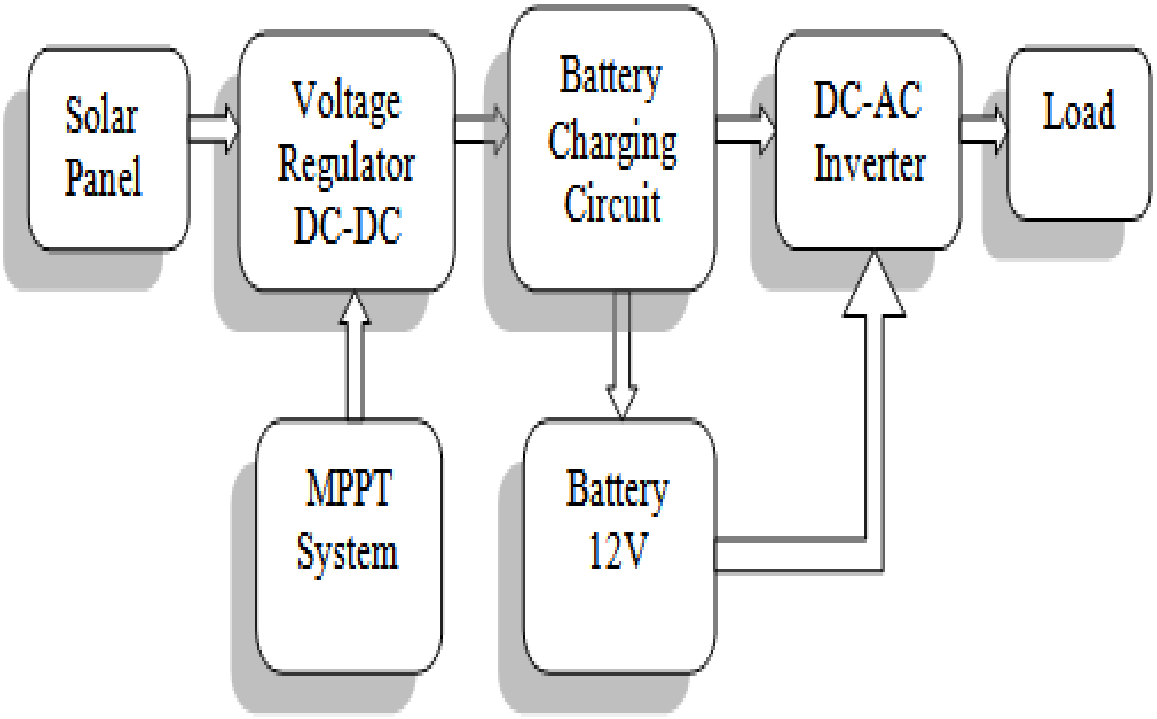

Figure 4-3 Schematic of the PV system modelled

Basis for computer simulation is a 'model' of a real system which is based on a theoretical analysis of the various physical processes occurring in a system, and of all factors influencing

those processes. Mathematical equations (mathematical models) describing quantitatively the system characteristics are formulated from this analysis and translated into computer codes to be used in the simulation process.

Digital simulation serves for the purpose of understanding the operational behaviour of these components and the interaction among them, since by simulating the system performance; one can trace all steps of energy conversion and identify the losses throughout the system in detail. Computer simulation allows a range of system parameters to be varied, and the operating characteristics of the system to be investigated as a function of these parameters, it also may be helpful for optimization in the design process of such systems. Another use of computer simulation is in the evaluation of operation strategies for the control of a system and permits the extrapolation of a system design to other localities, with different meteorological conditions and makes it possible to compare different systems.

The physical model in PSim was used for the verification and validation of the PV panels. Figure 4-4 shows the GUI input parameters palette for the PV panel.

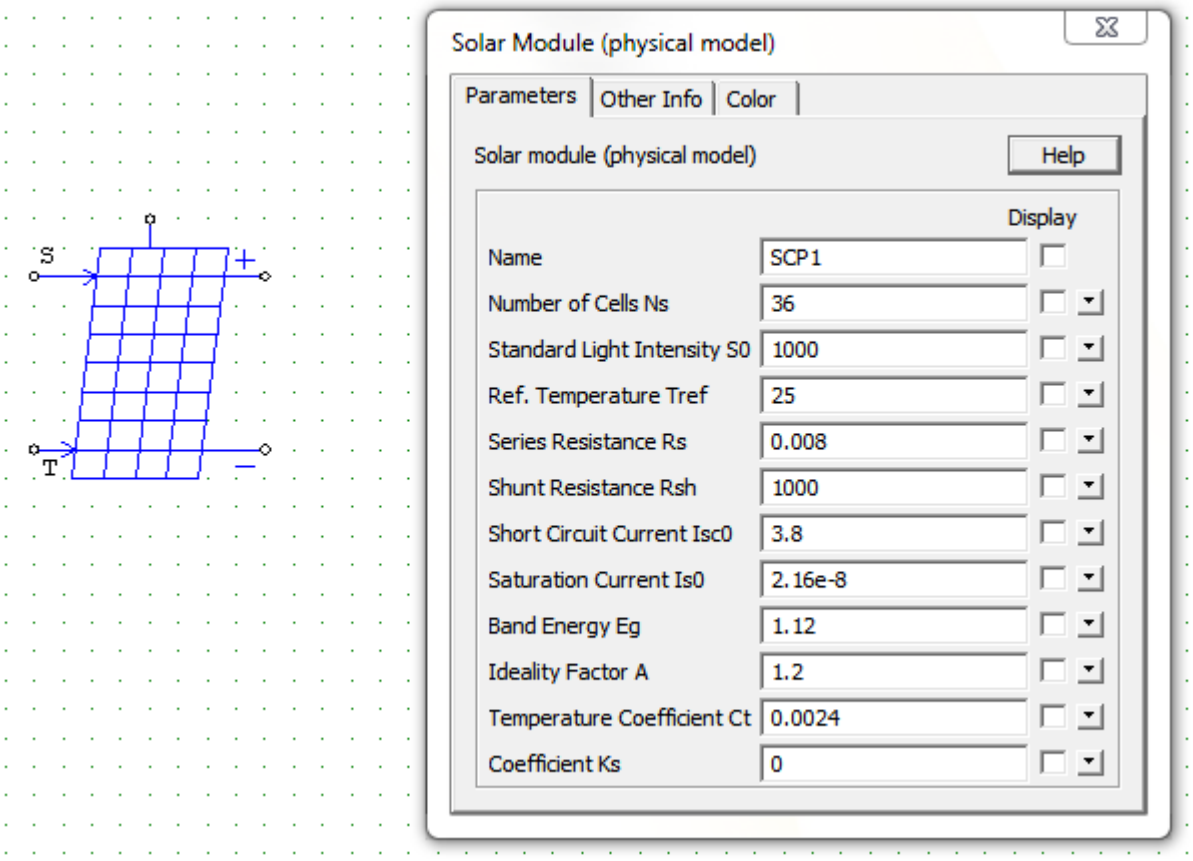

Figure 4-4 PSIM PV panel physical model

Figure 4-5 CDPES PV system setup

Figure 4-6: Solar panels mounted on the roof of electrical engineering department CPUT

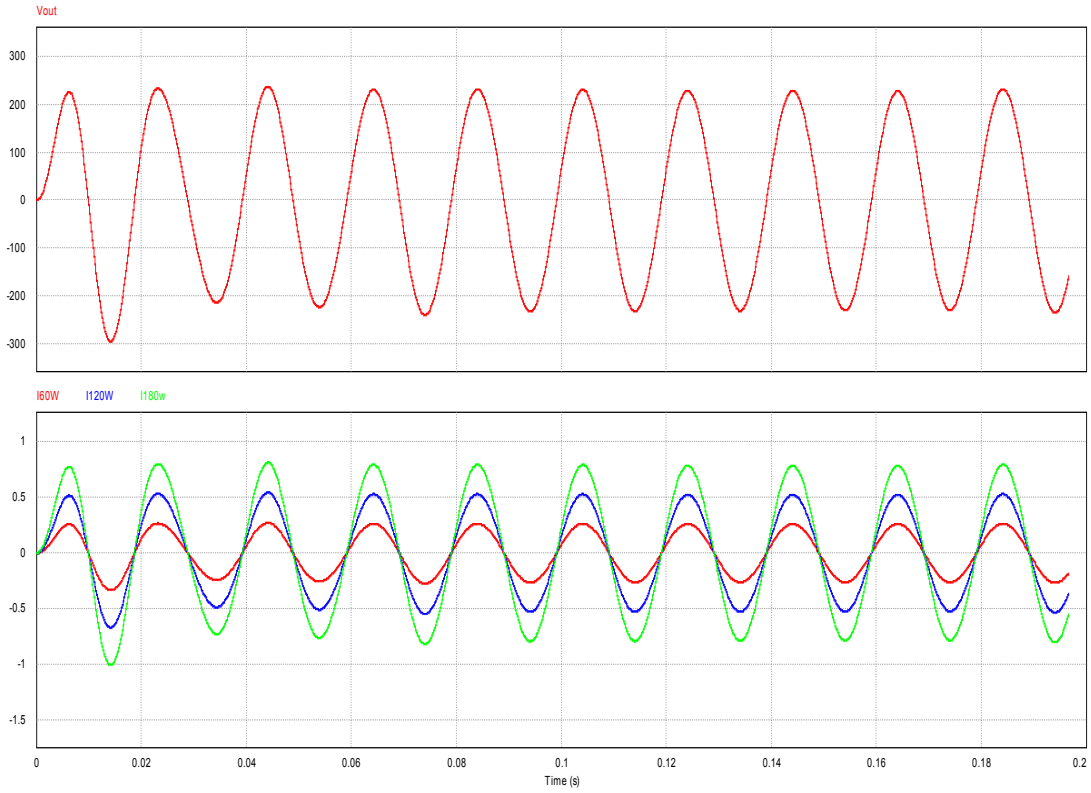

Figure 4-7 Output voltage and current waveforms of the simulated model

Table 4-1 PV system theoretical calculations

Load (W)	Voltage (Vrms)	Current (mA)	Power (W)
60	230	261	60
120	230	522	120
180	230	783	180

Table 4-2 PV system simulated results

Load (W)	Voltage (Vrms)	Current (mA)	Power (W)
60	228.8	259.5	59.37
120	228.8	519.1	118.77
180	228.8	778.4	178.09

Table 4-3: PV system experimental works results

Load (W)	Voltage (Vrms)	Current (mA)	Power (W)
60	229	240	54.96
120	230	460	105.8
180	229	730	169.17

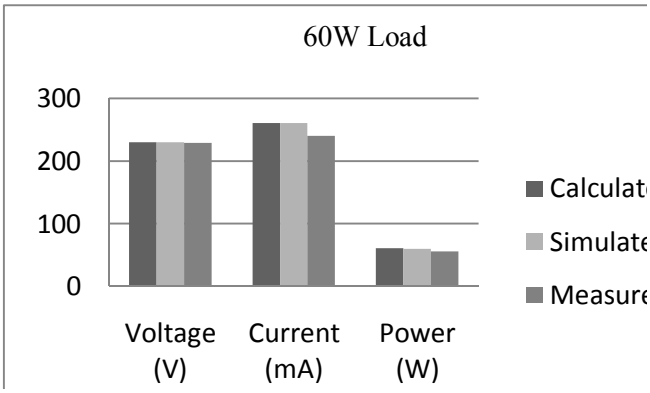

Figure 4-8 60W Linear load

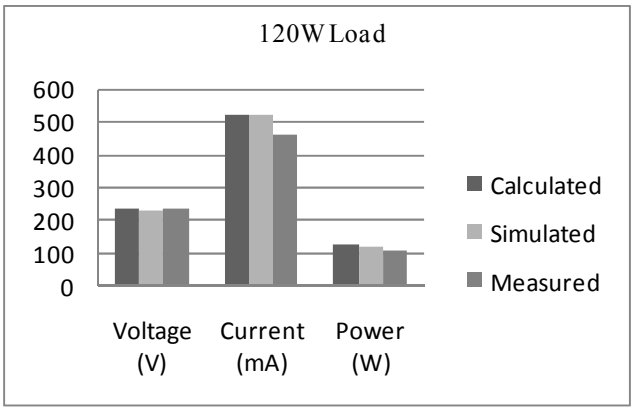

Figure 4-9 120 W Linear load

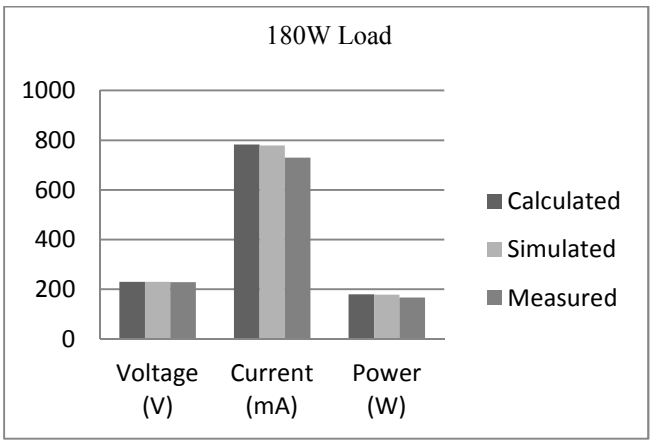

Figure 4-10 180 W Linear load

The results obtained for the system theoretical calculations and simulation results agree with the experimental work carried in the laboratory.

4.3 Common mode voltage and ground leakage current analysis

Leakage current is the current that flows through the protective ground conductor to ground. In the absence of a grounding connection, it is the current that could flow from any conductive part or the surface of non-conductive parts to ground if a conductive path was available (such as a human body).

When no transformer is used, a galvanic connection between the ground of the grid and the PV array exits through the parasitic capacitance. As a result, a common mode resonant circuit appears. This resonant circuit consists of the parasitic capacitance of the PV array, the ground, the dc and ac filter elements and the grid impedance as shown in figure 4-11.

Most photovoltaic panels have a metallic structure, which is required to be earthed in almost all countries, in order to comply with the safety regulations and standards. Since PV panels have a considerable surface area, this with the metallic frame forms a stray capacitance which is environmentally dependent, shown as $C_{G\text{-}PV}$ in Fig. 4-12

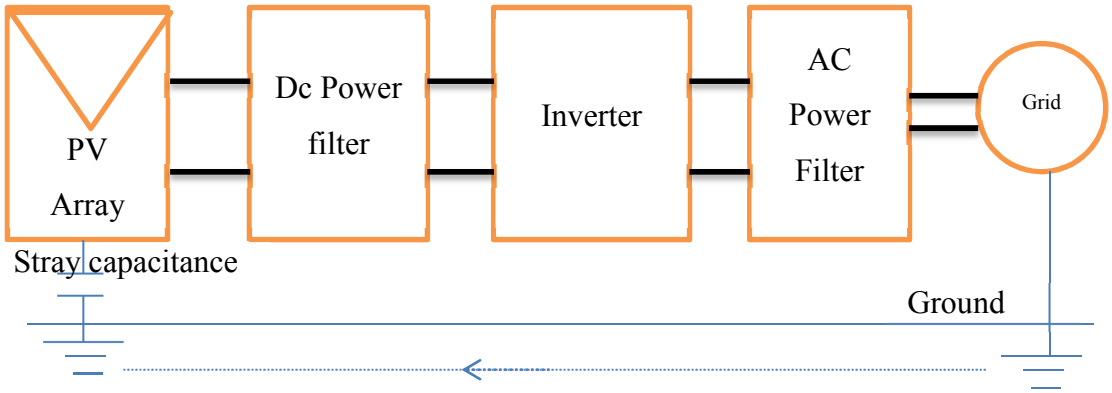

Figure 4-11 Common mode current in a transformerless system

A varying common-mode voltage depends on many factors as listed below:

- PV panel
- Frame structure
- Surface of cells
- Distance between cells
- Module frame
- Weather conditions
- Humidity and dust covering the PV panel

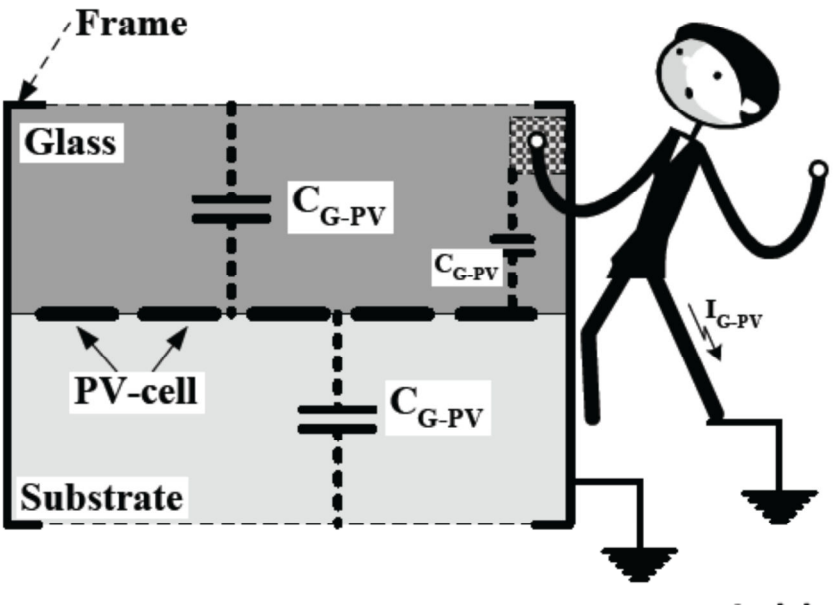

Figure 4-12 Parasitic capacitance in PV

In (Kerekes et al 2007), it is mentioned that a typical value of 100-200 pF exist between the PV cells and the ground. But on condition that the surface of the panel is covered with water, this parasitic capacitance will increase to 9 nF, 60 times its previous value. In case of a solar array having a considerable surface, the resulting stray capacitance will have value between 50-150 nF/kW, depending on the weather conditions and panel structure.

According to the German DIN VDE 0126-1-1 standards, in case of transformerless PV inverters connected to the grid, it is mandatory to install a Residual Current Monitoring Unit (RCMU) which is sensitive to both AC and DC currents and can as well sense DC fault currents. It must be possible to disconnect PV systems from the grid within 0,3 second when the leakage current with respect to the ground is greater than 300 mA.

In the single-phase full bridge circuit it is possible to eliminate leakage current by making the common mode voltage constant.

Most photovoltaic panels have a metallic frame, which is required to be grounded in almost all countries, in order to comply with the safety regulations and standards. Since PV panels have a considerable surface area, this with the metallic frame forms a parasitic capacitance, shown as C_{G-PV} in Fig. 4-12

4.3.1 Simplified common mode leakage current model

In full bridge circuit shown in figure 4-12, voltages VAO and VBO are controlled by the four switches S1, S2, S3 and S4.

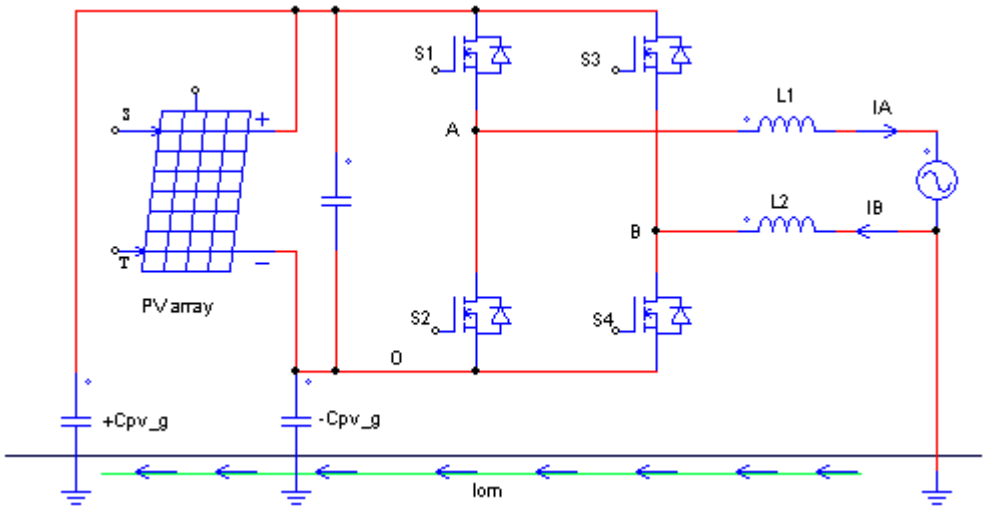

Figure 4-13 Common mode leakage current model of single phase full bridge inverter

When the upper switch is on, the corresponding voltage is equal to VDC while the lower switch corresponding voltage is zero (reference O). Therefore we can replace the DC bus and switches with two PWM voltage sources as shown in figure 4-13.

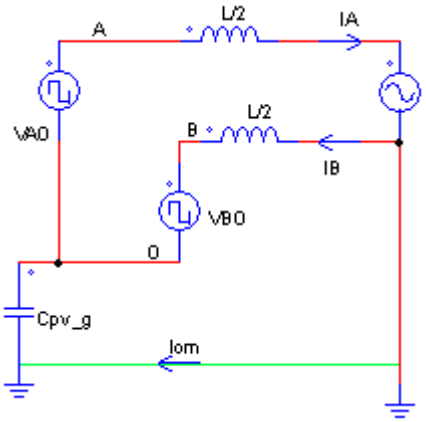

Figure 4-14 Simplified common mode leakage current mode of a single-phase full bridge inverter

According to the superposition theorem, the total leakage current is the sum of the currents generated by the grid and the two PWM voltage sources. Figure 4-14 shows the leakage current

generated by the grid. The leakage current generated by the two PWM voltage sources is shown in figure 4-15.

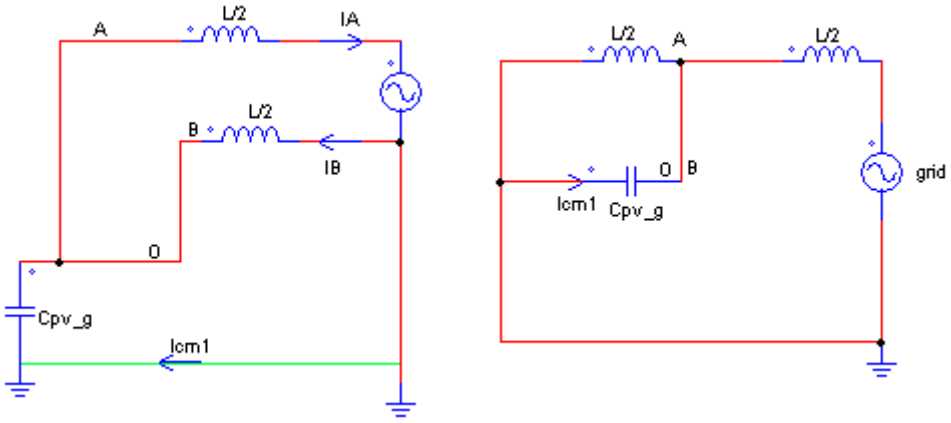

Figure 4-15 Equivalent circuit model of the leakage current generated by the grid

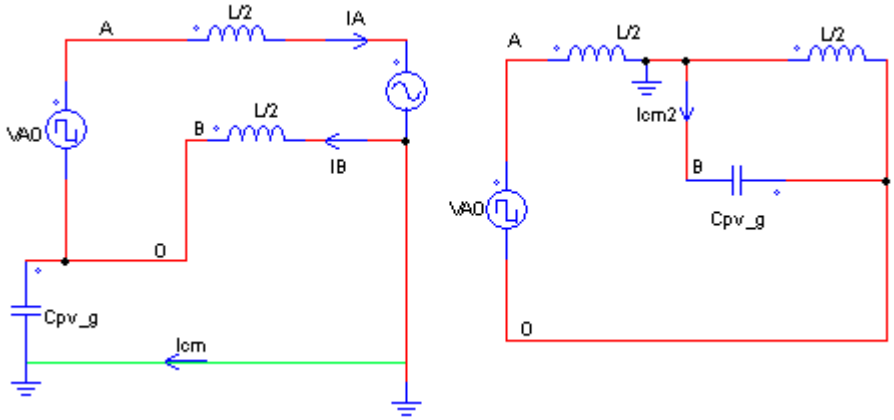

Figure 4-16 Equivalent circuit of the leakage current generated by the two PWM voltage sources.

As shown in figure 4-15, the leakage i_{cm1} generated by the grid can be given as:

$$i_{cm1} = \frac{-\frac{1}{2} j v_{grid}}{-\frac{1}{4}\omega_{grid} L + \frac{1}{\omega_{grid} C_{pv\_g}}} \qquad 4\text{-}15$$

As shown in figure 4-16, the leakage i_{cm2} and i_{cm3} generated by the PWM voltage sources can be given as:

$$i_{cm2} = \frac{\frac{1}{2} j v_{AO}}{-\frac{1}{4}\omega L + \frac{1}{\omega C_{pv\_g}}} \qquad 4\text{-}16$$

$$i_{cm3} = \frac{\frac{1}{2} j v_{BO}}{-\frac{1}{4}\omega L + \frac{1}{\omega C_{pv\_g}}} \qquad 4\text{-}17$$

Compared to the switching frequency, the grid frequency is low, thus I_{cm1} can be ignored. In many literatures the leakage current caused by the grid is not discussed, but it truly exists even when the common mode voltage is kept constant during all commutation states.

Combining equations 4-16 and 4-17, the total leakage current i_{cm} and common mode voltage v_{cm} are given in equations 4-18 and 4-19 respectively.

$$i_{cm} = \frac{j v_{cm}}{-\frac{1}{4}\omega_{cm} + \frac{1}{\omega_m C_{pv\_g}}} \qquad 4\text{-}18$$

$$v_{cm} = \frac{1}{2}\left(v_{AO} + v_{BO}\right) \qquad 4\text{-}19$$

According to equation 4-19, the equivalent circuit model of common mode leakage current can be obtained as shown in figure 4-17.

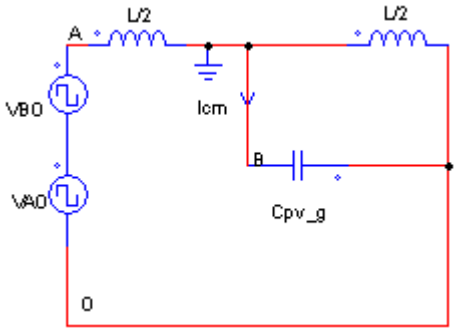

Figure 4-17 Equivalent circuit of the common mode leakage current model

As shown in figure 4-17 it is concluded that if the common mode voltage is kept constant during all the commutation states, leakage current could be restricted to nearly zero (assuming that the leakage current contributed by the grid is negligible).

Chapter 5 : TRANSFORMERLESS GRID CONNECTED PHOTOVOLTAIC INVERTERS

5.1 Photovoltaic power conversion technology

PV power conversion systems can be divided into two types. One set of PV power converters possess DC-DC converter for voltage matching for the power inverter system to operate efficiently and or implement maximum power point algorithm. The maximum power point algorithm ensures that maximum is extracted from the PV panel under different irradiance levels. If this DC-DC converter is not present, then the MPPT function can be shifted to the inverter stage. The connection between the Dc side and AC the grid can be galvanically isolated or connected by using transformers. Figures 5-1 shows how PV power conversion system is categorized.

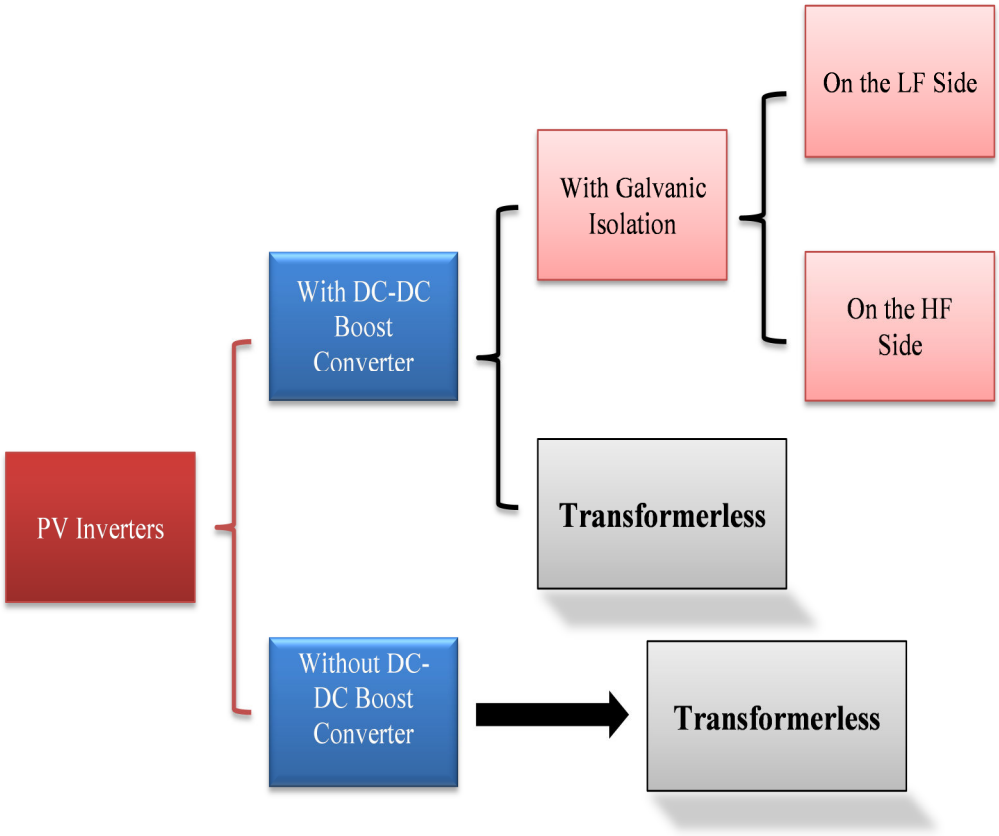

Figure 5-1 PV inverter technologies

If a high switching frequency transformer is to be deployed then the galvanic isolation is performed within the DC-DC conversion stage. A line frequency transformer is implemented at the output of the inverter stage. This transformer inclusion causes the system overall efficiency to decrease as well as increasing the system installation cost. The size, weight, volume are other factors that may make line frequency transformer undesirable in PV power conversion system.
A grid-connected transformerless PV power conversion system is shown in figure 5-2. The grid side controller is used to ensure that the injected grid current comply to the grid codes and standard in term of power quality while the input controller may include MPPT.

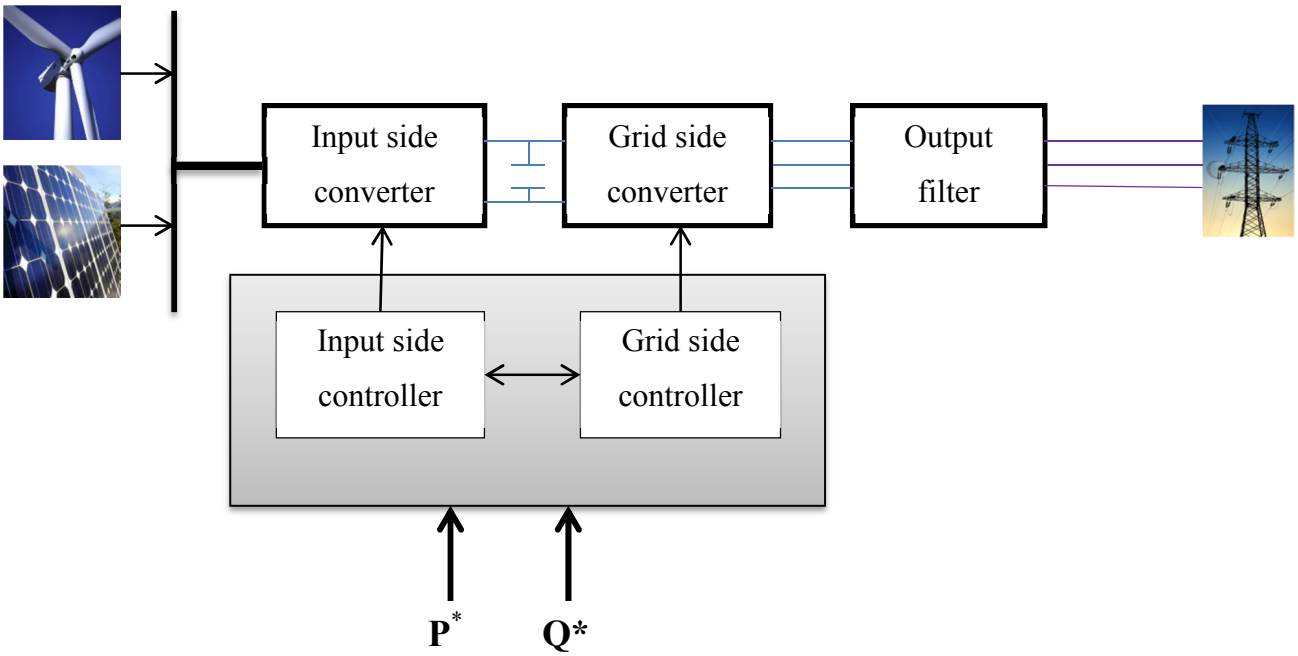

Figure 5-2 General Structure of a Transformerless Renewable Energy DPGS and its main Control Features

5.2 Solar power conversion structures

The PV inverter is the key section of grid connected PV power system. The main task is to convert the DC power produced by PV panels into grid-synchronized AC power. In order to increase the efficiency-to-cost ratio of PV systems, new designs have continuously been designed and developed.
Depending on the PV power plant configuration, the PV power inverter can be classified as:

- Module integrated power inverters, typically in the 50 - 400 W power rating range for very small PV plants (one module) as shown in figure 5-3 (a). An AC module is made up of a single solar module connected to the grid through its own inverter. The advantage of this configuration is that there are no mismatch losses, due to the fact that every single solar panel has its own inverter and MPPT, thus maximizing the power production. The power extraction is much better optimized than in the case of String inverters. One other advantage is the modular structure, which simplifies the modification of the whole system because of its "plug & play" characteristic. Two major disadvantages are the low overall efficiency due to the high-voltage amplification needed, and the price per watt which is still higher than in the other configurations to be discussed in next subsections. But in the future can be overcome by mass production, leading to low manufacturing and retail costs.

- String power inverters, typically in the 0,4 – 2,0 kW power rating for small roof-top plants with panels connected in one string as shown in figure 5-3 (b). They are based on a modular concept, where PV strings, made up of series- connected solar panels, are connected to separate inverters. The string inverters are paralleled and connected to the grid. If the string voltage is high enough - no voltage boosting is necessary, thereby improving the efficiency. Fewer PV panels can also be used, but then a DC-DC converter or a line frequency transformer is needed for a boosting stage.
  The advantages compared to the central inverter are as follows: no losses in string diodes (no diodes needed), separate MPPTs for each string better yield, due to separate MPPTs and lower price due to mass production.

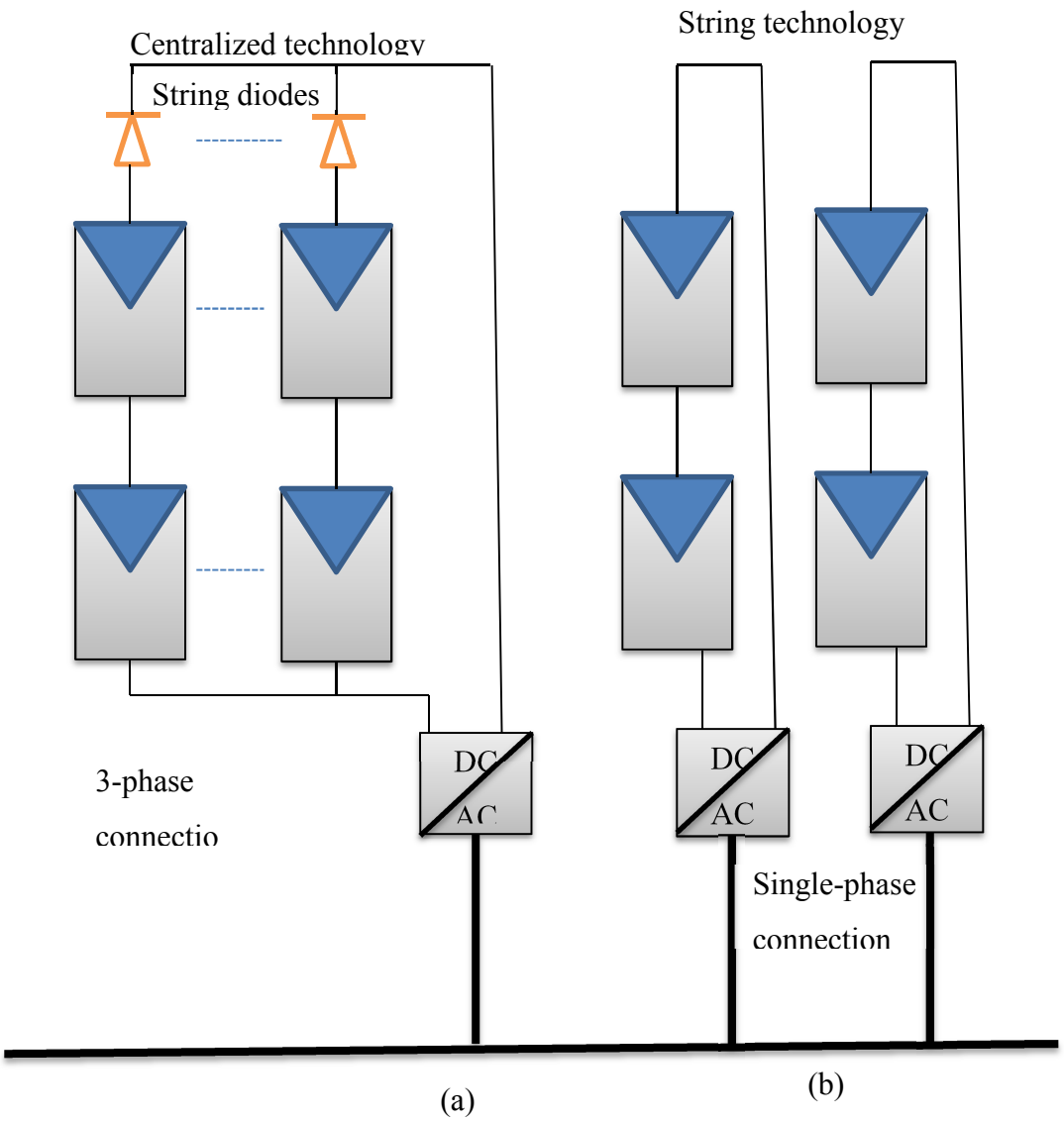

Figure 5-3 (a) Centralized technology (b) String technology

- Multistring power inverters, typically in the 1,5 – 6,0 kW power rating range for medium large roof-top plants with panels configured in one or two strings as shown in figure 5-4 (a). Multi-String inverters have recently appeared on the PV market. They are an intermediate solution between String inverters and Module inverters. A Multi-String inverter, shown in Fig. 23d, combines the advantages of both String and Module inverters, by having many DC- DC converters with individual MPPTs, which feed energy into a common DC-AC inverter. This way, no matter the nominal data, size, technology, orientation, inclination or weather conditions of the PV string, they can be connected to one common grid connected inverter. The Multi-String concept is a

flexible solution, having a high overall efficiency of power extraction, due to the fact that each PV string is individually controlled.

Multi-string technology

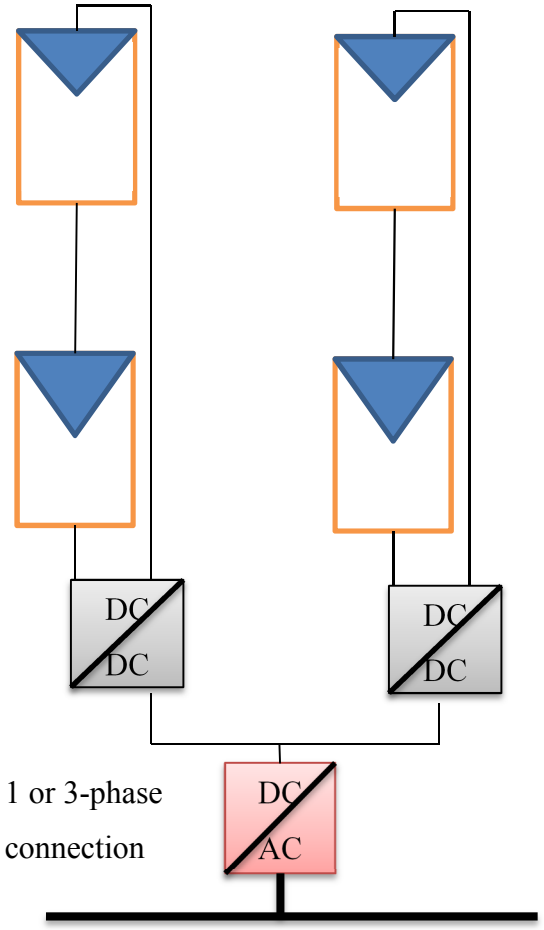

Figure 5-4 Multi-string technology

- Mini central power inverters, typically greater than 6,0 kW with three phase topology and modular design for larger roof-tops or smaller power plants in the range of 100 kW and typical units of 6, 8,10 and 15 kW.
- Central power inverters, typically in the 100 – 1000 kW power rating range with three-phase topology and modular design for large power plants ranging to tenths of a MW and typical unit sizes of 100, 150, 250,500 and 1000 kW.

  PV plants arranged in parallel strings are connected to one common central inverter. At first, line commutated thyristor-based inverters were used for this purpose. These were slowly replaced by force commutated inverters using IGBTs, because the efficiency of these inverters was higher and their cost was lower. However

the list of its disadvantages is significant. Need for high-voltage DC cables between PV panels and inverter, power losses due to common MPPT, power loss due to module mismatch losses in the string diodes, reliability of the whole system depends on one inverter.

Due to the high cost of solar energy system, the PV inverter technology has been driven primarily by efficiency. Thus a very diversity of PV inverter structures can be seen on the market. In comparison with motor drives inverters, the PV inverters are more complex in both hardware and functionalities. Thus the need to boost input voltage, grid connection filter, grid disconnection relay and DC switch are the most important aspects responsible for increased hardware complexity. Maximum power point tracking, anti-islanding, grid synchronization and data logger are typical functions required for the PV inverters.

New innovative power topologies have recently been developed for PV inverter with the main purpose of increasing efficiency and reducing manufacturing cost. As the lifetime of PV panels is typically longer than 20 years, efforts to increase the operating lifetime of PV inverters are gathering momentum.

The first method used to increase the efficiency was to eliminate the galvanic isolation transformer typically provided by high-frequency type in the DC-DC or by a line-frequency type on the output before interconnection with the grid. Thus a typical efficiency increase of 1-2% can be obtained. Such configurations are generally referred to as transformerless PV inverters.

Problems of DC current injection and safety issues due to leakage current require more complex solutions. Systems that are based on monitoring leakage current for personal safety reason as an indication of faults will be compromised. The capacitance appearing between the transformerless PV structures and the earth can vary greatly, depending on the PV panel construction and weather conditions and reference (Lopez O et al, 2007) typical value of 100 nF/kW are measured. The deployment of such topology especially for grid interconnection is dictated by regional grid codes. While currently transformerless PV inverters are accepted in some European countries, the opposite is the case in North America especially USA but recently allowed grid connected transformerless PV topologies.

Another important design issue that is driving the development of new topologies is the ability of exhibit high efficiency also at partial loads that is during the periods with reduced irradiation levels. Actually a weighted efficiency called “European efficiency” has been defined that takes into account the periods for different irradiation levels across Europe.

The PV inverters topologies that will be discussed in this thesis centered on two well developed and deployed, which are H-bridge and Neutral Point Clamped (NPC). Advantages, disadvantages and important remarks about H-bridge and NPC will discussed in the nest sub sections.

5.2 H-Bridge Inverter Topology

The H-bridge has an importance reference in power electronics converter technology development since its invention by W. Mcmurray in 1965 (Mcmurray W, 1965). It was the first structure to take advantage of the first available partially controllable forced-commutated semiconductor devices. The H-bridge topology is very versatile, being able to be used for both DC-DC and DC-AC conversion and can also be implement if full bridge (with two switching legs) or in half bridge form (with one switching leg).

The practical inverter topology based on the full-bridge inverter is shown in figure 5-4. Three main modulation strategies commonly used are:

Bipolar switching modulation technique as shown in figure 5-5 Switch pair S1/S4 and S2/S3 are switched at high frequency complementarily. Thus AC voltage can be generated as shown in figure 5-5 for both the positive and negative output currents. No zero output voltage state is possible.

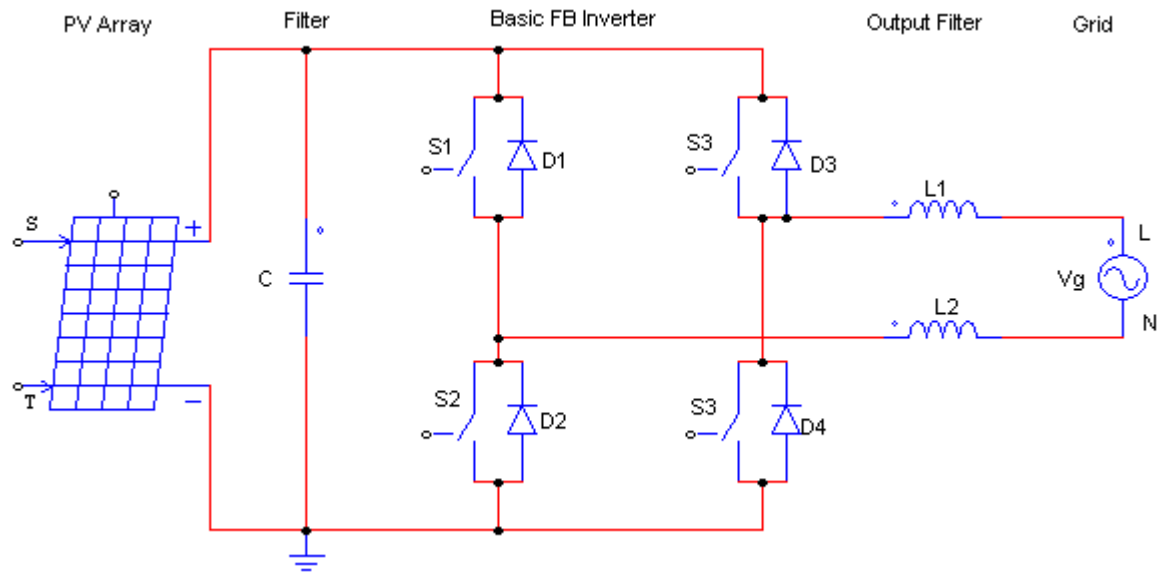

Figure 5-5 Basic Full Bridge Inverter with PV Module

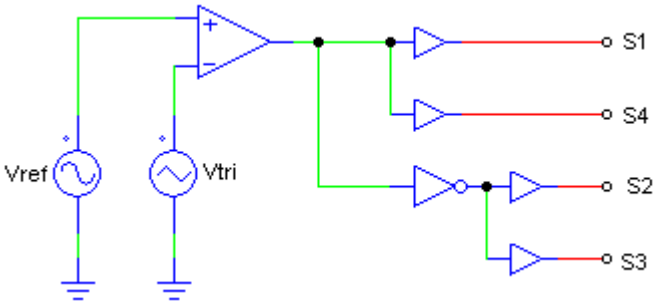

Figure 5-6 Bipolar SPWM switching control logic circuit

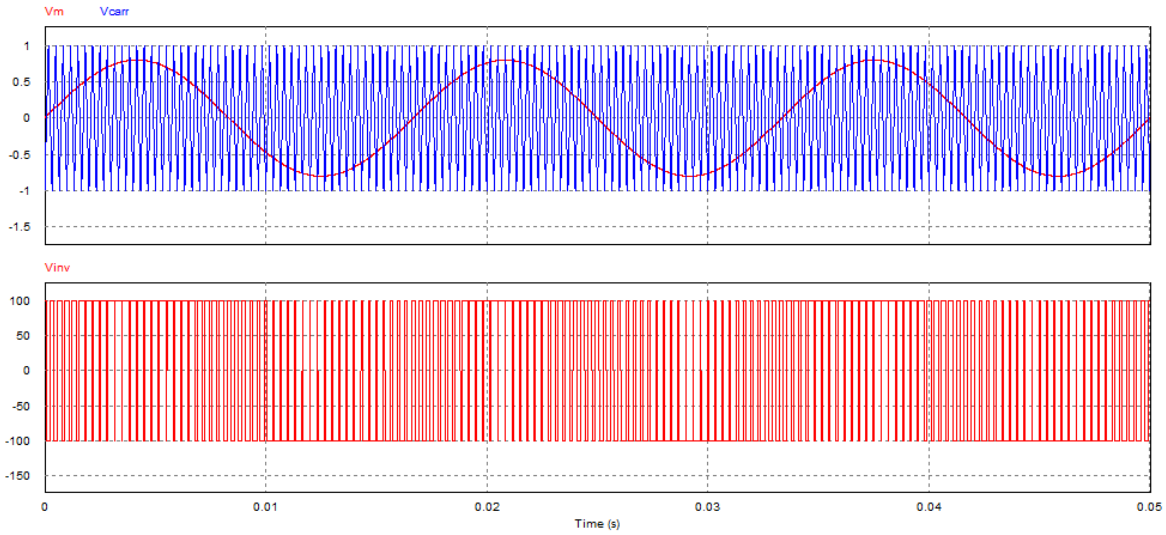

Figure 5-7 Bipolar switching waveforms

The advantage is that the leakage PV voltage has only a grid frequency component and switching complements, producing a very low leakage current and electromagnetic interference (EMI) if the topology is implement in transformerless architecture.

The disadvantages are: current ripple frequency equals the semiconductor device switching, resulting to higher filtering requirements, the voltage variation across the filter is bipolar producing high magnetic core losses, lower efficiency due to reactive power exchange between output inductance and the DC link capacitor because two switches are always simultaneously (theoretically) every switching period.

Same full bridge power topology that is used for bipolar is used for unipolar switching modulation strategy as shown in figure 5-5. Switch pair S1/S2 and S3/S4 are switched at high frequency with mirrored reference signals. Each leg of the inverter has its own reference and two zeros output are possible. Advantages of this topology are: the switching ripple frequency is

twice the switching frequency, producing lower filtering requirement, the voltage across the filter is unipolar, yielding lower core losses, high efficiency due to the losses during zero voltage states.

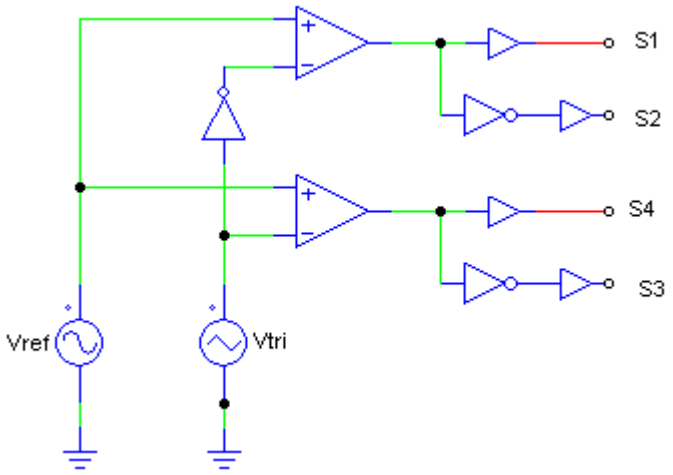

Figure 5-8 Unipolar SPWM switching control logic circuit

The control logic circuit for unipolar switching strategy is depicted in figure 5-8. Figure 5-9 shows the simulated output voltage waveforms of the topology with unipolar switching strategy.

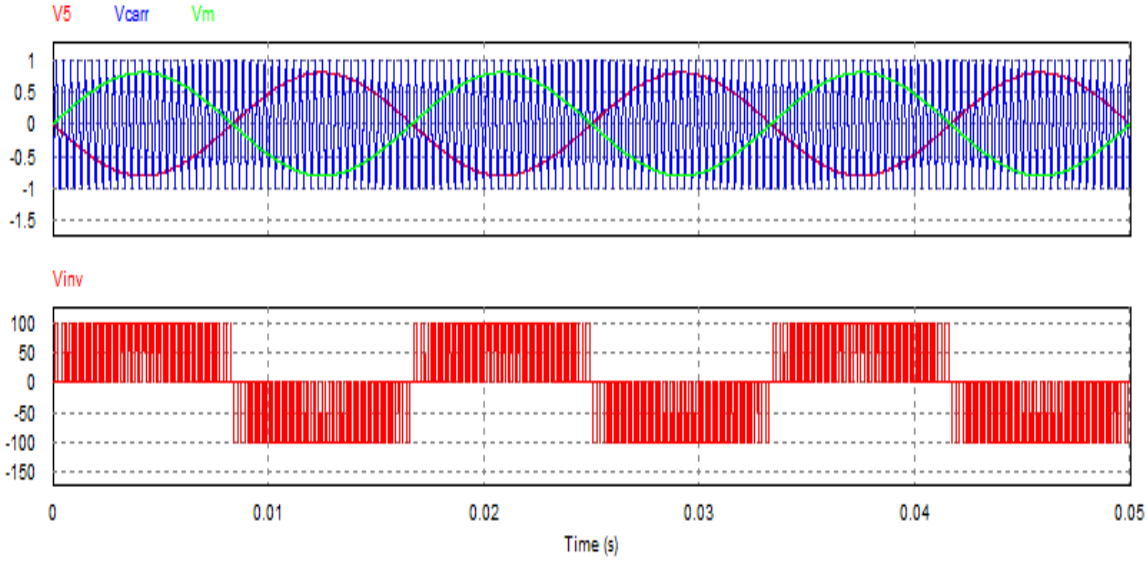

Figure 5-9 Unipolar switching waveforms

Main drawback is that the leakage current has switching frequency components, producing high leakage EMI. As such it cannot make use the advantage of high efficiency offered by transformerless topologies.

Hybrid switching modulation strategy as waveforms as shown in figure 5-11 and switching logic circuit is shown in figure 5-10. One of the inverter legs is switched at high frequency and the other one at the grid frequency.

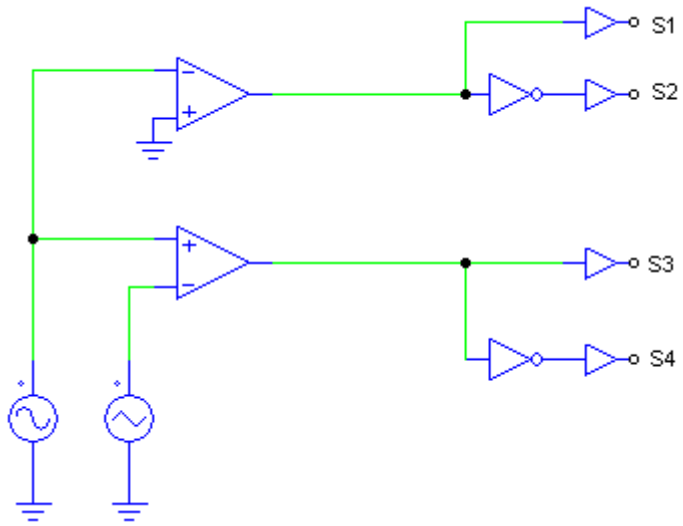

Figure 5-10 Hybrid switching control logic circuits

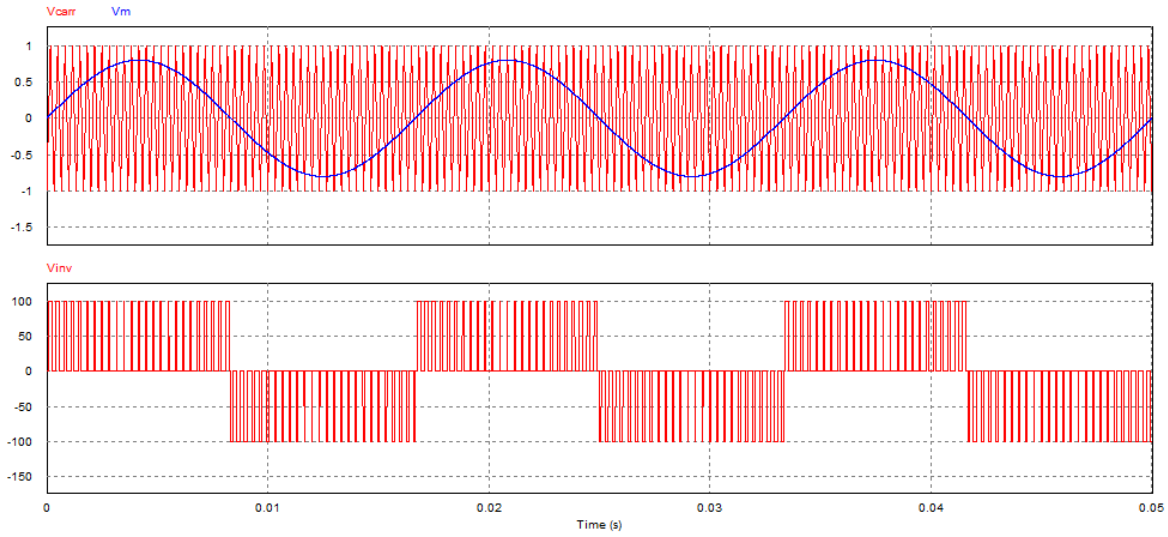

Figure 5-11Hybrid SPWM Waveforms

5.3 Neutral point clamped topology

Nabae, Magi and Takashasi in 1981 introduced the neutral point clamped (NPC) topology showing great improvement in terms of lower dV/dt and switch stress in comparison with classical two-level full-bridge inverter. The NPC topology is also very versatile and can be used in both single and three-phase inverters.

The main concept is that zero voltage state can be achieved by clamping the output to the grounded (middle point) of the DC bus using D+ or D- depending on the sign of the current (figure 5-12). The switching states for generating positive and negative current are explained as follows.

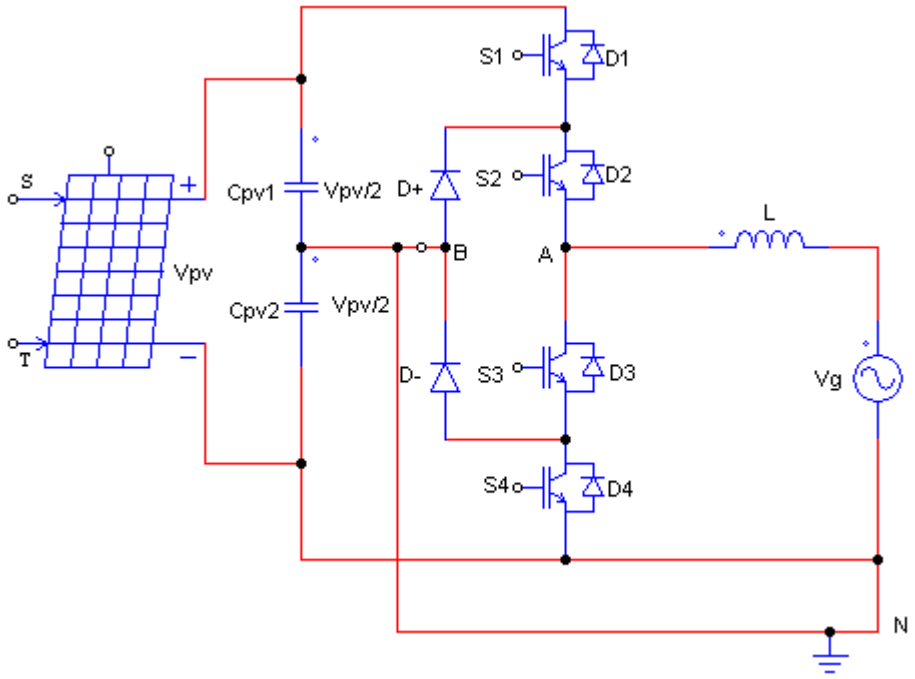

Figure 5-12 Neutral clamped half-bridge topology

Figures 5-13, 5-14, 5-15, and 5-16 show the switching states for the neutral clamped half bridge inverter topology.

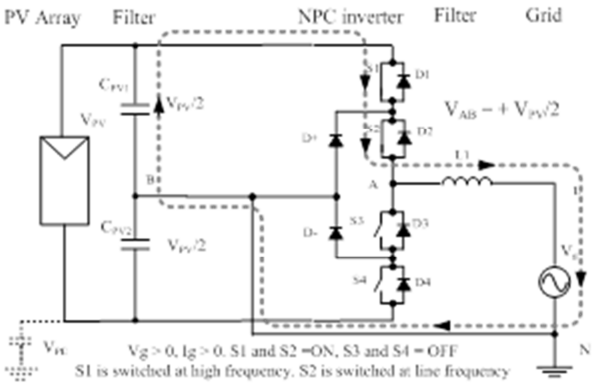

Figure 5-13 NPC Vg>0, Ig>0, S1 and S2 On, S3 and S4 Off

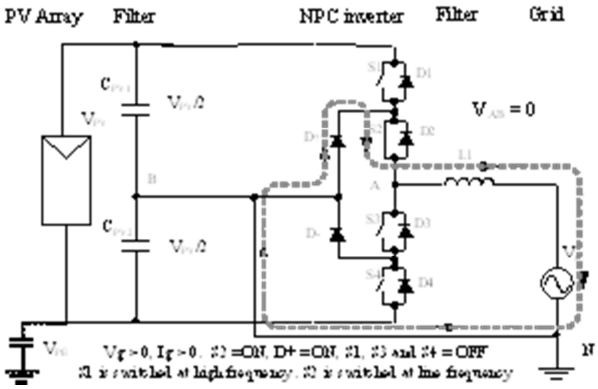

Figure 5-14 NPC Vg>0, Ig>0, D+ and S2 On, S3, S1 and S4 Off

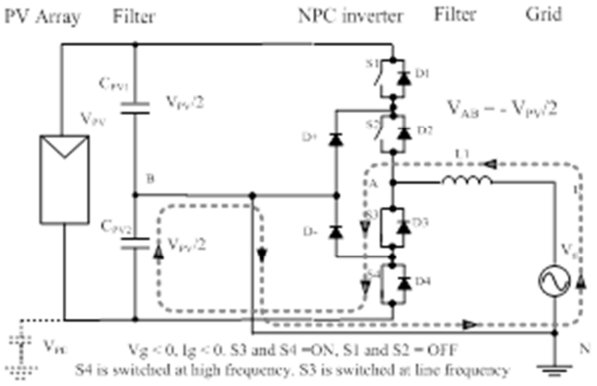

Figure 5-15 NPC Vg<0, Ig<0, S3 and S4 On, S1 and S2 Off

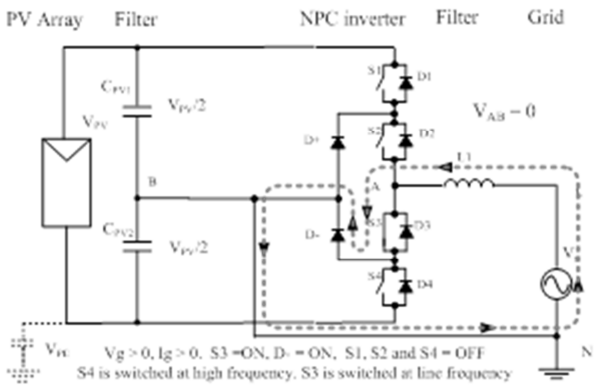

Figure 5-16 NPC Vg>0, Ig>0, S3 and D- On, S1, S4 and S2 Off

The main features of this topology are:

- S1 (S4) is switched at high frequency and S2 (S3) at grid frequency.
- Two zero voltage states are possible: S2, D+ = ON and S3, D- = ON. For operation out of unitary power factors S1 and S2 switch in opposition for $V_g > 0$, $I_g < 0$, and S2 and S4 for $V_b < 0$, $I_g > 0$.

Advantages are:

- Voltage across the filter in unipolar
- Higher efficiency of up to 98% since there is no reactive power exchange between output inductance and the PV parasitic capacitance during the zero voltage switching state and to the lower switching frequency in one leg.
- The voltage rating of outer switches can be reduced to a quarter of the DC link voltage resulting in switching losses.
- The voltage across the parasitic capacitance is maintained constant and is equal to half of the DC link voltage without any switching components, yielding very low leakage current and EMI.

Disadvantages:

- Two extra diodes
- Requires double voltage input in comparison with full bridge topologies.
- Unbalance switch losses: higher on the higher/lower switches and lower on the middle switches.
- Any inductance introduced in the neutral connection by, for example, EMI filters generates high frequency common voltage, which will lead to leakage current.

A variant of NPC of the classical NPC is a half-bridge with the output clamped to the neutral using a bidirectional switch realized with two series back-to-back IGBT as patented by Conergy as depicted in figure 5-17. An alternative realization of the same concept is presented in reference, where the unidirectional clamping switches are connected in parallel rather in in series and a full-bridge is used instead of a half-bridge.

The main concept of the Conergy NPC inverter is that zero voltage can be achieved by clamping the output voltage to the ground middle point of the DC bus using S+ or S- depending on the sign of the current.

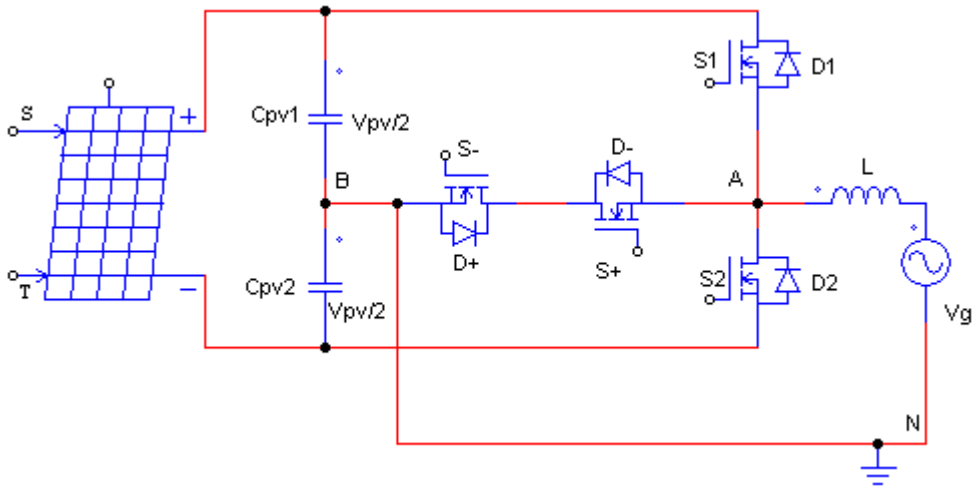

Figure 5-17 Conergy NPC inverter topology

The main features of this converter are:

- S1 (S2) and S+ (S-) is switched at high frequency.
- Two voltage zero voltage states are possible: S+, D+ = ON (S-, D- = 0N)

Figures 5-18, 5-19,5-20 and 5-21 show the switching states of Conergy NPC inverter topology.

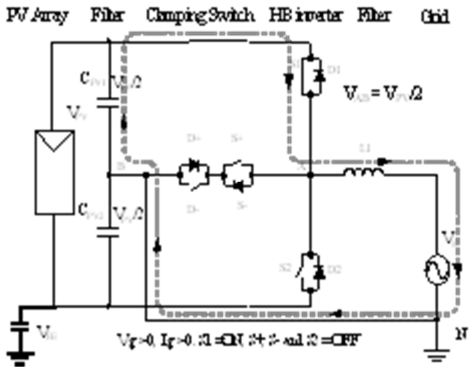

Figure 5-18 Conergy Vg>0, Ig>0, S1 = ON, S+, S- and S2 =OFF

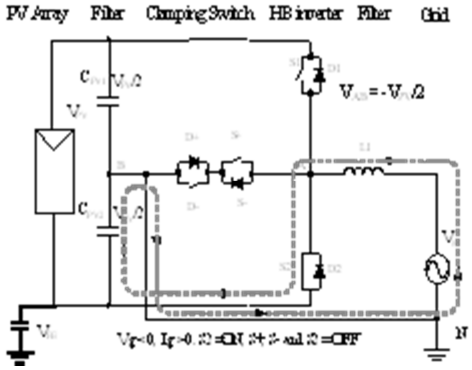

Figure 5-19 Conergy Vg<0, Ig>0, S2 = ON, S+, S- and S1 =OFF

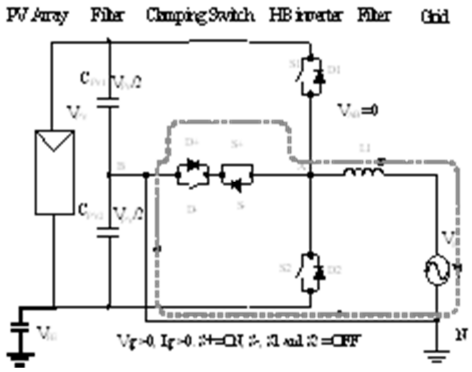

Figure 5-20 Conergy Vg>0, Ig>0, S+ = ON, S-, S1 and S2 =OFF

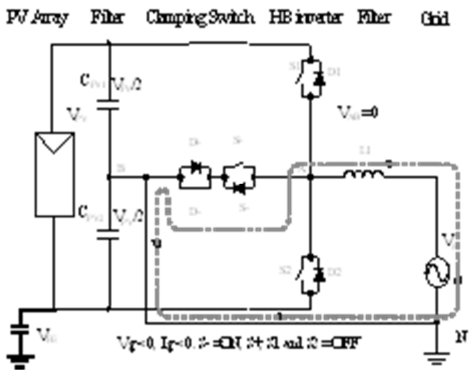

Figure 5-21 Conergy Vg<0, Ig<0, S- = ON, S+, S- and S2 +OFF

Advantages

- Voltages across the filter is unipolar ($0 \rightarrow +V_{pv} \rightarrow 0 \rightarrow -V_{pv} \rightarrow 0$) yielding lower core losses
- Higher efficiency of up to 98% is due to no reative power exchange between inductance L and the parasitic capacitance of the PV cells during zero voltage and to a reduced voltage drop across as only one switch is conducting during active states of the Conergy NPC inverter.
- V_{pv} is constant and is equal to $-V_{pv}/2$ without switching frequency components, yielding a very low leakage current and EMI.
- Balanced switching losses in contrast with classical NPC.

Drawbacks:

- The voltage rating of S1 and S2 is double in comparison with the outer switches in the NPC
- Requires double voltage input in comparison with full bridge topologies.
- Any inductance introduced in the neutral connection by, for example, EMI filters generates high frequency common-mode voltage, which will lead to leakage current.

5.3 NPC derived commercialized transformerless topologies

5.3.1 H5 inverter

H5 topology is a modified full bridge topology by adding an extra switch S5 in the positive bus of the DC link side of the bridge inverter as shown in figure 5-22. The upper pair of switches S1 and S3 is operated at fundamental grid frequency while the lower switch pair S2 and S4 is operated at high switching frequency. In the positive half cycle, S5 and S4 are switched simultaneously at high switching frequency while S1 is turned on continuously. Current flows through S5, S1 and S4.

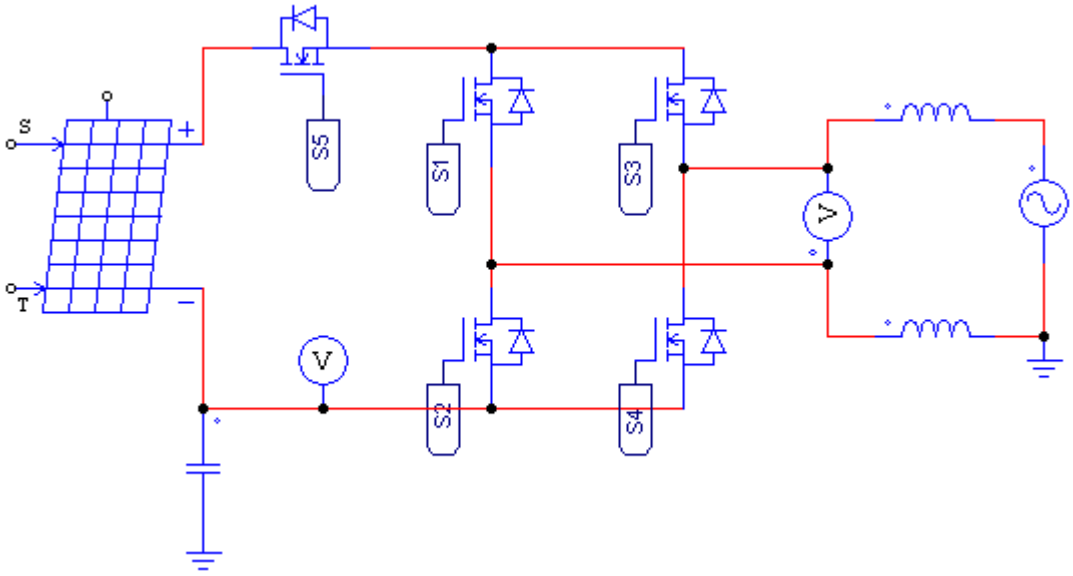

Figure 5-22 H5 inverter topology

During the positive zero voltage vector, S5 is turned off, disconnecting the PV module from the grid. Current freewheels through S1 and the anti-parallel diode of S3. On the other hand, in the negative half cycle, S5 and S2 are switched simultaneously while S3 is switched on continuously. Current flows through S5, S2 and S3. During the negative zero voltage vector, S5 is turned off and current freewheels through S3 and the anti-parallel diode of S1. The logic control circuit and control signals for H5 inverter topology are simulated and shown in figures 5-23 and 5-24. This switching sequence is illustrated in figures 5-25, 5-26, 5-27 and 5-28.

H5 inverter topology is also known as DC decoupling topology where the photovoltaic module is disconnected from the grid by disconnecting S5 in the DC side of the inverter topology.

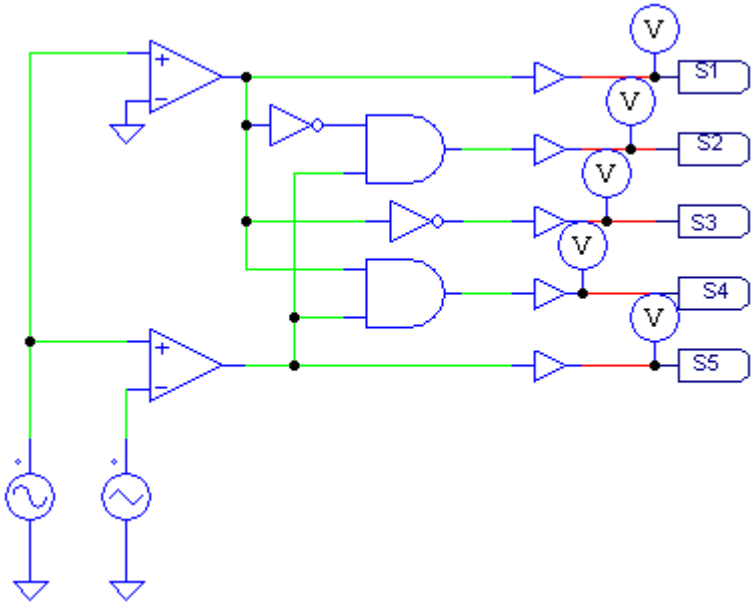

Figure 5-23 H5 switching logic control circuit

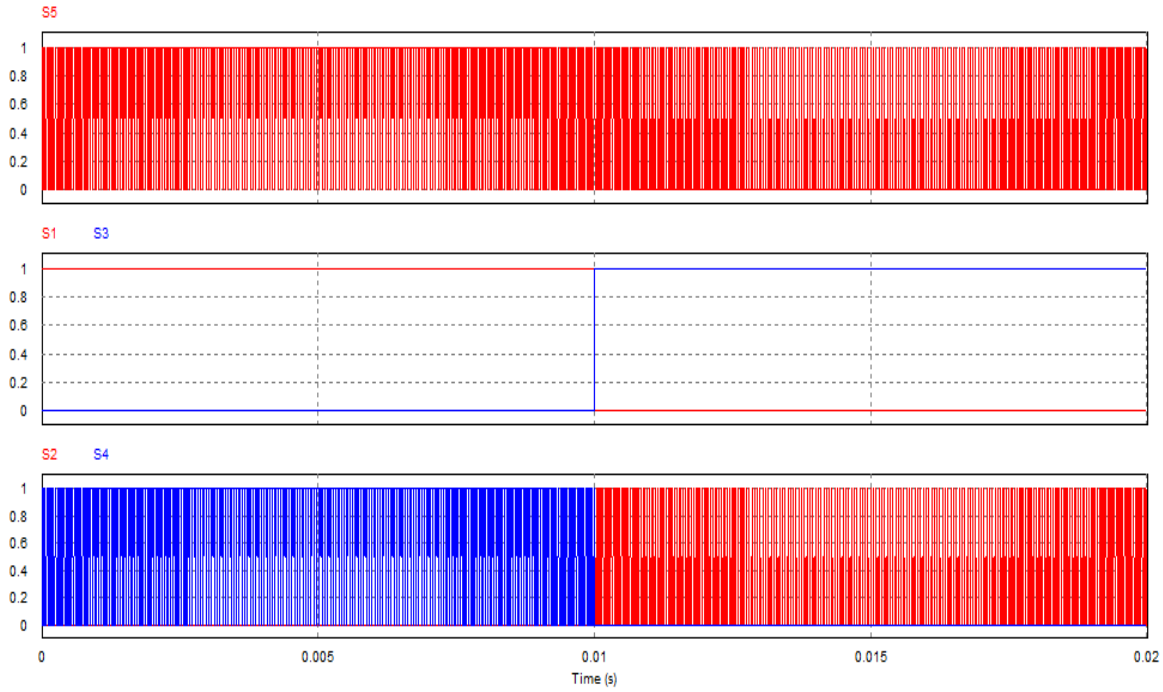

Figure 5-24 H5 control signal waveforms

Advantages of H5 inverter topology are:

- Voltage across the filter is unipolar, producing lower core losses.
- Higher efficiency of up to 98% is due to no reactive power exchange between the output inductance and the DC link capacitance during the zero voltage state and to the lower frequency switching in one switching in the switching sequence.
- Voltage across the PV module parasitic capacitance has only grid frequency component and no switching frequency components, yielding a very low leakage current and EMI.

The disadvantages of H5 inverter topology are:

- One extra switch used in the DC link side
- Three switches are conducting during the active switching instants leading to higher conduction losses.

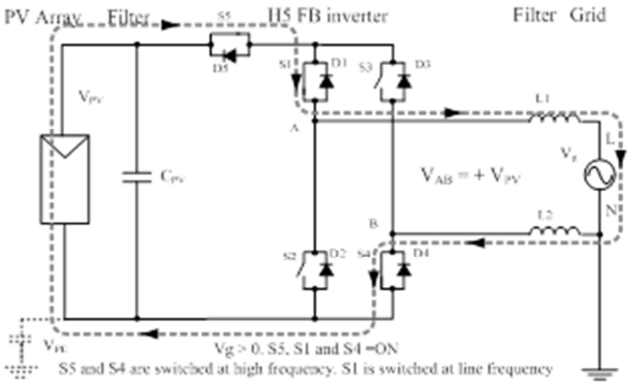

Figure 5-25 H5 Vg>0, S5, S1 and S4 On

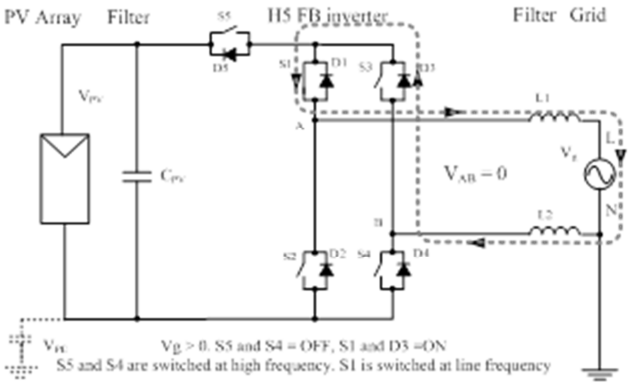

Figure 5-26 H5 Vg>0, S5 and S4 Off and D3 On

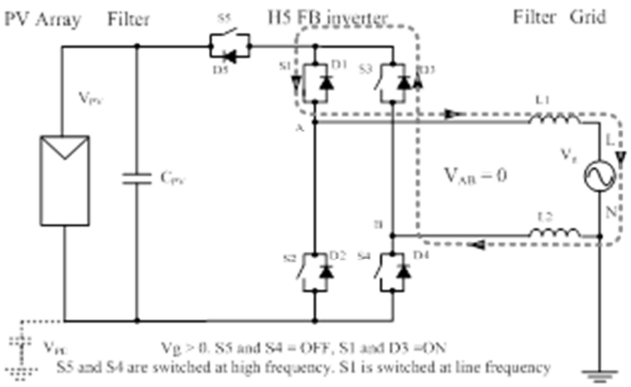

Figure 5-27 H5 Vg>0, S5 and S4 Off, S1 and D3 On

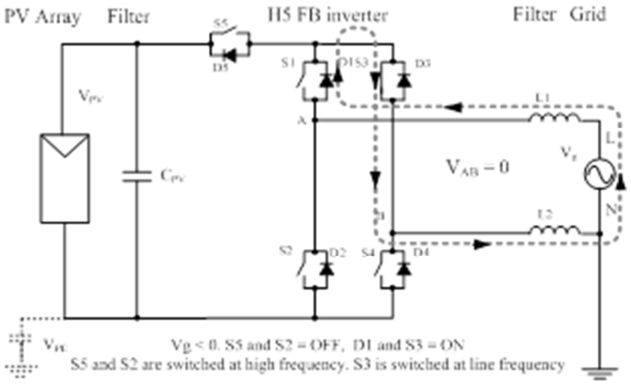

Figure 5-28 H5 Vg<0, S5 and S2 Off, D1 and S3 Off

H5 inverter topology is patented by SMA. It is widely used in transformerless grid-connected PV system. Leakage current is kept within the permissible limit due to constant common mode voltage. High efficiency is guaranteed as the generated output is the same as a unipolar PWM.

5.3.2 HERIC inverter

HERIC topology derived its acronym from Highly Efficient and Reliable Inverter Concept. It is designed by a modification of full bridge topology with two extra switches connected across the AC output side of the inverter as shown in figure 5-29.

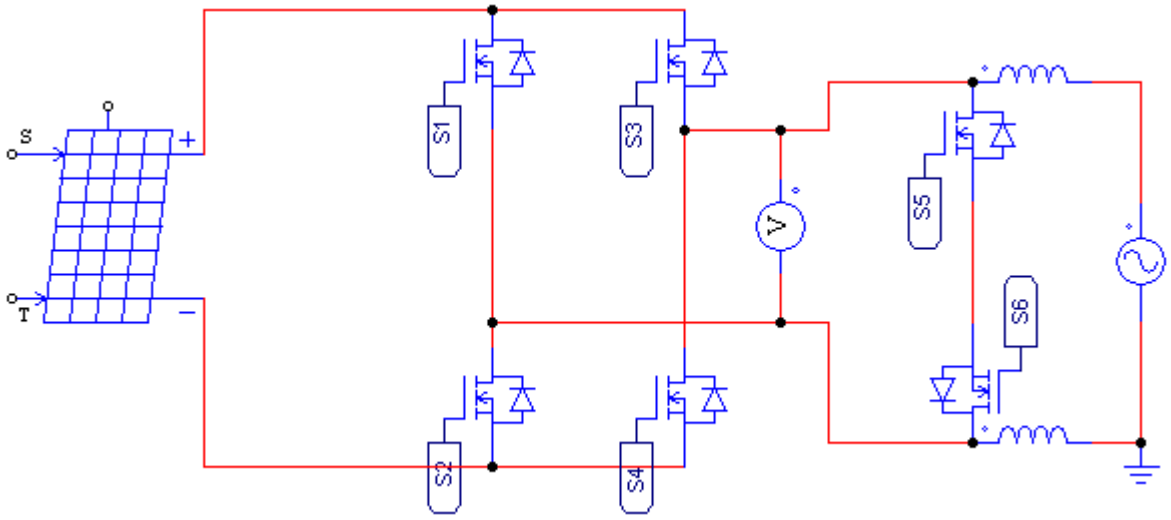

Figure 5-29 HERIC inverter topology

Each pair of the diagonal switches is operated at high switching frequency during one half of the grid voltage. During the zero voltage state, S5 is turned on during the positive half cycle. Current freewheels through the anti-parallel diode of S6, S5 and the grid. On the other hand, S6 is turned on during the negative half cycle and output current freewheels through the anti-parallel diode of S5, S6 and the grid. The PV module is disconnected from the grid during the zero voltage vectors because S1, S4 or S2, S3 are all in off state. The logic control circuit and control signals for HERIC inverter topology are shown in figure 5-30 and 5-31 respectively.

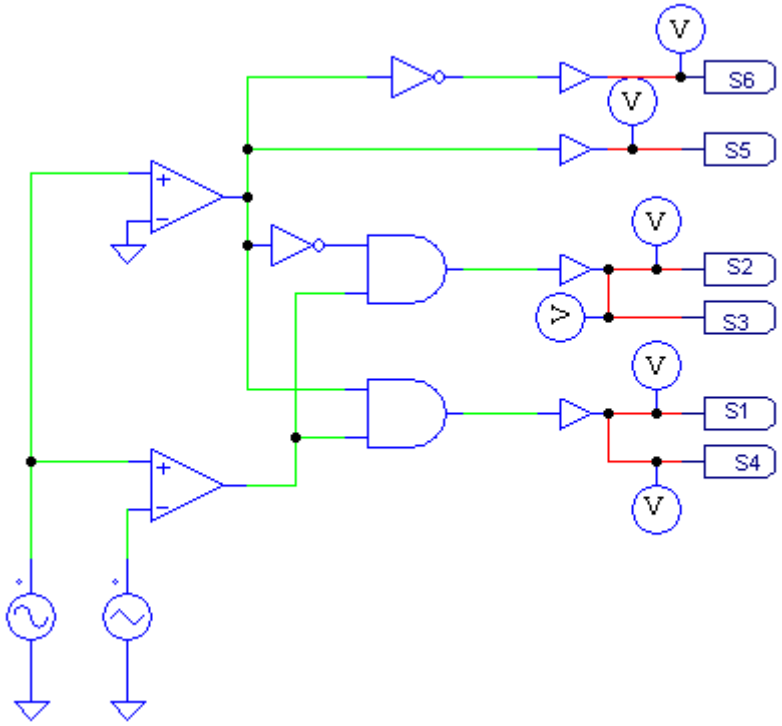

Figure 5-30 HERIC switching logic control circuit

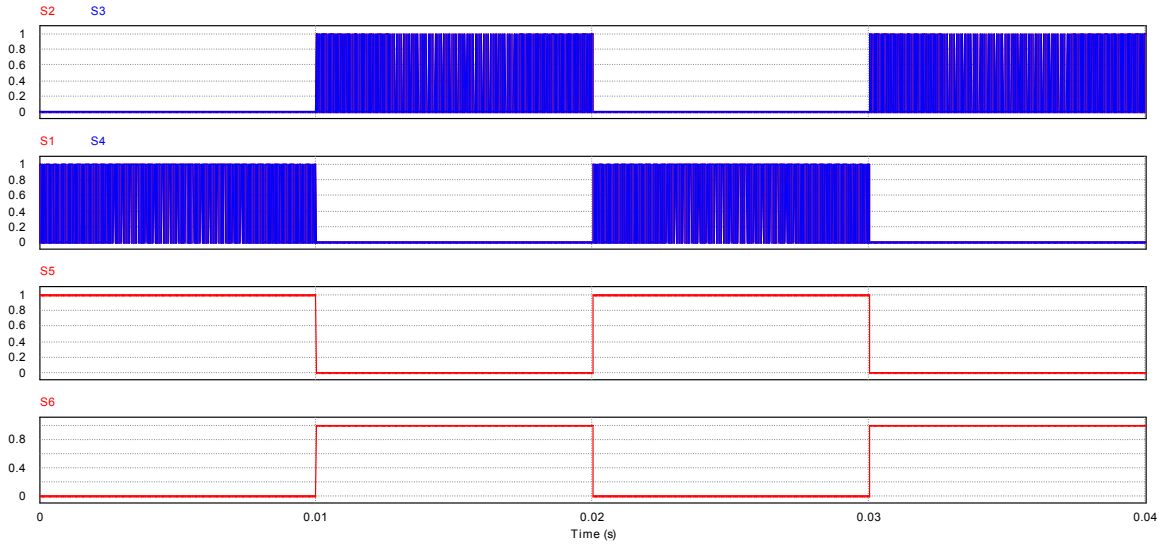

Figure 5-31 HERIC switching waveforms

HERIC inverter topology is also known as AC decoupling topology because the PV module is disconnected from the grid by short-circuiting the AC side of the inverter during the zero voltage states. All the switching states are shown in figures 5-32, 5-33, 5-34 and 5-35.

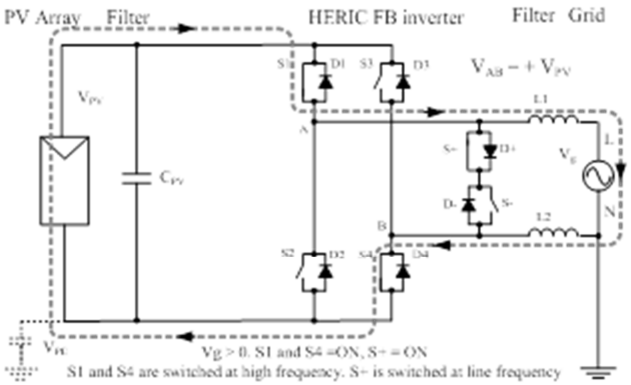

Figure 5-32 HERIC Vg>0, S1 and S4 On, S_ On

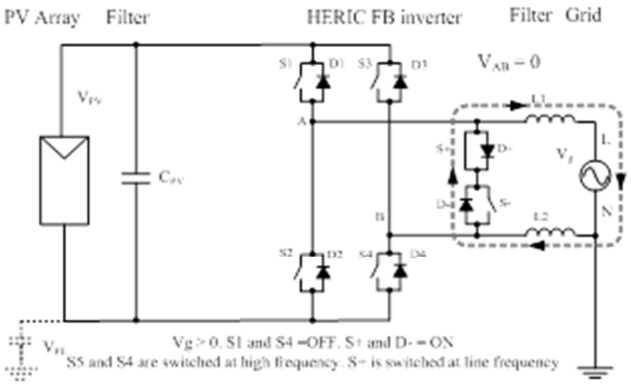

Figure 5-33 HERIC Vg>0, S1 and S4 Off, S+ and D- On

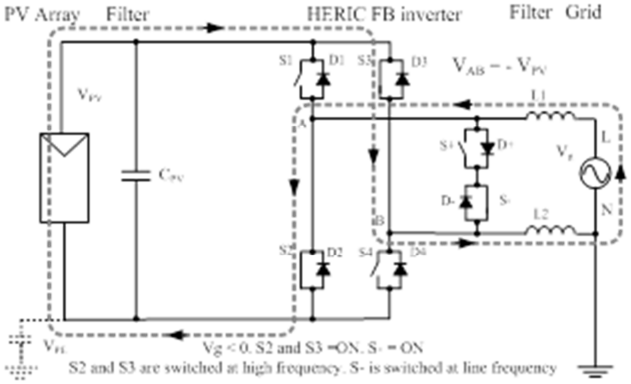

Figure 5-34 HERIC Vg>0, S2 and S3 On, S- On

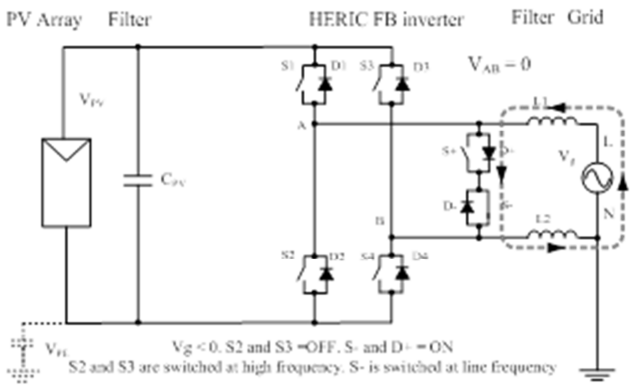

Figure 5-35 HERIC Vg<0, S2 and S3 Off, S- and D+ On

Advantages of HERIC inverter topology are:

- Voltage across the output filter inductance is unipolar
- Higher efficiency of up to 97% is due to no reactive power exchange between the DC link capacitance and the output inductance during the zero voltage state. Lower switching loss due to grid frequency switching in the AC bypass switches.
- Voltage across the parasitic capacitance of the PV module has only a grid frequency component yielding very low leakage current and EMI.
- Two switches are conducting during the active switching instants leading to lower conduction losses compared to H5 inverter topology.

The only disadvantage is the two extra switches used to implement the AC decoupling function during the zero voltage states.

5.3.3 REFU inverter

Figure shows the REFU (H6) inverter topology derived from the classical H-bridge topology. This topology was patented by REFU Solar in 2007 (Teodorescu et al, 2011:15). The topology actually uses a half-bridge within the AC side bypass and a by-passable DC-DC converter as shown in figure 5-36.

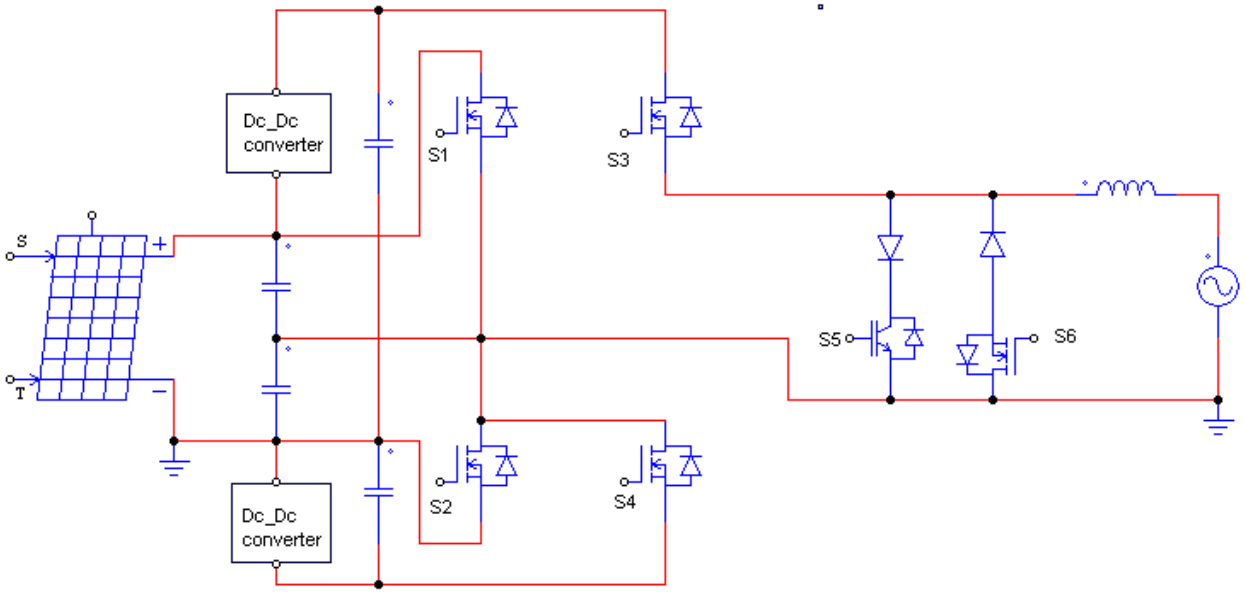

Figure 5-36 REFU transformerless PV inverter topology

The AC bypass is implemented in a different way compared to HERIC, which is by using unidirectional switches composed of standard IGBT modules with diodes in series to cancel the freewheeling path. Another specific characteristic of this topology is the use of a boost converter, which is activated only when the input is lower than the grid voltage.

Two additional active switches S5, S6 and diodes D5, D6 are added to the convectional full bridge inverter topology. Thus this topology is also derived from H-bridge inverter topology.

The main features of this converter are:

- S1 (S2) are switched at high switching frequency when there is no need for the voltage boost conversion that is the PV terminal voltage is greater than the absolute value of the AC grid voltage
- S3 (S4) are switched at high switching frequency when the voltage boost conversion is activated that is the PV terminal voltage is less than than the absolute value of the AC grid voltage
- S+ (S-) are switched at grid frequency depending on the voltage polarity.

Advantages of the REFU inverter are:

- Voltage across the filter is unipolar ($0 \rightarrow +V_{PV} \rightarrow 0 \rightarrow -V_{PV} \rightarrow 0$) yielding lower core losses.
- Higher efficiency of up to 98 % is due to no reactive power exchange between the link inductor and the DC link capacitance, C_{PV} during the zero voltage vector state, boost only when necessary and to lower frequency switching in the AC decoupling switches.

Drawbacks:

- Needs double Dc voltage resulting into poor DC link voltage utilization.
- Two extra active and two passive diodes but switched at grid frequency.

The switching sequence without consideration for the boost converters switching instants are illustrated in figures 5-37, 5-38, 5-39, 3-40, 5-41 and 5-42 (Teodorescu et al, 2011:16).

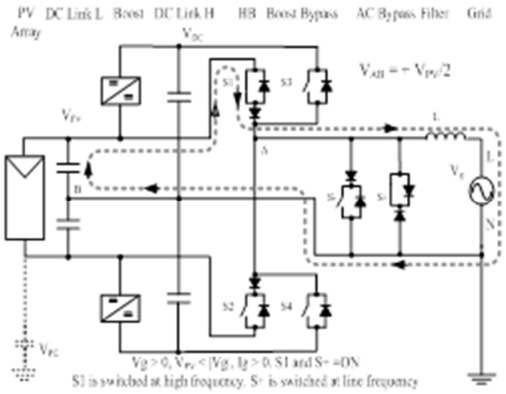

Figure 5-37 REFU Vg>0, Vpv<|Vg|, Ig>0. S1 and S+ = ON

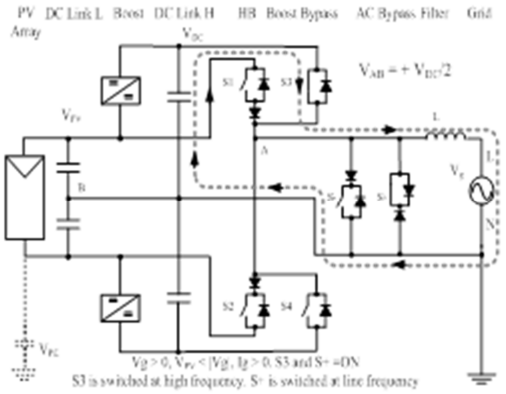

Figure 5-38 REFU Vg>0, Vpv<|Vg|, Ig>0. S3 and S+ = ON

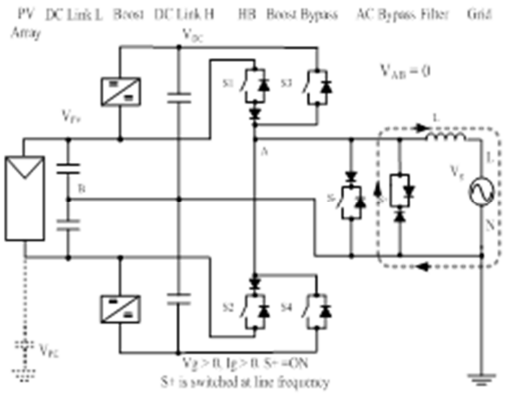

Figure 5-39 REFU Vg>0, Ig>0. S+= ON

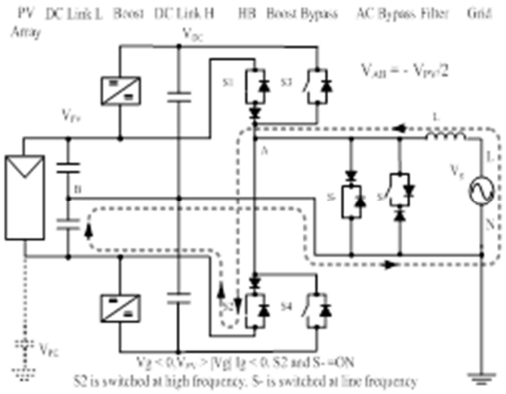

Figure 5-40 REFU Vg>0, Vpv<|Vg|, Ig<0. S2 and S- = ON

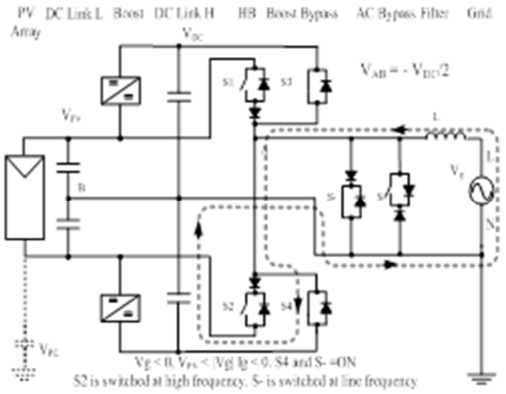

Figure 5-41 REFU Vg<0, Vpv<|Vg|, Ig<0. S4 and S- = ON

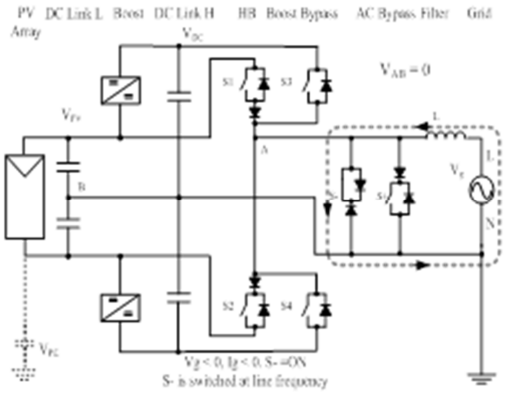

Figure 5-42 REFU Vg<0, Ig<0. S-= ON

5.3.4 Ingeteam inverter

Another modified full bridge inverter topology is the full bridge with DC bypass. This topology is the classical H-bridge topology with two extra switches in the DC link and also two extra diodes clamping the output to the grounded middle point of the DC bus as shown in figure 5-24. The DC switches provide the separation of the PV panels from the grid during the zero voltage states and the clamping diodes ensures that the zero voltage is grounded, in opposition to HERIC or H5 where the zero voltage is floating.

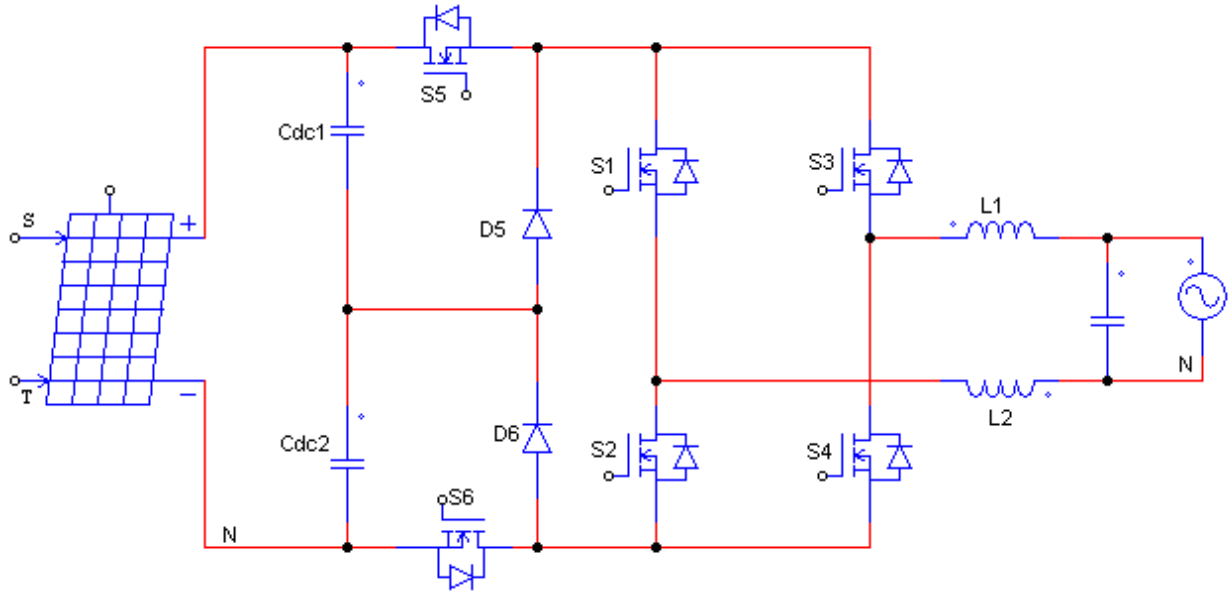

Figure 5-43 H6 inverter topology

In the positive half cycle, S1 and S4 are turned on continuously. S5 and S6 commutate simultaneously at high switching frequency while S2 and S3 commutate together and complimentarily to S5 and S6. Current flows through S5, S1, S4 and S6. During the positive zero voltage vector, S5 and S6 are turned off and S2 and S3 are turned on. Hence, freewheeling currents find paths in two ways: S1 and the anti-parallel diode of S3, and S4 and the anti-parallel diode of S2. The logic current circuit for the H6 modulation and switching signals for the H6 inverter topology are shown in figure 5-43 and figure 5-44 respectively (Teodorescue et al, 2011:17).

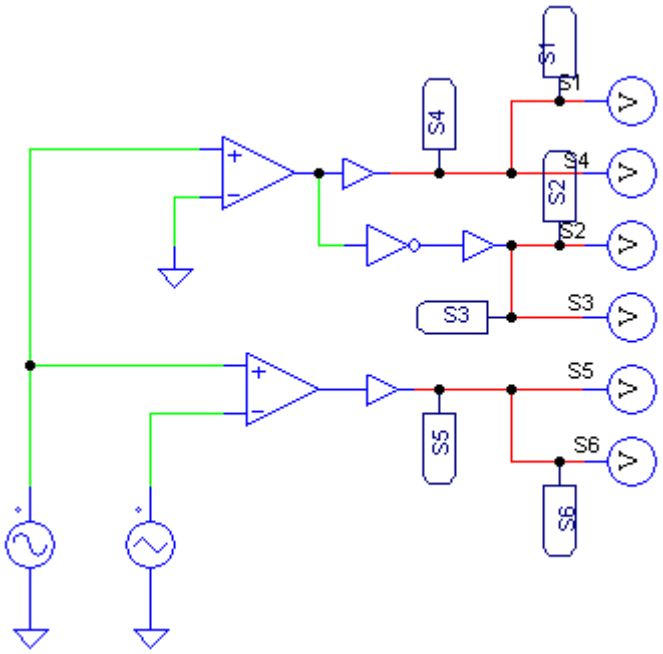

Figure 5-44 H6 switching control logic circuit

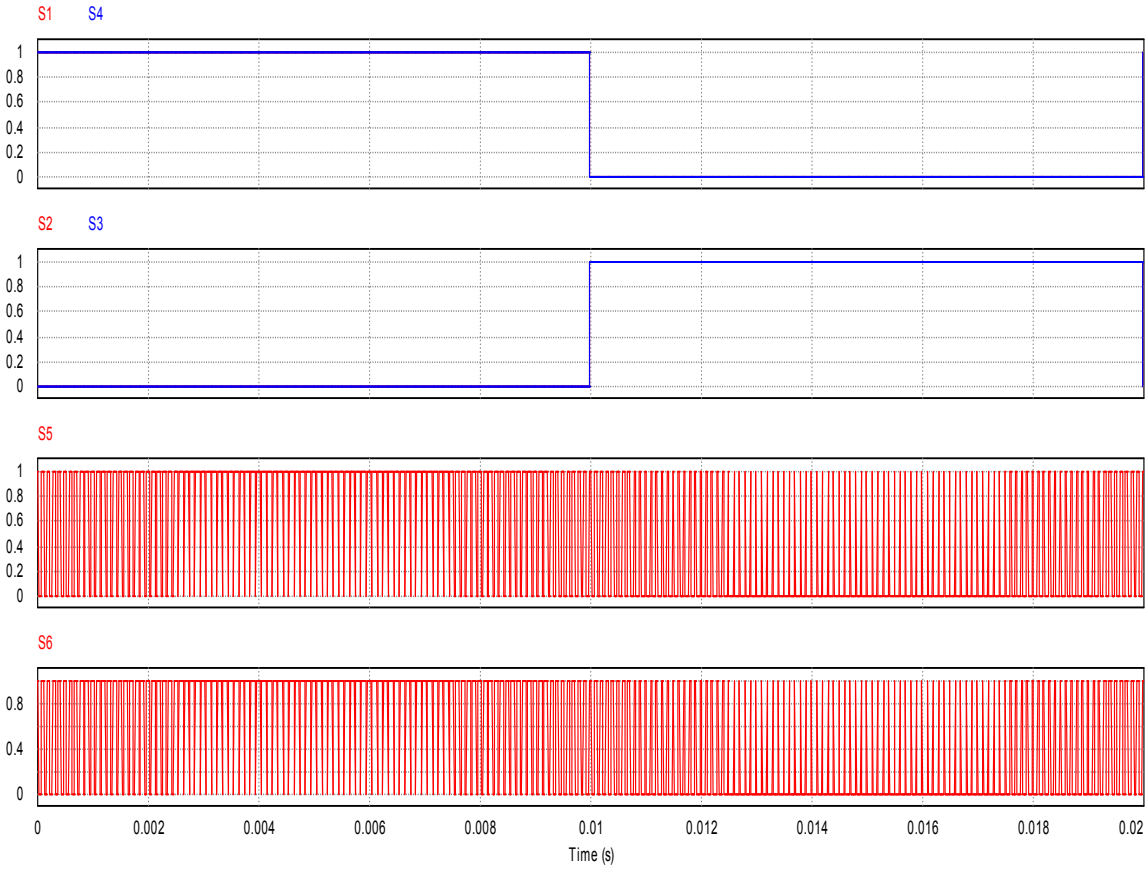

Figure 5-45 H6 switching waveforms

On the other hand, in the negative half cycle, S2 and S3 are turned on continuously. S5 and S6 commutate simultaneously at high switching frequency while S1 and S4 commutate together and complementarily to S5 and S6. During the negative zero voltage vector, S5 and S6 are turned off and S1 and S4 are turned on. Hence freewheeling current find its path in two ways: S3 and the anti-parallel diode of S1, and S2 and the anti-parallel diode of S4. PV module is disconnected from the grid by the use of S5 and S6.
The output voltage of the H6 inverter topology consists of three levels. The topology and control strategy guarantees constant common mode voltage which generates very small leakage current.

Advantages of H6 inverter topologies are:

- Voltage across the filter is unipolar
- The rating of the DC bypass switches is half of the DC link voltage

Voltage across the PV module has only a grid frequency component and no switching frequency components, producing a very low leakage current and EMI.

Drawbacks are:

- Two extra switches and two extra diodes
- Four switches are conducting during the active switching vector leading to higher conduction losses.

The switching states are shown in figures 5-45, 5-46, 5-47 and 5-48 as follows.

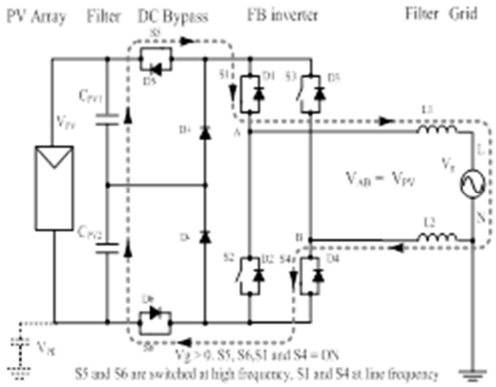

Figure 5-46 Ingeteam Vg>0. S5, S6, S1 and S4 = ON

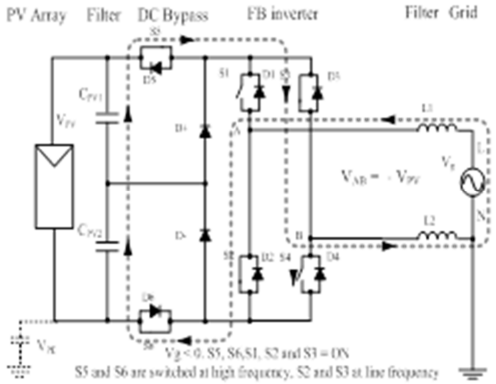

Figure 5-47 Ingeteam Vg<0. S5, S6, S1, S2 and S3 = ON

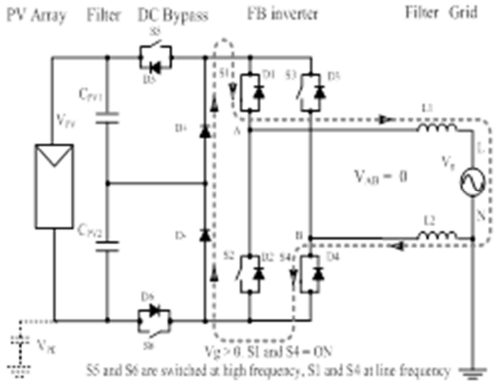

Figure 5-48 Ingeteam Vg>0. S1 and S4 = ON

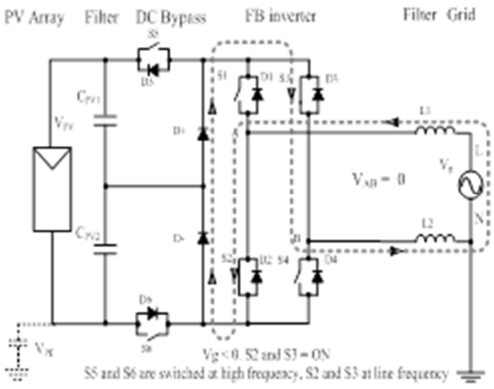

Figure 5-49 Ingeteam Vg<0. S2 and S3 = ON

5.3.5 FB-ZVR inverter

Another modified inverter topology by Kerekes et al that is suitable for transformerless PV system design is Full Bridge Zero Voltage Rectifier (FB-ZVR) topology as shown in figure 5-49. It is derived from HERIC inverter topology but the bidirectional grid short-circuiting switch is implemented using a diode bridge, one active switch and a diode clamped to the DC midpoint. Zero voltage state is achieved by turning the full bridge rectifier off and turning S5 on.

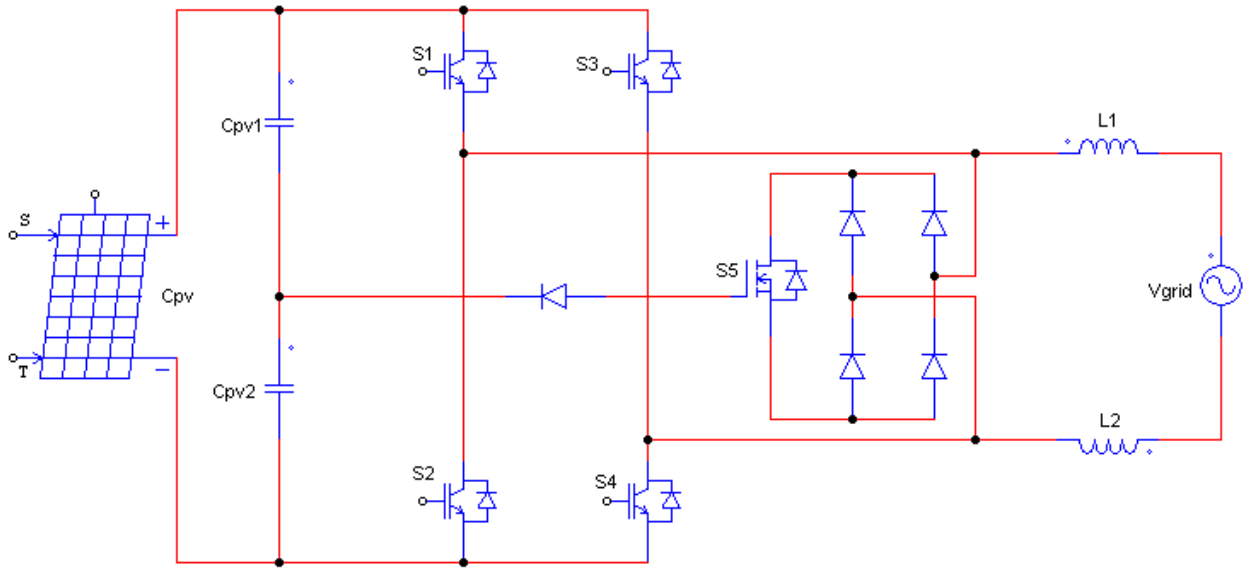

Figure 5-50 FB-ZVR inverter topology

The switches within the full bridge are switched diagonally same way in bipolar modulation switching scheme. The zero voltage state is introduced after each switching instant by turning all the switches of the full bridge off and turning S5 off (Teodorescu et al, 2011:19-20). The logic control circuit for this topology is shown in figure 5-50 and the modulation signals is also shown in figure 5-51.

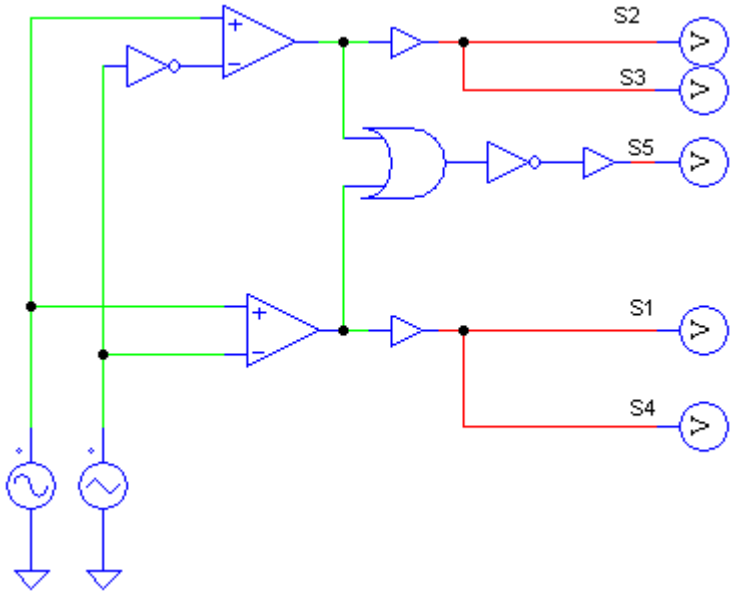

Figure 5-51 FB-ZVR switching modulation circuit

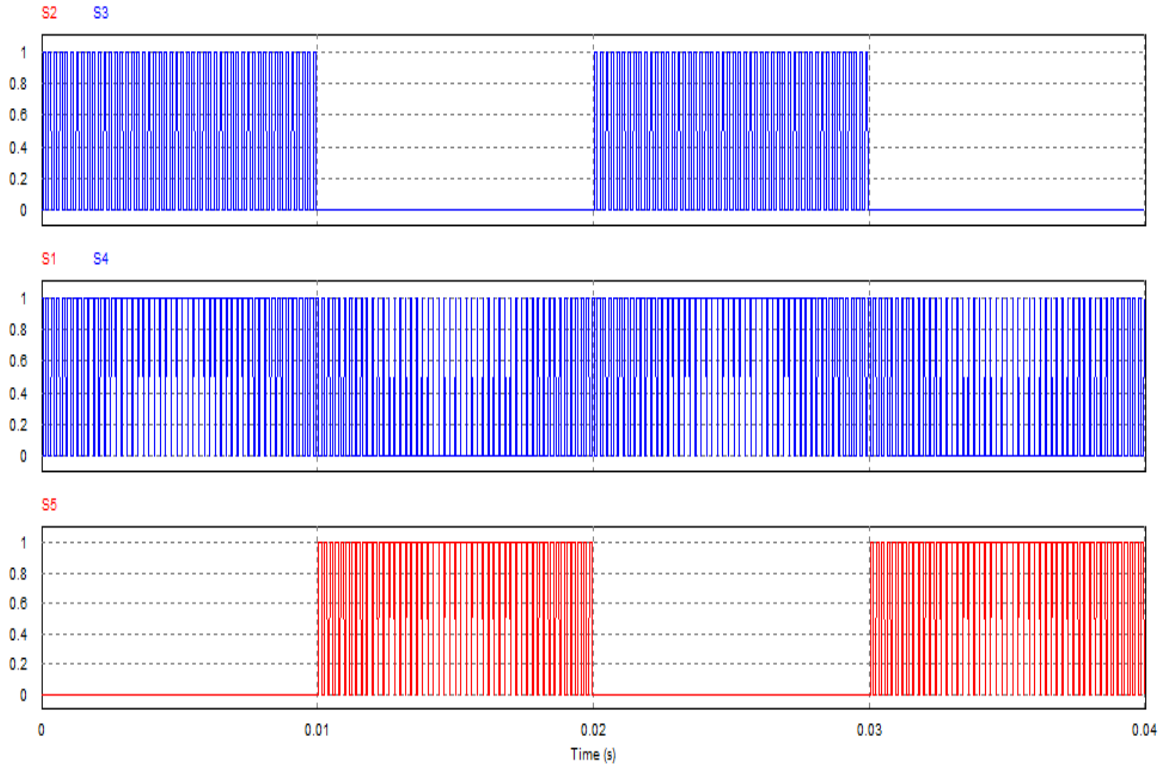

Figure 5-52 FB-ZVR modulation signal waveforms

Advantages are:

- Voltage across the filter is unipolar
- High efficiency of up to 96% is due to no reactive power exchange between the filter inductance and the DC link capacitance during zero voltage state.
- Voltage across the PV module has a grid frequency component and no switching frequency component producing very low leakage current and EMI

Drawbacks are:

- One extra switch and four diodes
- During deadtime clamping, bipolar output voltage is obtained leading to increased core losses across the output filter.

Chapter 6 : COMMON MODE VOLTAGE AND GROUND LEAKAGE CURRENT

6.1 Introduction

The main problem with transformerless PV inverter topologies is the ground leakage current. This ground leakage current can be a safety problem in both residential and industrial applications. This concern is already highlighted in chapter two of this work under various grid interconnection standards and codes. The only grid code that explicitly stated the requirement for grid connected PV transformerless PV inverter topologies is the German code VIN VDE 0126-1-1 that has been thoroughly scrutinized in chapter two.

Common mode voltage generation that produces ground leakage current is evaluated. PSIM simulation software is a dedicated and optimised simulation environment for simulating power electronics systems and drives systems. Thermal module is an add-on package from PSIM 7.0.5 that is very useful to calculate semiconductor power losses and hence determine power electronics system efficiency based on the accuracy of the semiconductor manufacturers' datasheet. However, PSIM 9 released in 2011 is used in this work.

Section 6.2 provides an overview of PSIM thermal module and shows the limitations of using it for semiconductor power devices losses determination. Sections 6.3 and 6.4 analyses the common mode voltage and ground leakage current for full bridge inverter topology with both bipolar unipolar switching strategies. The parasitic capacitance is modelled with 100 nF as described in (kerekes, 2007). Section 6.5 provides the PSIM model and simulation results for the performance evaluation for different inverter topology parameters variations.

6.2 Thermal module

The thermal module is an add-on module to the basic PSIM simulation software. This module allows the power losses of semiconductor devices such as MOSFET, IGBT, power diodes etc. the model is constructed by introducing a database from the manufacturer' datasheet if it is not already part of the software library. This device model is used in the simulation. In the simulation the model takes into account the static characteristics of the device such as conduction voltage drop, on-state resistance etc. The dynamic characteristics such as turn on and turn-off transients are taken not taken into account. So this is one limitation that will affect the simulated results but the power losses associated with the dynamic characteristic can be

accounted for and use to adjust the simulated results for better accuracy. Using the voltages and currents calculated during simulation, PSIM accesses the device database and then calculate the switching and conduction power losses. At this point it is necessary to take into that these losses calculations are only an approximation and its accuracy depends on the accuracy of the device's datasheet supplied by the manufacturer. This loss estimation procedure can also be used for thermal management design and estimating the device operating junction temperature to ascertain if it is less than the device maximum junction temperature plus headroom.

In the simulation processes there is a parameter under which the power losses can be calculated based on the switching frequency of the semiconductor. For example, if the switching frequency is 10 kHz and parameter is set to 10 kHz, then the power losses will be calculated for one switching period. However, if the parameter frequency is set to 50 Hz, then the losses will be the value for a switching period of 20 ms.

6.2.1 Diode power losses calculation

The diode power losses are calculated as follows:

Conduction loss: the power diode conduction is calculated using equation 6-1.

$$P_{cond\_cal} = V_D * I_F * D \qquad 6\text{-}1$$

where

V_D is the power diode voltage drop

I_F is the power diode forward conduction current and

D is the duty cycle

Switching power losses: when calculating the switching losses, the power diode turn-on losses are neglected. The power diode turn-off losses due to the reverse recovery is calculated as shown in equations 6-2 and 6-3.

$$P_{SW\_off} = E_{rr} * f \tag{6-2}$$

$$P_{SW\_off} = \frac{1}{4} * Q_{rr} * V_R * f \tag{6-3}$$

where
E_{rr} is the reverse recovery energy losses
Q_{rr} is the reverse recovery charge
V_R is the reverse blocking voltage and
f is the frequency as defined in the input parameter *frequency*

The reverse recovery charge Q_{rr} is defined as shown in equation 6-4

$$Q_{rr} = \frac{1}{2} * t_{rr} * I_{rr} \tag{6-4}$$

Where E_{rr} is given in the database, the losses will be calculated based on E_{rr}. If E_{rr} is not given, the losses will be calculated based on Q_{rr}. If Q_{rr} is not given, the losses will be calculated based on t_{rr} and I_{rr}. If both are not given, then losses will be considered zero.

6.2.2 IGBT power losses calculation

The power losses are calculated as follows:
Conduction losses: the IGBT conduction losses are calculated using equation 6-5.

$$P_{cond\_cal} = V_{ce(sat)} * I_C \quad \text{6-5}$$

where
$V_{ce(sat)}$ is the trnsistor collectror-emitter saturation voltage and
I_C is the collector current

Switching losses: the transistor switching losses during turn-on processes is calculated using equation 6-6.

$$P_{turn\_on} = E_{on} * f \quad \text{6-6}$$

where
E_{on} is the transistor turn-on energy losses and
f is the frequency as defined in the parameter *frequency*

On the other hand, the transistor turn-off losses are calculated with equation 6-7.

$$P_{turn\_off} = E_{off} * f \quad \text{6-7}$$

where
E_{off} is the transistor turn-on energy losses and
f is the frequency as defined in the parameter *frequency*

The loss calculation for the anti-parallel diode or free-wheeling diode is the same as described above. PSIM 2006 manual provides in depth details on information about the thermal module working principles and its limitations as well (PSIM, 2006).

6.3 Full bridge with bipolar switching inverter: Common mode voltage and ground leakage current

Full bridge with unipolar switching inverter is modelled and simulated with PSIM software to carry out the performance analyses. The two performance indexes used for the inverter topology are common mode voltage, ground leakage current (EMI). Simulation parameters are listed here for easy of reference as follows:

Table 6-1 Parameters used in case of the simulation

Switching frequency	fsw= 10 kHz
Single phase DC voltage	Vdc1=350 V
DC-link capacitance	Cdc=1 mF
Output filter inductance	Lf=1.8 mH
Output filter capacitance	Cf=2 mF
Grid voltage (peak of phase to neutral voltage)	Vg=325 V
Grid frequency	fg=50 Hz
Grid inductance	Lg=50 uH
All IGBTs' = IXYS IXGH40N60C2	

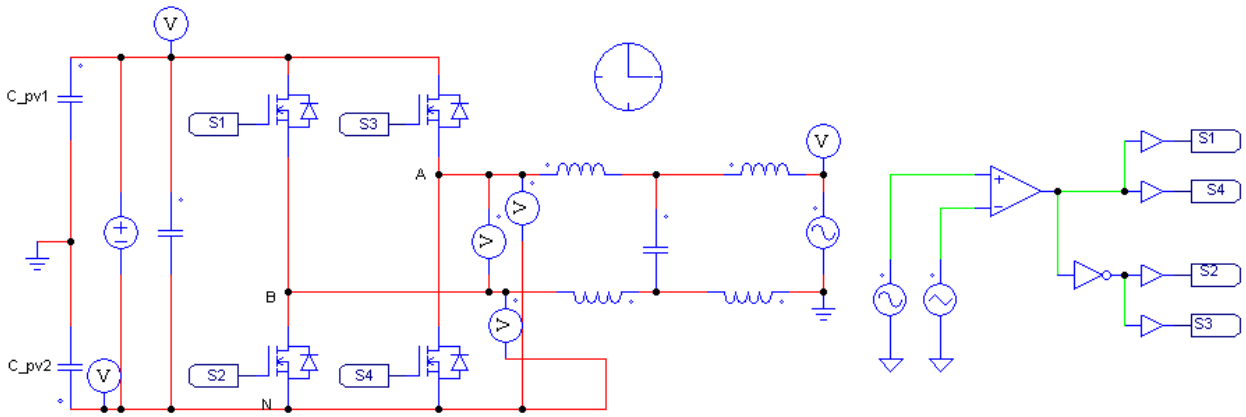

Figure 6-1 FB transformerless grid-connected topology with bipolar modulator

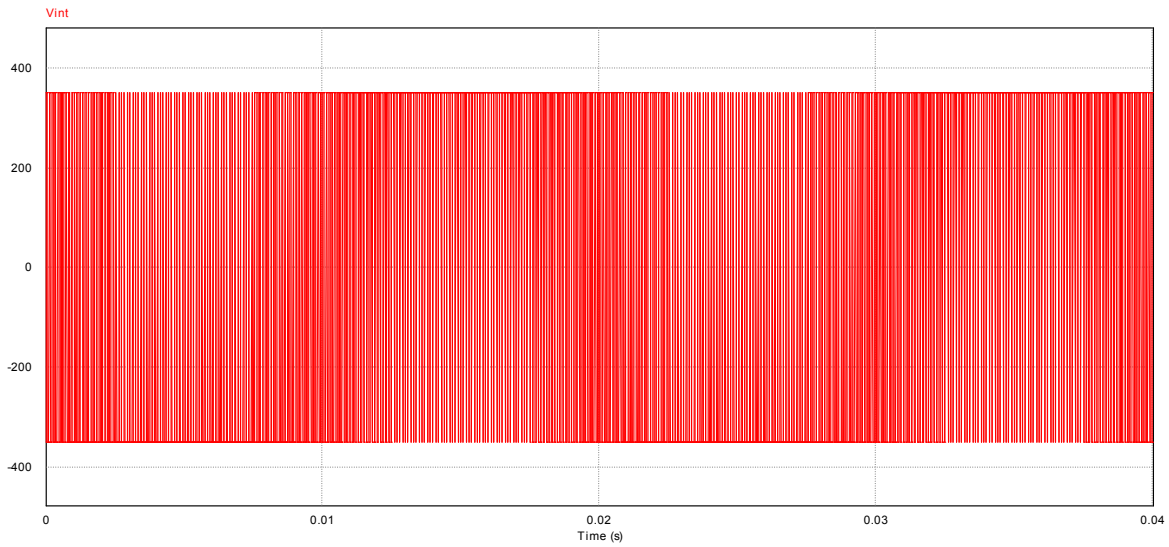

Figure 6-2 FB bipolar inverter output voltage

Figure 6-2 shows the inverter output voltage changing between +Vdc and –Vdc with switching frequency of 10 kHz. The common mode voltage is depicted in figure 6-3. The RMS value is 175V and the peak value is 175v (Vdc/2) with the grid frequency. This common mode voltage is impressed on the PV array terminal parasitic capacitance to induce the ground leakage.

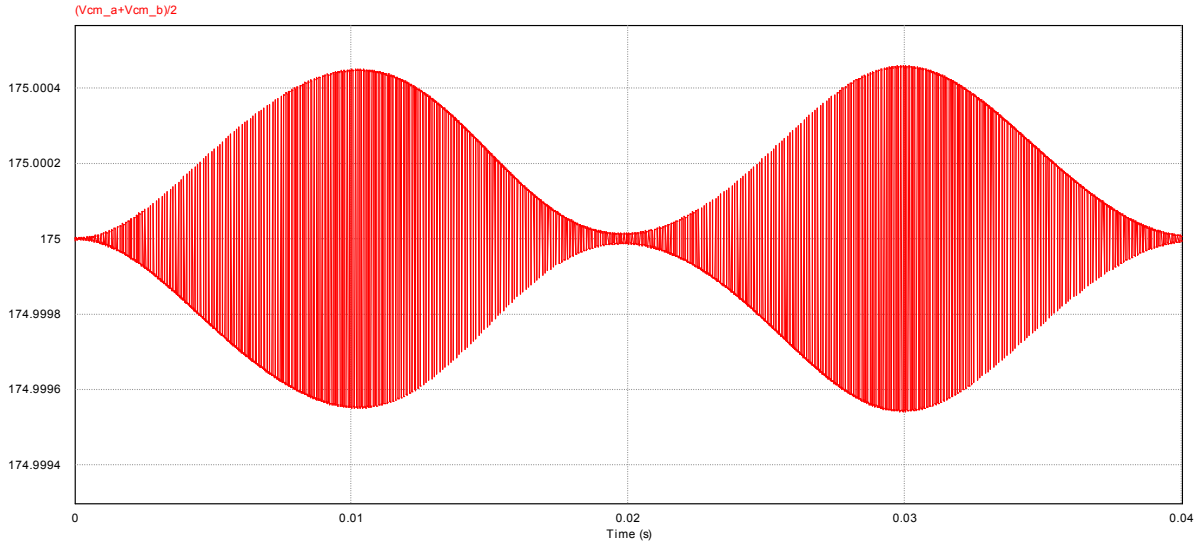

Figure 6-3 FB bipolar common mode voltage

Figure 6- 4 shows the grid output voltage having a root mean square value of 220V with a grid frequency of 50 Hz. The voltage across the PV array is depicted in figure 6-5 with a peak value of 350 V and root mean square value of 207 V with a of 50 Hz grid frequency.

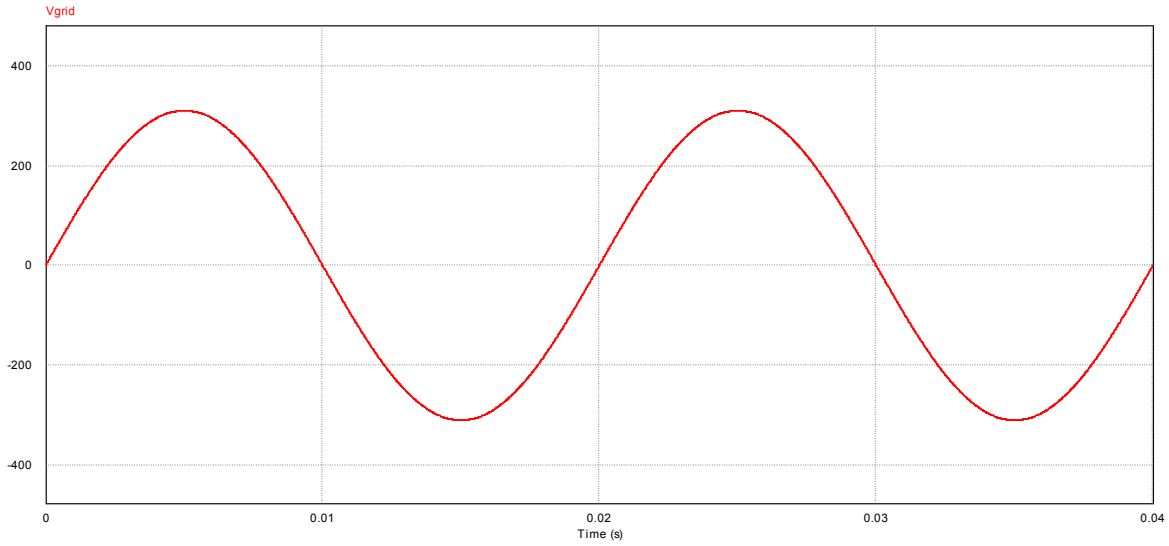

Figure 6-4 FB bipolar grid terminal voltage

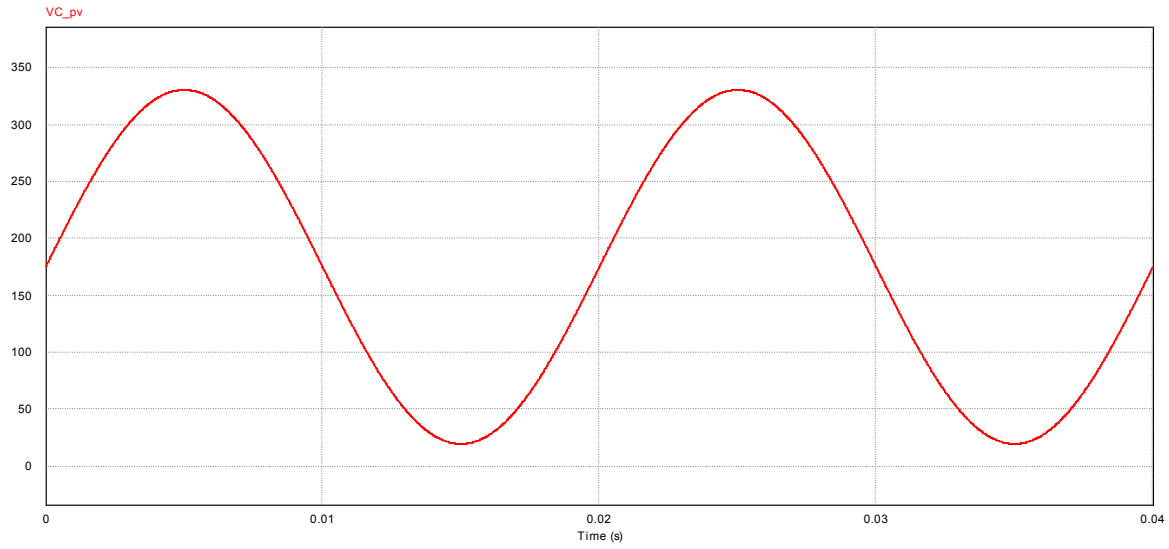

Figure 6-5 FB bipolar PV array terminal voltage

The ground leakage current waveform is shown in figure 6-6 having only the grid frequency component. The instantaneous peak value is 7,686 mA and the average leakage current is 3,111 mA. The root mean square value of the ground leakage current is 3,458 mA. These values

comply with the requirement stated in VDE 0126-1-1 safety requirement, thus this topology can be used as grid-connected transformerless PV inverter topology. However, the efficiency is low because of the reactive power exchange between the inverter output inductance and the Dc link capacitance.

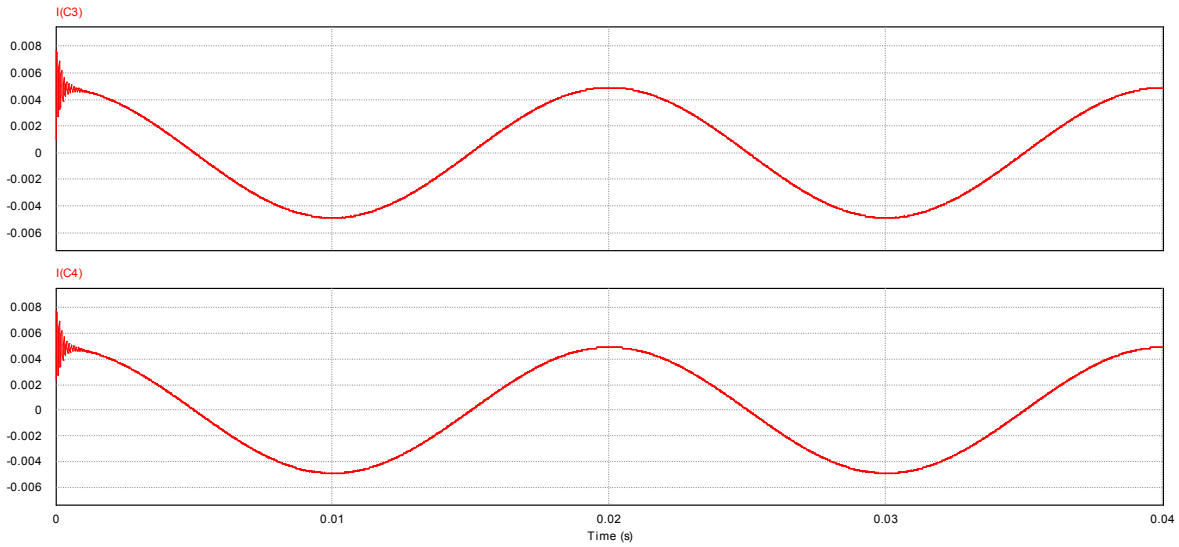

Figure 6-6 FB bipolar ground leakage current

The only frequency component present in the ground leakage current is the grid frequency of 50 Hz with peak vluae of 4,886 mA as shown in figure 6-7.

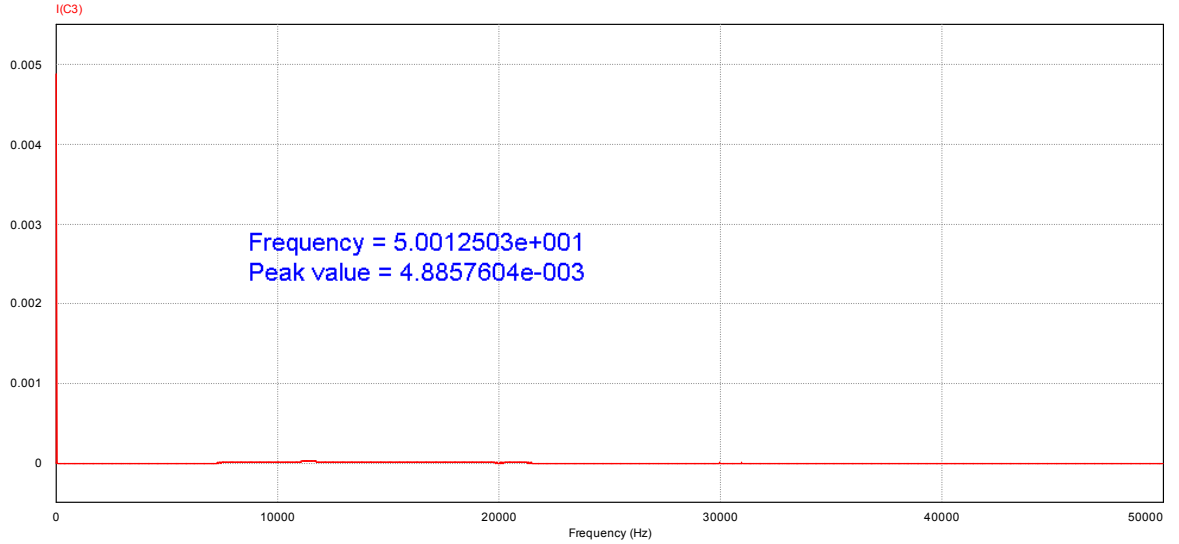

Figure 6-7 Ground leakage current FFT

6.5 Full bridge with unipolar switching inverter: Common mode voltage and ground leakage current

A Full bridge with unipolar switching inverter is modelled and simulated with PSIM software to carry out the performance analyses. The two performance indexes used for the inverter topology are common mode voltage, ground leakage current (EMI). Simulation parameters are in table 6-3.

Table 6-2 Parameters used in case of the simulation

Switching frequency	**fsw = 5 kHz**
Single phase DC voltage	Vdc1 = 350 V
DC-link capacitance	Cdc =1 mF
Output filter inductance	Lf = 0,9 mH
Output filter capacitance	Cf = 1 mF
Grid voltage (peak of phase to neutral voltage)	Vg = 325 V
Grid frequency	Fg = 50 Hz
Grid inductance	Lg = 50 uH
All IGBTs' = IXYS IXGH40N60C2	

The schematic of a FB transformerless grid-connected inverter topology with unipolar modulator is shown in figure 6-8 as modelled in the PSIM software environment.

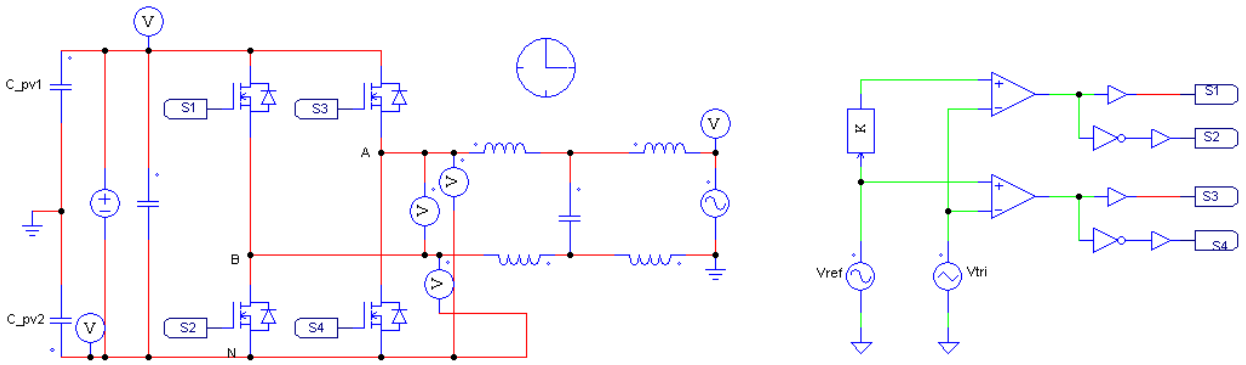

Figure 6-8 FB transformerless grid-connected topology with unipolar modulator

The inverter ouput voltage is shown in figure 6-9 changing from positive peak value to zero and then to negative peak values. The three voltage vector states enable the topology to be switched with half the switching frequency with the same component parameters as a full bridge with bipolar switching strategy. This provides the advantage of lower filter requirements and reduce the core lossess of the filter inductor. In order to be able to make comparative analysis with the full bridge with bipolar switching strategy a switching frequency of 5 Khz is used and the filter parameters are halfed as shown in table 6-2.

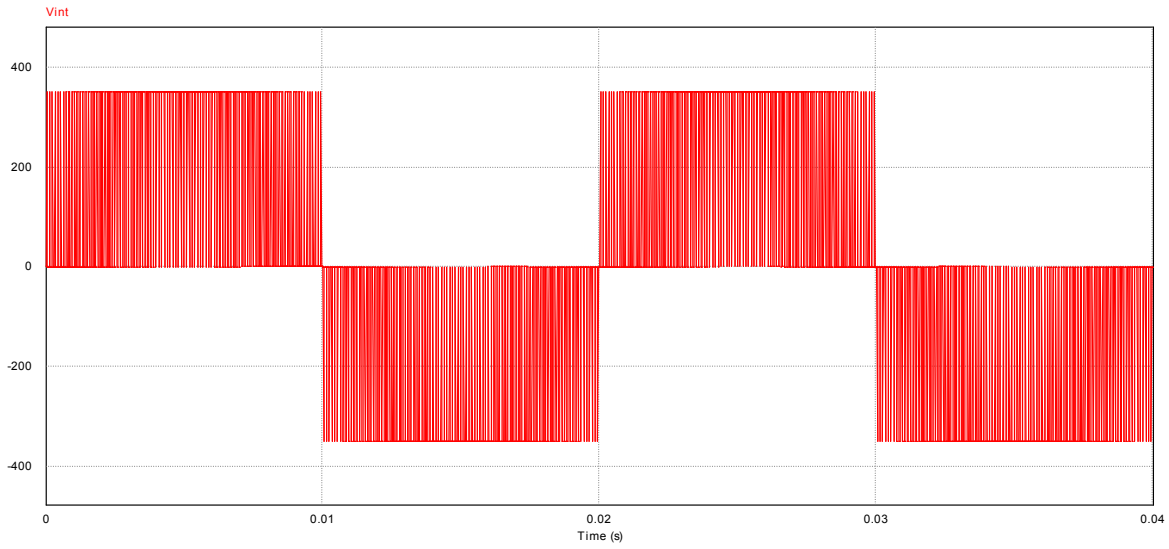

Figure 6-9 FB unipolar inverter output voltage

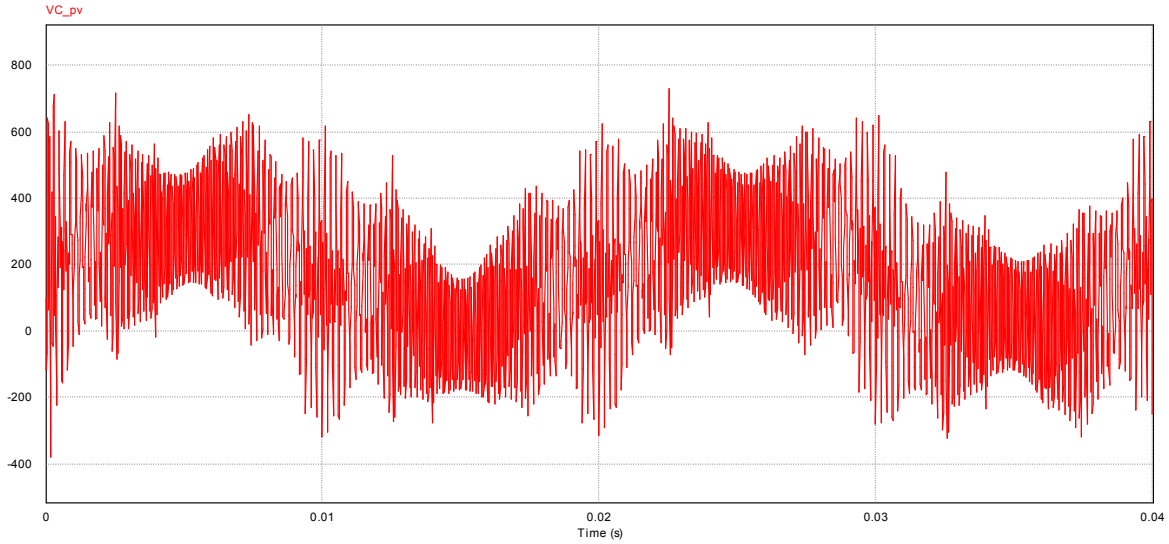

Figure 6-10 PV array terminal voltage

The PV array terminal voltage across the PV array parasitic capacitance is shown in figure 6-11 to contain harmonics of switching frequency. The peak value of the PV array terminal voltage is 730 V and the average value is 223 V. The root mean square value is 271 V. Ground leakage current is only limited by the PV array parasitic capacitance.

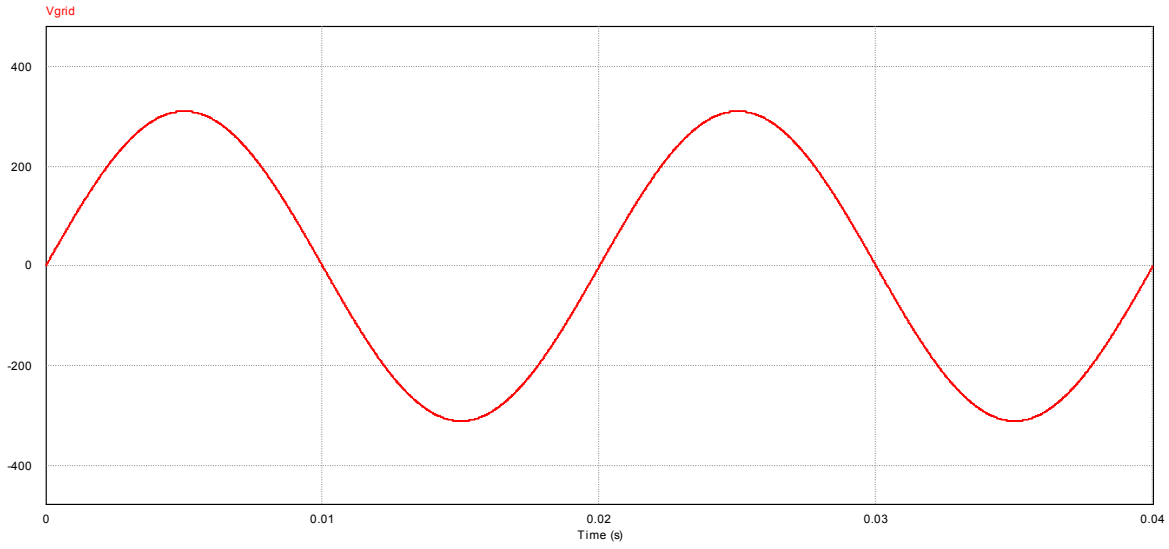

Figure 6-11 Grid terminal voltage

The grid waveform with frequency of 50 Hz and root mean square value of is 220 V and peak value of 311 V depicted in figure 6-12.

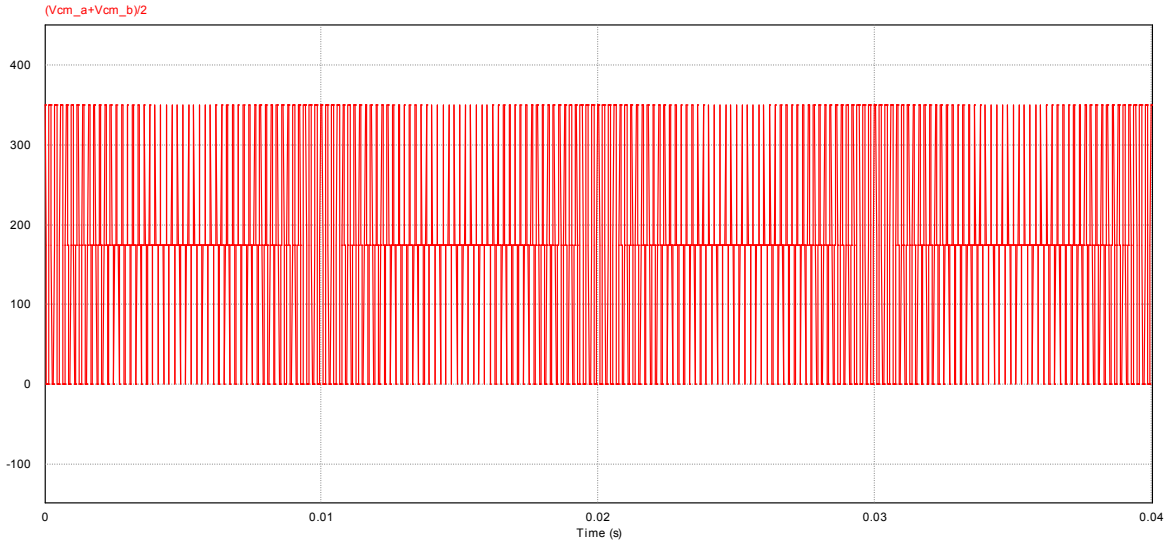

Figure 6-12 FB unipolar Common mode voltage

The common mode voltage imposed on the PV array parasitic capacitance is shown in figure 6-13. The peak value is 350 V which is the DC link voltage value and its root mean square is 210 V.

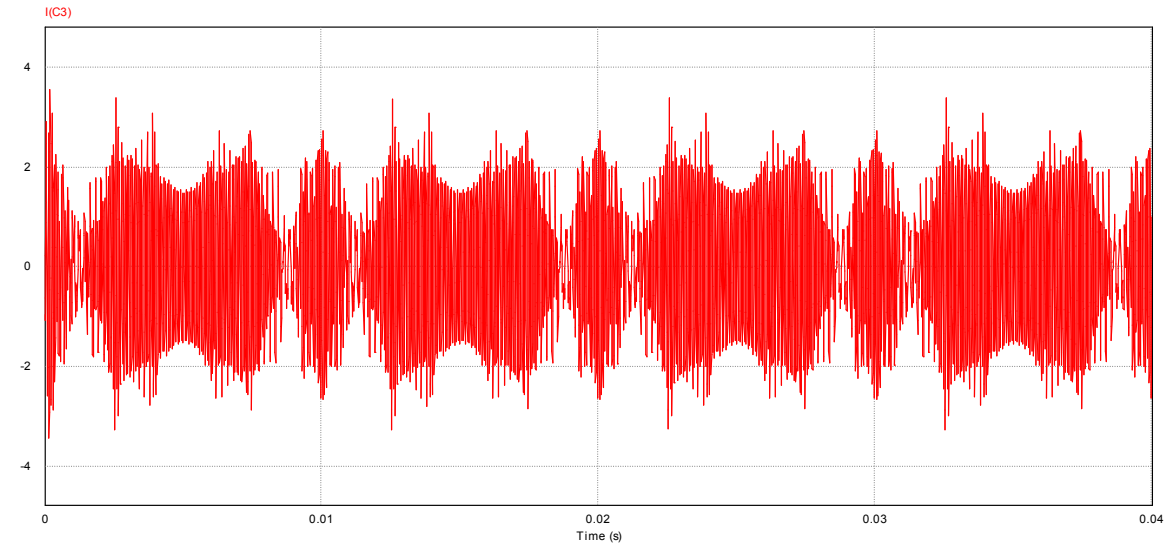

Figure 6-13 FB unipolar ground leakage current

The leakage current through the PV array parasitic capacitance is shown in figure 8-14. It contains harmonics of the switching frequency. The peak value of the ground leakage current is 3,552 A and the average value is 1,164 A. The root mean square value is 1,345 A.

Figure 6-15 shows the FFT of the ground leakage current. Based on the simulation results, the FB with unipolar switching is not acceptable for PV transformerless configuration because it does not comply with the safety requirement of VDE 0126-1-1.

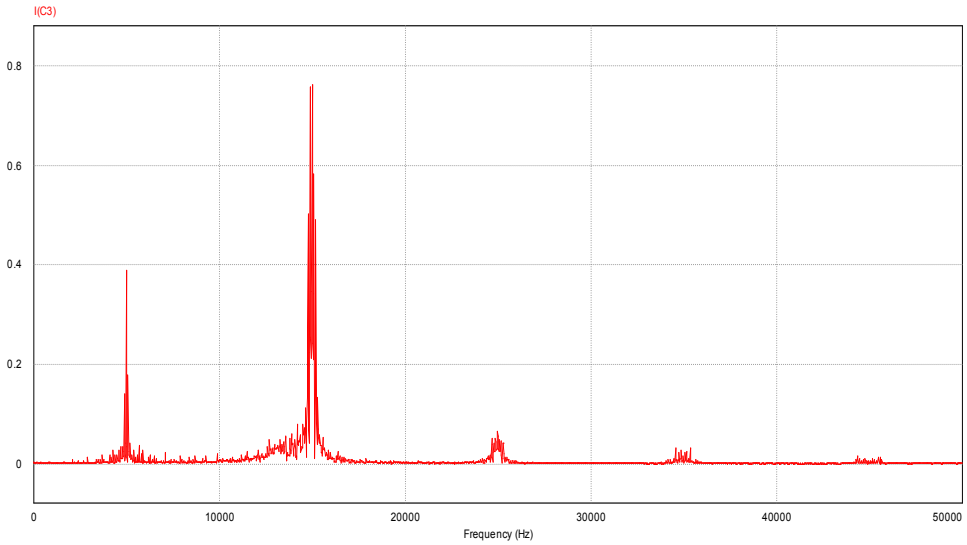

Figure 6-14 FB unipolar ground leakage current FFT

6.6 Energy efficiency determination of FB transformerless inverter topology

The energy efficiency of the full bridge transformerless inverter topology is determined by using the manufacturer's datasheet in PSIM. Only the switches power losses are considered in the energy efficiency determination. Inductor core losses, connectors losses, capacitance equivalent series resistance and inductance, power consumed by the control circuits and other auxiliary circuits such as sensors, signal conditioners etc. are not taken into consideration. Simulation parameters listed in table 6-3 is reproduced here for easy of reference as table 6-4.

Table 6-3 Parameters used in case of the simulation (unipolar switching)

Switching frequency	**fsw= 5 kHz**
Single phase DC voltage	Vdc1=350 V
DC-link capacitance	Cdc=1 mF
Output filter inductance	Lf=1.8 mH
Output filter capacitance	Cf=2 mF
Grid voltage (peak of phase to neutral voltage)	Vg=325 V
Grid frequency	fg=50 Hz
Grid inductance	Lg=50 uH
All IGBTs' = IXYS IXGH40N60C2	

Modulation index of 0.85 and PV array parasitic capacitance values of 100 nF is used. Input power is determined by multiplying the average input current with the DC bus voltage. Output power is determined by subtracting the total power losses of all the four switches. Equation 6-8 is used to calculate the efficiency of the power inverter.

$$\eta = \frac{P_{out}}{P_{in}} = 1 - \frac{P_{Loss}}{P_{in}} \qquad 6\text{-}8$$

Figure 6-15 shows the schematic diagram simulated in PSIM. The grid is modeled as an infinity current sink able to sink any amount of power delivered by the power converter.

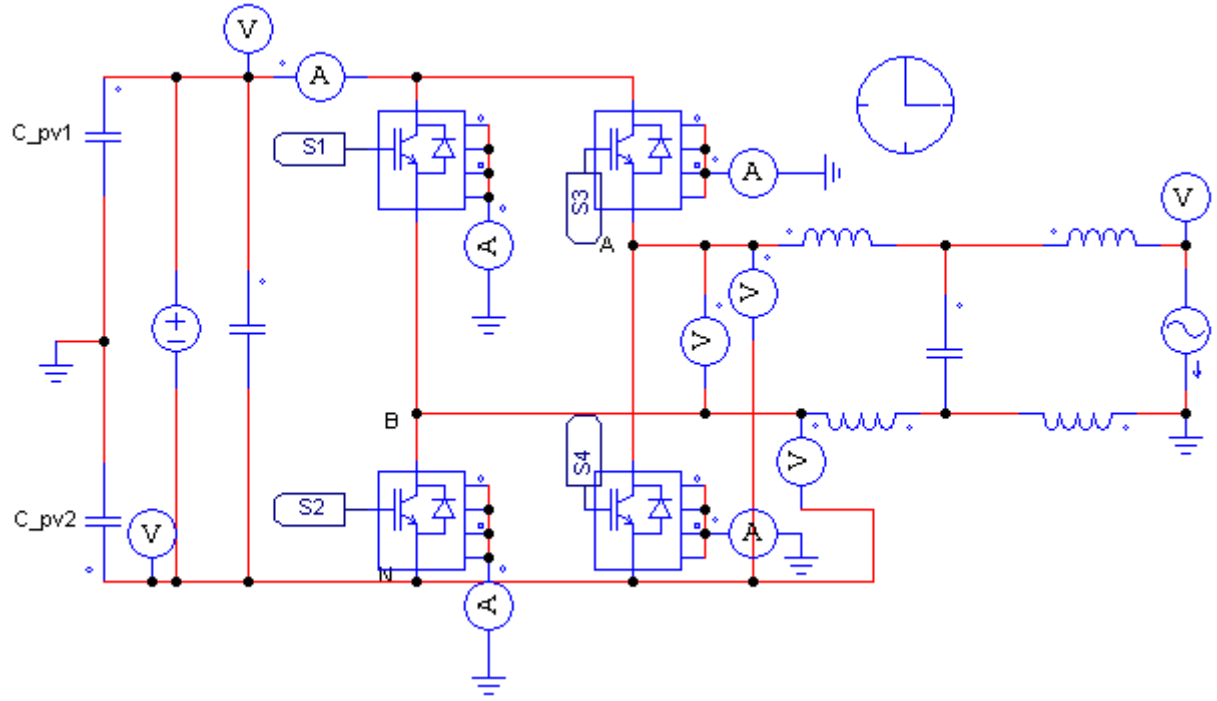

Figure 6-15 Efficiency model of transformerless PV FB inverter topology

The sum of the average power losses in each switch is shown in figure 6-16.

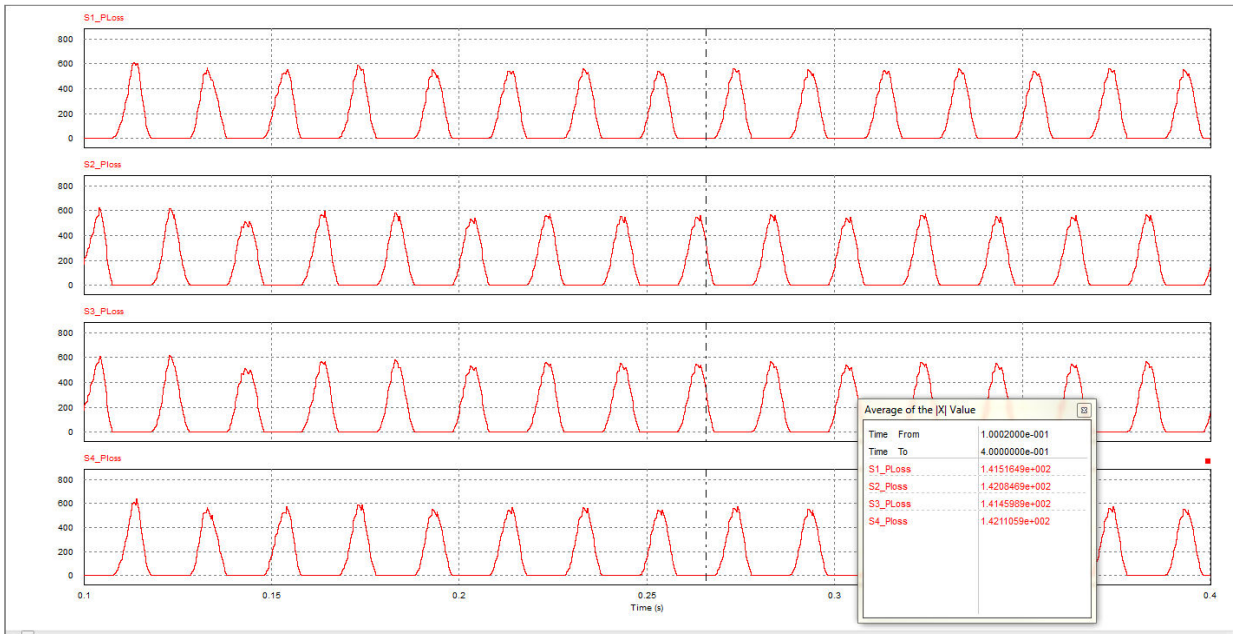

Figure 6-16 Average semiconductor power switch losses with bipolar switching

The total average power loss in the four IGBT switches is 567,17 W. The average input power is calculated by multiplying the DC link voltage (350 V) by the average input current. The waveform for the average input power is shown in figure 6-17.

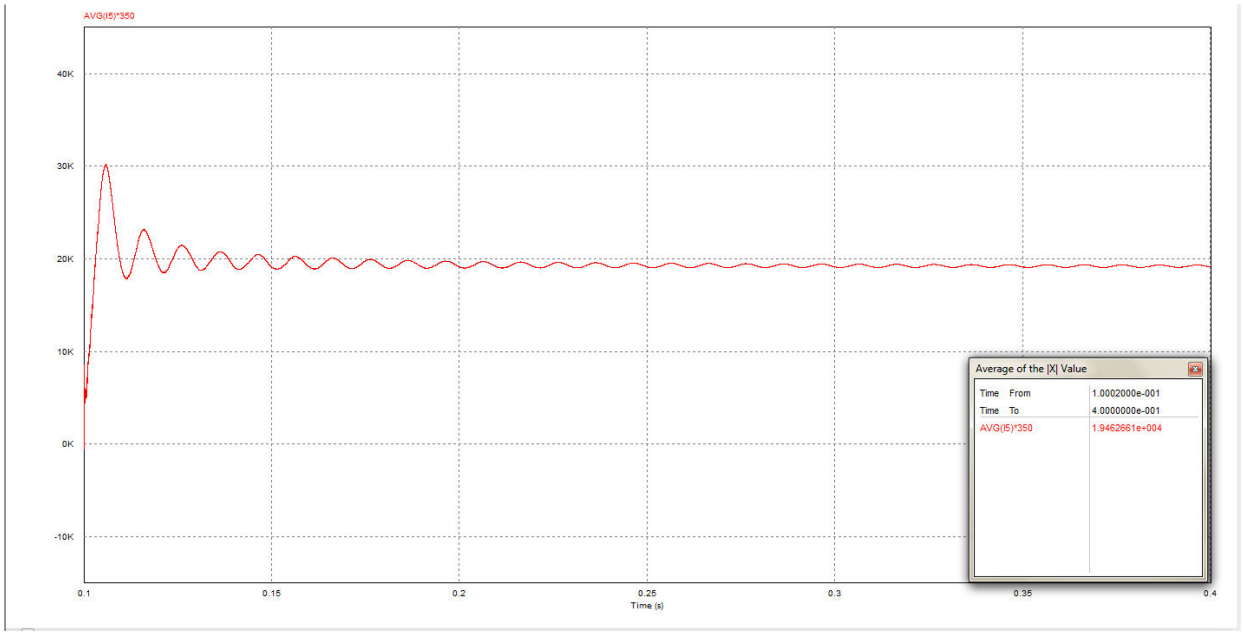

Figure 6-17 Average input power of FB topology with unipolar switching

The efficiency is calculated to be 97,09%. The value does not consider other losses in the inverter topology system. The real or practical efficiency value will be less than this calculated value. However, since the same assumptions will be used in other efficiency determination technique carried out in this work the conclusion will be qualitative.

The manufacturers' datasheet used for the switching power semiconductors (IXYS IXGH40N60C2) is provided in appendix A2.

The same schematic diagram in figure is used for the determination of the FB inverter topology with a bipolar switching modulator. Simulation parameters used are listed in table 6-4.

Table 6-4 Parameters used in case of the simulation (bipolar switching)

Switching frequency	**fsw= 10 kHz**
Single phase DC voltage	Vdc1 = 350 V
DC-link capacitance	Cdc = 1 mF
Output filter inductance	Lf = 0,9 mH
Output filter capacitance	Cf = 1 mF
Grid voltage (peak of phase to neutral voltage)	Vg = 325 V
Grid frequency	fg=50 Hz
Grid inductance	Lg=50 uH
All IGBTs' = IXYS IXGH40N60C2	

The average input power and total average power losses for the four IGBT switches are shown in figure 6-18 and 6-19 respectively.

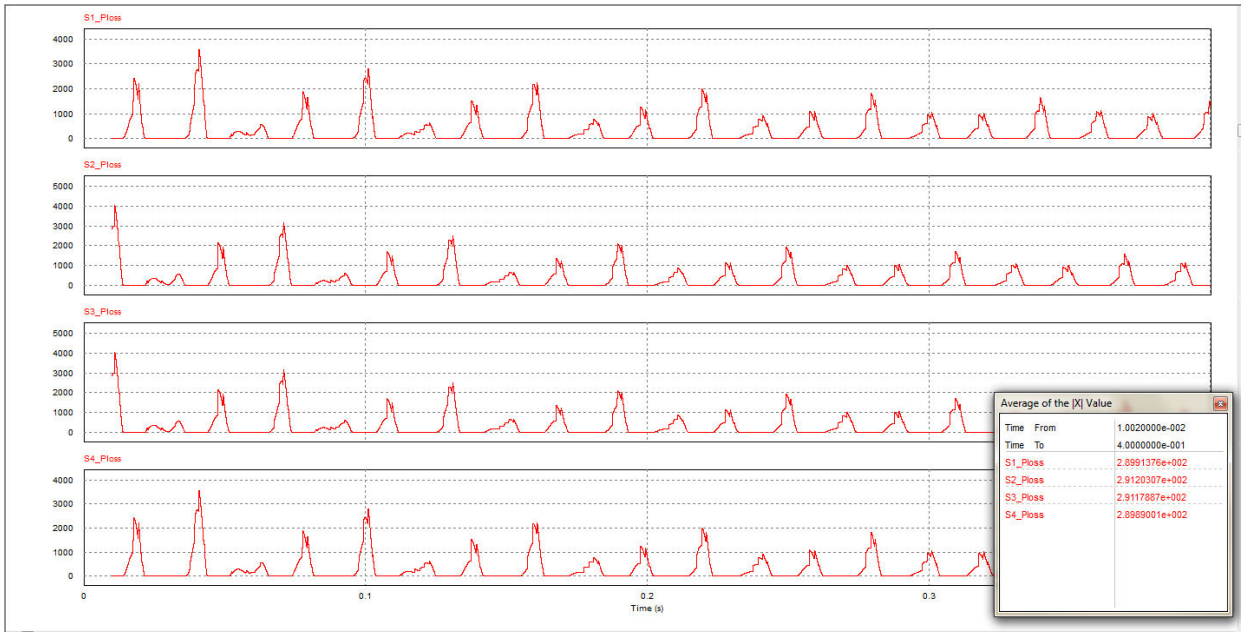

Figure 6-18 Average semiconductor power switch losses with bipolar switching

The total average power dissipated in the four IGBT switches is 1162.19 W. The average input power is determined from the waveform shown in figure 6-19. The efficiency value is calculated by multiplying the average input current by the DC bus voltage of 350 V. Average input power

is determined from the waveform shown in figure 6-19 to be 2537,11 W. The efficiency is calculated to be 95,42%

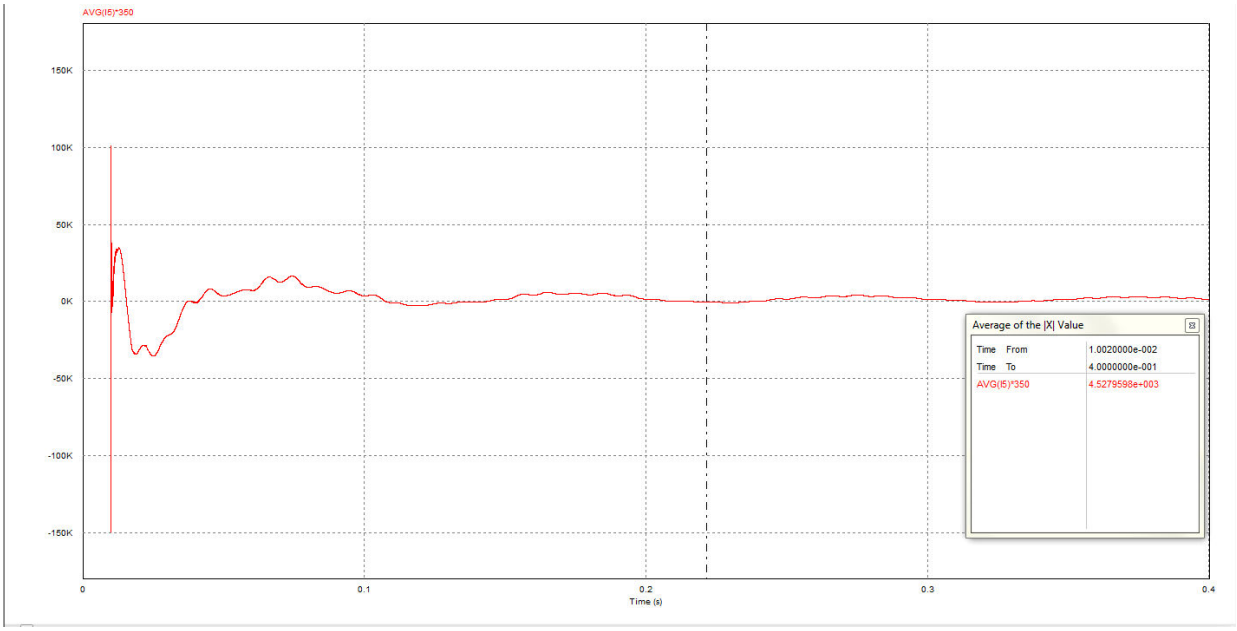

Figure 6-19 Average input power of FB topology with bipolar switching

The qualitative conclusions drawn from the power efficiency determination technique used in this work is that transformerless full bridge PV inverter topology with unipolar switching strategy has higher efficiency than the same configuration but implementing bipolar switching strategy. However, high frequency ground leakage current and its high values make it unsuitable as a grid-connected system. The better advantage of low frequency component of full bridge with bipolar switching scheme and higher power efficiency of the full bridge with unipolar switching strategy is explored in the new topology proposed in the next chapter.

Chapter 7 : NOVEL TRANSFORMERLESS GRID-CONNECTED PV TOPOLOGY

7.1 Introduction

A novel transformerless PV topology invented and developed is evaluated for common mode voltage and ground leakage current in this chapter. The PV array parasitic capacitance is modelled with a simple capacitor in PSIM. Both the positive and negative terminals of the PV panel are connected to ground through the parasitic value of 100 nF capacitance as reported in (Kerekes, 2007).

Common mode voltage and ground leakage current are analysed in this section. Mitigations methods are also highlighted.

Bipolar and unipolar switching strategies are investigated for the novel topology. Particular attention is paid to the voltage change across the PV parasitic capacitance and some mitigation techniques are implemented. A conclusion is given at the end of the simulation results analysis.

7.2 A novel transformerless grid-connected PV topology

A variant of the full bridge PV transformerless inverter topology investigated in this chapter is given in figure 7-1. Extra features added to the fundamental full bridge topology are two diodes and two active switches to achieve zero voltage vector switching states similar to HERIC and REFU inverter topologies that are fully discussed in sections 5.3.2 and 5.3.3. The main difference the previously mentioned topologies is the output grid filter and the switching strategy. During the zero voltage vectors switching states the grid is not short circuit through the inverter side inductor but rather through the inverter side capacitor and the grid side inductor.

The common mode voltage and ground leakage current is investigated for PV inverter topology presented in this section for both bipolar and unipolar switching strategies.

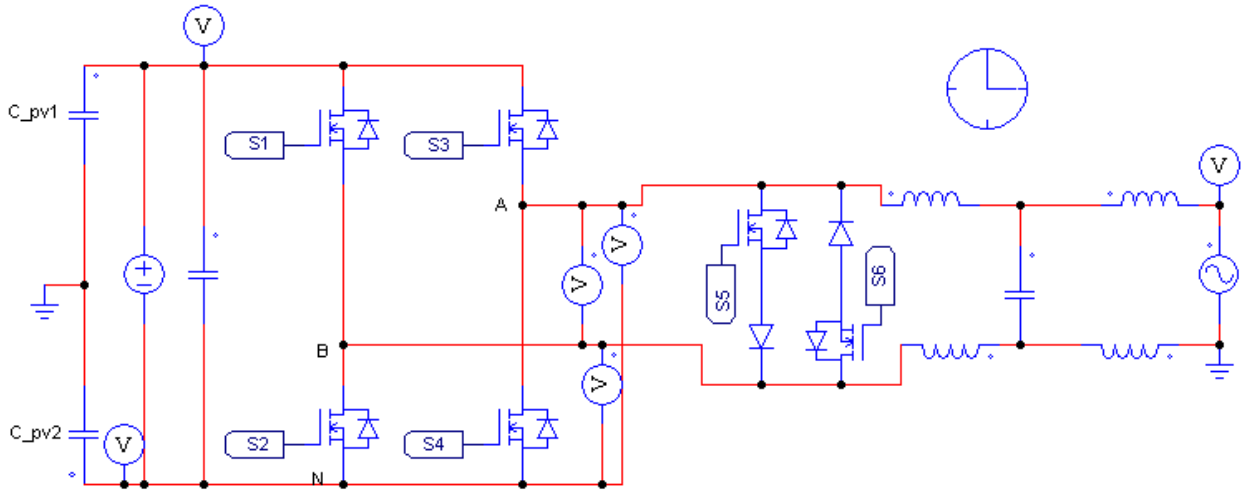

Figure 7-1 FB VZS AC decoupled dual-parallel switch

7.2.1 FB VZS AC decoupling dual-parallel switch with unipolar modulator.

The FB VZS AC decoupling dual-parallel transformerless inverter topology is shown in figure 7-1, the PV array is disconnected from the grid utility through the zero voltage vector switching states thereby preventing reactive power circulation between the DC link capacitance and the output filter inductance. This increases the efficiency of the system.

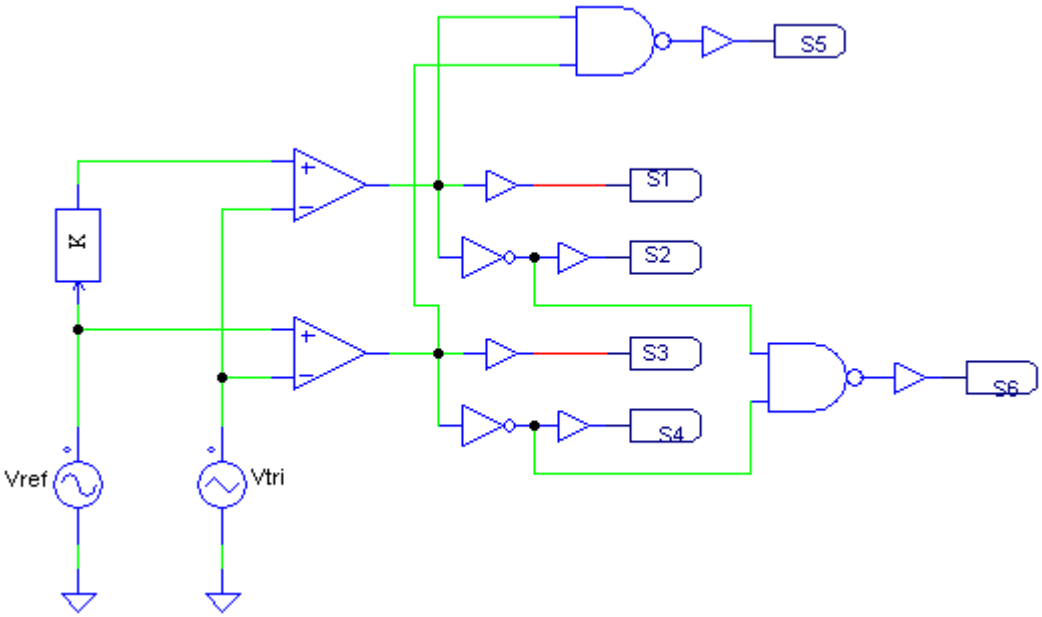

Figure 7-2 FB VZS AC decoupling dual-parallel switch unipolar modulator circuit

The anti-parallel AC decoupling switches perform the freewheeling roles of the anti-parallel diodes of the main bridge semiconductor switches. The grid current direction determines which of the AC decoupling switch conducts according to the switching strategy presented in figure 7-2. During the zero voltage vector state the output of the inverter is short-circuited across the output filter input when S1 and S3 or S2 and S4 or S1, S1, S2 and S4 are off. The number of zero voltage vector states can thus be increased to three.

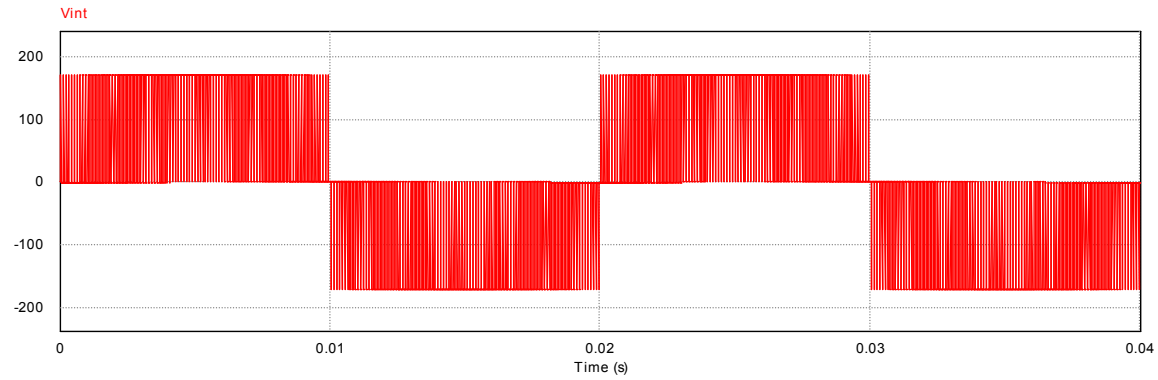

Figure 7-3 FB VZS AC decoupling dual-parallel switch inverter output voltage (Unipolar)

Figure 7-3 shows the output of the FB VZS AC decoupled inverter topology with the output voltage changing from positive 175 V to negative 175 V that is +Vdc/2 to –Vdc/2.

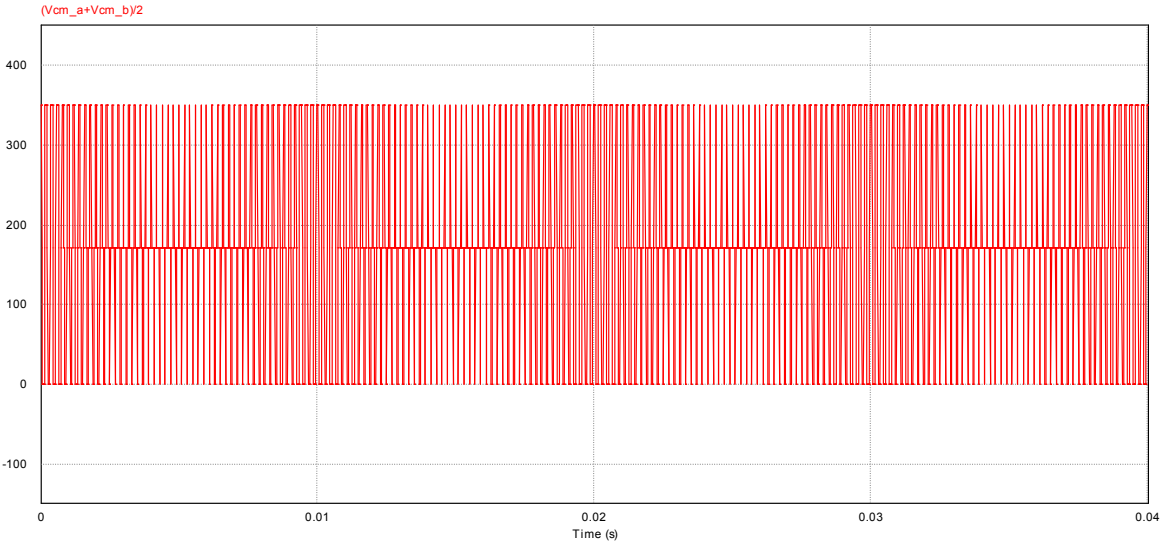

Figure 7-4 FB VZS AC decoupling dual-parallel switch common mode voltage (Unipolar)

The common voltage impressed across the PV parasitic capacitance is depicted in figure 7-4 with a peak value of 350 V that is Vdc.

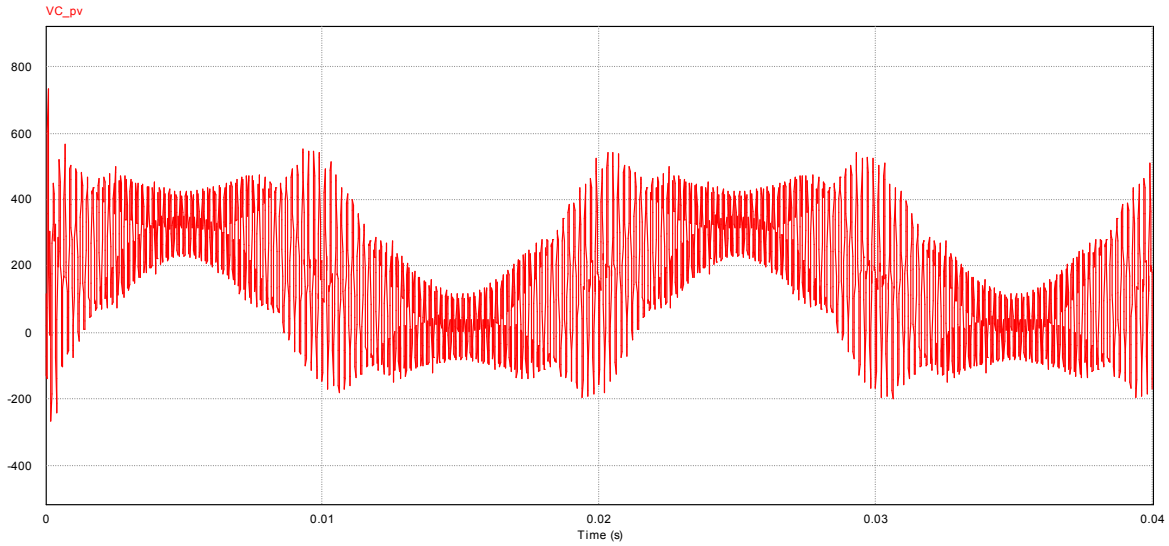

Figure 7-5 FB VZS AC decoupling dual-parallel switch PV array terminal voltage (unipolar)

The voltage impressed across the PV array capacitance is shown in figure 7-5 and its harmonics content in figure 7-6. The instantaneous peak value of this waveform is 732 V and its average is 203 V. The PV parasitic capacitance determines the limit of the ground leakage current.

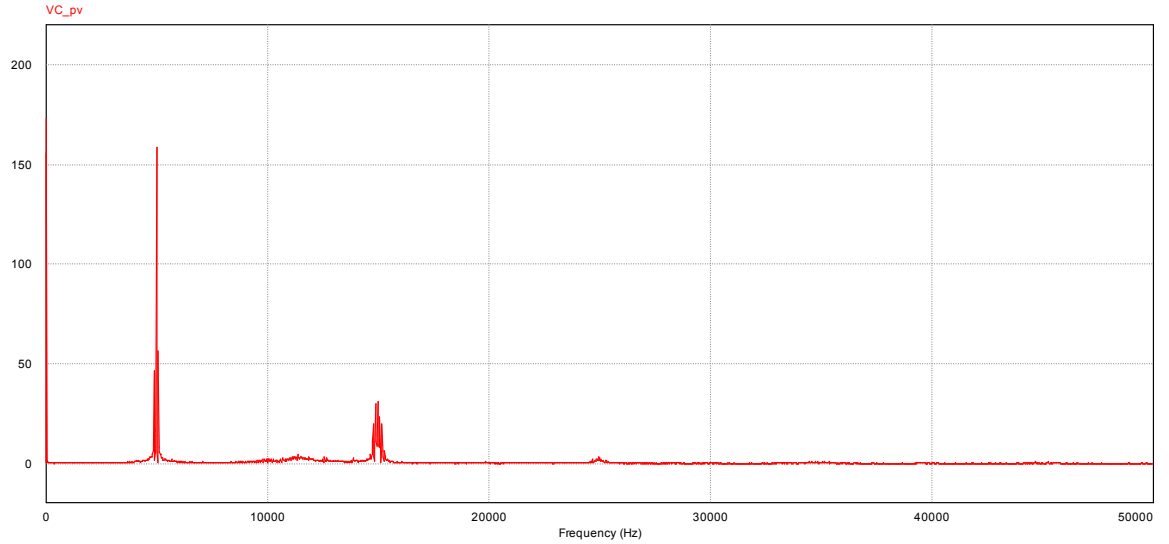

Figure 7-6 PV array terminal voltage FFT

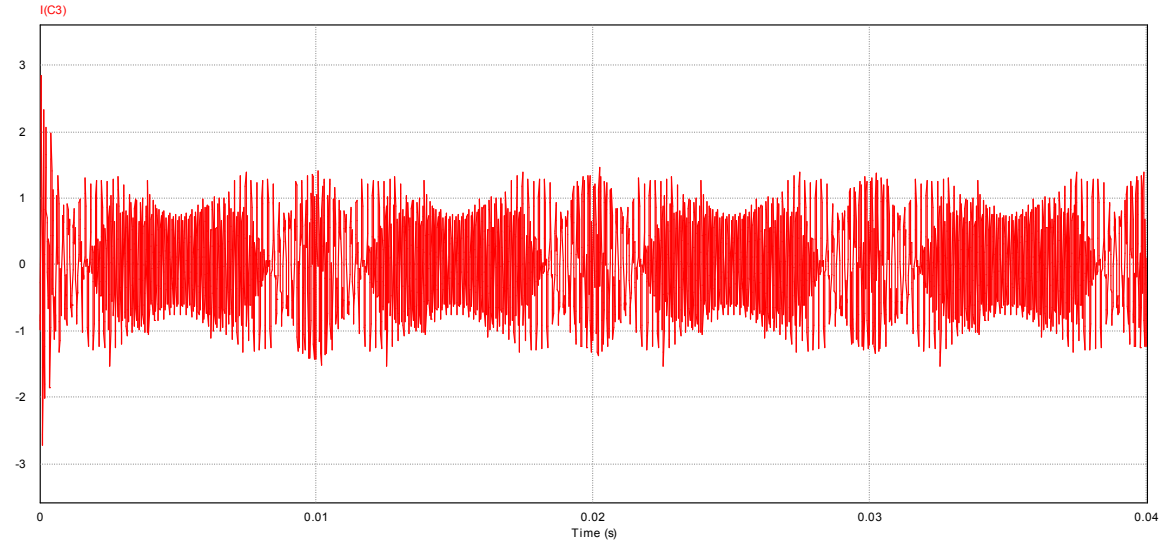

Figure 7-7 FB VZS AC decoupling dual-parallel switch PV ground leakage current (Unipolar)

The ground leakage current with PV array parasitic capacitance value of 100 nF is shown in figure 7-7 and its harmonics content in figure 7-8. The instantaneous peak value is 2,85 A and it average value is 564,00 mA. The root mean square value is 677,32 V. This topology with unipolar switching strategy is not acceptable for transformerless grid-connected system because of safety reason. The safety requirements stated in VDE 0126-1-1 is far exceeded.

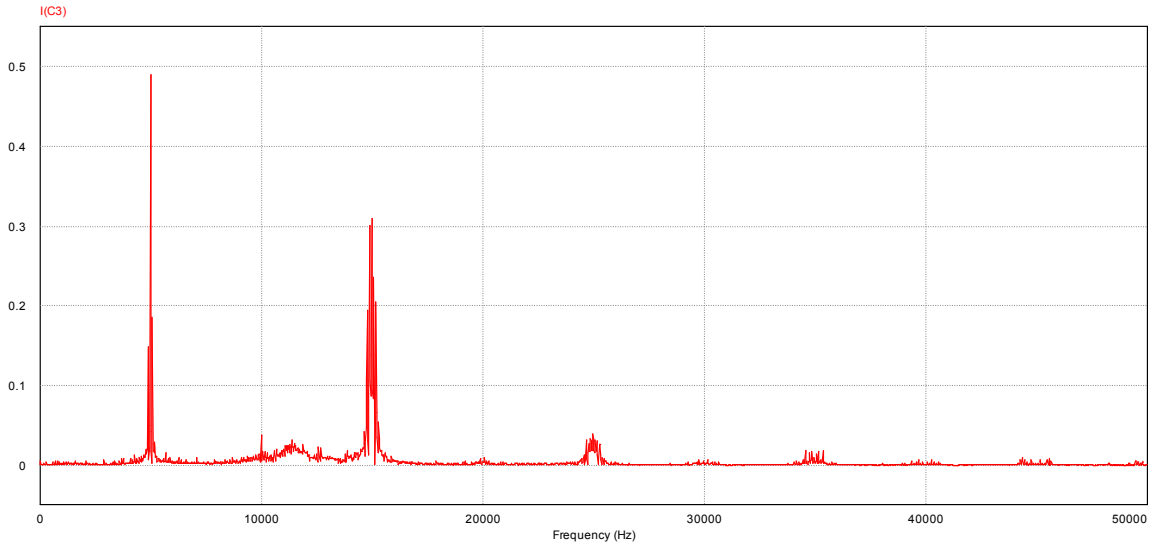

Figure 7-8 FB VZS AC decoupling dual-parallel switch PV ground leakage current FFT (Unipolar)

The harmonics content of the ground leakage current is depicted in figure 7-8. It contains harmonics at integral multiple of the switching frequency with a peak value at the switching

frequency (5 kHz). The peak value of this harmonic is 489,64 mV. The harmonics contain in this ground leakage current may cause electromagnetic interference problem for communication equipment and other low power control systems. Electromagnetic compatibility problem may arise.

7.2.1 FB VZS AC decoupling dual-parallel switch with bipolar modulator.

The FB VZS AC decoupling dual-parallel transformerless inverter topology is shown in figure 7-9 for easy of reference, the PV array is disconnected from the grid utility through the zero voltage vector switching states thereby preventing reactive power circulation between the DC link capacitance and the output filter inductance. This increases the efficiency of the system.

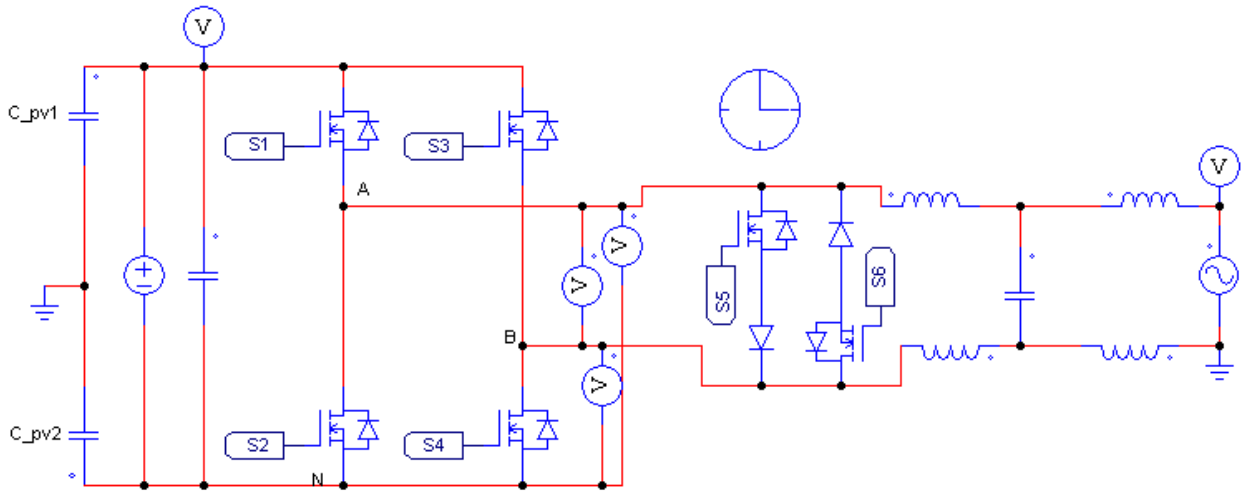

Figure 7-9 FB VZS AC decoupling dual-parallel switch with bipolar modulator

The anti-parallel AC decoupling switches perform the freewheeling roles of the anti-parallel diodes of the main bridge semiconductor switches. The grid current direction determines which of the AC decoupling switch conducts according to the switching strategy presented in figure 7-10.the bipolar switching modulating strategy is employed. During the zero voltage vector switching state the output of the inverter is short-circuited across the output filter input when S1 and S3 or S2 and S4 or S1, S1, S2 and S4 are off. The number of zero voltage vector switching states can thus be increased to three.

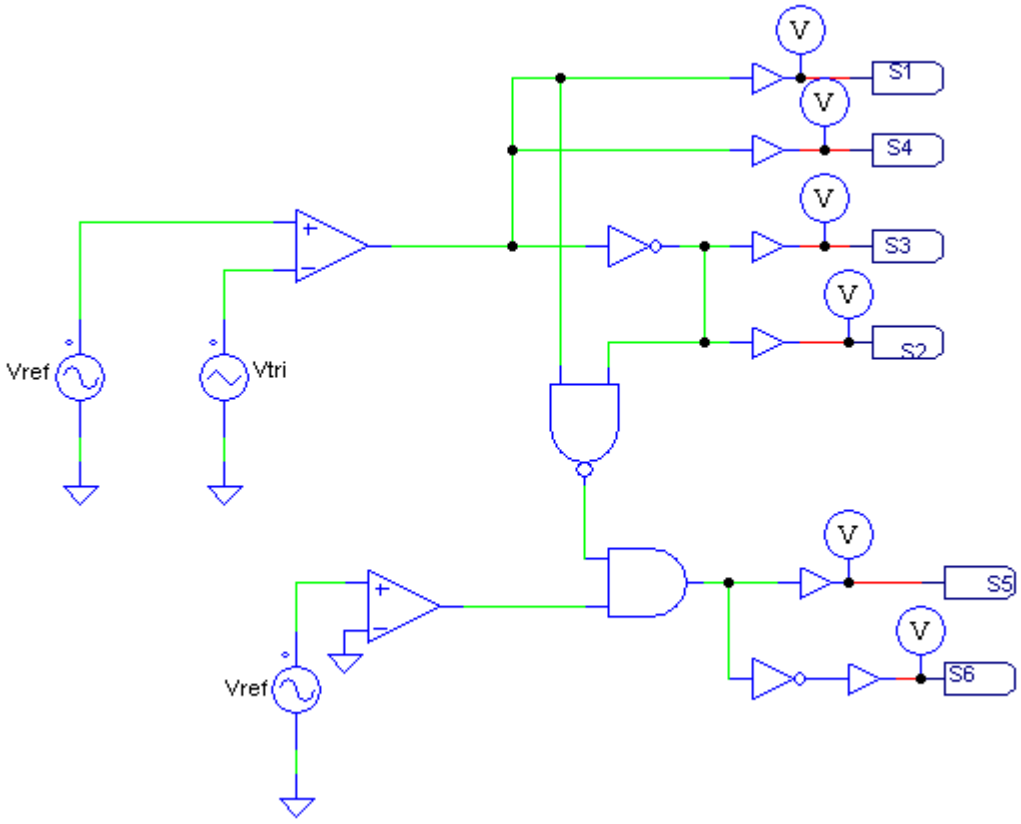

Figure 7-10 FB VZS AC decoupling dual-parallel switch bipolar modulator circuit

Figure 7-11 shows the output of the FB VZS AC decoupling inverter topology with the output voltage changing from positive 170 V to zero voltage to negative 350 V in the positive half cycle and positive 350 V to zero voltage to negative 170 V in the negative half cycle. This switching sequence actually reduces the voltage stress imposed on the output inductance thereby reducing the core losses of the inductor. Reduction the core losses translate into higher efficiency.

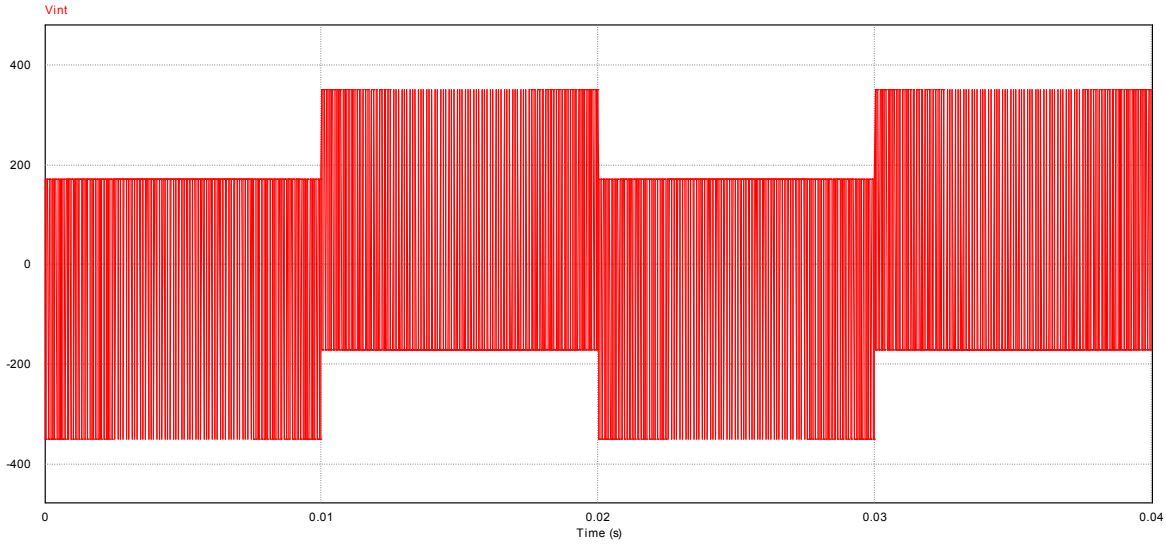

Figure 7-11 FB VZS AC decoupling dual-parallel switch inverter output voltage (bipolar)

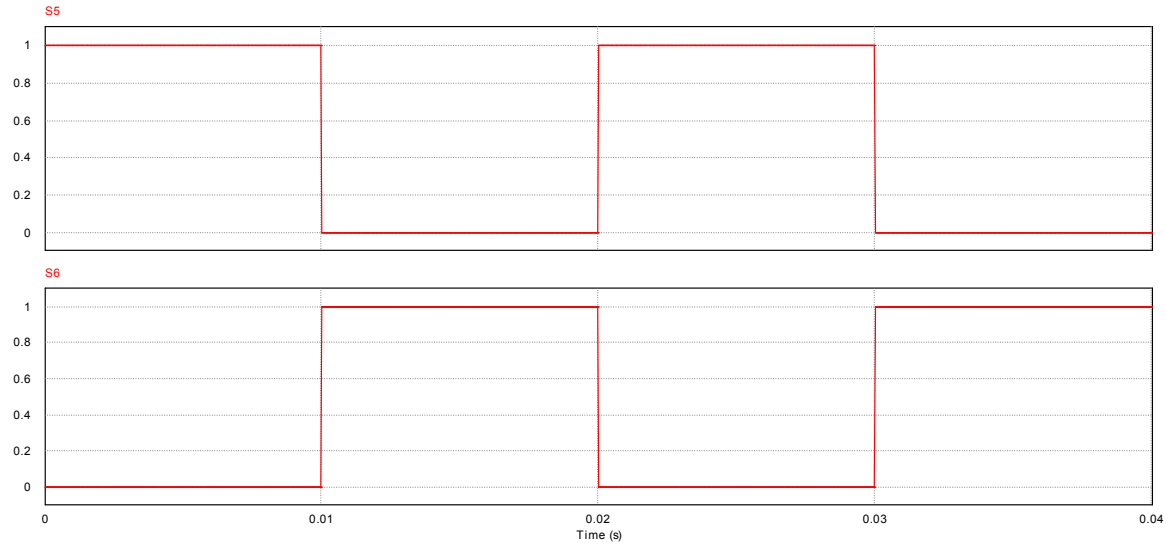

Figure 7-12 FB VZS AC decoupling dual-parallel switching signals (bipolar)

The switching signal for the AC coupling switches is shown in figure 7-12. Switch S6 is switched on continuously with the grid frequency during the positive grid current. Switch S5 is switched on continuously with the grid frequency during the negative grid current. These switching actions decouple the inverter topology from the DC link thereby preventing reactive power circulation.

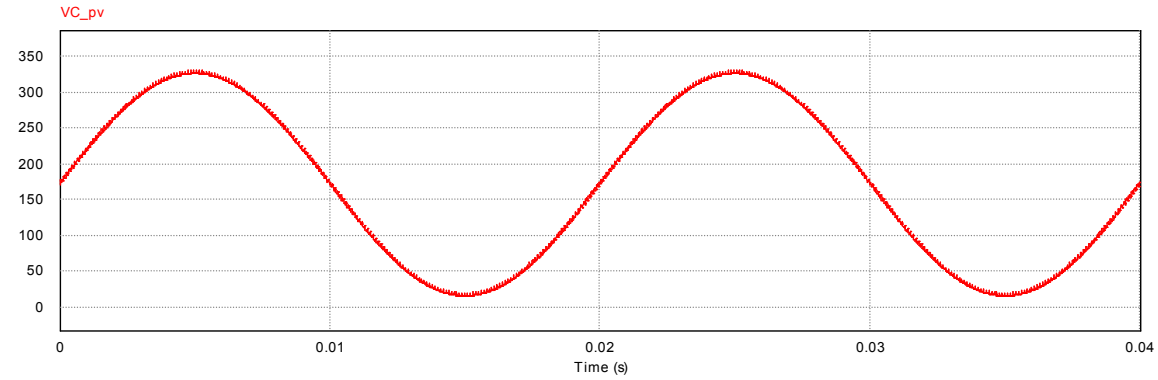

Figure 7-13 FB VZS AC decoupling dual-parallel switch PV array terminal voltage (bipolar)

The voltage impressed across the PV array capacitance is shown in figure 7-13 and its harmonics content in figure 7-14. The instantaneous peak value of this waveform is 330,55 V and its average is 171,71 V. The PV parasitic capacitance value determines the limit of the ground leakage current.

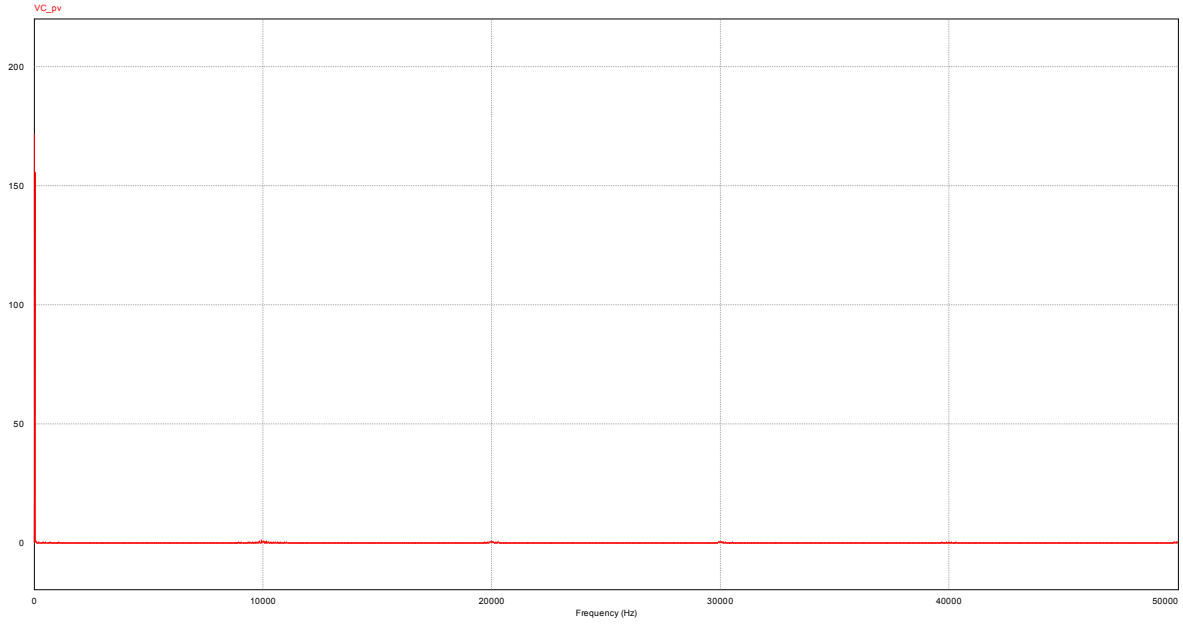

Figure 7-14 FB VZS AC decoupling dual-parallel switch PV array terminal voltage FFT (bipolar)

The common voltage mode impressed across the PV parasitic capacitance is depicted in figure 7-15 with a peak value of 175 V that is Vdc/2 and minimum value of 170V. The voltage impressed across the parasitic capacitance is very small that is about 5V. This common mode voltage

produces the ground leakage current shown in figure 7-16. The harmonics content of the leakage current is displayed in figure 7-17.

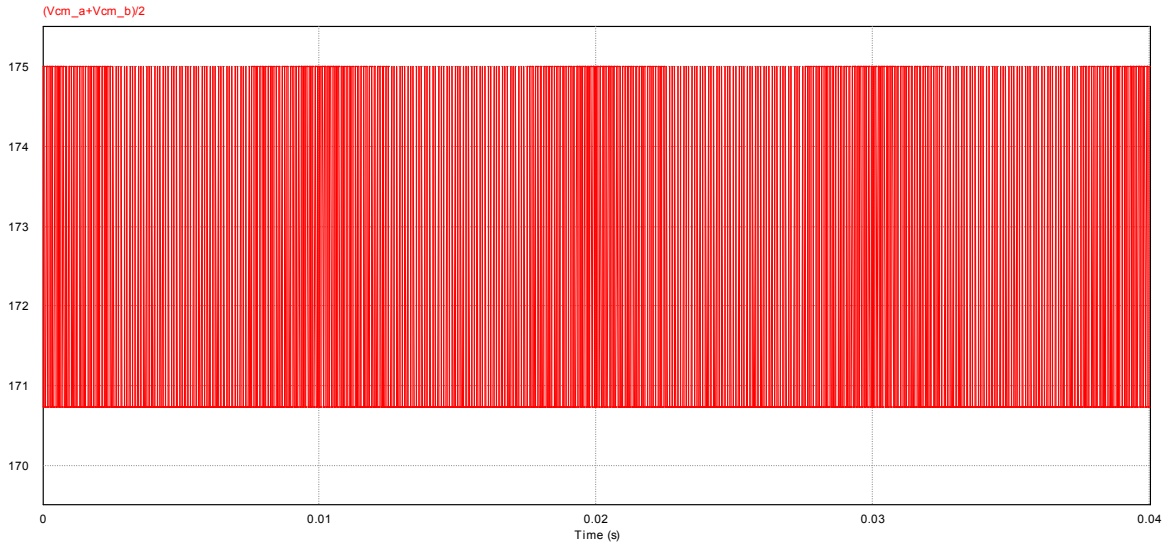

Figure 7-15 FB VZS AC decoupling dual-parallel switch Common mode voltage (bipolar)

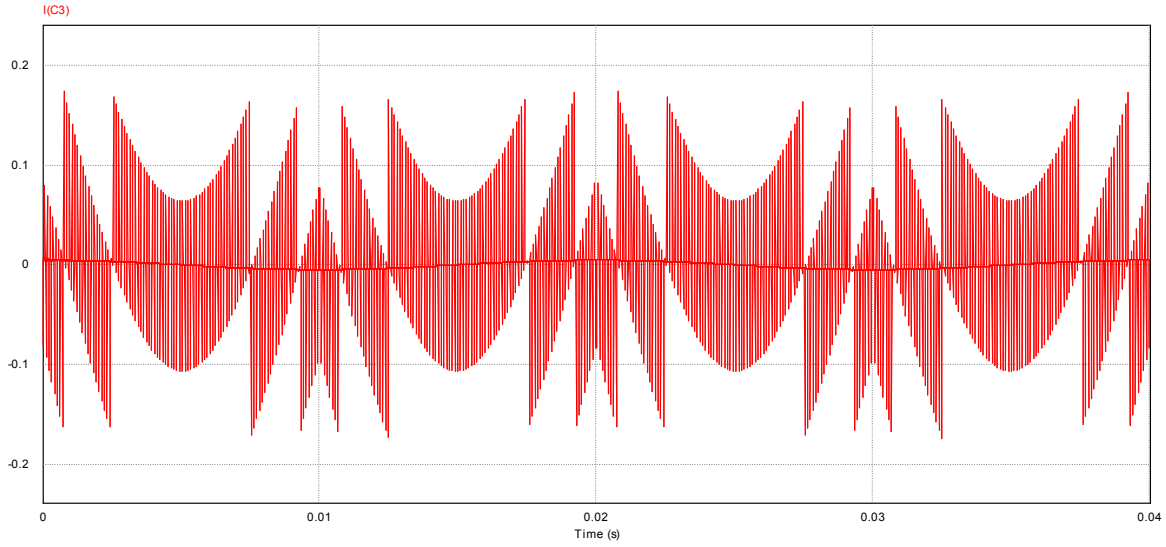

Figure 7-16 FB VZS AC decoupling dual-parallel switch PV ground leakage current (Bipolar)

The ground leakage current with PV array parasitic capacitance value of 100 nF is shown in figure 7-16 and its harmonics content in figure 7-17. The instantaneous peak value is 174 mA

and it average value is 19,56 mA. The root mean square value is 42,88 mV. This topology with bipolar switching strategy is acceptable for transformerless grid-connected system because the safety compliance requirements in VDE 0126-1-1.

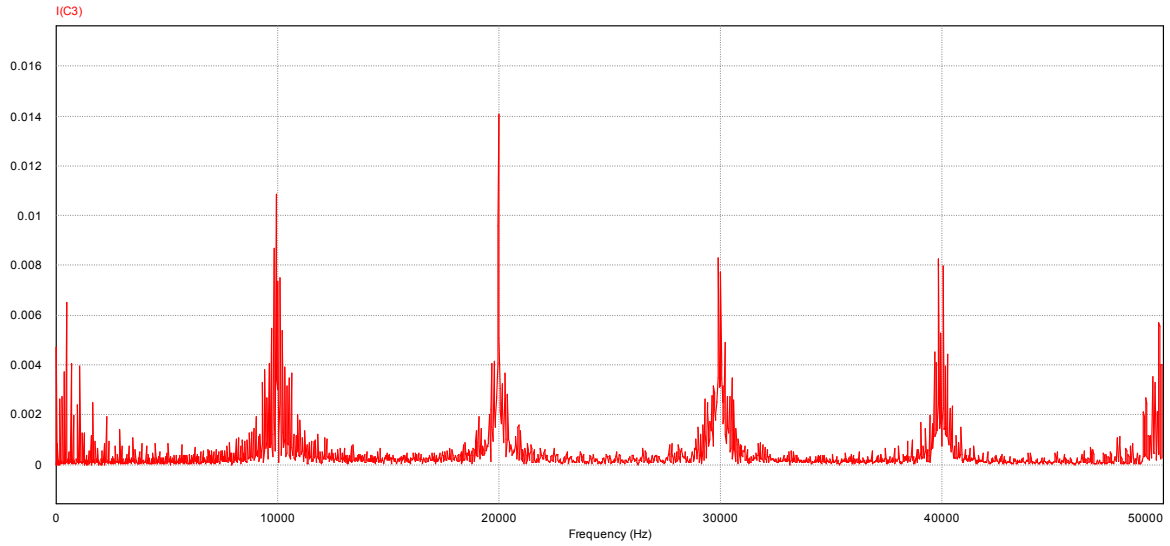

Figure 7-17 FB VZS AC decoupling dual-parallel switch PV ground leakage current FFT (Bipolar)

The harmonics content of the ground leakage current is depicted in figure 7-17. It contains harmonics at integral multiple of the switching frequency with a peak value at the switching frequency (20 kHz). The peak value of this harmonic is 174 mV.

7.3 Advantages of the proposed PV transformerless inverter topology

The new proposed PV transformerless inverter topology performs better than the REFU topology as highlighted below.

- Better use of the DC bus voltage: While the REFU inverter uses half the DC bus voltage, the proposed topology uses the full DC bus voltage providing higher root mean square quantities.
- DC-DC converters are not needed in the proposed topology thereby increasing the overall efficiency of the inverter topology.
- The problem of balancing the mid-point of the two DC capacitors is avoided in the proposed topology that may cause non symmetric output voltage.
- Possibility of non-symmetric AC voltage output that may result into injecting DC current into the utility grid is avoided in this topology.

- Efficiency wise, the proposed inverter topology uses six semiconductor switches with two of them operated at the grid frequency while the REFU topology uses some the three power converter stages in the structure thereby reducing the overall system efficiency.
- The proposed inverter topology is more reliable compared to REFU because its uses one power conversion stage.

The proposed PV transformer inverter compared well with the REFU topology on the basis of low EMI and ground leakage current.

Chapter 8: CONCLUSION AND RECOMMENDED FUTURE WORKS

8.1 Conclusions

The unlimited availability of the solar energy makes it an energy source that can be eternally used without concerns for its' source depletion nor its environmental degradation effects like fossil fuels (e.g. coal, oil, gas) and nuclear energy systems.

The cost of PV panels has been decreasing in recent times that gird parity is very close without government subsidies. One way of increasing the efficiency-cost ratio of a photovoltaic system is to eliminate the transformer used in almost PV inverter topologies. This technique not only decrease the overall system cost but also increase the overall system efficiency as well as the installation cost reduction of the system. However removing this device that provides the galvanic isolation creates some problems. The galvanic isolation can be provided by another method using the control capability offered by power electronics technology.

The safety problem of the transformerless inverter topologies is the generated ground leakage current as a result of the common mode voltage applied across the PV array terminals. This common mode voltage can be eliminated by appropriate inverter topology and switching strategy. The ground leakage current can never be eliminated completely in a grid connected system because a small common mode current is created by the grid voltage variations. However, the contribution of such common mode current created by the grid voltage variation is very minimal and contains only grid frequency component. Thus no problems of electromagnetic interference signals that can affect other sensitive equipment nearby exist.

Transformerless photovoltaic system does not use transformer but use provide galvanic isolation by disconnecting the PV arrays from the AC side during the zero voltage vector switching states. Different transformerless topologies have been developed and commercialized in recent times. Many single-phase transformerless PV inverter topologies are reviewed in this work with different switching strategies. Some that are suitable for transformerless configurations with respect to safety include full bridge with bipolar switching, H5, HERIC, Coenergy, Ingeteam, REFU.

A new transformerless PV inverter topology called FB VZS AC decoupling dual-parallel switch with bipolar switching strategy that can be used as a transformerless PV system is developed and analysed in this research work. The common mode voltage and ground leakage current of the new topology complies with the German code VDE-0126-1-1 safety requirements.

Advantages of the proposed transformerless PV inverter topology are: better use of the DC bus voltage - while the REFU inverter uses half the DC bus voltage, the proposed topology uses the full DC bus voltage providing higher root mean square quantities, DC-DC converters are not needed in the proposed topology thereby increasing the overall efficiency of the inverter topology, the problem of balancing the mid-point of the two DC capacitors is avoided in the proposed topology that may cause non symmetric output voltage and the possibility of non-symmetric AC voltage output that may result into injecting DC current into the utility grid is avoided in this topology.

Efficiency wise, the proposed inverter topology uses six semiconductor switches with two of them operated at the grid frequency while the REFU topology uses some the three power converter stages in the structure thereby reducing the overall system efficiency.

The minimum requirements that should be stipulated for grid interconnection of small-scale distributed generation systems are the power quality and safety issues foe people and system equipment. The control capability and flexibility of voltage source converter as a power electronics interface system can ensure that these important requirements are met with great reliability.

The adoption and implementation of the smart grid initiative will fasten the integration and interconnection of alternative energy systems with the electric power system providing energy security, adequate energy and robust system stability. The synergy of digital information technology, communication technology and the controllability of power energy electronics systems technology is ultimately going to lead to the development of robust and reliable electric power system of the future.

8.2 Recommended future works

The issue of DC current injection is of great interest in transformerless PV inverters as this cause distribution system saturation which may overload them. The new topology developed in this work should be investigated for DC injection capability and the amount of this thereof.

In Chapter 7 a novel FB VZS AC decoupling dual-parallel switch transformerless topology has been proposed. The main index used for the suitability as a grid-connected transformerless topology is the common mode voltage and ground leakage current that complies with the safety requirement stipulated in the German code VDE 0126-1-1. Further investigations are required to improve the efficiency of the proposed topology, by choosing better components by using silicon carbide semiconductors technology.

The modelling of the proposed transformerless should be developed in appropriate software such as PSIM or MATLAB/Simulink for efficiency determination and experimentally validated.
Ways to further increase the efficiency-cost ratio of existing and new transformerless topologies should be investigated for quick deployment in order to contribute adequate power to the depressed electricity system.
Since thin-film modules (or other newly developed PV modules) may become more important in the future PV module market, a PV inverter should have the capability to make one pole from the panel side to be grounded; or the dv/dt on the conductor poles of a photovoltaic module can be controlled to be in an acceptable range. Considering these facts, the development of future PV inverter may follow two different trends:

- Transformerless inverters: it is easier to realize high efficiency. Thus the objective for transformerless inverters is to reduce the PV module side voltage fluctuation (dv/dt) or, if possible, achieve PV side positive/negative pole grounding.
- For inverters with transformer: The advantage to this kind of inverter is that galvanic isolation is inherently realized and as a result, it is very easy for PV module side grounding.

Thin film PV technology has been reported to increase the parasitic capacitance which inadvertently increase the ground leakage current that may violate the safety margin stipulated in the German VDE0126-1-1 code.
Therefore, the objective for PV inverters with transformer is to achieve a higher efficiency which can be compared with that of transformerless inverters so that the efficiency-cost ratio can be increased.
The effects of ground leakage currents on the PV module lifetime and energy yield deterioration should be investigated especially for the thin film PV technology that is likely to have higher penetration in the solar energy systems.

8.3 Conference papers and DHET accredited journal publications

1. ***Raji AK*** *and Kahn MTE*, "Distributed Energy Resources for Domestic Electricity Users", *Domestic Use Energy Conference*, Cape Town, South Africa, 11-12 April, 2011, pp. 138-144

2. Raji AK *and Kahn MTE*, "Fuel cell systems as an efficient domestic distributed generation unit", *Domestic Use Energy Conference*, Cape Town, South Africa, 2-4 April, 2013, pp. 91-94

3. Raji AK *and Kahn MTE*, "Analysis of distributed energy resources for domestic electricity users", *Journal of Energy of Southern Africa,* Vol. 23, no 1, 2012, pp. 50-55

4. Haltor Mataifa, ***Atanda, K. Raji*** *and MTE Kahn*, "Effective Anti-Islanding Algorithm for Synchronous Distributed Energy Resources", *South Africa Institute of Electrical Engineers SAIEE (submitted -under review)*

REFERENCES

_____, 2012, "PV Industry set for growth", *25^0 in Africa*, Vol. 7, Nr 2, pp. 26-27

Ackermann Thomas, 2007, "Distributed resources and re-regulated electricity markets", *Electric Power System Research*, Vol. 77, pp. 1148-1159

Ackermann Thomas, Anderson Gran and Sder Lennart, 2007, "Distributed generation: a definition", *Electric Power Systems Research*, Vol.57, pp. 195-204

Alahmoud M., Chaaban A and Lau S., K. , (2011), "An Adaptive Photovoltaic-Inverter Topology", *Annual IEEE Industrial Electronics Society Conference*, Nov. 2–6, 2003, vol. 3, pp. 2338–2343.

Aldo Viers da Rosa, (2009), *Fundamental of Renewable Energy Processes*, 2nd Edition, Burlington, MA 0183, USA, Elsivier

Arajo S., V., Zacharias P., and Mallwitz R., (2010) "Highly Efficient Single-Phase Transformerless Inverter for Grid-Connected Photovoltaic Systems, *IEEE Transaction on Industrial Electronics*, Vol. 57, no. 9, pp. 3118-3128.

Arman M. F. and Zhong L., (1997) "A new, transformerless, photovoltaic array to utility grid interconnection," *in Proceeding International Conference in Power Electronics and Drive Systems*, May 26–29, 1997, vol. 1, pp. 139–143.

Arulampalam A., Barnes M., Engler A., Goodwin A. and Jenkins, 2004 "Control of power electronics interfaces in distributed generation Microgrids", *International Journal of Electronics*, Vol. 91, No. 9, pp. 503-523

Azah Mohamed, Muhammad Nizam and A. A. Salam**,** (2009), "Performance Evaluation of Fuel Cells and Microturbine as Distributed Generators in a Microgrid", *European Journal of Scientific Research*, Vol.30 No.4, pp.554-570

Azbe V and R Mihalic, 2006, "Distributed generation from renewable sources in an isolated DC

network", *Renewable Energy*, Vol. 31, pp. 2370-2384

Azri M. and Rahim N. A., (2011), "Design Analysis of Low-Pass Passive Filter in Single-Phase Grid-Connected Transformerless Inverter", *IEEE First Conference on Clean Energy and Technology CET*, pp. 348-353

Baifeng C., Pengwei S., Chuang L, Chien-Liang C., Lai J-S and Yu W., (2012), "High Efficiency Transformerless Photovoltaic Inverter with Wide-Range Power Factor Capability", pp. 575-582

Balaji Siva Prasad, Sachim Jain and Vivek Agarwal, (2008), "Universal Single-Stage Grid-Connected Inverter", *IEEE Transaction on Energy Conversion*, Vol. 23, no. 1, pp. 128-137

Barater D., Buticchi G, Crinto A. S., Franceschini and Lerenzani E (2009), "A new proposal for ground leakage current reduction in Transformerless Grid-Connected Converters for Photovoltaic Plants". *Industrial Electronics, IECON '09. 35th Annual Conference of IEEE* pp.4531-4536

Bassoon T. S., 2008, "High-Penetration, Grid-Connected Photovoltaic Technology Codes and Standards", *33rd IEEE Photovoltaic Specialists Conference* San Diego, California, pp. 1-4

Battaglini A, Lilliestam J, Hass A. and Patt A, 2009, "Development of SuperSmart Grids for a more utilization of electricity from renewable sources", *Journal of Cleaner Production*, doi:10:1016/j.clepro.2009.02.006, pp. 1-8

Bayod-Rjula A. A., 2009, "Future development of the electricity systems with distributed generation", *Energy*, Vol. 34, pp. 377-383

Billy M T and Henry Shu-Hung, 2005, 'An integrated Inverter With Maximum Power Tracking for grid-connected PV Systems; *IEEE Transaction On Power Electronics,* Vol. 20,no. 4, July, pp. 953-962

Bimal K B, 2000, “Energy, Environment, and Advances in Power Electronics”, *IEEE Transaction on Power Electronics*, Vol. 15, No. 4, pp. 688-701

Blaabjerg F., Zhe Chen and Søeren Baekhoej Kjaer, 2004, “Power Electronics as Efficient Interface in Dispersed Power Generation Systems”, *IEEE Transaction on Power Electronics*, Vol. 19, No. 5, pp. 1184-1194

Blaabjerg F., Teodorescu R., Chen Z., Liserre M., 2004, “Power Converters and Control of Renewable Energy Systems”, *Proceedings of the 6-th International Conference on Power Electronics*, 18-22 October 2004 (plenary session)

Blaabjerg F., Teodorescu R., Liserre M., and Timbus A.V., 2006, “Overview of Control and Grid Synchronization for Distributed Power Generation Systems”, *IEEE Transactions on Industrial Electronics*, Vol. 53, No. 5, pp. 1398-1409

Bouffard F. and Kirschen D. S., 2008, “Centralized and Distributed electricity systems”, *Energy Policy*, Vol. 36, pp. 4504-458

Bouzguenda M., Salmi T., Gastli A and Masmoudi A., (2010), “Assessment of Topologies to minimise Leakage Currents in Transformerless PV Inverters*”, IEEE International Energy Conference*, pp. 417-422

Bradaschia F., Cavalcanti M. C., Ferraz P. E. P., Neves F., A., S., dos Santos E. C. and Joas H. G. M. da Silva, (2011), “Modulation for Three-Phase Transformerless Z-Source Inverter to Reduce Laekage Currents in Photovoltaic Systems”, *IEEE Transaction on Industrial Electronics*, Vol. 58, no. 12, pp. 5385-5395

Brndllinger R. and Bletterie B., (20050, “Unintentional islanding in distribution grids with a high penetration of inverter-based DG: Probability for islanding and protection methods”, *Power Tech*. *IEEE Russia*, pp. 1-7

Bull S R and Billman L. L, (2000), “Renewable Energy: Ready to meet Its Promise?”, The Center for Strategic and International Studies and International Studies and the Massachusetts Institute of Technology, *The Washington Quarterly*, 23:1, pp. 229-244,

Byung-Geuk Cho, Seung-Ki Sul, Hyunjae Yoo and Seung-Min Lee, (2011), "LCL Filter Design and Control for Grid-connected PWM Converter", *8th International Conference on Power Electronics* – ECCE Asia, pp. 756-763

Calais M. and Agelidis V. G., (1998) "Multilevel converters for single phase grid connected photovoltaic systems — an overview," *in Proceeding IEEE International Symposium on Industrial. Electronics.* 1998, vol. 1, pp. 224–229.

Calais M., Myrzik J. M. A., and Agelidis V. G., (2001) "Inverters for single phase grid connected photovoltaic systems—Overview and prospects," *in Proceeding 17th European. Photovoltaic Solar Energy Conference*, Munich, Germany, Oct. 22–26, 2001, pp. 437–440.

Calais Martina, Agelidis G. Vassillios and Meinhardt Mike, (1999), "Multilevel Converters for Single-phase Grid connected Photovoltaic Systems: An Overview", *Solar Energy*, Vol.66, No. 5, pp. 325-335

Calais Martina, Myrzik Johanna, Spooner Ted and Vassilios G Agelidis (2002), "Inverter for Single-Phase Grid Connected Systems – An Overview", *Power Electronics Specialists Conference*, PESC 02. 2002 IEEE 33rd Annual, Vol. 4, pp. 1995-2000

Carrasco J.M., Franquelo L. G., Bialasiewicz J. T., Galvn E., Guisado R. C. P., Prats M, Len and Moreno-Alfonso N., (2006), "Power-Electronics Systems for the Grid Integration of Renewable Energy Sources: A Survey", *IEEE Transactions on Industrial Electronics*, Vol. 53, No. 4, August, pp. 1002-1016

Cavalcati M. C., de Oliveria K. C., de Farias A. M., Neves F. A. S., Azevedo G. M. S. and Camboim F. C., (2010), "Modulation Techniques to Eliminate Leakage Currents in Transformerless Three-Phase Photovoltaic Systems", *IEEE Transaction on Industrial Electronics*, Vol. 57, no. 4, pp. 1360-1368

Chen Y. and Smedley K. M., (2004), "A cost-effective single-stage inverter with maximum

power point tracking," *IEEE Transaction Power Electronics*, vol. 19, no. 5, pp. 1289–1294, Sep. 2004.

Chen Y. and Smedley, (2008), 'Three-Phase Boost-Type Grid-Connected Inverter', *IEEE Transactions on Power Electronics*, Vol. 23, No. 5, September, pp. 23012309

Chicco G. and Mancarella P., (2009), "Distributed multi-generation: A comprehensive view", *Renewable and Sustainable Energy Review*, Vol. 13, pp. 535-551

Chowdhury S. P, Chowdhury S, Ten C. F. and P. A. Crossley, (2008), "Islanding Protection of Distribution Systems with Distributed Generators A Comprehensive Survey Report", *Power and Energy Society General Meeting,* Conversion and Delivery of Electrical Energy in the 21st century, IEE, pp. 1-8

Ciobotaru M., Kerekes T., Teodorescu R. and Bouscayrol A.,(2006) PV inverter simulation using MATLAB/Simulink graphical environment and PLECS blocksets, *IEEE Industrial Electronics*, IECON, pp.5313 – 5318 *Conference on Power Electronics and Applications*, pp1-10

Conti Stefania, (2009), "Analysis of distribution network protection issues in presence of dispersed generation", Electric Power System Research, Vol. 79, pp. 49-56

Dash P. P. and Yazdani A, (2008), "A Mathematical Model and Performance Evaluation for a Single-Stage Grid-Connected Photovoltaic (PV) Systems," International Journal of Emerging Electric Power Systems, Vol. 9, Issue 6, Article 5

Delesposte Paulino, H., Mello Menegaz, P.J., Lyrio Simonetti, D.S., (2011), "A review of the main inverter topologies applied on the integration of renewable energy resources to the grid" *Power Electronics Conference (COBEP)*, Brazilian , pp. 963 - 969

Dicorato M. and Travato G. F., (2008), "Environmental-concerned energy planning using energy-efficiency and distributed-generation facilities", *Renewable Energy*, Vol. 33, pp. 1297-1313

Engler Alfred, (2005), "Applicability of droops in low voltage grids", *DER Journal*, no. 1, January, pp.1-5

Farret A. Felix, and Dimoes M. Godoy, (2006), Integration of Alternative Sources of Energy, John Wiley & Sons, Inc, Hoboken, New Jersey

Fernndez L. M., Garia, Saenz J. R. and Jurado F., (2009), "Equivalent models of wind farms by using aggregated wind turbines and equivalent winds", *Energy Conversion and Management*, Vol. 50, pp. 691-704

Franke W.-Toke, Oestreich N. and Fuchs F. W., (2010), "Comparison of Transformerless Converter Topologies for Photovoltaic Applications concerning Efficiency and Mechanical Volume", pp. 724-729

Freddy T K S, Nasrudin A. Rahim, and W.P. Hew, (2011) "Modelling, Analysis and Control of Various Types of Transformerless grid Connected PV Inverters" *IEEE First International Conference on Clean Energy and Technology*, pp.51-56

Gao F. and Iravin M. R., (2008), "A Control Strategy for a Distributed Generation Units in Grid-Connected and Autonomous Modes of Operation", *IEEE Transaction on Power Delivery*, Vol. 23, No.2, April, pp. 850-859

Gonzalez R., Gubia E., Lopez J and Marroyo L., (2008), "Transformerless Single-Phase Multilevel-Based Photovoltaic Inverter", IEEE Transaction on Industrial Electronics, Vol. 55, no. 7, pp. 2694-2702

Grid Code Requirements for Wind Turbines Connected to Distribution or Transmission Systems in South Africa version 4.4, http://www.nersa.org.za/Admin/Document/Editor/file/Electricity/TechnicalStandards/RSA%20Grid%20Code%20Connection%20Requirements%20for%20Wind%20Energy%20Facilitie.pdf available online (04/06/2010)

Guerrero J M, Blaabjerg F, Zhelev T, Hemmes K, Monmasson E, Jemei S, Comech M P,

Granadino R and Frau J I, (2010), "Distributed Generation: Toward a New Energy Paradigm", *IEEE Industrial Electronics Magazine*, pp. 52-64

Harald Winkler, (2005), "Renewable energy policy in South Africa: policy options for electricity", *Energy Policy*, Vol. 33, pp. 27-38

Hinz H. and Mutschler, (1998), "Voltage Source Inverters for Grid Connected Photovoltaic Systems", *2nd World Conference and Exhibition on Photovoltaic Solar Energy*, Vienna, July, pp. 2024-2048

Hosseini M., Shayanfar H. A. and Fotuhi-Firuzabad, (2009), "Reliability improvement of distribution systems using SSVR", *ISA Transactions*, Vol.48, pp. 98-106

Hyong Sik Kim and Dylan Dah-Chuan Lu, (2010), "Review on Wind Turbine Generators and Power Electronics Converters with the Grid-Connection", *Universities Power Engineering Conference (AUPEC)*, 2010 20th Australasian, pp.1 - 6

IEEE 1547.1, (2005), IEEE Standard Conformance Test Procedures for Equipment Interconnecting Distributed Resources with Electric Power Systems.

IEEE Standard 1547, (2003), "IEEE Standard for Interconnecting Distributed Energy Resources with Electric Power System*",* 28 July, pp.1-16

Jiayi H., Chuanwen J. and Rong X, (2008), "A review on distributed energy resources and Microgrid", *Renewable and Sustainable Energy Reviews*, Vol. 12, pp. 2472-2483

Jurado Francisco and Carpio Jos, (2005), "Enhancing the distribution networks using distributed generation", *The International Journal for Computational and Mathematics in Electrical and Electronics Engineering*, Vol.24, No. 1, pp. 107-126

Katiraei F., Iravin M. R., and Lehn P.W., (2007), "Small-signal dynamic model of a micro-grid including conventional and electronically interfaced distributed resources", *IET Gen. Trans. Distr.*, Vol. 1, No.3, pp. 369-378

Kazmierkowski M. P., (1998), "*Current Control Techniques for Three-Phase Voltage-Source PWM Converters: A Survey",* IEEE Transactions on Industrial Electronics, Vol. 45, No 5, pp. 691-703

Kerekes T, R Teodorescu and U Borup, (2007), "Transformerless Photovoltaic Inverters Connected to the Grid", *Applied Power Electronics Conference*, APEC 2007 - Twenty Second Annual IEEE , pp.1733-1737

Kerekes T., Teodorescu R. and Borup U., (2007) Transformerless Photovoltaic Inverters Connected to the Grid; *Twenty Second Annual IEEE Applied Power Electronics Conference,* APEC, pp.1733-1737

Kerekes T., Teodorescu R., Klumpner C., Sumner M., Floricau D., Rodriguez P.,(2007), "Evaluation of three-phase transformerless photovoltaic inverter topologies", *European*

Kerekes T., Teodorescu R., Liserre M., Mastromauro R., Dell'Aquila A., (2008) MPPT algorithm for voltage controlled PV inverters; *11th International Conference on Optimization of Electrical and Electronic Equipment*, 2008. OPTIM 2008; 22-24 May 2008, pp.427-432

Keyhani Ali, (2011), *Design of Smart Power Grid Renewable Energy Systems*, John Wiley & Sons, Inc, Hoboken, New Jersey

Keyhani Ali, Marwali N. Mohammad and Dai Min, (2010), *Integration of Green and Reneweable Energy in Electric Power Systems Renewable Energy Systems*, John Wiley & Sons, Inc., Hoboken, New Jersey

Khajehoddin S. A., Jain P. and Bakhshai, (2007), "Cascaded Multilevel Converters and their Applications in Photovoltaic Systems", *2nd Canadian Solar Building Conference*, Calgary, June 10-14, pp. 1-6

Khani D. and Yazdankhah A. Sadeghi, "Control of Inverter-interfaced Distributed Generation Systems in Different Operation Modes", *2nd IEEE International Symposium on Power Electronics for Distributed Generation systems*, pp.681-684

Kjaer S. B., Pedersen J. K., Blaabjerg and F., (2005), "A review of single phase grid-connected inverters for photovoltaic modules," *IEEE Transaction on Industrial Applications*, vol. 41, no. 5, pp. 1292–1306, Sep./Oct. 2005.

Kojabadi H. M., Bin Yu, Gadoura I. A., Liuchen Chang and Ghribi M., (2006), "A Novel DSP-based Current-controlled PWM Strategy for Single Phase grid connected inverters", *Power Electronics IEEE Transaction on*, Vol. 21, Issue 4, July, pp. 985-993

Koutroulis E. and Blaaabjerg F., (2011), "Design Optimization of Grid-Connected PV Inverters", pp. 691-698.

Kudo M., Takeuchi, Nozaki, Endo H. and Sumita J, (2007), "Forecasting Electric Power Generation in a Photovoltaic Power System for an Energy Network", *Electrical Engineering Journal in Japan*, Vol. 167, No. 4, pp. 847-853

Lamont A. D., (2008), "Assessing the long-term system value of intermittent electric generation technologies", *Energy Economics*, Vol. 30, pp. 1208-1231

Lasseter R. H. and Piagi P., (2004), "Microgrid: A Conceptual Solution", *Proc. 35th Annual Conference IEEE* PESC04 Aachen, Germany, 20-25, June, p 4285-4290

Lasseter R. H., (2007), "Microgrid and Distributed Generation", *Journal of Energy Engineering, America Society of Civil Engineers*, Sept., Vol. 133, Issue 3, pp. 144-149

Lee S-H., Song S-G., Park S-J., Moon C-J. and Lee M-H., (2008), "Grid-Connected Photovoltaic System using Current-Source Inverter", Solar Energy, Vol. 82, pp. 411-419

Li. S. Ding M, Wang J. and Zhang W., (2008), "Voltage control capability of SVC with VAR dispatch and slope setting", *Electric Power Systems Research*, doi:10.1016/j.epsr.2008.11.001

Lopez O., Freijedo F. D., Yepes A. G., Fernandez-Comessana P., Malvar J., Teodorescu R. and DovalGandoy J., (2010), "Eliminating Ground Current in a Transformerless Photovoltaic application", *IEEE Transaction on Energy Conversion*, Vol. 25, no. 1, pp. 140-147

Lopez O., Teodorescu R., Freijedo F. and DovalGandoy J., (2007), "Leakage current evaluation of a single phase transformerless PV inverter connected to the grid", *Applied Power Electronics Conference,* APEC 2007 - Twenty Second Annual IEEE , pp. 907-912

Lopez O., Teodorescue R., Freijedo F., and DovalGandoy J., (2007), "Leakage Current Evaluation of a Single-Phase Transformerless PV Inverter Connected to the Grid" *In Apllied Power Electronics Conference, APEC 2007 – Twenty Second Annual IEEE* 25, February – 1 March 2007, pp. 907 -912

Marwali M. N., Jung J-W. and Keyhani A., (2004), "Control of Distributed Generation Systems Part II: Load Sharing Control", *IEEE Transaction on Power Electronics*, Vol. 19, no. 6, November, pp. 1551-1561

Mastromauro R., Dell'Aquila A., Liserre M., and Kerekes T., (2009) "A Single-Phase Voltage Controlled Grid Connected Photovoltaic System with Power Quality Conditioner Functionality"; *IEEE Transactions on Industrial Electronics*; Industrial Electronics, IEEE Transactions on Volume: 56, Issue 11, pp. 4436 – 4444

Mcmurray W., (1965), "Inverter Circuits", US Patent 3207974, September 1965

Mienski R., Gburczyk P., Pawalek R. and Wasiak I., (2007), "Laboratory of Distributed Generation in Institute of Electrical Power Engineering of Technical University of Lodz", *9th International Conference of Electrical Power Quality and Utilisation*, Barcelona, October, pp. 9-11

Mondol J. D., Yohanis Y. G. and Norton B., (2007), "Comparison of measured and predicted long term performance of grid a (sic) connected photovoltaic system", *Energy Conversion and Management*, Vol. 48, pp. 1065-1080

Myrzik J. M. A. and Calais M., (2003) "String and module integrated inverters for single-phase

grid connected photovoltaic systems—A review," *in Proceeding IEEE Power Technical Conference*, Bologna, Italy, Jun. 23–26, 2003, vol. 2, pp. 1–8.

Myrzik J. M. A. and Calais M., *(*2003), "String and Module Integrated Inverters for Single-Phase Grid Connected Photovoltaic Systems: A Review", *IEEE Bologna Power Tech Conference*, June 23rd - 26th, Bologna. Italy

Nishida Y., Nakamura S., Aikawa N., Sumiyoshi S., Yamashita H., and Omori H., (2004),"A novel type of utility-interactive inverter for photovoltaic System," *Power Electronics and Motion Control Conference*, IPEMC 2004. The 4th International, Vol.3, pp. 1785 - 1790

Omar Abdel-Rahim, Mohamed Orabi and Mahrous Ahmed, (2010), "High Performance Power Conditioning for Grid Connected PV Module', *Proceeding of the 14th International Middle East Power Systems conference (MEPCON '10)*, pp. 728-733

Paula Mints, (2011), "Remote Markets for Photovoltaic Technologies, 1974 to Present and Ten Year Forecast", *Photovoltaic Specialists Conference (PVSC)*, 37th IEEE, pp.1848-1851

Peas Lopes J. A., Hatziargyriou N., Mutale J., Djapic P. and Jenkins N., (2007), "Integration distributed generation into electric power systems: A review of drivers, challenges and opportunities", Electric *Power Systems Research*, Vol. 77, pp. 1189-1203

Pedrasa M. A. and Spooner T., (2006), "A survey of Techniques Used to Control Microgrid Generation and Storage during island Operation", Proceeding of the *Australasian Universities Power Engineering Conference* (AUPEC 06)

Peng F. Z., Shen M. and Huang Y., "Z-Source Inverter for Residential Photovoltaic Systems", IEEE Transaction on Power Electronics, Vol. 21, no. 6, November, pp. 1776-1782

Pepermans G., Driesen J., Haeseldonckx D., Belmans R. and Dhaeseleer W., (2005), "Distributed generation: definition, benefits and issues", *Energy Policy*, Vol. 33, pp. 787-798

Photong C., Klumpner C and Wheeler P., (2010) "Evaluation of Single-Stage Power Converter Topologies for Grid-Connected Photovoltaic", *Industrial Technology (ICIT)*, IEEE International Conference on, pp.1161-1168

Pierquet B. J. and Perrault D. J., (2010) "A Single Phase Photovoltaic Inverter Topology with a Series-Connected power Buffer", *Energy Conversion Congress and Exposition (ECCE)*, IEEE, pp. 2811-2818

Powersim Inc., (2006), "PSIN, User's Guide" version 7.0, Release 5, July 2006, Copyright 2001-2006, Powersim Inc.

Rahamn M. F. and Zhong L, (1997), "A new Transformerless Photovoltaic Array to Utility Grid Interconnection", *Power Electronics and Drive Systems Proceedings*, International Conference on, Vol.1, pp. 139 - 143

Ramakrishna K. S. and Bhatti T. S., (2008), "Automatic generation control of single area power system with multi-source power generation", *Journal of Power and Energy*, Proc. IMechE Vol. 222 Part A, pp. 1-11

Renders B., Ryckaert, De Gussem, Ryckaert W. R. and Vandevelde, (2009), "Converter-connected Distributed Generation Units with Integrated Harmonic Voltage Damping and Harmonic Compensation Function", *Electric Power Systems Research*, 79, pp. 65-70

Renders B., Ryckaert, De Gussem, Stockman K. and Vandevelde, (2008), "Improving the Voltage Dip Immunity of Converter-Connected Distributed Generation Units", *Renewable Energy*, Vol. 33, pp. 1011-1018

Rodriguez J., Lai J-S., and Peng F.Z., (2002), "Multilevel Inverters: A survey of Topologies, Controls, and Applications", *IEEE Transactions on Industrial Electronics*, Vol. 49, No. 4, August, pp. 724-738

Salam A. A, Mohamed A, and Hannan M. A, (2008), "Technical Challenges on Microgrids",

ARPN *Journal of Engineering and Applied Sciences*, Vol. 3, No. 6, December, p. 64-69

Salamah A.M., Finney S.J. and Williams B.W, (2009), "Single-Phase Voltage Source Inverter With a Bidirectional Buck-Boost Stage for Harmonic Injection and Distributed Generation", *IEEE Transactions on Power Electronics*, Vol. 24. No. 2, February, pp. 376-387

Schimdf F. and Norum L. E., (2008), "Grid connected Converters for Photovoltaic, State of the Art, Ideas for Improvement of Transformerless Inverters", *Nordic Workshop on Power and Industrial Electronics*, June 9-11, pp.

Shen J-M., Jou H-L and Wu J-C,, (2012), "Novel Transformerless Grid-Connected Power Converter With Negative Grounding for Photovoltaic Generation System", *IEEE Transaction on Power Electronics*, Vol. 27, no. 4, pp. 1818-1829

Siddiqui A. S. and Maribu K, (2009), "Investment and upgrade in distributed generation under uncertainty", *Energy Economics*, Vol. 31, pp. 25-37

Skjellnes Tore, Skjellnes Asle and Norum Lars E., (2002), "Load sharing for parallel inverters without communication", *Nordic Workshop on Power and Industrial Electronics*, August, pp.12-14

Sorensen Bent, (2011), *Renewable Energy: Physics, engineering, environmental, impacts, economics & planning*, 4th Edition, Burlington, 01803, USA

Suan F. T. K., Rahim N., A. and Hew W. P., (2011), "Modelling, Analysis and Control of Various Types of Transformerless Grid Connected PV Inverters", *IEEE First Conference on Clean Energy and Technology CET*, pp. 51-56

Suul J. A., Molinas M, Norum and Undeland T, (2008), "Tuning of Control Loops for Grid Connected voltage Source Converters", *Power and Energy Conference*, 2008. PECon 2008. IEEE 2nd International, pp. 797-802

T. Kerekes, R. Teodorescu, M. Liserre, (2008), "Common mode voltage in case of

transformerless PV inverters connected to the grid" *IEEE International Symposium on Industrial Electronics*, pp. 2390 – 2395

Teoderescu Remus, Liserre Marco and Rodríguez Pedro, (2011), "Grid Converter for Photovoltaic and wind Power System, IEEE John Wiley & Sons, LTD

Teodorescu R. and Liserre M, (2006), "*Power Electronics for Renewable Energy,* Slides presented at the course PERES, Aalborg, Denmark, March 2006

Teodorescu R., Blaabjerg F. and Liserre M, (2004), "Proportional-Resonant Controllers: A New Breed of Controllers Suitable for Grid-Connected Voltage-Source Converters", *Proceedings of OPTIM'04*, 20-21 may 2004, Brasov, Vol. III, pp. 9-14

Teodorescu R., Blaabjerg F. and Liserre M, (2004), "Breed of Controllers Suitable for Grid-Connected Voltage-Source Converters", *Proceedings of OPTIM'04*, 20-21 May 2004, Brasov, vol. III, pp. 9-14

Teodorescu R., Blaabjerg F., Liserre M. and Borup U., (2004), "A New Control Structure for Grid-Connected PV Inverters with Zero Steady-State Error and Selective Harmonic Compensation", *Proceedings of APEC'04*, Anaheim, CA

Thomas S. Basso, (2008), "High-Penetration, Grid-Connected Photovoltaic technology Codes and Standards, Photovoltaic Specialists Conference, PVSC '08, 33rd IEEE, pp. 1 – 4

Timbus A., Teodorescu R. and Blaabjerg F., (2005), "Synchronization Methods for Three-Phase Power Generation Systems: An overview and Evaluation", *Power Electronics Specialists*, 2005 IEEE 36th Conference, 11-14 Sept.

Tong S., Kleinberg M. and Miu Karen, (2005), "A Distribute Slack Bus Model and Its Impact on Distribution System Application Techniques, Circuits and Systems", *ISCAS 2005 IEEE International Sysmposium on*, Vol. 5, 23-26 May, pp. 4743-4746

Tsikalakis A.G. and Hatziargyriou, (2007), "Environmental benefit of distributed generation

with and without emission trading", *Energy Policy*, Vol. 53, pp. 3395-3409

UL 1741, (2005), Inverters, Converters, Controllers, and Interconnection System equipment for Use with Distributed Energy Resources.

Valtchev V., Van den Bossche A., Ghijselen J. and Melkbeek J, (2000), "Autonomous renewable energy conversion system", *Renewable Energy*, 19, p. 259-275

Variath, R.C., Andersen, M.A.E., Nielsen, O.N., Hyldgard, A., (2010), "A review of module inverter topologies suitable for photovoltaic systems", *IPEC, 2010 Conference Proceedings* pp.310 - 316

Vazquez, G., Kerekes, T., Rolan, A., Aguilar, D., Luna, A., Azevedo, G. (2009), *Industrial Electronics*, IEEE International Symposium on , pp.544 – 548

Wenzhou L U, Keliang Z and Yang Yunhu, "A General Internal Model Based Control Scheme for CVCF PWM Converters", *2nd IEEE International Symposium on Power Electronics for Distributed Generation systems*, pp.485-489

Xiaomeng Su, Yaojie Sun, Yandan Lin, (2011),"Analysis on Leakage Current in Transformerless Single-Phase PV Inverters Connected to the Grid", *Power and Energy Engineering Conference (APPEEC),* Asia-Pacific, pp. 1 – 5

Xue Y, Chang L., Kjr S. B, Bordonau J. and Shimizu T, (2004), "Topologies of Single-Phase Inverters for Small Distributed Power Generators: An Overview", *IEEE Transaction on Power Electronics*, Vol. 19, No. 5, September, pp. 1305-1314

Yan Xu, Tolbert L. M, Rizy D.T and Kueck J.D, (2007), "Non-active Power-Related Ancillary Services Provided by Distributed Energy Resources", *Power Engineering Society General Meeting*, IEEE, 24-28 June, pp. 1-7

Yaosuo Xue, Liuchen Chang, Soren Baekhoj, Josep Bordonau and Toshihisa shimizu, (2004), "Topologies of Single-Phase Inverter for Small Distributed Power Generators: An Overview", *IEEE Transaction on Power Electronics*, Vol. 19, no. 5, pp. 1305-2004

Yen-Shin Lai and Fu-San Shyu, (2004), "Optimal Common-Mode Voltage Reduction PWM Technique for Inverter Control with Consideration of the Dead-Time effects – Part 1: Basic Development", *IEEE Transaction on Industry Applications*, Vol. 40, no. 6, pp.1605-1612

Zeineldin H. H., El-Saadany E. F. and Salama M. M A., (2006), "Islanding detection of inverter-based distributed generation", *IEE Proc-Generation Distribution*, Vol. 153, No. 6, November, pp.

Zeng Q. and Chang L., (2005), "Study of Advanced Current Control Strategies for Three-Phase Grid-Connected PWM Inverters for Distributed Generation", *Proceeding of the IEEE Conference on Control Applications* Toronto, Canada, August 28-31, pp. 1311-1316

Zhang L, Harnefors L and Nee H-P, (2010), "Power-Synchronization Control of Grid-Connected Voltage-Sources Converters", *IEEE Transaction on Power Systems*, Vol. 25, no. 2, pp. 809-820

Zhe Chen, Josep M. Guererro and Frede Blaajerg (2008), "A review of the State of the Art of Power Electronics for Wind Turbines", *IEEE Transaction on Power Electronics,* Vol. 24, no. 8, pp.1859-1875

BIBLIOGRAPHY

Markvart T., *Solar Electricity,* 2nd ed. England: John Wiley & Sons Ltd, 2000

Mohan N.,Undeland T.M, William R.P, *Power Electronics,* 3rd ed. USA: John Wiley & Sons, Inc, 2003

Erickson R.W, *Fundamentals of Power Electronics,* USA: Chapman & Hall, 1997

Kazmierkowski M.P, Krishnan R., Blaabjerg F., *Control in Power Electronics Selected Problems,* USA, AcademicPress,2002

APPENDIXE A

A1 Model of the power converter

In the following the mathematical model of the L filter-based and LCL filter-based inverters are presented. These models are relevant for the study of the AC voltage control and AC current control.

The state of the three-phase inverter is modeled by means of a switching space vector defined with the switching functios $p_j(t)$ (j=a,b,c) equal to 1 when the upper switch is closed and 0 when the lower switch is closed in order to avoid current shoot-through fault resulting in the damage of the converter.

$$\overline{p}(t) = \frac{2}{3}(p_a(t) + \alpha p_b(t) + \alpha^2 p_c(t)) \qquad \text{A-1}$$

where $\alpha = e^{j2\pi/3}$

Hence the inverter produces on the AC side the following voltage:

$$\overline{v}(t) = \overline{p}(t) v_c(t) \qquad \text{A-2}$$

If the converter is connected to the grid through an L filter, the equation that describes the evolution of the grid current is

$$\overline{v}(t) = \overline{e}(t) + R\overline{i}(t) + L\frac{d\overline{i}(t)}{dt} \qquad \text{A-3}$$

$\overline{v}(t)$ is the space vector of the inverter voltages, $\overline{i}(t)$ is the space vector of the inverter input currents and $\overline{e}(t)$ is the space vector of the input line voltages. Each of these vectors can be obtained by substituting in A-1 the phase converter voltages, the phase currents and the phase grid voltages respectively.

The mathematical model of the system written in the state-space form is

$$\frac{d\bar{i}(t)}{dt} = \frac{1}{L}[-R\bar{i}(t) - \bar{e}(t) + \bar{p}(t)v_{dc}(t)] \qquad \text{A-4}$$

A commonly adopted approach in analyzing three-phase systems is to use a stationary or rotating reference frame. In the first case the frame will be denoted as αβ and in the second as *dq* and also called synchronous reference frame. In fact the *dq* frame is synchronous with the angular speed ω (where $\omega = 2\pi f$ and f is the fundamental frequency of the power grid voltage waveform). The space vectors that express the inverter electrical quantities are projected on the α axis and β axis or the *d* axis and *q* axis.

The following transformation can be used to obtain the switching functions in the αβ frame and *dq* frame knowing the switching functions for each inverter leg:

$$\begin{bmatrix} p_\alpha \\ p_\beta \end{bmatrix} = \frac{2}{3}\begin{bmatrix} 1 & -1/2 & -1/2 \\ 0 & -\sqrt{3}/2 & \sqrt{3}/2 \end{bmatrix}\begin{bmatrix} p_a \\ p_b \\ p_c \end{bmatrix} \qquad \text{A-5}$$

$$\begin{bmatrix} p_\alpha \\ p_\beta \end{bmatrix} = \begin{bmatrix} \cos\theta & \cos(\theta - \frac{2\pi}{3}) & \cos(\theta + \frac{2\pi}{3}) \\ \sin\theta & \sin(\theta - \frac{2\pi}{3}) & \sin(\theta + \frac{2\pi}{3}) \end{bmatrix}\begin{bmatrix} p_a \\ p_b \\ p_c \end{bmatrix} \qquad \text{A-6}$$

Equation A-5 can easily be derived from equation A-4 by setting θ = 0. The same transformations can be adopted for all electrical quantities involved in equation A-3.

The mathematical model in the αβ reference frame is

$$\begin{cases} \dfrac{di_\alpha(t)}{dx} = \dfrac{1}{L}[-Ri_\alpha(t) - e_\alpha(t) + p_\alpha(t)v_{dc}(t)] \\ \dfrac{di_\beta(t)}{dx} = \dfrac{1}{L}[-Ri_\beta(t) - e_\beta(t) + p_\beta(t)v_{dc}(t)] \end{cases} \qquad \text{A-7}$$

The particular feature of the *dq* reference frame is that if a space vector with constant magnitude rotates at the same angular speed of the frame, it has constant *d* and *q* components while if it

rotates at a different speed or it has a time-variable magnitude it has pulsating components. Thus in a *dq* reference frame rotating at the angular speed ω becomes

$$\begin{cases} \dfrac{di_d(t)}{dx} - \omega i_q(t) = \dfrac{1}{L}[-Ri_d(t) - e_d(t) + p_d(t)v_{dc}(t)] \\ \dfrac{di_q(t)}{dx} + -\omega i_d(t) = \dfrac{1}{L}[-Ri_q(t) - e_q(t) + p_q(t)v_{dc}(t)] \end{cases} \qquad \text{A-10}$$

in the dq reference frame, the d and q differential equations for the current are dependent due to the cross-coupling terms $\omega i_q(t)$ and $\omega i_d(t)$.

The mathematical model of a single-phase voltage source inverter in the case where L filter is connected on the grid can be obtained from equation A-5 simply by considering one of the two equations.

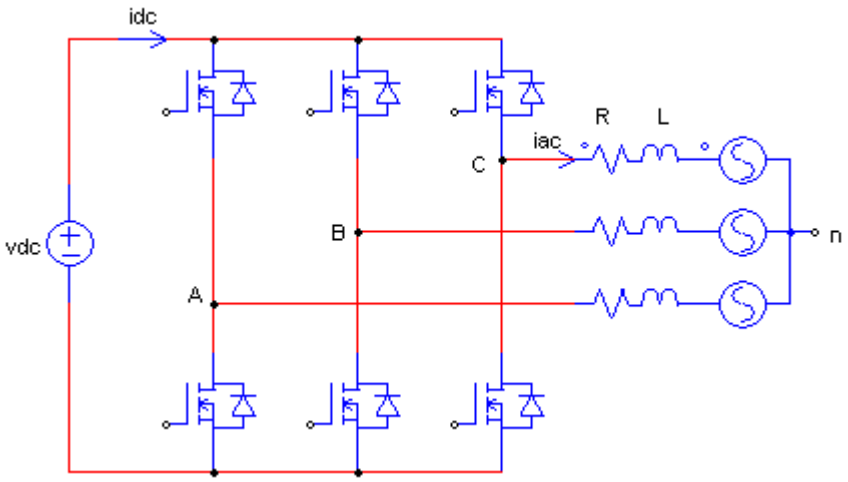

Figure A-1 Grid-connected L-Filter inverter

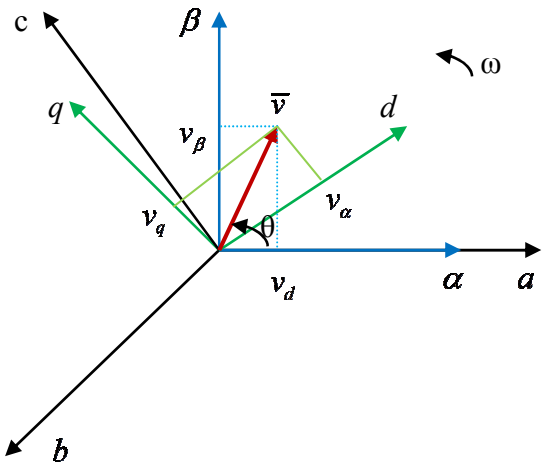

Figure A-0-1 Stationary and rotating reference frame

A2 IXYS HiPerFASTTM IGBT datasheet

IXYS

HiPerFAST™ IGBT
C2-Class High Speed IGBTs

IXGH 40N60C2
IXGT 40N60C2

V_{CES} = 600 V
I_{C25} = 75 A
$V_{CE(sat)}$ = 2.7 V
$t_{fi typ}$ = 32 ns

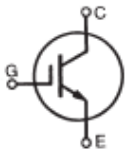

TO-268 (IXGT)

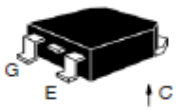

TO-247 (IXGH)

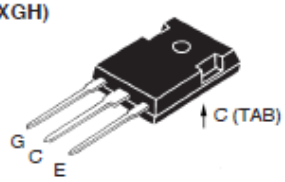

G = Gate, C = Collector,
E = Emitter, TAB = Collector

Symbol	Test Conditions	Maximum Ratings	
V_{CES}	T_J = 25°C to 150°C	600	V
V_{CGR}	T_J = 25°C to 150°C; R_{GE} = 1 MΩ	600	V
V_{GES}	Continuous	±20	V
V_{GEM}	Transient	±30	V
I_{C25}	T_C = 25°C (limited by leads)	75	A
I_{C110}	T_C = 110°C	40	A
I_{CM}	T_C = 25°C, 1 ms	200	A
SSOA (RBSOA)	V_{GE} = 15 V, T_{VJ} = 125°C, R_G = 10 Ω Clamped inductive load @ ≤ 600 V	I_{CM} = 80	A
P_C	T_C = 25°C	300	W
T_J		-55 ... +150	°C
T_{JM}		150	°C
T_{stg}		-55 ... +150	°C
Maximum lead temperature for soldering 1.6 mm (0.062 in.) from case for 10 s		300	°C
Plastic body		200	°C
M_d	Mounting torque (M3)	1.13/10	Nm/lb.in.
Weight	TO-247	6	g
	TO-268	4	g

Symbol	Test Conditions		Characteristic Values (T_J = 25°C unless otherwise specified) min.	typ.	max.	
$V_{GE(th)}$	I_C = 250 µA, V_{CE} = V_{GE}		3.0		5.0	V
I_{CES}	V_{CE} = V_{CES} V_{GE} = 0 V	T_J = 25°C T_J = 150°C			50 1	µA mA
I_{GES}	V_{CE} = 0 V, V_{GE} = ±20 V				±100	nA
$V_{CE(sat)}$	I_C = 30 A, V_{GE} = 15 V	T_J = 25°C T_J = 150°C		2.2 2.0	2.7	V V

Features

- Very high frequency IGBT
- Square RBSOA
- High current handling capability
- MOS Gate turn-on
  - drive simplicity

Applications

- PFC circuits
- Uninterruptible power supplies (UPS)
- Switched-mode and resonant-mode power supplies
- AC motor speed control
- DC servo and robot drives
- DC choppers

Advantages

- High power density
- Very fast switching speeds for high frequency applications

Symbol	Test Conditions (T$_J$ = 25°C unless otherwise specified)	min.	typ.	max.	
g_{fs}	I_C = 30 A; V_{CE} = 10 V, Pulse test, t ≤ 300 µs, duty cycle ≤ 2 %	20	36		S
C_{ies}	V_{CE} = 25 V, V_{GE} = 0 V, f = 1 MHz		2500		pF
C_{oes}			180		pF
C_{res}			54		pF
Q_g	I_C = 30 A, V_{GE} = 15 V, V_{CE} = 300 V		95		nC
Q_{ge}			14		nC
Q_{gc}			36		nC
$t_{d(on)}$	**Inductive load, T$_J$ = 25°C**		18		ns
t_{ri}	I_C = 30 A, V_{GE} = 15 V		20		ns
$t_{d(off)}$	V_{CE} = 400 V, R_G = R_{off} = 3 Ω		90	140	ns
t_{fi}			32		ns
E_{off}			0.20	0.37	mJ
$t_{d(on)}$	**Inductive load, T$_J$ = 125°C**		18		ns
t_{ri}	I_C = 30 A, V_{GE} = 15 V		20		ns
E_{on}	V_{CE} = 400 V, R_G = R_{off} = 3 Ω		0.3		mJ
$t_{d(off)}$			130		ns
t_{fi}			80	240	ns
E_{off}			0.50		mJ
R_{thJC}				0.42	K/W
R_{thCK}	(TO-247)		0.25		K/W

TO-247 AD Outline

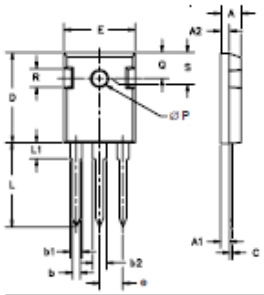

Dim.	Millimeter Min.	Max.	Inches Min.	Max.
A	4.7	5.3	.185	.209
A_1	2.2	2.54	.087	.102
A_2	2.2	2.6	.059	.098
b	1.0	1.4	.040	.055
b_1	1.65	2.13	.065	.084
b_2	2.87	3.12	.113	.123
C	.4	.8	.016	.031
D	20.80	21.46	.819	.845
E	15.75	16.26	.610	.640
e	5.20	5.72	0.205	0.225
L	19.81	20.32	.780	.800
L1		4.50		.177
ØP	3.55	3.65	.140	.144
Q	5.89	6.40	0.232	0.252
R	4.32	5.49	.170	.216
S	6.15 BSC		242 BSC	

TO-268 Outline

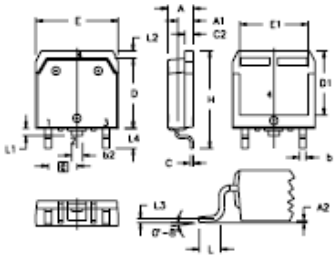

SYM	INCHES MIN	MAX	MILLIMETERS MIN	MAX
A	.193	.201	4.90	5.10
A1	.106	.114	2.70	2.90
A2	.001	.010	0.02	0.25
b	.045	.057	1.15	1.45
b2	.075	.083	1.90	2.10
C	.016	.026	0.40	0.65
C2	.057	.063	1.45	1.60
D	.543	.551	13.80	14.00
D1	.488	.500	12.40	12.70
E	.624	.632	15.85	16.05
E1	.524	.535	13.30	13.60
e	.215 BSC		5.45 BSC	
H	.736	.752	18.70	19.10
L	.094	.106	2.40	2.70
L1	.047	.055	1.20	1.40
L2	.039	.045	1.00	1.15
L3	.010 BSC		0.25 BSC	
L4	.150	.161	3.80	4.10

Min. Recommended Footprint
(Dimensions in inches and mm)

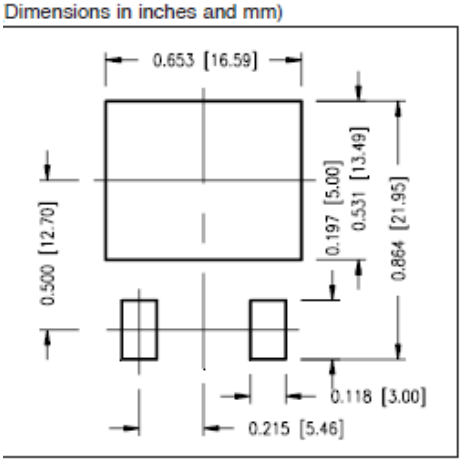

Fig. 1. Output Characteristics @ 25 Deg. C

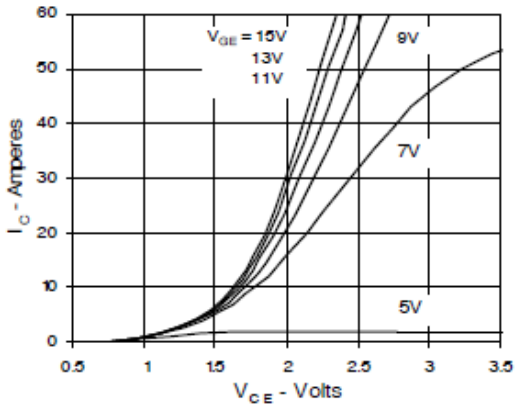

Fig. 2. Extended Output Characteristics @ 25 deg. C

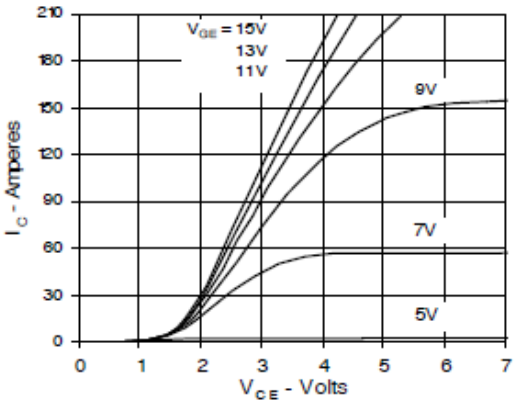

Fig. 3. Output Characteristics @ 125 Deg. C

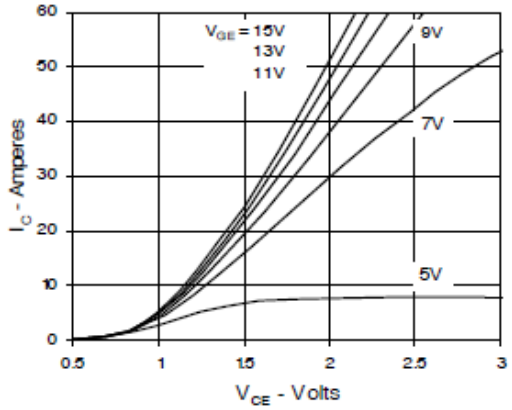

Fig. 4. Temperature Dependence of $V_{CE(sat)}$

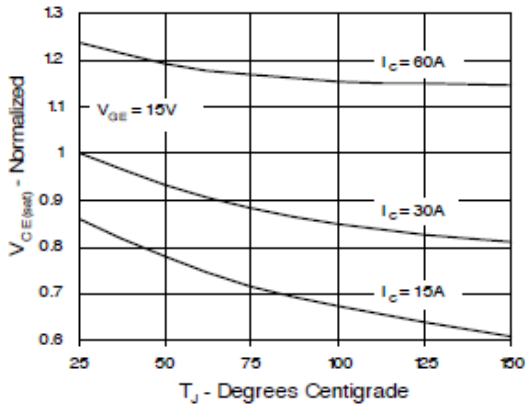

Fig. 5. Collector-to-Emitter Voltage vs. Gate-to-Emitter voltage

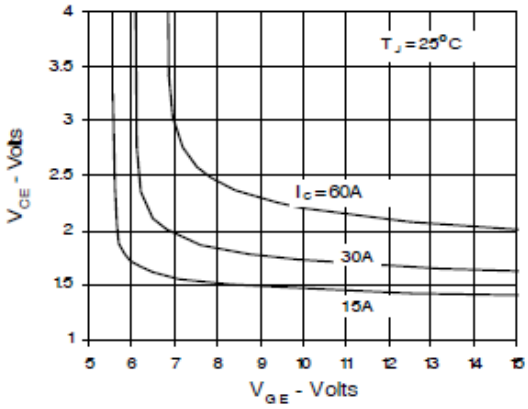

Fig. 6. Input Admittance

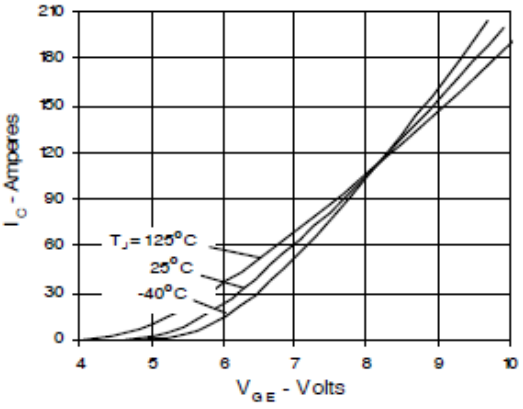

Fig. 7. Transconductance

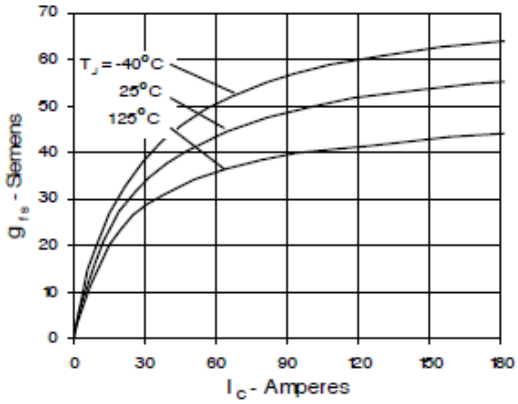

Fig. 8. Dependence of E_{off} on R_G

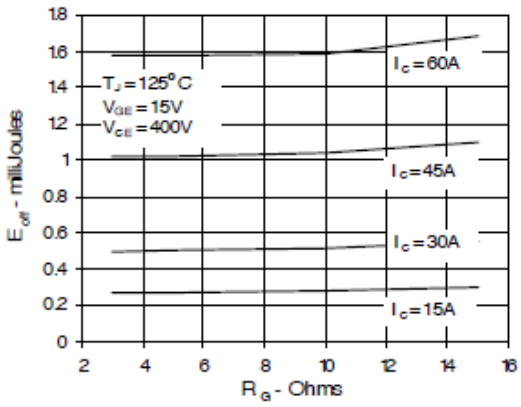

Fig. 9. Dependence of E_{off} on I_C

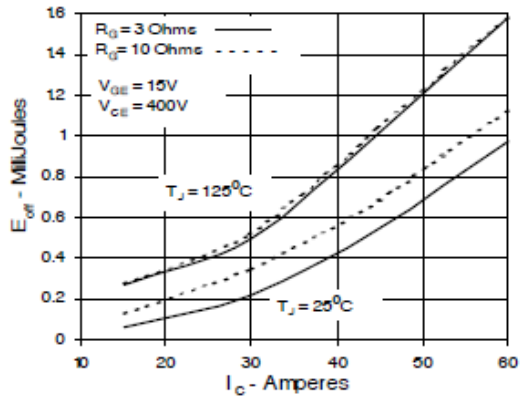

Fig. 10. Dependence of E_{off} on Temperature

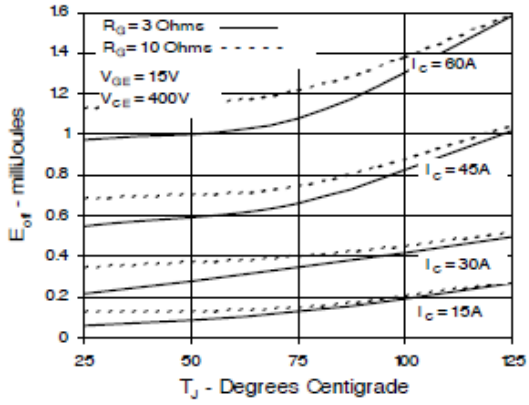

Fig. 11. Gate Charge

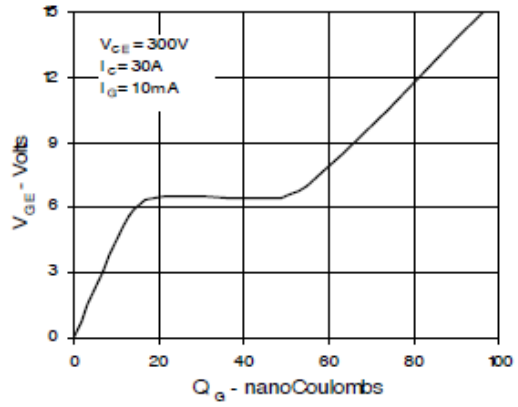

Fig. 12. Capacitance

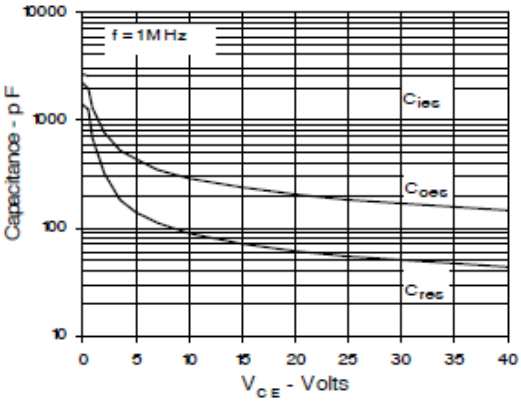

Fig. 13. Maximum Transient Thermal Resistance